Morphological, physiological, and molecular studies on the effect of shoot architecture on phase change and floral transition in *Eucalyptus occidentalis* and *Metrosideros excelsa*

Elizabeth. S.K.D. Jaya

2007

Morphological, physiological, and molecular studies on the effect of shoot architecture on phase change and floral transition in *Eucalyptus occidentalis* and *Metrosideros excelsa*

A thesis presented in partial fulfilment of the
requirements for the degree of

Doctor of Philosophy

in

Plant Biology

at

Massey University, Palmerston North,
New Zealand

Elizabeth S.K.D. Jaya

2007

Abstract

Shoot morphogenesis in *Eucalyptus occidentalis* and *Metrosideros excelsa* was analysed at the morphological, physiological and molecular levels to understand the regulation of phase change and the floral transition. Study of the regulation of these developmental plant processes is limited in woody species due to their long juvenile phase.

Six ecotypes of *E. occidentalis* were grown to two predetermined architectures (free branching or single stem). Free branching plants of ecotype 13648 displayed adult shoot phenology (lanceolate leaves) earlier than single stem counterparts. In addition, changes in leaf morphology in free branching plants were accompanied with changes in leaf anatomy and gas exchange signifying that in *E. occidentalis* complexity of shoot architecture had a significant effect on rate of phase change. Flowering was observed in all but one ecotype irrespective of architecture demonstrating that vegetative phase change and floral transition are temporally uncoupled in this species.

To understand the floral transition at the molecular level in *E. occidentalis*, partial homologues of the inflorescence meristem identity gene *TERMINAL FLOWER1* and floral meristem identity genes *LEAFY* and *APETALA1* were isolated. The expression patterns of these meristem identity genes during development of free branching and single stem plants were analysed by quantitative real-time PCR. Increased levels of expression of *EOLFY* and *EOAP1* (relative to *α-TUBULIN)* were displayed at more proximal nodes in free branching plants than in single stem plants. Elevated floral meristem identity gene expression levels correlated with flower initiation.

Further, effects of architecture and environment on gene expression were monitored in *E. occidentalis*. The overriding effect of shoot architecture on the floral transition was observed under warm long day and ambient environments. Elevated levels of *EOLFY* and *EOAP1* were correlated with floral bud score and *EOAP1* was found to be a reliable marker of floral transition in *E. occidentalis*. Low levels of *EOTFL1* expression were detected in buds irrespective of their position on the plant leading to the suggestion that this might have contributed to the precocious flowering observed in this species.

In contrast to *E. occidentalis*, *M. excelsa* attained adult shoot phenology (pubescent leaves) faster when grown as single stem plants than as free branching plants. It appears that growth as height is required for vegetative phase change in this species. However, floral transition occurred only once single stem plants were allowed to branch. Vegetative phase change and the transition to flowering seem to be coordinated in this species with the former being a pre-requisite for the latter.

Acknowledgements

My heart felt gratitude to my main supervisor Professor Paula Jameson for giving the opportunity to undertake this project, continual support, guidance, advice and encouragement throughout. I would like to convey my sincere gratitude to my co-supervisor Dr. John Clemens for valuable suggestions, discussions, guidance, and encouragement.

I would like to thank my co-supervisor Dr. Huaibi Zhang for advice in setting up molecular experiments. I am thankful to my co-supervisor Prof. Michael McManus for allowing me to continue my experiments in the lab and providing support.

I am also thankful to Dr. Southerton for kindly providing *E. occidentalis* seed and information about the provenances.

My special thanks are due to Dr. Dave Kubien for advice in conducting photosynthesis experiments and to Dr. Jason Song for introducing me to real-time PCR analyses. I am thankful to Prof. Peter Lockhart for advice in the construction of phylogenetic trees.

I would like to thank Dr. Alasdair Noble for the expert statistical advice and Mrs. Lesley Taylor and Plant Growth Unit staff for the assistance provided to grow the plants and conduct experiments in greenhouses.

I would like to express my appreciation to my lab mates Jan Binnie, Susanna Leung and Anu Sooda for their support and friendship during the study and the Institute of Molecular BioSciences for the facilities provided.

I am grateful to my husband Raj and my children Joseph and Joel for their encouragement and love, which made this endeavor a success.

I acknowledge thankfully the funding provided by the Public Good Science Fund, Crop and Food Research, Massey University for awarding a Doctoral Scholarship, and IMBS and NZSPB for sanctioning travel grants to attend conferences.

Finally I am grateful to my Lord Jesus for His abiding presence and enabling me to complete this study successfully.

Table of Contents

	Page
Abstract	ii
Acknowledgements	iv
Table of Contents	v
List of Figures	ix
List of Tables	xiii
List of Abbreviations	xv
Chapter 1. Introduction	
1.1 Overview	1
1.2 Models of phase change	3
1.3 Phase change in herbaceous species	6
1.4 Phase change in perennial species	9
1.4.1 Morphological and anatomical markers	10
1.4.2 Physiological markers	11
1.4.3 Genetic markers	13
1.4.4 Phase change and shoot architecture	14
1.4.5 Acceleration of phase change	16
1.5 Floral transition in herbaceous species	17
1.5.1 Floral transition models	17
1.5.2 Flower development pathways in *Arabidopsis*	18
1.5.2.1 Photoperiod response pathway	20
1.5.2.2 The vernalization response pathway	21
1.5.2.3 The autonomous pathway	22
1.5.2.4 The gibberellin (GA) pathway	23
1.5.2.5 Integration pathway	23
1.5.3 Meristem identity genes	25
1.5.3.1 *LEAFY*	25
1.5.3.2 *APETALA1*	27
1.5.3.3 *TERMINAL FLOWER1*	27
1.6 Floral transition in woody perennials	29
1.6.1 Expression patterns of *LEAFY* homologues	29
1.6.2 Expression patterns of *APETALA1* homologues	32
1.6.3 Expression patterns of *TERMINAL FLOWER1* homologues.	35
1.7 Definition of terms	36
1.8 Summary of phase change, floral transition and shoot architecture in *M. excelsa* and *E. occidentalis*	37
1.9 Aims and objectives	39
Chapter 2. Phase change and flowering in *Eucalyptus occidentalis* in relation to shoot architecture: morphological study	
2.1 Introduction	41
2.2 Materials and Methods	42
2.2.1 Plant material	42
2.2.2 Leaf morphology	43

2.2.3 Flowering 43
2.2.4 Statistical analysis 45
2.3 Results 45
2.3.1 Leaf morphology 45
2.3.2 Flowering 58
2.4 Discussion 62

Chapter 3. Phase change in *Eucalyptus occidentalis* in relation to shoot architecture (physiological studies)
3.1 Introduction 65
3.2 Materials and Methods 65
3.2.1 Plant material and treatments 65
3.2.2 Gas exchange 67
3.2.3 Leaf anatomy 68
3.2.4 Leaf mass per unit area (LMA) 68
3.2.5 Leaf mineral analysis 69
3.2.6 Statistical analysis 69
3.3 Results 70
3.3.1 Gas exchange 70
3.3.2 Leaf anatomy 78
3.3.3 Leaf mass per unit area 79
3.3.4 Mineral concentration 79
3.4 Discussion 86
3.4.1 Gas exchange 86
3.4.2 Leaf anatomy 88
3.4.3 Leaf mass per unit area and mineral concentrations 89

Chapter 4. Floral transition in *Eucalyptus occidentalis* in relation to shoot architecture (molecular studies)
4.1 Introduction 91
4.2 Materials and Methods 92
4.2.1 Plant material 92
4.2.2 Total RNA extraction 92
4.2.2.1 Hot borate RNA extraction 92
4.2.2.2 QIAGEN RNA extraction 95
4.2.3 Genomic DNA isolation 96
4.2.4 Quantification of total nucleic acids 96
4.2.5 Reverse transcription reaction (RT) 97
4.2.6 Polymerase chain reaction (PCR) 98
4.2.7 Agarose gel electrophoresis and band purification 98
4.2.8 Isolation of the partial homologues of meristem identity genes 98
4.2.9 Reference genes 99
4.2.10 Sequencing of isolated meristem identity and reference genes 99
4.2.11 Sequence verification 100
4.2.12 Phylogenetic analysis 101
4.2.13 Southern analysis 101
4.2.13.1 Electrophoresis of DNA digests and blotting 101

4.2.13.2 Probe preparation 102
4.2.13.3 Hybridisation and detection of non-radioactive probes 102
4.2.14 Temporal expression of meristem identity genes 103
4.2.14.1 Primers used for quantification of meristem identity genes 103
4.2.14.2 Quantitative real time PCR assay 103
4.2.14.3 Optimisation of real-time PCR conditions 104
4.2.14.4 Selection of reference gene for relative quantification 104
4.2.14.5 Calculation of PCR efficiencies 104
4.2.14.6 Relative quantification of meristem identity genes 105
4.3 Results 106
4.3.1 Meristem identity gene isolation and analysis 106
4.3.1.1 *LEAFY* (*LFY*) 106
4.3.1.2 *TERMINAL FLOWER1* (*TFL1*) 112
4.3.1.3 *APETALA1* (*AP1*) 117
4.3.2 Isolation and identification of reference genes 122
4.3.2.1 α-*TUBULIN* 122
4.3.2.2 *GAPDH* 122
4.3.2.3 *18S RNA* 124
4.3.2.4 *β-ACTIN* 124
4.3.3 Southern analysis 126
4.3.4 Temporal expression of meristem identity genes using qRT-PCR 127
4.3.4.1 Total RNA extraction from bud samples 127
4.3.4.2 Reference gene validation by RT-PCR 127
4.3.4.3 Real time PCR optimisation: determination of template and $MgCl_2$ concentration 131
4.3.4.4 Performance of *α-TUBULIN* in LightCycler™ experiments 133
4.3.4.5 PCR amplification efficiency determination 133
4.3.4.6 Melting curve analysis 134
4.3.4.7 Meristem identity gene expression in relation to architectural manipulation and flowering in *E. occidentalis* 137
4.4 Discussion 141
4.4.1 Identification of partial homologues of meristem identity genes 141
4.4.2 Optimisation and advantages of real-time qRT-PCR assay 143
4.4.3 Gene expression in architecturally manipulated plants 144

Chapter 5. Effect of environment and shoot architecture on floral transition and gene expression in *Eucalyptus occidentalis*
5.1 Introduction 147
5.2 Materials and Methods 147
5.2.1 Plant material 147
5.2.2 Plant growth and flowering 148
5.2.3 Bud collections 149
5.2.4 Statistical analysis 149
5.2.5 Temporal expression of meristem identity genes 149
5.2.5.1 Total RNA extractions 149
5.2.5.2 cDNA preparations 149
5.2.5.3 Quantification of *EOLFY*, *EOAP1* and *EOTFL1* 149

5.3 Results 151
5.3.1 Plant growth and flowering 151
5.3.2 Floral score and meristem identity gene expression 153
5.3.2.1 Floral score 153
5.3.2.2 Expression of meristem identity genes 153
5.4 Discussion 158

Chapter 6. Effect of environment and shoot architecture on gene expression in relation to phase change and floral transition in *Metrosideros excelsa*
6.1 Introduction 161
6.2 Materials and Methods 162
6.2.1 Plant material and growth conditions 162
6.2.2 Leaf anatomy 163
6.2.3 Bud collection and cymule scale scar count 163
6.2.4 Statistical analysis 165
6.2.5 Total RNA extractions 165
6.2.6 cDNA preparations 165
6.2.7 Isolation and quantification of *MEL*, *MESAP1* and *METFL1* 165
6.3 Results 167
6.3.1 Leaf anatomy 167
6.3.2 Bud scale scar counts 167
6.3.3 Quantification of meristem identity genes 167
6.4 Discussion 173
6.4.1 Leaf anatomy 173
6.4.2 Floral transition and expression of meristem identity genes 173

Chapter 7. Final Discussion 176

Appendices
Appendix 1 p values of ANOVA analyses 180
Appendix 2 Candisk analysis-1 187
Appendix 3 Candisk analysis-2 191
References 198

List of Figures

Page

Figure 1.1 Simple model of the four pathways controlling flowering time in *Arabidopsis thaliana* (from Corbesier and Coupland, 2006) 19

Figure 1.2 Genetic regulatory networks controlling flowering in *Arabidopsis* Showing four pathways (from Welch et al., 2004). 19

Figure 2.1 Typical *Eucalyptus occidentalis* juvenile (A) and adult leaves (B). *E. occidentalis* ecotype 15416 grown in single stem (C) and free branching (D) architecture in a greenhouse under conditions specified in Section 2.2.1. 44

Figure 2.2 Leaf length to maximum width ratio differences between ecotypes of *E. occidentalis* (shown in panels) from node 10 to 60 54

Figure 2.3A Two-way interaction between ecotype and node number for the variable roundness in *E. occidentalis*. 55

Figure 2.3B Two-way interaction between architecture and node number for the variable roundness of single stem and free branching plants in *E. occidentalis*. 55

Figure 2.3C Two-way interaction between ecotype and architecture for the variable roundness of single stem and free branching plants in *E. occidentalis*. 56

Figure.2.4 Two-way interaction between ecotype and architecture, for the variable petiole length of single stem and free branching plants in *E. occidentalis*. 56

Figure 2.5 Axes Can1 and Can2 of canonical ordinations of morphological data of *E. occidentalis*. 59

Figure 2.6 Axes Can1 and Can2 of canonical ordinations of morphological data of architecture and ecotype treatments of *E. occidentalis*. 60

Figure 2.7 Percentage of plants shown at each bar of six ecotypes of *E. occidentalis* that initiated flower buds nine months after sowing when grown with either free branching or single stem architecture. 61

Figure 3.1 Experimental treatments for gas exchange, leaf mass per unit area, and leaf mineral analysis of *E. occidentalis*. + F, supplementary fertiliser; – F, no supplementary fertiliser. 66

Figure 3.2 The response of net photosynthesis rate (A) (mean ± S.E.) to intercellular CO_2 (C_i) in *E. occidentalis* of ecotypes 13648 and 15416. 71

Figure 3.3 Correlation between V_{cmax} and J_{max} parameters in *E. occidentalis* estimated for January and February 2004 gas exchange measurements. 73

Figure 3.4 The response of photosynthesis (A) (mean ± S.E.) to intercellular CO_2 (C_i) in *E. occidentalis*. 75

Figure 3.5 Correlation between V_{cmax} and J_{max} parameters in *E. occidentalis* estimated for March and April 2004 gas exchange measurements (+/– supplementary fertiliser application). 77

Figure 3.6 Photomicrographs of traverse sections of representative single stem and free branching leaves of *E. occidentalis* ecotype 13648 and 15416 at node 30, 40 and 50 on the main stem. Each section has incorporated scale size bar of 100 μm. 81

Figure 4.1 Typical example showing sites of bud collection for meristem identity gene expression analysis. 93

Figure 4.2A Isolation of partial homologue of *LFY* (270 bp) from *E. occidentalis*. 107

Figure 4.2B Isolation of partial homologue of *LFY* (1000 bp) from *E. occidentalis*. 107

Figure 4.3 Comparison of the amino acid sequence of EOLFY with LFY-like protein sequences from GenBank. 109

Figure 4.4 Phylogenetic relationship of some *LFY* homologues derived from plants from a wide range of angiosperm species using the neighbour joining method and TreeView software. 110

Figure 4.5 Deduced gene structure of *EOLFY* sequence. 111

Figure 4.6 Isolation of partial homologue of *TFL1* (170 bp) from *E. occidentalis* 113

Figure 4.7 Comparison of the amino acid sequence of EOTFL1 with TFL1-like protein sequences from GenBank. 114

Figure 4.8 Phylogenetic relationships of some *TFL1* homologues derived from plants from a wide range of angiosperms using the neighbour joining method and TreeView software. 115

Figure 4.9 Deduced gene structure of the *EOTFL1* sequence 116

Figure 4.10 Isolation of partial homologue of *AP1* (650 bp) from *E. occidentalis*. 118

Figure 4.11 Comparison of amino acid sequence of EOAP1 with AP1-like protein sequences from GenBank. 119

Figure 4.12 Phylogenetic relationship of some *AP1* homologues derived from plants from a wide range of angiosperms using neighbour joining method and TreeView software. 120

Figure 4.13 Deduced gene structure of the *EOAP1* sequence. 121

Figure 4.14 Isolation of partial homologue of α-*TUBULIN* (650 bp) and *GAPDH* (380 bp) from *E. occidentalis*. 123

Figure 4.15 Isolation of partial homologue of *18S RNA* (180 bp) from *E. occidentalis*. 125

Figure 4.16 Isolation of partial homologue of *β-ACTIN* (450 bp) from *E. occidentalis*. 125

Figure 4.17 Southern analysis of *E. occidentalis* genomic DNA after restriction digestion. 126

Figure 4.18 Example of total RNA (RNA integrity) used for gene expression assays. 128

Figure 4.19 Expression of potential reference genes *18S RNA* and *α-TUBULIN* in random bud samples of *E. occidentalis*. 129

Figure 4.20A and B Expression of potential reference genes *β-ACTIN* and *GAPDH*, respectively in random bud samples of *E. occidentalis*. 130

Figure 4.21 Amplification curves obtained for cDNA template and $MgCl_2$ concentration optimisation assay. 132

Figure 4.22 Amplification performance of *α-TUBULIN* in five randomly selected bud samples. 133

Figure 4.23 Standard curves showing the starting cDNA log concentration verses Cp values in PCR amplification programme. 135

Figure 4.24 Melting curve analysis of meristem identity and reference genes. 136

Figure 4.25 Percent floral score of paired axillary buds. 138

Figure 4.26 Expression of meristem identity genes (*EOLFY*, *EOTFL 1* and *EOAP 1)* in (A) free branching and (B) single stem plants. 139

Figure 4.27 The ratios of expression of floral meristem identity genes *EOLFY* (A) *EOAP1* (B) as compared to shoot identity gene *EOTFL1*. 140

Figure 5.1 *Eucalyptus occidentalis* ecotype 13648 plants grown with free branching (A) and single stem-free branching architectures (B). 150

Figure 5.2A-D Plant growth and flowering pattern in *E. occidentalis* grown in Warm/long day and Ambient treatments. 152

Figure 5.3 Percent floral scores of paired axillary buds on plants grown in different environments with different architectures. 155

Figure 5.4 Relative quantification of meristem identity gene expression in plants grown under Warm/LD conditions with different shoot architecture. 156

Figure 5.5 Relative quantification of meristem identity gene expression in plants grown under Ambient conditions with different shoot architecture. 157

Figure 6.1 Schematic diagram of the inflorescence and one cymule of *M. excelsa* (Sreekantan et al., 2001). 164

Figure 6.2 Typical leaf sections (200 X) of *M. excelsa* at node 20, 40, 55 and 75 on the main stem of SsFb plants. 169

Figure 6.3 Number of bud scale scar pairs at distal ends of branches of plants grown under different environments with architecture modification. 170

Figure 6.4 Relative quantification of meristem identity gene expression on three occasions in *M. excelsa* plants grown under different environmental and architecture treatments. 171

Figure 6.5 A-D Plots showing the expression ratios of *MEL/METFL1* and *MESAP1/METFL1* on three occasions in plants grown under Ambient and Warm/LD environments with architecture modification. 172

List of Tables

Page

Table 1.1 Traits showing changes during phase change in *Z. mays* (Table adapted from Poethig, 1990). 7

Table 2.1 *Eucalyptus occidentalis* provenances used in this study. 42

Table 2.2 Morphological attribute: leaf area (cm^2) measured in six ecotypes of *E. occidentalis* at nodes 10, 20, 30, 40, 50 and 60 on the main stem of free branching and single stem plants. 46

Table 2.3 Morphological attribute: leaf perimeter (cm) measured in six ecotypes of *E. occidentalis* at nodes 10, 20, 30, 40, 50 and 60 on the main stem of free branching and single stem plants. 47

Table 2.4 Morphological attribute leaf roundness measured in six ecotypes of *E. occidentalis* at nodes 10, 20, 30, 40, 50 and 60 on the main stem of free branching and single stem plants. 48

Table 2.5 Morphological attribute leaf length (cm): measured in six ecotypes of *E. occidentalis* at nodes 10, 20, 30, 40, 50 and 60 on the main stem of free branching and single stem plants. 49

Table 2.6 Morphological attribute leaf maximum width measured in six ecotypes of *E. occidentalis* at nodes 10, 20, 30, 40, 50 and 60 on the main stem of free branching and single stem plants. 50

Table 2.7 Morphological attribute leaf length/width ratio measured in six ecotypes of *E. occidentalis* at nodes 10, 20, 30, 40, 50 and 60 on the main stem of free branching and single stem plants. 51

Table 2.8 Morphological attribute petiole length (cm) measured in six ecotypes of *E. occidentalis* at nodes 10, 20, 30, 40, 50 and 60 on the main stem of free branching and single stem plants. 52

Table 3.1 Mean values (± S.E.) of the parameters V_{cmax} (μmol m^{-2} s^{-1}) and J_{max} (μmol m^{-2} s^{-1}) of ecotypes 13648 and 15416 of *E. occidentalis*. 72

Table 3.2 Mean values (± S.E.) of the parameters V_{cmax} (μmol m^{-2} s^{-1}) and J_{max} (μmol m^{-2} s^{-1}) for ecotypes 13648 and 15416 of *E. occidentalis* with or without supplementary fertiliser application. 76

Table 3.3 Leaf anatomical characteristics (mean values ± S.E.) of single stem and free branching plants at different nodes for *E. occidentalis* ecotypes 13648 and 15416. 80

Table 3.4 Leaf mass per unit area (g m^{-2}), of leaves of free branching and single stem plants for two ecotypes of *E. occidentalis* prior to supplem entary fertiliser application 82

Table 3.5 Leaf mass per unit area (g m^{-2}), of leaves of free branching and single stem plants for two ecotypes of *E. occidentalis* following supplementary fertiliser treatment to half of the plants. 82

Table 3.6 Mean values (± S.E.) of leaf mineral concentration of single stem and free branching plants of *E. occidentalis* at different nodes prior to supplementary fertiliser application. 83

Table 3.7 Mean values (± S.E.) of leaf mineral concentration of single stem and free branching plants of *E. occidentalis* following supplementary fertiliser treatment to half of the plants. 85

Table 4.1 Primers used for isolating meristem identity genes. 99

Table 4.2 Primers used for isolating reference genes. 100

Table 4.3 Primers used for real-time quantitative RT-PCR. 103

Table 4.4 Optimisation of real time PCR with cDNA derived after RT reaction for template dilution and $MgCl_2$ concentrations. 131

Table 6.1 Primers used for real-time quantitative RT-PCR of *Metrosideros excelsa*. 166

Table 6.2 Anatomical parameters of *Metrosideros excelsa* leaves collected from SsFb plants. [1, 2] 168

List of Abbreviations

ANOVA	analysis of variance
bp	base pair
cDNA	complementary deoxyribonucleic acid
CSIRO	Australian Commonwealth Scientific and Research Organization
DEPC	diethyl pyrocarbonate
EDTA	ethylene diamine tetracetic acid
FMI	floral meristem identity
JPEG	joint photographic experts group
Kb	kilo base
LED	light emitting diode
LMA	leaf mass per unit area
ORF	open reading frame
Pa	Pascal
PCR	polymerase chain reaction
rpm	revolutions per minute
SE	standard error
SDS	sodium dodecyl sulphate
Tris-HCl	tris (hydroxymethyl) aminomethane hydrochloride
UV	ultraviolet

Chapter 1
Introduction

1.1 Overview

Production of ornamental plants is of importance worldwide. According to IBISWorld research reports, nursery and floriculture production industry revenue in the United States alone was US $229.5 billion in 2005 and the domestic demand worth US $323 billion. In New Zealand, the export value for flowers, foliage and plants was NZ $81 million in 2002 (Anon., 2003). These figures suggest a significant potential for future growth. The Public Good Science Fund (PGSF) supported an ongoing study through a Crop and Food Research subcontract of the various morphological, physiological and molecular attributes contributing to phase change and flowering under the Native Ornamental Plants Programme aimed at the development of new ornamental crops. Under this programme *Metrosideros excelsa* (pohutukawa), a member of the Myrtaceae, was identified as having potential as an ornamental flowering crop either as a cut flower or as a flowering container plant. Until now, *Metrosideros* has attracted attention only as a foliage plant (Vitousek, 1998). *Metrosideros excelsa* is a large, mass-flowering tree endemic to northern New Zealand. Prior to the present study, *M. excelsa* had been studied at the morphological, physiological (Henriod, 2001; Sismilich, 2001) and molecular levels (Sreekantan, 2002). To gain a deeper understanding of the mechanisms underlying phase change and the transition to flowering in woody species, this project formed the basis of a comparative study combining the previous information obtained for *M. excelsa* with new research using *Eucalyptus occidentalis*, a non-native perennial, but also a member of the Myrtaceae, as the model species.

In angiosperms, three post-embryonic developmental phases have been recognised: juvenile, adult vegetative and adult reproductive (Poethig, 1990). *Metrosideros excelsa* is a homoblastic species, which exhibits a gradual transition between juvenile and adult vegetative characteristics during phase change (Dawson, 1968) and it generally takes several years for seedlings and over three years for rejuvenated plants from micro

propagation to flower (Clemens et al., 1999). *Eucalyptus occidentalis* (flat-topped yate) is a native to the southwest of Western Australia. It exhibits neoteny, which is the retention of juvenile characteristics into the adult reproductive plant (Wiltshire et al., 1998). Further, precocious flowering after only 12 weeks from sowing was observed in container-grown plants of *E. occidentalis* (Bolotin, 1975). This is of interest commercially because the development of woody plants from seed may include a juvenile phase, lasting up to 15 to 20 years in certain commercially important forest trees (Hackett, 1985).

There has been significant interest in accelerating phase change in woody plants and a variety of methods have been tested including physical methods such as shoot and root restriction in *M. excelsa* (Clemens et al., 1999), application of the plant hormone gibberellic acid to *Eucalyptus* species (Scurfield and Moore, 1958), shoot restriction (single stem growth) coupled with the application of paclobutrazol in *Citrus* species (Snowball et al., 1994), fertiliser treatment in *Eucalyptus nitens* (Williams et al., 2004) and long day treatment in *E. occidentalis* (Bolotin, 1975). In several studies, limiting growth to a single stem by removal of axillary buds before bud break or elongation has been shown to reduce the time to flower (Davis, 1991). Clemens et al. (1999) demonstrated that architecturally modified (single stem) *M. excelsa* plants became progressively mature with increasing node position, and developed downy tomentum on the abaxial surface, characteristic of mature leaves. However, it has been proposed that the attainment of reproductive competence in *M. excelsa* is a consequence of the tree reaching a certain degree of branching complexity (Clemens et al., 2002; Sismilich et al., 2003).

Unlike herbaceous plants such as *Arabidopsis* and *Zea mays* there is paucity of information and understanding with regard to the molecular basis of phase change and floral transition in woody perennials. In spite of significant differences in growth habit between herbaceous and woody plants, it would not be unreasonable to expect that the mechanisms underlying flowering control would be similar (Battey and Tooke, 2002). Previous work has demonstrated the presence of the floral meristem identity genes *LEAFY* (*LFY*), *APETALA1* (*AP1*) and the inflorescence meristem identity gene *TERMINAL FLOWER1* (*TFL1*) in woody plants such as *M. excelsa* (Sreekantan et al., 2004), *E. globulus* (Kyozuka et al., 1997; Southerton et al., 1998; Dornelas and

Rodriguez, 2005), *Cedrela fissilis* (Dornelas and Rodriguez, 2006), and *Citrus sinensis* (Pena et al., 2001; Pillitteri et al., 2004).

Combining the previous lines of evidence in woody plants, in this study an attempt has been made to understand the shoot restriction methods versus crown complexity and environmental cues in relation to phase change and first flowering in *E. occidentalis*. Further the molecular basis of the floral transition was investigated after isolating the *LFY*, *AP1* and *TFL1* homologues of *E. occidentalis* and employing quantitative real-time PCR (qRT-PCR) to monitor gene expression. The ultimate objective is to use the knowledge generated to accelerate both phase change and flowering in ornamental woody species such as *M. excelsa*.

The following review covers the available literature including models of phase change, phase change in herbaceous and perennial species, floral transition in herbaceous and perennial species, meristem identity genes, and definition of terms adopted in this thesis.

1.2 Models of phase change

Classical models described by Lawson and Poethig (1995) depend on hypotheses based on size of the plant, distance between root and shoot, number of leaves, and time. If the root system were to produce a factor that promoted the juvenile phase or inhibited adult development, shoot maturation might occur when this factor fell below a certain level because of the absolute distance. If the change of phase was regulated by plant size, then mutations that affect the size of the shoot or root system would affect the identity of leaves at particular positions on the shoot. If phase change were time-dependent, then mutations in this mechanism would cause leaves to assume early or late vegetative fates depending on when they appeared in the real time (Lawson and Poethig, 1995).

The relationship between age or size and reproductive maturity has been investigated in woody species by growing plants under conditions that retard or accelerate growth (Lawson and Poethig, 1995). Large, rapidly growing plants flower earlier than smaller, more slowly growing ones, suggesting that reproductive maturation is a size-dependent

not an age-dependent process (Longman and Wareing, 1959). One of the explanations for this type of effect is that by increasing the rate of shoot growth , the measurement of developmental time has also been accelerated, leading to an earlier phase transition both in terms of plant size (physiological age) and plant age (developmental time) (Lawson and Poethig, 1995).

Various models have been proposed based on the developmental changes during phase change. Kester (1976) proposed a model based on woody species and explained the coexistence of juvenile and adult characteristics during plant ontogeny along the main shoot axis and the lateral branches by noting that these are expressed at different locations on the plant. The juvenile characteristics usually occupy the lower part of the stem; after some time the plant produces intermediate characteristics and then the adult traits, which take up the upper portions and the periphery of the plant body.

In the combinatorial model, Poethig (1990) proposed a model similar to Kester's (1976). This model implies that the development of the shoot is specified by a series of independently regulated, but overlapping programmes that modify the expression of a common set of processes that are required for shoot growth, rather than by a series of mutually exclusive developmental programmes coming from many different sources (Poethig, 1990). For example, in *Zea mays* during the phase transition from juvenile to adult growth, the leaves have a combination of juvenile and adult cell types and also a variety of other traits that are expressed in a quantitatively intermediate fashion (Poethig, 1990; Lawson and Poethig, 1995). Similarly, in woody plants, such as *Eucalyptus* species, the transition from a juvenile to an adult phase of development is accompanied by the production of intermediate patterns of shoot development that combine cellular and morphological traits from each phase (Hackett, 1976).

Hackett and Murray (1997) proposed a set of alternative models for phase change. The important aspects of these models are that phase change is not controlled by a single step process but by a composite of processes or programmes. The models emphasise the importance of studying the regulation of individual phase-specific characteristics to understand the whole picture of phase change (Zhang, 1998). These models can be used to explain the results obtained from mutants in genetic analysis of phase change where there is either a prolonged expression of the juvenile phase (Poethig, 1988a, 1988b;

Bassiri et al., 1992) or the accelerated appearance of the mature programme (Sung et al., 1992; Haughn et al., 1995; Amasino, 1996). Such genetic analyses indicate that the pathways involved in phase change are likely to be complex with frequent branch points and many interacting pathways as proposed by Lawson and Poethig (1995). Physiological studies also show that the changes of individual phase-specific traits may not be closely linked temporally or mechanically (Greenwood, 1992; Hackett et al., 1992) but display differential time courses (Steele et al., 1989; Greenwood et al., 1989; Browne, 1995). The differential sensitivity of various morphological and physiological traits to rejuvenation (phase reversal) by gibberellic acid (GA_3) in *Hedera helix* (ivy) is an example of such complexity (Rogler and Hackett, 1975).

Greenwood (1995) suggested that, while applying the models to study the developmental phases in woody species one must consider related mechanisms and account for the phenomena demonstrated experimentally in mutant plants, which include:

1. The onset of the mature state is usually gradual, but can be abrupt. For example, in several conifers abrupt maturation has been observed immediately following tissue culture propagation from adventitious buds induced on the cotyledons of mature embryos (Greenwood, 1995).
2. Phase change affects a wide variety of morphological, physiological and biochemical traits, but these traits appear to vary independently of one another.
3. Maturational traits are often persistent, and their maintenance is not always a function of tree size or proximity to roots.
4. There is evidence that the cells of the apical meristem itself become determined in some woody plants. Grafted apices from mature plants of *Citrus* or *Sequoiadendron* consisting of only the apical and one to two leaf primordia grow out into plants that have mature characteristics (Navarro et al., 1975; Monteuuis, 1991).
5. Rejuvenation methods bring about reversion to the juvenile condition.

According to these principles, Greenwood (1995) contends that the switch (of phase change) could reside within individual cells in the apical meristem and, once activated, would make that cell mature, so that the apex would progressively become a mosaic with an ever increasing percentage of mature cells. Expression of mature characteristics

would, therefore, be a function of the ratio of juvenile to mature cells in the apex at a given time. This hypothesis may explain why fully expanded leaves at intermediate stage of phase change possess phenotypic characters (or cell types) typical of both juvenile and adult phases as exhibited in many woody species (James and Bell, 2001).

The recent molecular model proposed by Battey and Tooke (2002) explains that in the vegetative state, the shoot meristem has vegetative identity and hence gives rise to a leaf plus its associated axillary meristem. Vegetative identity alters with a switch from the juvenile to adult condition. Signals generated within the plant as a function of developmental age, or following exposure to an appropriate environment, then cause the meristem to take a new identity - that of the inflorescence meristem - which gives rise to bracts and associated flowers. Finally, an inflorescence meristem may undergo transition to a floral meristem. In recent usage, switching between these different identities has equated with phase change (Battey and Tooke, 2002).

From the above suggested phase change models in herbaceous and perennial plants it would be appropriate to summarise that phase change could be under the control of complex networks of endogenous and environmental factors. Further, phase change is the critical aspect of shoot development in understanding the attainment of reproductive competency and the mechanisms underlying the life history evolution of a given species.

1.3 Phase change in herbaceous species

Vegetative phase change has been investigated more intensively in woody plants until recently. This was mainly due to the fact that the prolonged juvenile phase and the morphological differences between the phases are often more obvious in woody species (Lawson and Poethig, 1995). Generally, herbaceous plants do not have extreme morphological variation during phase change. However, it has been shown that *Zea mays* and *Arabidopsis thaliana* plants undergo discrete changes from the juvenile to the adult stage during the course of vegetative development (Poethig, 1988a; Moose and Sisco, 1994; Clark et al., 1997; Evans and Barton, 1997; Telfer et al., 1997; Tsukaya et al., 2000; Vega et al., 2002; Bollman et al., 2003).

In *Arabidopsis,* the appearance of abaxial trichomes on the third and later leaves, followed by the disappearance of adaxial trichomes later in development, is reported to be a phase specific marker (Lawson and Poethig, 1995). It has been postulated that there is a global inductive signal (possibly GA) for trichome production, the key level of which increases during the development of the rosette, and that the adaxial epidermis is less sensitive to this signal than the abaxial epidermis (Telfer et al., 1997).

In *Z. mays,* juvenile and adult vegetative plants have distinct features for a wide range of traits (Table 1.1) as described by Poethig (1990).

Table 1.1 Traits showing changes during phase change in *Z. mays* (Table adapted from Poethig, 1990).

Traits	Juvenile	Adult
Cuticle thickness	1 μm	3 μm
Epidermal cell shape	Circular	Rectangular
Epicuticular wax	Present	Absent
Aerial roots	Present	Absent
Epidermal hairs	Absent	Present
Bulliform cells	Absent	Present
Lateral buds	Tiller-like	Ears or absent
Anthracnose resistance	Poor	Good

Further, Orkwiszewski and Poethig (2000) reported that leaf identity can be regulated independently of the identity of the shoot apical meristem, and they explained that vegetative phase change was not initiated by a change in the identity of the shoot apical meristem.

Sylvester et al. (2001) conducted a comparative study of leaf shape and anatomy in maize, *Oryza sativa* (rice), and blue grass and reported that, in maize, juvenile leaves were coated with epicuticular wax, lacked specialised cells such as trichomes and

bulliform cells and had epidermal cell walls that stained a uniform purple colour. Adult maize leaves were pubescent, lacked epicuticular waxes and had crenulated epidermal cell walls that stained purple and blue. In contrast, all bluegrass and rice blades were pubescent and coated with epicuticular waxes, and showed purple and blue wall staining. In all three grasses, blade width steadily increased at each node until a threshold size was attained several nodes before reproductive competence was achieved. Blade to sheath length showed a similar trend of continuous change followed by discontinuous change prior to reproduction. Leaf development analysis demonstrated that maize primordia initiated more rapidly relative to blade and sheath growth compared with either blue grass or rice. This study concluded that leaf shape, as defined by blade width and blade to sheath ratio, was a reliable indicator of phase, whereas anatomy was not a universal indicator of phase change in the grasses (Sylvester et al., 2001).

Several genes involved in shoot maturation have been identified in maize and *Pisum*. In maize, such genes were defined by the dominant, gain-of-function mutations, *Teopod 1*, *2* and *3* (*Tp1*, *Tp2* and *Tp3*) and *Corngrass* (*Cg*) which prolong the expression of juvenile traits (Poethig, 1988b). These mutations all prolong the expression of early vegetative traits, such as epicuticular wax, but only delay slightly the onset of late vegetative traits, such as macrohair production (Evans et al., 1994). Even though the *Teopod* mutations cause a reduction in the size of reproductive structures (tassel and ear) it was shown that this was not due to the mutation, but to the increased number of leaves produced by the main shoot. These findings indicate that the *Teopod* mutations prolong the juvenile developmental program while leaving the late vegetative and reproductive development relatively unaffected (Lawson and Poethig, 1995). Further mutation studies identified *glossy15* (*gl15*) which, in contrast to the *Teopod* mutations caused the precocious expression of adult traits, and affected only the leaf epidermis. Subsequently, it was suggested that *Gl15* encodes an epidermal factor that initiates or maintains the expression of adult traits, and that it acts downstream of the *Teopod* genes (Lawson and Poethig, 1995). In maize the *epc* (*early phase change*) gene mutation and gibberellic acid specifically affected vegetative phase change: in certain genetic backgrounds *epc* mutations reduced the duration of the juvenile vegetative phase and caused early flowering but they had little or no effect on the number of adult leaves (Vega et al., 2002).

Telfer and Poethig (1998) analysed shoot maturation in *A. thaliana* by screening the mutations that affected the timing of abaxial trichome production, a trait that distinguishes juvenile and adult leaves and showed that *HASTY* (*HST*) may be a part of a developmental clock that regulates the timing of shoot maturation. It was also suggested that *HST* promoted a juvenile pattern of vegetative development and inhibited flowering by reducing the competence of the shoot to respond to *LFY* and *AP1*. The fact that *hst* affected both vegetative phase change and flowering time, raised the long - standing question about the relationship between these two aspects of shoot development (Telfer and Poethig, 1998).

Kazumi et al. (2002) have identified five recessive allelic mutations in rice, *mori1-1* to *mori1-5*, which drastically modified the shoot architecture of the plant. The most outstanding feature of *mori1* plants is a rapid production of small leaves and short branches. This mutation is a heterochronic mutation that suppresses the induction of the adult phase and the termination of the juvenile phase. They reported that *MORI1* plays an important role in the juvenile to adult phase change.

Recently, Poethig (2007) reported that, vegetative phase change in maize and *Arabidopsis* was regulated by several endogenous small (21 nt) RNAs. These were the trans-acting siRNA, tasi-ARF, and two miRNAs, miR156 and miR172. tasi-ARF represses the expression of the auxin-related transcription factors ETTIN/ARF3 and ARF4. miR156 and miR172 have complementary temporal expression patterns and target different families of transcription factors (Poethig, 2007).

As observed above, the recent studies in model organisms *Arabidopsis*, maize and rice have suggested that the phenomenon of vegetative phase change is not confined to woody species alone. Gene mutation studies have enabled some progress in understanding of phase change at the physiological and genetic levels due to the short life cycles of the model species.

1.4 Phase change in perennial species

The juvenile phase of woody plants has usually been considered a stage which may last up to 30 to 40 years in certain forest trees, during which flowering does not occur and cannot be induced under normal conditions (Hackett, 1985). The long juvenile phase is a serious constraint for traditional and transgenic breeding practices (Pillitteri et al., 2004). Therefore, studies on phase change in woody species are of practical and theoretical importance. Characterisation of phase change has been analysed in different species as given below by studying distinct markers during phase change.

1.4.1 Morphological and anatomical markers

Changes in leaf morphology (structure) among other changes in the plant often accompany phase change. Phase change in ivy is one of the best characterised among the woody species. A variety of features distinguish juvenile and adult parts of the plant. Obvious morphological transitions include a change from lobed to entire leaves, from alternate to spiral patterns of leaf production (phyllotaxis), from the presence to the absence of adventitious roots and from a trailing or climbing vine to a semi-erect shrub (Brink, 1962; Stein and Fosket, 1969).

New Zealand has a large number of strongly heteroblastic plants using the term as defined by Goebel (1900), the species that show pronounced vegetative morphological differences between juvenile and adult shoots. Cockayne (1912) estimated that 200 native species in 37 families have distinct juvenile and adult stages of vegetative development. For example, juvenile leaves of the *Pseudopanax crassifolius* (lancewood) as described by Gould (1993) are long, linear, deflexed, coriaceous and sharply toothed. They have a high specific weight, a thick, ornamented cuticle, a multiseriate hypodermis composed of collenchyma, a well developed palisade layer and many spongy mesophyll layers. Juvenile leaves were strong relative to adult leaves and to the leaves of other species; adult leaves were shorter, broader and less massive than juvenile leaves and the orientation was horizontal. The transitional leaves were morphologically intermediate between juvenile and adult leaves. However, the anatomy of juvenile, transitional and adult leaves was found to be similar (Gould, 1993).

Metrosideros excelsa exhibits both juvenile and adult vegetative phases, but in contrast to heteroblastic species, leaf morphology in *M. excelsa* progresses gradually from

glabrous, small and lanceolate leaves in the juvenile phase to those that are relatively hirsute, large and rounded in the adult vegetative phase (Clemens et al., 2002). Adult leaves of *M. excelsa* have deeper palisade and spongy mesophyll layers than juvenile or transitional foliage and as such resemble sun leaves (Kubien et al., 2007).

In *Eucalyptus globulus* ssp. *globulus* (Tasmanian blue-gum) there are dramatic differences in the leaf anatomy and morphology of the adult compared with the seedling (James et al., 1999); this vegetative phase change generally begins at one to three years of age. Juvenile leaves are typically blue-grey in colour, dorsiventral in structure, hypostomatous, and approximately horizontal in orientation (Johnson, 1926; Jacobs, 1955). In contrast, adult leaves are dark green in colour, isobilateral (adaxial and abaxial palisade), amphistomatous and nearly vertical in orientation (James et al., 1999). The transitional leaves are largely isobilateral in structure (James and Bell, 2001). However, *E. risdonii* and *E. occidentalis* retains juvenile foliage to floral transition without the requirement of vegetative phase change (Wiltshire et al., 1998).

Morphological and anatomical differences were recorded between old-growth trees and saplings of *Pseudotsuga menziesii* (Douglas-fir) (Apple et al., 2002). They reported that, compared with needles of old-growth trees, needles of saplings were longer and had proportionately smaller vascular cylinders, larger resin canals and few hypodermal cells.

Poethig (1990) suggested that the transition from juvenile to an adult phase of vegetative growth usually occurs gradually and may involve subtle changes in shoot morphology and physiology. However, as described above, the morphological changes appear to be more pronounced in woody species compared to herbaceous plants. Further, in woody species these changes may be gradual (homoblastic) as in *Metrosideros* with gradual changes in leaf morphology from juvenile to adult morphology (Clemens et al., 1999) or abrupt heteroblastic as in *Eucalyptus* which produces distinctly juvenile foliage for some time but, after a brief transition, produce significantly different new foliage (James and Bell, 2001).

1.4.2 Physiological markers

Physiological traits such as net photosynthetic rate have been shown to be influenced by phase change. The net photosynthetic capability of the mature foliage of *Larix laricina* (larch) was significantly greater than that of juvenile foliage and photosynthesis was positively correlated with the chlorophyll content of the foliage (Greenwood et al., 1989; Hutchison et al., 1990). In ivy, light saturated net CO_2 assimilation (A) and stomatal conductance (G_s) were about 50% higher in adult leaves than in juvenile foliage on the same individual and photosynthesis was higher in adult than juvenile leaves (Bauer and Bauer, 1980). In contrast, in other studies, with increasing ontogenetic development a concomitant decrease in net photosynthetic rate was reported in *Picea abies* (Kull and Koppel, 1987), *Sequoiadendron giganteum* (Grulke and Miller, 1994) and *Pinus ponderosa* (Kolb and Stone, 2000).

Day et al. (2001) studied the age related trends in needle morphology and gas exchange in a population of *Picea rubens* (red spruce). The differences were measured across a 2 to 120 year age range. Field study revealed significant age related trends in morphology including decreasing specific leaf area, increase in needle width, projected area and width/length ratio. Further, age-related declines in photosynthetic rates were observed which were due to non stomatal limitations. In a study with *Quercus* spp. (oak) seedlings and mature trees, the latter exhibited larger leaf mass per unit area (LMA), higher leaf N content and lower maximum stomatal conductance than seedlings. The extent of the difference between growth stages varied among the three species studied (*Q. ilex*, *Q. pyrenaica* and *Q. fraginea*) (Mediavilla and Escudero, 2003). Kruger and Volin (2006) reported that photosynthetic rates were well correlated with plant growth rates. Leaf anatomy was closely related with photosynthetic rate via its effect on light and CO_2 acquisition in C_3 plants (Evans, 1999; Pyankov et al., 1999).

Huang et al. (2003) studied the photosynthetic potential of *in vitro* grown juvenile, adult, and rejuvenated *Sequoia sempervirens* shoots. They found that juvenile and rejuvenated shoots showed higher rates of photosynthesis and respiration, evidenced by faster O_2 evolution and consumption. The photosynthetic rates were associated with more chlorophyll, especially chlorophyll *a*, in the juvenile and the rejuvenated shoots. Nevertheless, the authors suggested that the identical quantum efficiencies of photosystem II indicated that the same photosystems were operating and with equal effectiveness in juvenile, adult, and rejuvenated tissues.

Anatomical variation in juvenile *Eucalyptus* leaves accounts for differences in specific leaf area and CO_2 assimilation rates (Sefton et al., 2002). These authors showed that *E. occidentalis* has two well-defined closely packed, adaxial layers and sometimes a third adaxial layer. In addition a short, loosely packed abaxial palisade layer was usually distinguishable and had a higher assimilation rate in this species as compared to *E. grandis* and *E. camaldulensis* in a comparative study of juvenile leaves of different species (Sefton et al., 2002).

In *Metrosideros*, Sismilich et al. (2003) reported carbon isotope composition ($\delta^{13}C$) and leaf morphology were associated with vegetative phase change. Vegetative phase change occurred in juvenile and rejuvenated plants grown at 24/16 °C, and there was a corresponding increase in leaf $\delta^{13}C$ (from ca. −27% to −23%) in these two groups of plants. The authors suggested that increasing $\delta^{13}C$ in plants undergoing phase change is a result of reduced sink strength in single stem plants, and to a lesser extent within each branch of branched plants, causing reduced stomatal conductance and photosynthesis (Sismilich et al., 2003). In *M. excelsa*, adult foliage displayed lower Rubisco capacity (V_{cmax}) and a reduced rate of maximum electron transport (J_{max}) as compared to juvenile foliage (Kubien et al., 2007).

In woody species, there appears to be an age or ontogeny related influence on the gas exchange parameters. Comparative studies of different growth stages may provide essential information for understanding the strategies adopted by the species at different stages of their life cycle, as well as the selective pressures that operate in each stage (Mediavilla and Escudero, 2003).

1.4.3 Genetic markers

The studies on genes and genetic pathways regulating phase change in perennial species have been very limited due to long lifecycles. A downstream gene involved in the expression of a phase-specific trait has been defined by studying the genes required for anthocyanin production in ivy. Juvenile phase ivy produces anthocyanin under appropriate environmental conditions, whereas adult phase ivy does not. The inability of adult tissue to synthesise anthocyanin results, at least in part, from a lack of

transcription of the gene encoding the enzyme dihydroflavonol reductase (DFR) (Murray et al., 1994).

Carlsbecker et al. (2004) presented a detailed analysis of the activities of three regulatory genes with potential roles in phase transition (from juvenile and non-reproductive to adult reproductive) in Norway spruce: *DAL1*, a MADS-box gene related to the *AGL6* group of genes from angiosperms (deficiens-agamous-like (*DAL*) genes), and the two *LFY*-related genes *PaLFY* and *PaNLY*. *DAL1* activity was initiated in the shoots of juvenile trees at three to five years of age, and then increased with age, whereas both *LFY* genes were active throughout the juvenile phase. Constitutive expression of *DAL1* in transgenic *Arabidopsis* plants caused a dramatic attenuation of both juvenile and adult growth phases with flowers forming immediately after the embryonic phase of development in severely affected plants. These findings implicate a significant role of *DAL1* in phase change.

Even when phase change was characterised at morphological, anatomical, physiological and genetic levels in woody species, the vegetative phases of development were usually defined in terms of reproductive competence of the shoot (Poethig, 1990). Zimmerman et al. (1985) suggested that certain woody plants can be induced to flower in the juvenile phase. This was inconsistent with the idea that vegetative phase change is a prerequisite for floral transition and raised the possibility that these two phenomena, vegetative phase change and flowering time, were actually independent processes whose expression was coordinated by common regulatory factors (Telfer and Poethig, 1998). In a study of leaf heteroblasty and the timing of reproduction in *Eucalyptus*, Wiltshire et al. (1998) demonstrated a separate genetic control of the timing of the transition from juvenile to adult foliage and of the onset of reproduction in the *Eucalyptus risdonii – E. tenuiramis* complex. *Eucalyptus risdonii* reaches reproductive maturity earlier than its progenitor *E. tenuiramis* and begins to flower while still producing juvenile foliage (Wiltshire et al., 1998). Therefore, the control of phase change could involve species-specific plant processes.

1.4.4 Phase change and shoot architecture

Shoot architecture has been used to characterise and distinguish plants of different

ontogenetic states. Wareing and Frydman (1976) reported that the shoot system of trees undergoes several other types of morphological change such as seasonal change in vegetative metamers, as well as those associated with phase change, as the tree grows in size and the branch system increases in complexity. In ivy the attainment of a certain size was a requirement for the attainment of the adult condition and Wareing and Frydman (1976) suggested that the juvenile condition was promoted by and dependent on gibberellins produced in the roots. They again suggested by different experimental results that low gibberellin levels were a necessary but not a sufficient condition for the juvenile to adult transition. However, these classical interpretations assumed that the mechanism that regulates phase change is independent of the environmental conditions that retard or promote shoot growth (Lawson and Poethig, 1995).

More recently, Sismilich et al. (2003) studied the shoot architecture of *M. excelsa* in relation to phase change and described a mathematical model for topological mapping of trifurcating botanical trees. A number of attempts have been made to quantify such differences (Borchert and Tomlinson, 1984; Thornley and Johnson, 1990). Various methods have been used to quantify the architecture of trees exhibiting divaricating branching, in some of which the transition between the juvenile and adult ontogenetic states was marked by an abrupt change in branching pattern (Atkinson, 1992; Kelly, 1994; Day et al., 1997). In *M. excelsa* there were marked architectural differences observed between the juvenile and adult vegetative ontogenetic states of the plant (Clemens et al., 1999; Sreekantan et al., 2001). Sismilich et al. (2003) suggested that the *Metrosideros* model was capable of describing the dynamics of plant growth as expressed by changes in topological parameters over time and contributed the ability to separate the difference of growth in complexity from that of growth in size. Thus, *Metrosideros* shoot architecture studies have revealed the importance of size-complexity during phase change.

As observed above, plant growth and architecture result from the reiteration of modules and can be described as a consequence of the fate of the individual buds (Lovett-Doust, 1989). Individual plant architecture is partly based on genotype but it also has a strong ontogenetic component which reflects the developmental history of each plant (Tomlinson, 1983) and influences several plant functions such as reproduction by

constraining the number of meristems available for flowering (Preston, 1999).

1.4.5 Acceleration of phase change

One of the major obstacles to the breeding of woody plants is the long juvenile phase. The most successful method of shortening the juvenile period in a range of woody species has been to grow seedlings under conditions that encourage rapid growth to achieve the minimum size responsive to flower inductive conditions in the shortest possible time (Wareing and Robinson, 1963; Visser, 1964; Aldwinkle, 1975). In fruit breeding, various practical techniques have been attempted to accelerate the flowering and fruiting of seedlings (e.g. Snowball et al., 1994).

Williams et al. (2004) found that phosphorus fertiliser could induce earlier vegetative phase change in *Eucalyptus nitens*. Of all the treatments used to induce flowering in woody angiosperms, paclobutrazol (PP333, Bonzi®; Uniroyal, Middlebury, C.T., U.S.A.), a triazole, is used most commonly (Meilan, 1997). In a study with PP333, when applied as a collar drench, foliar spray, or trunk injection, PP333 could induce flower bud initiation in *E. globulus* and *E. nitens* trees ranging between 19 months and 17 years of age (Griffin et al., 1993; Hasan and Reid, 1995).

Circumferential girdles (removal of a ring of the bark, down to the phloem, around the entire stem) have been effective in a number of tree species. Wesoly (1985) demonstrated that complete stem girdles induced flowering in *Pinus silvestris* (Scots pine). Wire girdling is another method which involves encircling selected branches or the main stem with steel wire, which is twisted "tightly". The wire is adjusted as the plant grows to avoid killing parts distal to the wire (Meilan, 1997). This technique, also known as cincturing, has been shown to stimulate flowering in conifers (Greenwood and Schmidtling, 1981). Another method of initiating earlier flowering is training shoots to grow horizontally. Longman et al. (1965) demonstrated that it was possible to stimulate flowering by growing apple trees horizontally.

Seedling-grown plants of *M. excelsa* reached an adult reproductive phase within five to ten years, whereas cuttings from adult foliage were capable of flowering within one year and the preferred method of propagation for this species has been through the use of

micro-propagation (Oliphant, 1990). However, because micro-propagation caused a rejuvenation of parent material, an effective method was investigated to accelerate phase change. Clemens et al. (1999) applied shoot and root restriction treatments to accelerate phase change in *M. excelsa*. Shoot restriction was imposed by removing all lateral shoots to give single stem plants. Leaves of single stem plants became progressively mature with increasing node position and developed the downy tomentum on the abaxial surface characteristic of mature leaves, suggesting that accelerating the growth of the main stem during the rapid growth phase shortened the juvenile phase in *M. excelsa* (Clemens et al. 1999).

1.5 Floral transition in herbaceous species

Floral transition is the developmental turning point from the vegetative to the reproductive phase. For plants, the induction of flowering is critical, being the most important part of the life cycle from the standpoint of reproductive strategy and allocation of limited resources (Komeda, 2004). Environmental conditions and developmental regulations control flowering (Mouradov et al., 2002). The control of flowering has been reviewed frequently over the last few years (Levy and Dean, 1998; Simpson et al., 1999; Araki, 2001; Mouradov et al., 2002; Komeda, 2004; Putterill et al., 2004; Blazquez et al., 2006; Corbesier and Coupland, 2006).

1.5.1 Floral transition models

Physiological studies have led to three models for the control of flowering time (reviewed in Bernier, 1988; Thomas and Vince-Prue, 1997). The florigen concept (reviewed in Lang, 1952; Evans, 1971) was based on the transmissibility of substances or signals across grafts between reproductive donor shoots and vegetative recipients. In the second model, the nutrient diversion hypothesis which proposed that inductive treatments resulted in an increase in the amount of assimilates moving to the apical meristem, which in turn induced flowering (Sachs and Hackett, 1983; Bernier, 1988). The third model, the multi-factorial control model, proposed that a number of promoters and inhibitors, including plant hormones and assimilates were involved in controlling the developmental transition (Bernier, 1988).

Genetic analysis of flowering time in pea, cereals and *Arabidopsis* supports the hypothesis of the multi-factorial control model (Koornneef et al., 1998b). Recently in *Arabidopsis* many genes that control flowering time have been discovered. These genes function in 'cascades' within four promotive pathways, the 'photoperiodic', 'autonomous', 'vernalization', and 'gibberellin' pathways, which all converge on the 'integrator' genes *SUPPRESSOR OF OVEREXPRESSION OF CONSTANS 1 (SOC1)* and *FLOWERING LOCUS T (FT)*, which act upstream of the genes involved in floral morphogenesis such as *AP1* and *LFY* (Moon et al., 2003; Takada and Goto, 2003). *Arabidopsis thaliana* has become a key model plant for studies on the regulation of the floral transition by using molecular genetic approaches.

1.5.2 Flower development pathways in *Arabidopsis*

Genetic and physiological analysis of flowering time in *Arabidopsis* has led to the identification of a large number (>80) of flowering-time genes that regulate flowering time in response to environmental and endogenous cues (Simpson et al., 1999). Regulation occurs through a complex network of genetic pathways, with the two main pathways mediating environmental responses: the long day pathway and the vernalization pathway. Two additional pathways function independently of environmental cues: the autonomous pathway, which promotes flowering under all conditions and the gibberellin (GA) pathway, which is needed for flowering under non-inductive short day conditions. These pathways (Figures 1.1 and 1.2) converge in the induction of floral meristem identity genes and the floral transition (Welch et al., 2004; Corbesier and Coupland, 2006).

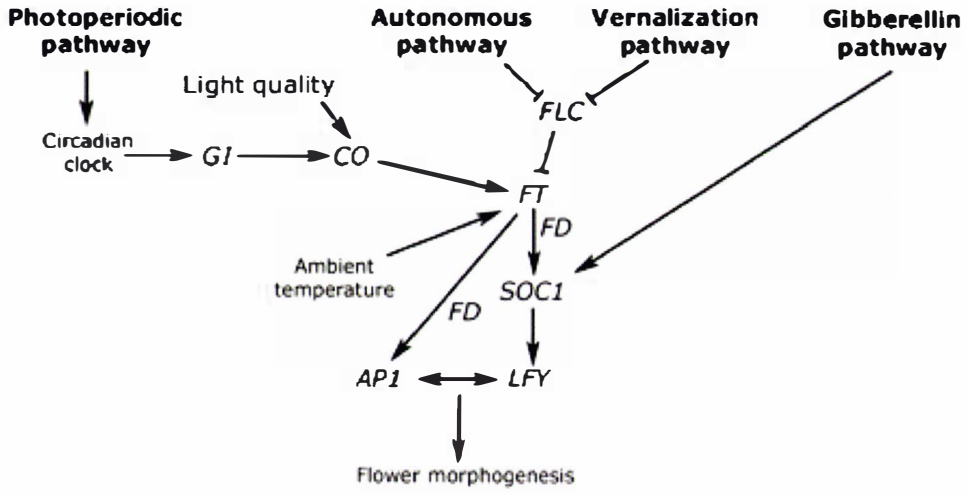

Figure 1.1 Simple model of the four pathways controlling flowering time in *Arabidopsis thaliana* (from Corbesier and Coupland, 2006).

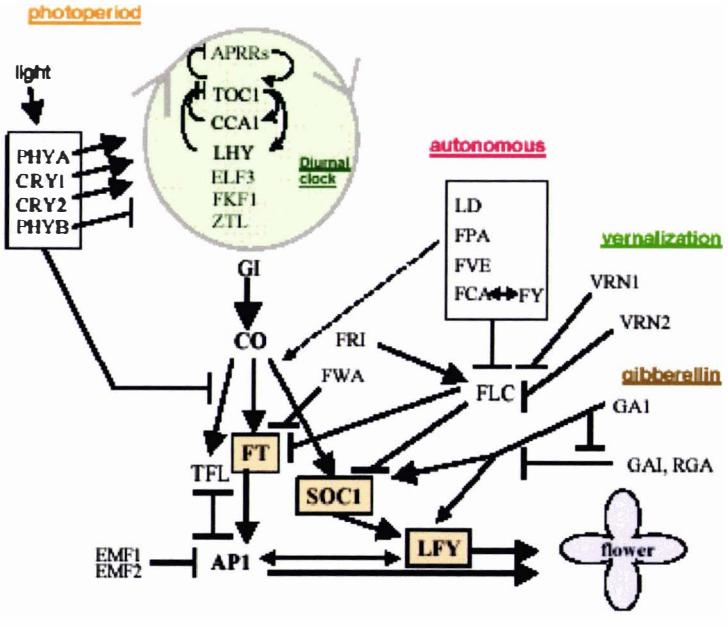

Figure 1.2 Genetic regulatory networks controlling flowering in *Arabidopsis* showing four pathways (from Welch et al., 2004).

1.5.2.1 Photoperiod response pathway

In temperate regions one of the most important factors affecting flowering is the duration of the daily light period or photoperiod. *Arabidopsis* is a facultative long day plant and flowers earlier in long days (Kyozuka, 2002; Mouradov et al., 2002). Photoperiod is perceived by the plant and transduced to a downstream signalling system by the interaction of photoperception mechanisms with the endogenous diurnal clock (Hayama and Coupland, 2003). The products of the five phytochrome genes *PHYTOCHROME A* (*PHYA*) through *PHYTOCHROME E* (*PHYE*) and the two cryptochrome genes *CRYPTOCROME 1* (*CRY1*) and *CRY2* have critical roles in sensing light, and entraining the circadian clock (Putterill et al., 2004; Welch et al., 2004).

There is a negative feedback loop in which *TIMING OF CAB 1* (*TOC 1*) stimulates expression of *LATE ELONGATED HYPOCOTYL* (*LHY*) and *CIRCADIAN CLOCK ASSOCIATED 1* (*CCA1*), which then feed back and repress *TOC1* expression (Alabadi et al., 2001). The details of the *Arabidopsis* circadian clock are reviewed elsewhere (Samach and Coupland, 2000; Devlin, 2002; Eriksson and Millar, 2003). The light and clock regulated expression of the flowering time gene *CONSTANS* (*CO*) is critical to the timing of flowering (Welch et al., 2004). *CO* appears to promote flowering by directly up-regulating the expression of the *FT* and *SOC1* genes (Hayama and Coupland, 2003).

FT and *SOC1* transcript levels are up-regulated in long day, compared to short day conditions, resulting in rapid flowering in long days and delayed flowering in short days (Putterill et al., 2004). *CO* regulates the synthesis or transport of a systemic flowering signal, thereby positioning the signal within the established hierarchy of regulatory proteins that control flowering (An et al., 2004). *CO* is expressed mainly in the leaf, where the CO protein is responsible for sensing the daylength signal (Takada and Goto, 2003; Yanovsky and Kay, 2003), *FT* is then induced in the leaf phloem by *CO* (An et al., 2004).

Recently, Lin et al. (2007) provided some of the strongest evidence to date that FT protein functions as a long-distance florigenic signal, from work performed in cucurbits (squash). The authors used a *Cucurbita moschata* accession responsive to inductive short day photoperiods, along with a potyvirus vector, *Zucchini* yellow mosaic virus, to drive *FT* expression under different daylength growing conditions. They also

performed grafting experiments between un-induced *C. moschata* and flowering *C. maxima*, a day-neutral species. Analysis of vascular tissue and phloem sap from photoperiodically induced and un-induced plants by real-time RT-PCR and mass spectrometry showed that the presence in the phloem of FT-like (FTL) proteins, but not *FTL* mRNA, was highly correlated with the onset of flowering. However, Eckardt (2007) mentioned that Lin et al. (2007) studies do not absolutely rule out a role for *FT* mRNA as part of the long-distance signal within the phloem and suggested that there are three aspects of long-distance transport that could require different signaling components:(1) phloem loading in source tissue, (2) long-distance transport through the phloem, and (3) unloading of the signal from the phloem to sink tissue (or SAM).

King et al. (2006) reported that transmitted signals in the grass *Lolium temulentum* may include gibberellins (GAs) and *FT* gene. Within 2 h of starting a florally inductive long day (LD), expression of GA 20-oxidase increases in the leaf; its product, GA_{20}, then increases 5.7-fold, its substrate GA_{19} decreases equivalently and a bioactive product GA_5 increases 4-fold. The early LD increase in leaf GA_5 biosynthesis coupled with a doubling of the GA_5 content at the shoot apex, King et al. (2006) suggested a substantial evidence for GA_5 as a LD florigen. LD signaling may also involve transport of *FT* mRNA or protein because expression of *LtFT* and *LtCO* increased rapidly, substantially (80-fold for *FT*), and independently of GA. However, because a LD from fluorescent lamps induced *LtFT* expression but not flowering, the nature of the light response of *FT* requires clarification. Thus a link between flowering, LD, and GAs, has been demonstrated (King et al., 2006).

1.5.2.2 The vernalization response pathway

Exposure to low temperature for several weeks will often accelerate flowering. Susceptibility to this treatment can differ markedly between ecotypes of a species (Mouradov et al., 2002). For example, many naturally occurring *Arabidopsis* ecotypes will flower very late if they are not exposed to a vernalization treatment but flower early if exposed to low temperatures for four to eight weeks (Michaels and Amasino, 2000). The genetic control of vernalization was addressed by crossing winter annual varieties that require vernalization with summer annual varieties that do not. These varieties differed at two loci, *FLOWERING LOCUS C* (*FLC*) and *FRIGIDA* (*FRI*), and dominant alleles at these loci in the winter annual are required to confer a vernalization treatment

(Clarke and Dean, 1994). *FLC* encodes a repressor of flowering and high level expression of *FLC* correlates with the vernalization requirement of winter annual varieties (Sheldon et al., 1999; 2000). The product of the *FRI* gene somehow increases *FLC* mRNA abundance. The fact that *FLC* expression is required for *FRI* to delay flowering is supported by the observation that loss-of-function *flc* mutations suppress the effect of *FRI* on flowering time (Mouradov et al., 2002).

Genetic approaches were undertaken to identify genes in the vernalization pathway by screening mutants that remain late flowering after a long cold treatment. *VERNALIZATION1* (*VRN1*) and *VERNALIZATION2* (*VRN2*) were identified in *Arabidopsis*. The study of *vrn1* and *vrn2* mutants has revealed that *FLC* is repressed during vernalization in the same way in these mutants and in wild type (Gendall et al., 2001; Levy et al., 2002). However, the repressed state of *FLC* is not stably maintained in *vrn1* and *vrn2* mutants upon return to warm conditions. Thus *VRN1* and *VRN2* are responsible for the stable maintenance of the vernalized state but not for its initial establishment. Lesions in *VRN2* also affect the chromatin structure of *FLC* (Gendall et al., 2001). The recent identification of *VERNALIZATION INSENSITIVE3* (*VIN3*; Sung and Amasino, 2004) gene provides an answer to the question of how *VRN1* and *VRN2*, rather ubiquitously and constitutively expressed genes, repressed *FLC* only after a *VERNALIZATION* cold treatment. In *vin3* mutants, the repression of *FLC* under extended cold conditions never occurs indicating that *VIN3* is responsible for the initial repression of *FLC* during cold exposure. The extent, if any, to which vernalization mechanisms are conserved among plant species, remains to be determined. Recent work in vernalization-requiring cultivars of wheat indicated that the genetically identified targets of the vernalization pathway in wheat are not related to *FLC* (Yan et al., 2003), but the basic mechanisms that sense the prolonged cold could be conserved (Sung and Amasino, 2004).

1.5.2.3 The autonomous pathway

The autonomous pathway was identified via a group of mutants that are late flowering under all photoperiods and are highly responsive to vernalization. These mutants include *fca*, *fy*, *fpa*, luminidependens (*ld*) and *fve* (Koornneef et al., 1991) and appear to delay flowering by causing increased expression of *FLC*. Although all of the autonomous pathway mutations act by increasing *FLC* expression, genetic evidence

suggested that they may not all act in a simple linear pathway.

FCA encodes a protein with two RNA recognition motifs (RRM domains) (Burd and Dreyfuss, 1994), a WW protein interaction domain (Macknight et al., 1997) and a domain interacting with AtSW13B (Samowski et al., 2002). *FY* is a conserved mRNA 3′ end processing factor that functions with *FCA* (Simpson et al., 2003). *FPA* also encodes an RNA-binding protein (Schomburg et al., 2001) and *LD* encodes a homeodomain protein (Lee et al., 1994b). *FVE* encodes a WD-40 repeat protein similar to human RbAp48, AtMS14, possibly involved in chromatin regulation (Morel et al., 2002). *FCA* and *FVE* function are especially responsive to temperature which may contribute to differential temperature dependent growth rates and flowering time (Welch et al., 2004).

1.5.2.4 The gibberellin (GA) pathway

The growth regulator, GA_3, promotes flowering of *Arabidopsis* under short days when the long day pathway is inactive (Simpson et al., 1999). The impact of GA on flowering and GA signalling is thoroughly reviewed by Olszewski et al. (2002). Under short day conditions, GA activates downstream molecular targets such as the floral meristem identity gene *LFY* through a signalling pathway that is independent of the long day pathway (Blazquez and Weigel, 2000). The *LFY* promoter is induced by long days in *ga1* mutants (Blazquez et al., 1998), but the magnitude of induction is reduced. These observations point to both GA-dependent and -independent effects in the photoperiodic control of *Arabidopsis* flowering. It has been shown previously that the concentration of active GAs increases in plants that are transferred from short to long days, coinciding with bolting (Xu et al., 1997). Further, Blazquez et al. (2002) showed that the GA contribution was not quantitatively important in the determination of flowering time by the photoperiod pathway. Therefore, the increase in GA concentration induced by long days might be relevant for cell expansion required during stem elongation, rather than determination of flowering time in *Arabidopsis*.

1.5.2.5 Integration pathway

The different floral pathways as described above converge into a limited number of downstream regulatory genes (Komeda, 2004). The photoperiod pathway promotes flowering specifically under long days. The transcription of the *GI* and *CO* genes is

regulated by the circadian clock, whereas light quality regulates CO protein abundance. The autonomous pathway negatively regulates the abundance of mRNA of the floral repressor *FLC*. *FLC* mRNA abundance is also repressed by vernalization independently of the autonomous pathway. Finally, gibberellin promotes flowering of *Arabidopsis*, particularly under short days. All four pathways appear to converge on the transcriptional regulation of the floral integrator genes *FT* and *SOC1* which promote expression of *AP1* and *LFY*, genes required to confer floral identity on developing floral primordia (Figure 1.1; Corbesier and Coupland, 2006). *LFY* regulates the transcription of *AP1*, *AP3*, and *AG* and gives floral identity to the shoot apical meristem (SAM). Thus, *LFY* is the switch of the floral development (Bernier, 1988). On the other hand, *FT* is considered to be the key to floral evocation (Kardailsky et al., 1999).

FT has high homology to *TFL1* (Bradley et al., 1997). Mutations in *TFL1* are semi-dominant and cause early flowering with a determinate inflorescence (Alvarez et al., 1992). Thus, *TFL1* codes for a repressor of flowering. The *tfl1* is an interesting mutation because it has mutations in two aspects for flowering: temporal (early flowering), and spatial (terminal-determinate flowering). The *TFL2* gene was initially identified as an enhancer mutation of the *tfl1* mutant (Larsson et al., 1998; Kotake et al., 2003). *TFL2* functions as a negative repressor of *FT* expression. *TFL1* transcription is inhibited by the FMI genes (Komeda, 2004).

The *CO* gene interacts directly with the *FT* gene (Samach et al., 2000), which is in turn regulated by *FLC,* a key of the autonomous and vernalization pathway. Another important gene in the integration pathway is *SOC1* or *AGL20* (Hepworth et al., 2002). *LFY* functions in part downstream of *SOC1* (Lee et al., 2000). The expression of *FT* and *SOC1* is regulated positively by the photoperiod pathway as well as the autonomous pathway acting through *FLC* repression. Also, the vernalization signal increases *SOC1* expression by down-regulation of *FLC* levels (Lee et al., 2000). Further, the gibberellin pathway up-regulates *SOC1* expression (Borner et al., 2000). Thus, *SOC1* and *FT* act as the converging point for all four pathways (Hepworth et al., 2002). A bZIP transcription factor, FD, preferentially expressed in the shoot apex is required for *FT* to promote flowering (Abe et al., 2005). FD and FT are interdependent partners through protein-protein interaction and act at the shoot apex to promote floral transition and to initiate floral development through transcriptional activation of a floral meristem

identity gene, *AP1*. If FT protein represents a long-distance signal, then it will get transported from leaves to interact with FD protein at the shoot apex as observed in *Cucurbits* (Lin et al., 2007).

1.5.3 Meristem identity genes

Meristem identity genes are the final players in the pathway to flowering. The outcome of the decision to flower is governed by the interplay of genes that promote vegetative shoot identity, such as *TFL1* and *TFL2* and those that promote floral identity such as *LFY* and *AP1* in *Arabidopsis* (Blazquez et al., 2001). The main evidence for the involvement of these proteins in the determination of floral identity is based on loss-and gain-of-function studies with corresponding function genes as shown by Blazquez et al. (2006) and similarities between loss-of-function mutants in orthologous genes from different species supports the idea that there is a common mechanism for the establishment of floral meristem identity.

1.5.3.1 *LEAFY*

LFY is a key floral meristem gene and its regulation is critical to the control of flower development. *LFY* is the earliest of the known floral identity genes to be expressed, and directly activates at least one of the later genes, *AP1* (Wagner et al., 1999). In *Arabidopsis*, *LFY* is a homeotic gene, the mutation of which causes inflorescence meristems to arise in the position normally occupied by floral meristems (Weigel et al., 1992). *LFY* promotes the transition from inflorescence to floral meristem largely by activating *AP1* (Mandel and Yanofsky, 1995; Wagner et al., 1999), but subsequently has a central and *AP1*-independent role in controlling floral development (Sablowski, 2007). In one study, Blazquez et al. (2002) used plants carrying fusions of the *LFY* promoter to the GUS marker gene and showed that the *LFY* promoter responded to both the long day and to GA. Further, they demonstrated that a deletion in a putative *myb* transcription factor binding site within the *LFY* promoter prevented activation by GA but not by the long day pathway. Analysis of double mutants and the effects of constitutive *LFY* expression in *fca* mutant background supports the idea of a positive regulation of *LFY* by the autonomous pathway (Page et al., 1999). Therefore, *LFY* is an ultimate target of the four flowering pathways. *LFY* has been shown to bind specific sequences present in the regulatory regions of the homeotic genes *AP1* (Parcy et al.,

1998), *APETALA3* (*AP3*) (Lamb et al., 2002) and *AGAMOUS* (*AG*) (Busch et al., 1999).

LFY homologues have been isolated and studied from several herbaceous plant species. The first *LFY* orthologue isolated was *FLORICAULA (FLO)* from *Antirrhinum*. *FLO* transcripts were abundant in bracts and in the early floral meristem (Coen et al., 1990). In *Arabidopsis*, the highest expression of *LFY* was found in regions of the inflorescence meristem that formed floral meristems and in newly formed floral meristems. However, *LFY* was also expressed at low levels during vegetative development (Weigel et al., 1992). In *Impatiens balsamina*, a *LFY* homologue (*IbLFY*) was identified. It was highly conserved at the sequence level and when expressed ectopically in *Arabidopsis* showed homologous function (Ordidge et al., 2005). RNA *in situ* hybridisation revealed that *IbLFY* was expressed in all meristem states, even in proliferating meristems (Chiurugwi et al., 2007).

In pea, the *LFY* orthologue, *UNIFOLIATA* (*UNI*) was visible at high levels during very early stages of leaf development, which suggests a role for *LFY/FLO* genes in leaf development, at least in legumes (Hofer et al., 1997). In tomato also, a change in leaf phenotype was observed when *FALSIFLORA* (*FALS*) was mutated (Molinero-Rosales et al., 1999). The *FLO/LFY* homologue of rice, *RFL* was expressed in vegetative tissue in the epidermal cells of very young leaves. Kyozuka et al. (1998) considered that *RFL* was required for maintenance of the proliferating branching pattern of the inflorescence. In maize the *FLO/LFY* homologue, *ZFL*, was expressed in vegetative apices but was strongly up-regulated during reproductive development (Bomblies et al., 2003).

Hence, among the meristem identity genes *LFY* gene stands out, because its expression precedes that of other meristem identity genes with flower specific expression. The gradual change in *LFY* expression during the vegetative phase in *Arabidopsis* suggested that the level of *LFY* expression might be an important determinant in flower initiation (Blazquez et al., 1997). The authors also suggested that the *LFY* gene is an important element of the transition from the vegetative to the reproductive phase, as *LFY* is both necessary and sufficient for the initiation of individual flowers. Thus, *LFY* combines properties of flowering time and floral meristem identity genes, indicating that *LFY* is a direct link between the global process of floral induction and the regional events

associated with the initiation of individual flowers and helps to determine the floral character of apices (Blazquez et al., 1997).

1.5.3.2 *APETALA1*

The *AP1* gene in *Arabidopsis* is a MADS-box gene and is important for promoting floral meristem identity. *AP1* is expressed throughout young floral meristems, shortly after the onset of *LFY* expression. However, the expression of *AP1* becomes restricted to the first and second whorls of the flower and to floral pedicels (Blazquez et al., 2006). The loss-of- function mutants of *AP1* produce shoots in place of early arising flowers and exhibit defects in floral meristems of late arising flowers indicating that the transition from inflorescence to floral meristem is not normal (Bowman et al., 1993). In *Antirrhinum,* the transition from inflorescence to flower development involves the action of the *AP1* homologue *SQUAMOSA* (*SQUA*) gene. Flowers in *squa* mutants are replaced by shoots that bear occasional flowers (Huijser et al., 1992).

Carr and Irish (1997) cloned homologues of *AP1* and characterised the expression pattern in *Brassica oleraceae* var *italica* (broccoli) and var *botrytis* (cauliflower). They reported that the *AP1* homologue was expressed in some of the meristems of arrest-stage cauliflower, providing evidence that this tissue is florally determined. In broccoli, both the *AP1* and *AP3* homologues were expressed. However, the spatial pattern of expression of the broccoli *AP1* homologue differed from that of *Arabidopsis.* Interestingly, Murai et al. (2003) suggested that in wheat, the *AP1* homolog (*WAP1*) plays a central role in the phase transition from vegetative to reproductive growth.

Ciannamea et al. (2006) analysed three AP1-like MADS- box proteins (LpMADS1-3) as well as a SHORT VEGETATIVE PHASE (SVP)-like MADS- box protein (LpMADS10) from the monocot perennial grass species *Lolium perenne.* Based on the expression pattern for LpMADS1 and the protein properties the authors suggested that the functional equivalent of *LpMADS1* is the *SOC1* and not the *Arabidopsis AP1* gene.

1.5.3.3 *TERMINAL FLOWER1*

The *TFL1* gene plays an important role in regulating flowering time and in maintaining the fate of the inflorescence meristem (Mimida et al., 2001). In *tfl1* mutants the inflorescences are replaced by flowers, cauline leaves subtend solitary flowers, rather

than shoots and the meristems of the inflorescence shoots are converted into floral meristems and form terminal flowers (Shannon and Meeks-Wagner, 1991) specifying the role of *TFL1* in inflorescence shoot identity. The *tfl1* mutants flower earlier than wild type, indicating a second function of *TFL1* as a repressor of the floral transition. *TFL1* is expressed in a small region at the centre of the inflorescence meristem (Bradley et al., 1997). Plants constitutively expressing *TFL1* have an enlarged rosette and a highly branched inflorescence which eventually produces normal flowers (Ratcliffe et al., 1998). This effect showed that all developmental phases of the shoot apex were being prolonged: vegetative, early inflorescence and late inflorescence, which was opposite to the phenotype of the *tfl1* mutant, where the phase transition occurred faster than in the wild type (Blazquez et al., 2006). It has been proposed that *TFL1* participates in a common mechanism underlying the major developmental transitions at the shoot apex rather than playing two separate roles repressing flowering and specifying shoot identity (Ratcliffe et al., 1998).

In *I. balsamina* 35S:*IbTFL1* plants bolted late and only three of the 14 plants produced flowers suggested that similar to *TFL1*, *IbTFL1* was capable of controlling both the transition from the vegetative to the inflorescence phase and the transition from the inflorescence phase to flowering (Ordidge et al., 2005).

The *TFL1* orthologue in *Antirrhinum, CENTRORADIALIS* (*CEN*), acts only towards inflorescence meristem maintenance. To understand the functions of *TFL1* homologues in pea, Foucher et al. (2003) isolated three *TFL1* homologues, which were designated as *PsTFL1a*, *PsTFL1b* and *PsTFL1c*. They observed that *PsTFL1a* corresponded to the *DETERMINATE* (*DET*) gene and *PsTFL1c* corresponded to the *LATE FLOWERING* (*LF*) gene. Thus different *TFL1* paralogues controlled two distinct aspects of plant development in pea whereas a single gene, *TFL1*, performs both functions in *Arabidopsis*.

TFL1/*CEN* (*RCN1* and *RCN2*)-like genes played important roles in determining plant architecture in rice, mainly by controlling the timing of phase transition (Nakagawa et al., 2002). In perennial rye grass (*Lolium perenne*), Jensen et al. (2001) isolated a *TFL1*-like gene, *LpTFL1*, to investigate the regulation of meristem identity and the control of floral transition for its function in flower development. They found that

LpTFL1 was a repressor of flowering and a controller of axillary meristem identity in rye grass.

To summarise meristem identity genes, Liljegren et al. (1999) highlighted the interactions among *AP1*, *LFY*, and *TFL1* in specifying the meristem fate in *Arabidopsis*. They presented evidence that *AP1* expression in lateral meristems was activated by at least two independent pathways, one of which is regulated by *LFY*. In *lfy* mutants, the onset of *AP1* expression is delayed, indicating that *LFY* is formally a positive regulator of *AP1*. They also found that *AP1*, in turn, can positively regulate *LFY*, because *LFY* is expressed prematurely in the converted floral meristems of plants constitutively expressing *AP1*. Shoot meristems maintain an identity distinct from that of flower meristems, in part through the action of genes such as *TFL1*, which bar *AP1* and *LFY* expression from the inflorescence shoot meristem. The authors showed that this negative regulation can be mutual because *TFL1* expression is down regulated in plants constitutively expressing *AP1*. Therefore, they concluded that the normally sharp floral transition between the production of leaves with associated shoots and formation of the flowers, which occurs upon floral induction, is promoted by positive feedback interactions between *LFY* and *AP1*, together with negative interactions of these two genes with*TFL1* (Liljegren et al.,1999).

1.6 Floral transition in woody perennials

In herbaceous species (annuals), as observed earlier, reproduction is the end of the life cycle, whereas perennials have a longer reproductive life cycle by producing vegetative and reproductive shoots every year, and a number of times in their life cycle. Although there are differences in lifespan, the genetic mechanisms underlying flower induction and floral organ formation appear to be similar among these species (Tan and Swain, 2006). The advances made in *Arabidopsis* genetic studies of floral transition have paved the way for similar investigations in woody species as reviewed below.

1.6.1 Expression patterns of *LEAFY* homologues

Homologues of the floral meristem identity gene *LFY* of *Arabidopsis* and *FLO* of *Antirrhinum* have been isolated and gene expression studies carried out in a number of

different woody species.

Southerton et al. (1998) cloned *ELF1* and *ELF2* from *E. globulus* with sequence homology to the genes *LFY* in *Arabidopsis* and *FLO* from *Antirrhinum*. They reported that *ELF1* was expressed in the developing *Eucalyptus* floral organs in a pattern similar to *LFY* while *ELF2* appeared to be a pseudogene. In *E. globulus*, *LFY* was expressed in young leaves and leaf primordia. However, when compared with floral buds, *LFY* expression was higher in floral tissue than in young vegetative shoots (Southerton et al., 1998). Dornelas et al. (2004) isolated *EgLFY* from *Eucalyptus grandis* and showed that it was preferentially expressed in the developing *Eucalyptus* floral organs in a pattern similar to *Arabidopsis LFY*.

The fragments of the *LFY*-equivalent, *MEL*, isolated from *M. excelsa* exhibited bimodal patterns of expression (Sreekantan et al., 2004). Expression was detected during early floral initiation in autumn, increased during cymule primordia initiation in late autumn and was followed by down-regulation during winter and up-regulation in spring as floral organogenesis occurred. Spatial expression patterns of *MEL* showed that it had greater similarity to *FLO* than to *LFY*, expressing in the apex of the inflorescence, on the cymule primordia, on floral primordia, in sepals and petals, in stamens and in the inner regions of the gynoecium and in anthers and ovules at late developmental stages. Sreekantan et al. (2004) considered that the interaction between *MEL* and *METFL1* was more similar to the interaction between *FLO* and *CEN* than that between *LFY* and *TFL1*. Consequently, Sreekantan et al. (2004) suggested that the three genes (*MEL*, *METFL1*and *MESAP1*) from *M. excelsa* fit a broader herbaceous model encompassing *Antirrhinum* as well as *Arabidopsis*.

The expression pattern of *STLFY* from *Sophora tetraptera* was analysed and a bimodal pattern detected. Expression was first detected in vegetative growth and increased rapidly as the inflorescences developed. Expression reached a peak when the inflorescences developed to their full length, and then decreased during the winter dormant period of the floral buds and increased during spring, co-incident with organogenesis (Song, 2005). In *Clianthus maximus*, no bimodal pattern was observed reflecting the species-specific developmental system (Song, 2005).

Rottmann et al. (2000) isolated the *LFY/FLO* homologue, *PTLF,* from *Populus trichocarpa.* They reported that over expression of the *PTLF* cDNA in *Populus* caused early flowering, albeit, infrequently. *In situ* hybridisation studies revealed that *PTLF* was expressed in the floral meristems and developing male and female flowers.

Partial homologues of *LFY* were isolated by Walton et al. (2001) from *Actinidia deliciosa* (kiwifruit) and showed that *ALF* exhibited a bimodel pattern of annual expression in developing first-order axillary buds and their subsequent shoots. The first period of expression was early in first-order bud development (late spring of the first growing season), when second-order meristems are initiated, and the second, approximately 10 months later, when those meristems differentiate flowers (late spring of the second growing season).

In apple, two homologues of *FLO/LFY*, *AFL1* and *AFL2*, were isolated from floral buds and both showed high homology to the *PTLF* and *PEAFLO* homologue of poplar and pea, respectively (Wada et al., 2002). *ALF1* was expressed only in the floral bud during the transition from vegetative to reproductive growth, whereas *ALF2* was expressed in the vegetative shoot apex, floral buds, floral organs and roots. The two copies of the *LFY* homologues in their genome could be due to complex polyploidy origin (Wada et al., 2002).

In another investigation, the *FLO/LFY* homologue, *VFL*, was isolated in grapevine and expression was reported in lateral meristems that gave rise to inflorescence and flower meristems. Further expression was also observed in other meristematic regions such as the vegetative shoot apical meristem and the lateral meristems that give rise to tendrils suggesting a role for *VFL* not only in flower meristem specification, but also in the maintenance of indeterminacy before the differentiation of derivatives of the apical meristem: flowers, leaves, or tendrils (Carmona et al., 2002).

Esumi et al. (2005) identified *LFY* from six fruit species. Two types of cDNAs for *LFY* homologues were isolated from each maloid species, *PpLFY-1* and *PpLFY-2* for Japanese pear, *PcLFY-1* and *PcLFY-2* for European pear, *CoLFY-1* and *CoLFY-2* for quince, *CsLFY-1* and *CsLFY-2* for Chinese quince, and *EjLFY-1* and *EjLFY-2* for

loquat. The presence of two different *LFY* homologues in maloid plants may reflect the polyploid origin of Maloideae.

Pena et al. (2001) studied acceleration of flowering time, and transformed juvenile *Citrus* seedlings to constitutively express the *Arabidopsis LFY* or *AP1* gene orthologues. The authors reported that both types of transgenic *Citrus* produced fertile flowers and fruits as early as the first year, and observed an appreciable shortening of the juvenile vegetative phase. Furthermore, expression of *AP1* was as efficient as *LFY* in the initiation of flowers, and did not produce any severe developmental abnormality. Flowering in both *AP1* and *LFY* transgenic trees was observed in consecutive years, and their flowering response was under environmental control (Pena et al., 2001).

From *Citrus sinensis*, Lovatt et al. (2004) isolated *CsLFY*. *CsLFY* expression was restricted almost exclusively to reproductive tissues. Ectopic expression studies showed early flowering phenotypes similar to *Arabidopsis LFY* (Lovatt et al., 2004). The authors also suggested that the *C. sinensis* has two easily distinguishable *CsLFY* alleles due to its hybrid origin.

Two *LFY* homologous *NEEDLY* (*NLY*) and *PRFLL* were found in *Pinus radiata*, a gymnosperm. *NLY* was expressed during vegetative development (Mouradov et al., 1998). *PRFLL* was expressed in male cones and not in the females during reproductive development (Mellerowicz et al., 1998).

From these studies, it appears that the function of homologues of *Arabidopsis* floral meristem identity gene *LFY* is conserved in woody perennials. In transgenic lines studied so far, the *LFY* homologues induced early flowering, a feature of interest to those keen to hasten flowering in perennial species. In most diploid plant species, the *LFY* gene exists as single copy, but in complex polyploidy species more than one copy was found. Thus, all *LFY/FLO*-like genes found in angiosperms appear to be orthologues of a single ancestral gene.

1.6.2 Expression patterns of *APETALA1* homologues

Homologues of the floral meristem identity gene *AP1* of *Arabidopsis* and *SQUA* of

Antirrhinum have been isolated and gene expression studies carried out in a number of different woody species.

In *Eucalyptus*, two functional equivalents of *AP1* were cloned and named *EAP1* and *EAP2* (Kyozuka et al., 1997). Both of these genes were expressed to higher levels in flower buds. RNA blot analysis showed that while *EAP1* was expressed at all stages of floral morphogenesis, *EAP2* was expressed more predominantly in young flower buds. Neither gene was expressed at a significant level in leaves, stems or roots (Kyozuka et al., 1997).

Walton et al. (2001) isolated partial homologues of *AP1* from kiwifruit. Expression studies showed that *AAP1* displayed bimodal patterns of annual expression in developing first-order axillary buds and their subsequent shoots consistent with a two-year cycle of axillary bud, flower and fruit development in this perennial woody species. Similarly, in *M. excelsa*, Sreekantan et al. (2004) studied the temporal expression patterns and showed that *MESAP1* exhibited a bimodal pattern of expression showing low levels in autumn, increasing during cymule primordia initiation in late autumn, decreasing during winter, and increasing again during organogenesis in spring. *In situ* hybridisation showed that *MESAP1* was first expressed on the cymule primordia in early developmental stages. Expression was also detected on the subtending bracteoles, mainly concentrated in their axils (Sreekantan et al., 2004).

Elo et al. (1996) cloned three MADS-box genes (*BpMADS3*, *BpMADS4* and *BpMADS5)* from silver birch (*Betula pendula*) homologous to *SQUA* and *AP1*. The *BpMADS3* expression was observed in the early stages of the transition to flowering and during inflorescence development. These three genes when over-expressed in transgenic tobacco caused an early flowering phenotype (Cseke and Podila, 2004).

An *AP1* homologue fragment (*MdAP1*) was isolated from *Malus sylvestris* var *domestica* (Kotoda et al., 2002) and expression studies showed that it was exclusively expressed in sepals and in the flesh of the cortex during fruit development. Another *Malus AP1* homologue, *MdMADS2*, was expressed at all stages of floral development. However, immuno-localisation showed that the MdMADS2 protein was excluded from

the stamen and carpel primordia during the later stages of development (Sung et al., 1999). *MdMADS12* (another *Malus AP1* homologue), was expressed in leaves, vegetative shoots and floral tissues (van der Linden et al., 2002) and these studies revealed that some aspects of *Malus* floral development probably differed from those observed in herbaceous species.

Lovatt et al. (2004) isolated *CsAP1* from *Citrus sinensis*. *CsAP1* expression was restricted almost exclusively to reproductive tissues but also found in the fourth whorl carpel tissue of mature flowers and this was distinct from other plant *AP1* genes. Ectopic expression of *CsAP1* in *Arabidopsis* showed early flowering phenotypes similar to *Arabidopsis AP1* (Lovatt et al., 2004). The authors also suggested that the *C. sinensis* has two easily distinguishable *CsAP1* alleles due to its hybrid origin.

Calonje et al. (2004) studied the early steps of flower initiation and development in *Vitis vinifera* (grapevine), and isolated two MADS-box genes, *VFUL-L* and *VAP1*, the putative *FUL*-like and *AP1* grapevine orthologues and analysed expression patterns during vegetative and reproductive development. Both genes were expressed in lateral meristems that can give rise to either inflorescences or tendrils and no expression was detected in leaves or roots. Both genes were also co-expressed in inflorescence and flower meristems. Expression patterns of *VAP1* suggested that it might have a role in floral transition and flower development (Calonje et al., 2004).

In *Sophora*, no *STAP1* was detected in adult leaves, vegetative and shoot tips. *STAP1* was expressed at lower levels in inflorescences compared to early stage floral buds. Only a very low level was detected in mid-stage flower buds (Song, 2005). Similar observations were recorded for *Clianthus*, except that in mid-stage floral buds high level of *CMAP1* was expressed to a high level (Song, 2005).

Therefore, similar to *LFY/FLO* gene homologues, homologues of *AP1/SQUA* are also important for the initiation of floral development in perennials. *AP1/SQUA* is also strongly expressed in floral meristems, consistent with a direct role in promoting floral fate. There are no *LFY*-related genes in the *Arabidopsis* genome, and the DNA-binding protein encoded by *LFY* is unrelated to other classes of transcription factors (Weigel et al., 1992; Parcy et al., 1998). In contrast, *AP1* belongs to the family of MADS box

genes, many of which encode transcription factors regulating different aspects of flower development (Mandel et al., 1992).

1.6.3 Expression patterns of *TERMINAL FLOWER1* homologues

Homologues of the inflorescence meristem identity gene *TFL1* of *Arabidopsis* and *CEN* of *Antirrhinum* were isolated and gene expression studies carried out in a number of different woody species.

Sreekantan et al. (2004) isolated *METFL1* from *M. excelsa* and showed that this gene was expressed throughout the period of inflorescence development and was expressed in the inflorescence meristem but not in the floral meristems as is also the case for *TFL1* in *Arabidopsis*.

Carmona et al. (2007) showed that the *FT/TFL1* gene family in *Vitis vinifera* was composed of at least five genes. Sequence comparisons with homologous genes identified in other dicot species grouped genes in three major clades, the *FT*, *MFT* and *TFL1* subfamilies, the latter including three of the *Vitis* sequences. Gene expression patterns showed that *VvTFL1A*, *VvTFL1B* and *VvTFL1C* could be associated with vegetative development and maintenance of meristem indeterminancy. Over expression of *VvTFL1A* did not affect flowering time but affected the determination of flower meristems, strongly altering inflorescence structure, which is consistent with the biological roles assigned to similar genes in other species (Carmona et al., 2007).

Two different types of cDNA for *TFL1* homologues were isolated from six maloid species (Esumi et al., 2005). They were *PpTFL1-1* and *PpTFL1-2* for Japanese pear, *PcTFL1-1* and *PcTFL1-2* for European pear, *MdTFL1-1* and *MdTFL1-2* for apple, *CoTFL-1* and *CoTFL1-2* for quince, *CsTFL1-1* and *CsTFL1-2* for Chinese quince and *EjTFL1-1* and *EjTFL1-2* for loquat. Maloid *TFL1* homologues were transcribed mainly in buds and *TFL1-1* and *TFL1-2* were expressed at high levels in buds before floral differentiation and their expression seemed to decrease after floral differentiation (Esumi et al., 2005).

Kotoda and Wada (2005) cloned *MdTFL1* from apple, a gene homologous to *TFL1* of *Arabidopsis*. Expression studies showed that *MdTFL1* mRNA was expressed preferentially in vegetative tissues such as apical buds, stems and roots of seedlings and expression peaked two weeks prior to floral bud differentiation. They suggested that *MdTFL1* was involved in the maintenance of the vegetative phase in apple and that it functions analogously to *TFL1*. Antisense expression of *MdTFL1* reduced the juvenile phase in apple (Kotoda et al., 2006).

A homologue of *TFL1* was isolated from the hybrid perennial tree crop Washington navel orange (*Citrus sinensis*) (*CsTFL*). Ectopic expression of *CsTFL* in wild type *Arabidopsis* plants showed late-flowering phenotypes, similar to the studies with over expression of *Arabidopsis TFL1* (Pillitteri et al., 2004). *CsTFL* transcripts were not detected in adult vegetative tissues but *CsTFL* RNAs were detected in all floral organs. Gene expression studies using real-time PCR showed that juvenility in *Citrus* was positively correlated with *CsTFL* transcript accumulation, and negatively correlated with the RNA levels of the floral regulatory genes, *LFY* and *AP1* (Pillitteri et al., 2004).

Three *TFL1/CEN* like genes were isolated from *Eucalyptus* and these were designated *ETCL1*, *ETCL2*, *ETCL3* (Collins and Campbell, 2001). Two of the genes were over-expressed in *Arabidopsis* and the resultant plants showed many characteristics with the plants that over expressed *Arabidopsis TFL1*. These findings revealed that *ETCL* genes shared functions with *TFL1* and had the ability to delay phase change considerably (Collins and Campbell, 2001).

The *TFL1* studies also suggest that, at least at a fundamental level, flowering genes and presumably, pathways are conserved between herbaceous and perennial species. The regulatory genes *TFL1/CEN* have drawn interest in perennials as this opens the prospect to reduce the prolonged juvenile development, which has been a major obstacle for effective tree breeding purposes.

1.7 Definition of terms

Poethig (1990) defines p*hase change* as the transition between all ontogenetic phases of

development. Subsequently, three primary *phases* of plant development following post-embryonic development have been defined: the *juvenile vegetative phase*, in which the plant is considered incapable of sexual reproduction; the *adult vegetative phase*, in which reproductive competency is established; and the *reproductive phase* in which reproductive structures such as inflorescences and flowers appear (Conway and Poethig, 1993; Greenwood, 1995; Kerstetter and Poethig, 1998). The transition between each of these phases [referred to as *phase change* (Brink, 1962; Poethig, 1990; Jones 1999)] is characterised by species-specific traits, although *maturation* (Wareing, 1959; Greenwood, 1995), and *ontogenetic ageing* (Fontanier and Jonkers, 1976) have also been used. This is different to physiological ageing as described by Wareing (1959), which is often associated with a reduced growth rate or vigour as a result of increasing size and complexity of the plant (Henriod, 2001).

In *E. occidentalis*, reproductive competency has been acquired while the plant is still apparently 'juvenile' and hence the above definitions cannot be readily applied. Consequently, the following definitions have been adopted in this thesis:
Vegetative phase change will refer to the progression from the juvenile to adult vegetative states irrespective of reproductive competency.
Floral transition will refer to the transition from the vegetative to the reproductive state as indicated by molecular and/or morphological markers (evidence of inflorescence development on shoot axes).
Adult/mature will refer to the ontogenetic phases occurring after the juvenile vegetative phase.

1.8 Summary of phase change, floral transition and shoot architecture in *M. excelsa* and *E. occidentalis*

Clemens et al. (1999) studied *M. excelsa* under root and shoot restriction treatments, a feature acknowledged to accelerate phase change. Single stem plants attained a greater number of nodes and greater shoot length as compared to free branching plants. At any particular node, leaves on free branching plants failed to attain the same degree of mature morphology as those from a comparable position in single stem plants. Thus, it could be concluded that vigorous growth tended to accelerate vegetative phase change

in *M. excelsa* (Clemens et al., 1999).

Further, Sismilich (2001) investigated the significance of shoot architecture for phase change by describing quantitative attributes. The theoretical model developed by analysing tree topology, suggested that complexity of crown architecture (rather than size) was critical for both the progress and characterisation of phase change (Sismilich et al., 2003). These studies found that the architectural component of phase change was the key to a plant achieving reproductive competence, with attainment of crown complexity occupying an important role (Clemens et al., 2002). Kubien et al. (2007) explored the differences in gas exchange physiology between juvenile and adult phase leaves and reported that, during vegetative phase change in *M. excelsa*, the control of water loss appears to shift from a physiological to a physical basis, possibly associated with a reallocation of leaf resources away from photosynthesis. It appears that the shoot development undergoes discrete stable developmental phases and that the vegetative phase change is a prerequisite for the reproductive phase change (Henriod, 2001).

Southerton (2002) studied *Eucalyptus occidentalis* for tree breeding purposes. Heterochrony has played a major role in the evolution of the *Eucalyptus* species (Hill and Johnson, 1995; Potts and Wiltshire, 1997). The main modes of heterochrony expressed in the *Eucalyptus* as described by Wiltshire et al. (1998) appear to be: i) *neoteny*, which is the retention of juvenile characteristics into the reproductively mature plant and the opposite process of ii) *acceleration* or iii) *pre-displacement*, which reduce the number of pairs of juvenile leaves, so that adult leaves, or leaves with adult characteristics, are expressed earlier in the ontogeny of descendents (Wiltshire et al., 1998). Further, precocious flowering was observed in *E. occidentalis* when grown in long day conditions (16 h) with first flowering occurring in less than a year (Bolotin, 1975). This precocious flowering phenomenon can be regarded as another heterochronic process, iv) *progenesis* (Wiltshire et al., 1998). Thus in *E. occidentalis,* it appears that due to neoteny, and precocious flowering, regulation of phase change and floral transition are temporally uncoupled.

It appears that the two species, *M. excelsa* and *E. occidentalis*, although from the same family have different growth and development strategies towards phase change and flowering. Although there are differences in shoot morphogenesis, it has been

suggested that the genetic control of the floral transition is conserved across the angiosperms (Tan and Swain, 2006). In this thesis a detailed physiological and molecular study of phase change and floral transition in relation to shoot architecture was carried out in *E. occidentalis*, along with a comparative investigation of *M. excelsa*, to gain insights into the mechanisms that control phase change and flowering processes in woody perennials.

1.9 Aims and objectives

The ultimate aim of this project was to understand the similarities and differences between *M. excelsa* and *E. occidentalis* in relation to phase change and flowering in order to gain access to mechanisms that could potentially accelerate phase change in ornamental New Zealand native species.

In this study, *E. occidentalis* seedlings were grown with two contrasting architectures, so that growth in terms of size (height) and growth in terms of complexity (free branching) could be separated. The rate of phase change was assessed at the morphological and physiological levels, with an aim to determining whether growth as height or growth as complexity is critical to phase change in this species.

Wiltshire et al. (1998), demonstrated that phase change and flowering are temporally uncoupled in *Eucalyptus risdonii*, and this may be the case for *E. occidentalis* as it also exhibits neoteny. Based on the previous studies in *Eucalyptus* species and *M. excelsa*, the following hypotheses were tested in *E. occidentalis*:

1. The rate of phase change is controlled primarily by the complexity of shoot architecture.
2. Phase change and flowering processes in *E. occidentalis* are temporally uncoupled and are under strong genetic control.

To test these hypotheses the provenances of *E. occidentalis* were grown in two architectures (single stem and free branching). The effects of architecture modification on seedlings of *E. occidentalis* were monitored by measuring changes in leaf morphology, shoot phenology, gas exchange characteristics and floral scores in relation to node positions

Pillitteri et al. (2004) monitored the expression of the *Citrus* equivalents of the meristem identity genes *LFY*, *AP1* and *TFL1* using real-time PCR and demonstrated that *CsTFL* transcript accumulation was positively correlated with juvenility whereas *CsLFY* and *CsAP1* were negatively correlated. In view of the published literature, and to improve our understanding of the key genes associated with the floral transition in *E. occidentalis* and *M. excelsa*, the temporal expression patterns of the meristem identity genes, *LFY, AP1, TFL1* were measured in plants grown under different environmental regimes and either as single stem or free branching plants. Relatively higher levels of *TFL1* were expected to reflect a more juvenile and/or vegetative condition, whereas relatively higher levels of *LFY* might reflect a more mature/reproductive condition. Expression of *AP1* was expected only in those tissues committed to flowering.

Chapter 2

Phase change and flowering in *Eucalyptus occidentalis* in relation to shoot architecture: morphological study

2.1 Introduction

The relationship between age or size and reproductive maturation has been investigated in woody species (Longman and Wareing, 1959; Lawson and Poethig, 1995). The practice of growing plants with a single stem, as opposed to allowing plants to branch freely, is suggested to encourage growth to a minimum size required for phase change to occur, since this feature is often inversely related to the length of the juvenile period (Hackett, 1976; 1985). Clemens et al. (1999) suggested that vigorous growth (limiting growth to a single stem) tended to accelerate vegetative phase change in *M. excelsa.* However, in a subsequent study of *M. excelsa,* an architectural component of phase change was found to be the key to a plant achieving reproductive competence, with attainment of crown complexity occupying an important role (Sismilch et al., 2003).

Wiltshire et al. (1998) demonstrated that the control of vegetative phase change is a genetically independent process from floral transition in *Eucalyptus risdonii*, and this may be the case for *E. occidentalis* as it also exhibits neoteny. Precocious flowering has been reported in *E. occidentalis* (Bolotin, 1975). The present study was conducted with *E. occidentalis*, to investigate the effect of shoot architecture, as growth as height (single stem architecture) or growth in terms of complexity (free branching architecture), on phase change and flowering. Six ecotypes were included in this study to investigate whether there were ecotypic differences in phase change in response to shoot architecture. Typically, *Eucalyptus* displays changes in leaf morphology from broader juvenile phase leaves to lanceolate leaves in the adult phase (James and Bell, 2001), a pattern also exhibited in *E. occidentalis* (Chippendale, 1973) (Figure 2.1A and B). These changes were monitored by recording morphological attributes of the leaf, including area, perimeter, length, width, length/width ratio, roundness and petiole length, at different ontogenetic stages. This morphological characterisation of phase

change in different ecotypes of *E. occidentalis* grown with two architectures could provide insights into the effect of shoot architecture on the phase change process. Observations on flowering could reveal whether there is a relationship between phase change and floral transition (flowering) of this model plant, which could lead to further understanding of the integration of developmental and evolutionary approaches of shoot and floral phenology. In the present investigation, the hypotheses tested were that the rate of phase change is controlled primarily by the complexity of shoot architecture, and that phase change and flowering processes in *E. occidentalis* are temporally uncoupled and are under strong genetic control.

2.2 Materials and Methods

2.2.1 Plant material

Seeds of six ecotypes (13648, 15416, 15395, 13644, 13636, and 13634) of *Eucalyptus occidentalis* of known provenance were obtained from the Australian Tree Seed Centre, CSIRO, Australia (Table 2.1). It is understood that each seedlot was made up from seeds collected from several trees within the each population.

Table 2.1 *Eucalyptus occidentalis* provenances used in this study.

Seedlot No.	Locality	latitude (S)	longitude (E)
13634	Broomehill	34° 02′	117° 38′
13636	Porongurup	34° 41′	117° 54′
13644	Thomas River	33° 48′	123° 00′
13648	Peak Charles	35° 121′	121° 10′
15395	Dumbleyung Lake	33° 20′	117° 40′
15416	Truslove	33° 20′	121° 43′

Several of these ecotypes had been used for preliminary work on precocious flowering for tree breeding purposes in Australia (Simon Southerton, personal communication). Seeds were germinated at room temperature, and seedlings transferred to small pots and finally to 10 l pots. The potting medium consisted of a mixture of peat and pumice (80:20 v/v) supplemented with a controlled release fertiliser (4.0 g l^{-1} of 8 to 9 month

release Osmocote Plus, Grace Sierra, Heerlen, The Netherlands). Between 4-25 replicate plants for each treatment were grown from April 2003 to June 2004 in a greenhouse at the Massey University Plant Growth Unit, Palmerston North, New Zealand. For temperature moderation the greenhouse was set to vent at 25 °C, and warmed when the temperature fell below 20 °C to give mean day/night temperature of 27 °C/18 °C, under ambient conditions of daylength. The plants from the six ecotypes were subjected to two architectural treatments: pruned to obtain single stem architecture by removing the axillary buds from the time the plants were 300 mm tall, and not pruned at all to obtain a free branching architecture (Figure 2.1C and D). During flowering, care was taken to retain floral buds on single stem plants while maintaining the single stem architecture.

2.2.2 Leaf morphology

When the plants were grown to over 60 nodes (April 2004), fully expanded leaves were collected from the main stem at nodes 10, 20, 30, 40, 50 and 60 for characterisation of morphological features. Nodes were numbered on the main axis of single stem as well as free branching plants. Data were collected from four to eight replicate plants of each ecotype. The leaf images were captured by photocopying. The photocopied images were digitised (JPEG format) by scanning. The leaf morphology attributes, leaf area (cm^2) perimeter (cm), roundness (4π perimeter^2/leaf area), length (cm) and maximum width (cm), length/width ratio and petiole length (cm) (Henriod, 2001) were measured using Image Pro® PLUS software (version 4.5.0.19, Media Cybernetics, Silver Spring, M.D., U.S.A.).

2.2.3 Flowering

Total number of plants with floral buds was recorded during January 2004 when the plants were nine months old. At this stage, floral buds were identifiable visually with the naked eye in leaf axils, on the main stem and on branches.

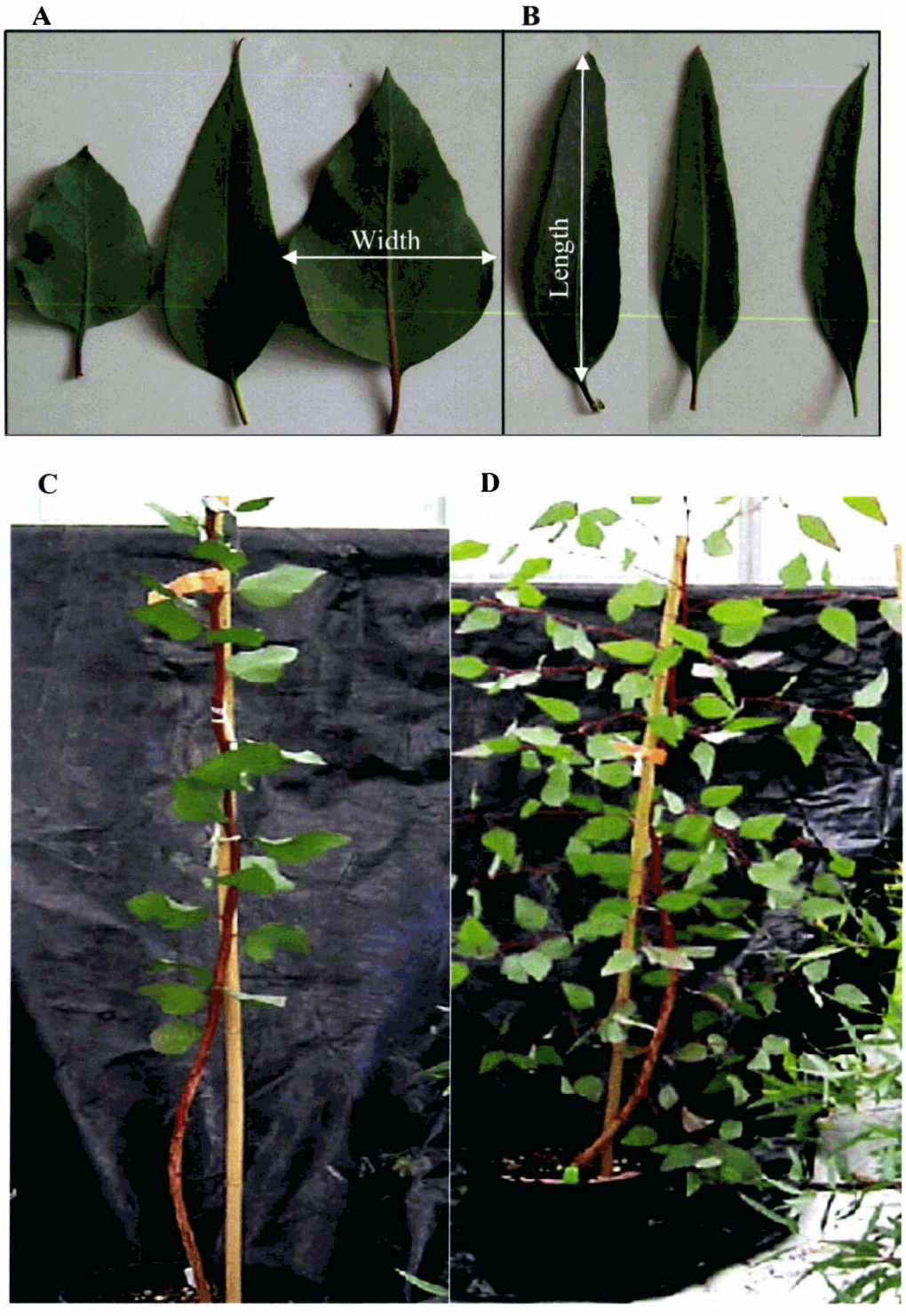

Figure 2.1 Typical *Eucalyptus occidentalis* juvenile (A) and adult leaves (B). *E. occidentalis* ecotype 15416 grown in single stem (C) and free branching (D) architecture in a greenhouse under conditions specified in Section 2.2.1.

2.2.4 Statistical analysis

Three-way repeated measures ANOVA was performed to determine the significance of main effects (ecotype, architecture, and node position) and their interactions on measured leaf morphology attributes (leaf area, leaf perimeter, leaf length, leaf maximum width, length/width ratio, leaf roundness and petiole length). For ANOVA analysis, six levels of ecotype (13648, 15416, 15395, 13644, 13636, and 13634), two levels of architecture (single stem and free branching) and six levels of node position (10, 20, 30, 40, 50, and 60) were used. Wherever the main effects and their interaction were found to be significant, pair-wise comparison between means and their significance was determined by Tukey's test. Computations were carried-out using SAS (SAS Institute, Cary, N.C., U.S.A.) program. To test for global differences in leaf morphology attributes between the ecotypes grown with different architectures, the spatial ordination of leaf morphological data was performed using canonical discriminant analysis. For spatial ordination analysis, six ecotypes were used as classes, measured leaf attributes as seven variables and a total of 468 observations (including six node positions) were used to demonstrate the ecotypic differences. Further, spatial ordination was also performed using 12 classes (six ecotypes × two architectures), measured leaf attributes as seven variables and a total of 468 observations to demonstrate the effect of architecture within the ecotypes.

2.3 Results

2.3.1 Leaf morphology

Three-way ANOVA with repeated measures was performed for leaf morphology attributes and the p-values were recorded in Appendix 1 (Table 1). The main effects ecotype, node, and architecture were significant ($p<0.0001$) for all the parameters analysed. Significant three-way interactions between ecotype, node, and architecture were observed for leaf area, perimeter, width ($p<0.05$), and a highly significant ($p<0.0003$) interaction for length/width. The mean values obtained for various morphological attributes are depicted in Tables 2.2 to 2.8. In general, the leaf morphological changes due to ontogeny as a marker of phase

Table 2.2 Morphological attribute: leaf area (cm^2) measured in six ecotypes of *E. occidentalis* at nodes 10, 20, 30, 40, 50 and 60 on the main stem of free branching and single stem plants.

Node	Ecotype 15416		Ecotype 13648		Ecotype 15395		Ecotype 13644		Ecotype 13636		Ecotype 13634	
	F.B	S.S	F.B	S.S	F.B	S.S	F.B	S.S	F.B	S.S	F.B	S.S
10	$21.8\pm2.8^{a,1}$	$32.6\pm3.7^{a,1}$	$4.8\pm0.7^{a,1}$	$22.3\pm2.9^{a,1}$	$29.3\pm2.0^{a,1}$	$31.1\pm4.8^{a,1}$	$43.6\pm4.8^{a,1}$	$58.0\pm0.9^{a,1}$	$38.5\pm5.5^{a,1}$	$28.8\pm6.2^{a,1}$	$31.4\pm3.0^{a,1}$	$31.3\pm2.0^{a,1}$
20	$31.7\pm4.0^{a,1}$	$47.2\pm5.7^{a,1}$	$13.7\pm2.6^{a,1}$	$27.3\pm3.9^{a,1}$	$21.9\pm2.1^{a,1}$	$53.6\pm8.8^{a,2}$	$25.5\pm5.2^{a,1}$	$75.5\pm9.6^{a,2}$	$44.5\pm5.3^{a,1}$	$54.0\pm7.5^{a,1}$	$32.8\pm2.9^{a,1}$	$51.6\pm4.2^{a,2}$
30	$27.7\pm2.1^{a,1}$	$56.8\pm5.5^{b,2}$	$9.9\pm1.5^{a,1}$	$26.3\pm1.5^{a,1}$	$19.1\pm1.1^{a,1}$	$62.0\pm4.6^{b,2}$	$24.0\pm1.3^{a,1}$	$58.7\pm6.1^{a,2}$	$27.5\pm2.3^{a,1}$	$59.5\pm4.5^{a,2}$	$23.8\pm2.9^{a,1}$	$58.6\pm4.2^{b,2}$
40	$23.4\pm1.4^{a,1}$	$64.5\pm9.5^{b,2}$	$10.6\pm2.7^{a,1}$	$20.6\pm2.2^{a,1}$	$21.9\pm1.4^{a,1}$	$56.4\pm8.1^{a,2}$	$25.4\pm3.3^{a,1}$	$80.8\pm7.8^{a,2}$	$27.0\pm3.8^{a,1}$	$60.8\pm6.4^{a,2}$	$24.0\pm1.6^{a,1}$	$55.0\pm5.9^{b,2}$
50	$25.3\pm2.9^{a,1}$	$45.0\pm4.2^{a,1}$	$5.8\pm1.1^{a,1}$	$20.4\pm2.2^{a,1}$	$24.8\pm3.7^{a,1}$	$60.7\pm4.7^{b,2}$	$22.9\pm3.6^{a,1}$	$82.4\pm14^{a,2}$	$26.6\pm1.7^{a,1}$	$57.5\pm4.8^{a,2}$	$19.8\pm1.5^{a,1}$	$46.5\pm7.1^{a,2}$
60	$24.6\pm3.6^{a,1}$	$41.0\pm6.4^{a,1}$	$7.5\pm1.1^{a,1}$	$19.5\pm2.9^{a,1}$	$23.2\pm2.2^{a,1}$	$45.8\pm6.2^{a,1}$	$19.7\pm2.2^{a,1}$	$56.1\pm8.8^{a,2}$	$14.6\pm2.4^{a,1}$	$41.4\pm6.2^{a,1}$	$14.5\pm2.0^{a,1}$	$33.6\pm2.8^{a,1}$

F.B: free branching; S.S: single stem. Values represent mean of four to eight replicates (±S.E.). Same alphabet superscripts indicate no significant ($p<0.05$) difference within each column. The comparisons were also made between architectures (between the respective columns) at the corresponding node position, different number superscripts indicate significant difference ($p<0.05$).

Table 2.3 Morphological attribute: leaf perimeter (cm) measured in six ecotypes of *E. occidentalis* at nodes 10, 20, 30, 40, 50 and 60 on the main stem of free branching and single stem plants.

Node	Ecotype 15416		Ecotype 13648		Ecotype 15395		Ecotype 13644		Ecotype 13636		Ecotype 13634	
	F.B	S. S	F.B	S.S	F.B	S.S	F.B	S.S	F.B	S.S	F.B	S.S
10	$18.0\pm1.1^{a,1}$	$21.9\pm1.3^{a,1}$	$10.4\pm1.0^{a,1}$	$21.1\pm1.9^{a,2}$	$20.8\pm0.7^{a,1}$	$21.4\pm1.9^{a,1}$	$24.2\pm1.4^{a,1}$	$29.2\pm0.1^{a,1}$	$23.4\pm2.3^{a,1}$	$19.9\pm2.0^{a,1}$	$21.7\pm1.0^{a,1}$	$21.7\pm0.7^{a,1}$
20	$21.5\pm1.3^{a,1}$	$26.7\pm1.6^{a,1}$	$17.3\pm1.6^{a,1}$	$23.9\pm1.7^{a,1}$	$18.4\pm1.2^{a,1}$	$27.6\pm2.1^{a,1}$	$19.6\pm2.1^{a,1}$	$34.5\pm2.8^{a,2}$	$25.5\pm1.4^{a,1}$	$27.9\pm2.0^{a,1}$	$22.4\pm1.1^{a,1}$	$28.8\pm1.4^{a,1}$
30	$20.6\pm0.9^{a,1}$	$30.3\pm1.5^{b,2}$	$16.3\pm1.3^{a,1}$	$24.4\pm1.1^{a,1}$	$17.4\pm0.5^{a,1}$	$30.6\pm1.0^{a,2}$	$19.7\pm1.4^{a,1}$	$31.1\pm2.0^{a,2}$	$20.8\pm0.7^{a,1}$	$30.3\pm0.9^{a,1}$	$21.0\pm0.9^{a,1}$	$31.0\pm1.2^{b,2}$
40	$19.6\pm0.9^{a,1}$	$31.3\pm2.7^{b,2}$	$17.2\pm1.0^{a,1}$	$22.9\pm1.2^{a,1}$	$20.2\pm0.8^{a,1}$	$28.5\pm1.7^{a,1}$	$22.1\pm2.7^{a,1}$	$37.7\pm1.4^{a,2}$	$22.6\pm2.0^{a,1}$	$30.6\pm1.6^{a,1}$	$22.8\pm0.7^{a,1}$	$29.8\pm1.9^{a,1}$
50	$21.5\pm1.6^{a,1}$	$26.1\pm1.5^{a,1}$	$14.3\pm1.0^{a,1}$	$22.7\pm1.0^{a,1}$	$22.6\pm1.6^{a,1}$	$30.6\pm1.4^{a,1}$	$21.7\pm2.1^{a,1}$	$40.9\pm4.4^{a,2}$	$25.2\pm1.0^{a,1}$	$32.5\pm1.5^{b,1}$	$22.5\pm0.9^{a,1}$	$28.7\pm2.5^{a,1}$
60	$21.0\pm1.7^{a,1}$	$26.9\pm2.3^{a,1}$	$14.5\pm0.7^{a,1}$	$21.1\pm1.2^{a,1}$	$22.3\pm0.7^{a,1}$	$27.3\pm2.0^{a,1}$	$19.9\pm0.1^{a,1}$	$35.0\pm3.6^{a,2}$	$19.2\pm2.0^{a,1}$	$27.3\pm2.5^{a,1}$	$18.7\pm0.8^{a,1}$	$27.3\pm0.7^{a,2}$

F.B: free branching; S.S: single stem. Values represent mean of four to eight replicates (±S.E.). Same alphabet superscripts indicate no significant ($p<0.05$) difference within each column. The comparisons were also made between architectures (between the respective columns) at the corresponding node position, different number superscripts indicate significant difference ($p<0.05$).

Table 2.4 Morphological attribute leaf roundness measured in six ecotypes of *E. occidentalis* at nodes 10, 20, 30, 40, 50 and 60 on the main stem of free branching and single stem plants.

Node	Ecotype 15416		Ecotype 13648		Ecotype 15395		Ecotype 13644		Ecotype 13636		Ecotype 13634	
	F.B	S.S	F.B	S.S	F.B	S.S	F.B	S.S	F.B	S.S	F.B	S.S
10	1.21±0.0	1.19±0.0	1.88±0.2	1.60±0.1	1.18±0.0	1.20±0.0	1.18±0.0	1.17±0.0	1.2±0.1	1.16±0.0	1.21±0.0	1.21±0.0
20	1.19±0.2	1.21±0.0	1.88±0.2	1.70±0.1	1.23±0.1	1.18±0.0	1.23±0.1	1.26±0.0	1.2±0.0	1.19±0.0	1.23±0.0	1.29±0.1
30	1.23±0.0	1.31±0.0	2.20±0.2	1.80±0.1	1.26±0.0	1.22±0.1	1.29±0.1	1.32±0.0	1.3±0.1	1.25±0.1	1.55±0.1	1.33±0.0
40	1.31±0.1	1.24±0.0	2.60±0.3	2.18±0.3	1.5±0.1	1.19±0.0	1.53±0.2	1.43±0.1	1.5±0.2	1.25±0.0	1.75±0.1	1.31±0.1
50	1.48±0.1	1.23±0.1	3.10±0.3	2.20±0.2	1.68±0.1	1.24±0.0	1.67±0.1	1.65±0.1	1.9±0.1	1.49±0.1	2.06±0.1	1.56±0.1
60	1.50±0.1	1.49±0.1	2.40±0.3	1.98±0.2	1.74±0.1	1.33±0.0	1.65±0.2	1.83±0.3	2.1±0.2	1.49±0.1	2.05±0.1	1.85±0.2

F.B: free branching; S.S: single stem. Values represent mean of four to eight replicates (±S.E.).

Table 2.5 Morphological attribute leaf length (cm) measured in six ecotypes of *E. occidentalis* at nodes 10, 20, 30, 40, 50 and 60 on the main stem of free branching and single stem plants.

Node	Ecotype 15416		Ecotype 13648		Ecotype 15395		Ecotype 13644		Ecotype 13636		Ecotype 13634	
	F.B	S.S	F.B	S.S	F.B	S.S	F.B	S.S	F.B	S.S	F.B	S.S
10	6.7±0.3	7.9±0.5	4.7±0.5	9.4±0.9	7.5±0.3	7.8±0.8	8.9±0.3	10.4±0.3	8.3±1.0	6.9±0.58	8.0±0.3	8.0±0.2
20	7.8±0.5	9.8±0.7	7.71±0.8	10.8±0.8	6.9±0.5	9.9±0.7	7.0±0.8	13.0±1.3	9.3±0.6	10.0±0.8	8.4±0.4	10.6±0.7
30	7.6±0.4	11.7±0.7	7.6±0.6	11.0±0.5	6.9±0.3	11.1±0.3	7.6±0.9	12.3±1.0	8.6±0.3	11.1±0.5	8.8±0.4	11.7±0.6
40	7.9±0.4	12.3±1.2	8.1±0.4	10.4±0.6	8.6±0.4	10.5±0.4	9.4±1.3	15.4±0.6	9.9±1.1	12.1±0.7	10.1±0.3	11.4±0.7
50	9.1±0.7	10.2±0.8	6.8±0.5	10.5±0.5	9.9±0.8	11.8±0.7	9.6±0.9	17.6±2.3	11.6±0.5	13.8±0.8	10.3±0.4	12.0±1.0
60	8.9±0.8	11.1±1.1	6.7±0.3	9.6±0.6	9.8±0.3	11.1±0.8	8.7±0.1	15.0±2.1	8.8±1.0	11.6±1.3	8.4±0.3	11.9±0.5

F.B: free branching; S.S: single stem. Values represent mean of four to eight replicates (±S.E.).

Table 2.6 Morphological attribute leaf maximum width measured in six ecotypes of *E. occidentalis* at nodes 10, 20, 30, 40, 50 and 60 on the main stem of free branching and single stem plants.

Node	Ecotype 15416		Ecotype 13648		Ecotype 15395		Ecotype 13644		Ecotype 13636		Ecotype 13634	
	F.B	S.S	F.B	S.S	F.B	S.S	F.B	S.S	F.B	S.S	F.B	S.S
10	$4.75\pm0.4^{a,1}$	$6.21\pm0.3^{a,1}$	$1.56\pm0.1^{a,1}$	$3.55\pm0.2^{a,1}$	$5.87\pm0.3^{a,1}$	$5.81\pm0.5^{a,1}$	$7.28\pm0.6^{a,1}$	$8.03\pm0.3^{a,1}$	$6.62\pm0.5^{a,1}$	$5.56\pm0.7^{a,1}$	$5.70\pm0.3^{a,1}$	$5.74\pm0.2^{a,1}$
20	$6.02\pm0.4^{a,1}$	$7.34\pm0.4^{a,1}$	$2.62\pm0.3^{a,1}$	$3.73\pm0.2^{a,1}$	$4.97\pm0.2^{a,1}$	$7.74\pm0.7^{a,2}$	$5.43\pm0.6^{a,1}$	$8.99\pm0.3^{a,2}$	$7.05\pm0.4^{a,1}$	$7.8\pm0.6^{a,1}$	$5.90\pm0.4^{a,1}$	$7.71\pm0.3^{a,1}$
30	$5.69\pm0.3^{a,1}$	$7.62\pm0.3^{a,1}$	$2.03\pm0.2^{a,1}$	$3.79\pm0.2^{a,1}$	$4.51\pm0.1^{a,1}$	$8.19\pm0.6^{b,2}$	$5.10\pm0.2^{a,1}$	$7.58\pm0.4^{a,1}$	$4.84\pm0.2^{a,1}$	$8.24\pm0.4^{a,2}$	$4.48\pm0.3^{a,1}$	$7.85\pm0.3^{b,2}$
40	$4.67\pm0.2^{a,1}$	$7.84\pm0.6^{a,2}$	$1.96\pm0.4^{a,1}$	$3.25\pm0.3^{a,1}$	$4.35\pm0.2^{a,1}$	$7.81\pm0.7^{a,2}$	$4.52\pm0.1^{a,1}$	$8.37\pm0.5^{a,2}$	$4.22\pm0.3^{a,1}$	$7.5\pm0.5^{a,2}$	$4.00\pm0.2^{a,1}$	$7.31\pm0.5^{a,2}$
50	$4.47\pm0.3^{a,1}$	$6.47\pm0.4^{a,1}$	$1.35\pm0.2^{a,1}$	$3.14\pm0.3^{a,1}$	$4.08\pm0.3^{a,1}$	$7.70\pm0.4^{a,2}$	$3.83\pm0.4^{b,1}$	$7.58\pm0.5^{a,2}$	$3.66\pm0.2^{a,1}$	$6.74\pm0.5^{a,2}$	$3.16\pm0.2^{b,1}$	$5.91\pm0.6^{a,2}$
60	$4.30\pm0.3^{a,1}$	$5.86\pm0.6^{a,1}$	$1.71\pm0.2^{a,1}$	$3.12\pm0.3^{a,1}$	$4.06\pm0.2^{a,1}$	$6.12\pm0.5^{a,1}$	$3.60\pm0.3^{b,1}$	$6.21\pm0.8^{a,1}$	$2.71\pm0.2^{b,1}$	$5.42\pm0.4^{a,2}$	$2.95\pm0.3^{b,1}$	$4.83\pm0.9^{a,1}$

F.B: free branching; S.S: single stem. Values represent mean of four to eight replicates (±S.E.). Same alphabet superscripts indicate no significant ($p<0.05$) difference within each column. The comparisons were also made between architectures (between the respective columns) at the corresponding node position, different number superscripts indicate significant difference ($p<0.05$).

Table 2.7 Morphological attribute leaf length/width ratio measured in six ecotypes of *E. occidentalis* at nodes 10, 20, 30, 40, 50 and 60 on the main stem of free branching and single stem plants.

Node	Ecotype 15416		Ecotype 13648		Ecotype 15395		Ecotype 13644		Ecotype 13636		Ecotype 13634	
	F.B	S.S	F.B	S.S	F.B	S.S	F.B	S.S	F.B	S.S	F.B	S.S
10	$1.43\pm0.1^{a,1}$	$1.26\pm0.0^{a,1}$	$3.13\pm0.5^{a,1}$	$2.62\pm0.1^{a,1}$	$1.28\pm0.0^{a,1}$	$1.34\pm0.1^{a,1}$	$1.20\pm0.1^{a,1}$	$1.31\pm0.1^{a,1}$	$1.25\pm0.1^{a,1}$	$1.29\pm0.1^{a,1}$	$1.42\pm0.0^{a,1}$	$1.4\pm0.0^{a,1}$
20	$1.29\pm0.0^{a,1}$	$1.33\pm0.1^{a,1}$	$3.11\pm0.4^{a,1}$	$2.89\pm0.1^{a,1}$	$1.38\pm0.1^{a,2}$	$1.29\pm0.0^{a,1}$	$1.31\pm0.2^{a,1}$	$1.44\pm0.1^{a,1}$	$1.30\pm0.1^{a,1}$	$1.30\pm0.1^{a,1}$	$1.46\pm0.1^{a,1}$	$1.37\pm0.1^{a,1}$
30	$1.33\pm0.1^{a,1}$	$1.53\pm0.1^{a,1}$	$3.83\pm0.3^{a,1}$	$2.94\pm0.2^{a,1}$	$1.52\pm0.1^{a,2}$	$1.39\pm0.1^{a,1}$	$1.52\pm0.3^{a,1}$	$1.63\pm0.1^{a,1}$	$1.80\pm0.1^{a,1}$	$1.36\pm0.1^{a,1}$	$2.03\pm0.2^{a,1}$	$1.51\pm0.1^{a,1}$
40	$1.68\pm0.1^{a,1}$	$1.54\pm0.1^{a,1}$	$4.74\pm0.6^{b,1}$	$3.48\pm0.5^{a,1}$	$1.99\pm0.1^{a,2}$	$1.38\pm0.1^{a,1}$	$2.07\pm0.3^{a,1}$	$1.85\pm0.1^{a,1}$	$2.39\pm0.3^{a,1}$	$1.64\pm0.1^{a,1}$	$2.60\pm0.2^{a,1}$	$1.58\pm0.1^{a,1}$
50	$2.03\pm0.1^{a,1}$	$1.58\pm0.1^{a,1}$	$5.42\pm0.5^{b,1}$	$3.63\pm0.4^{a,2}$	$2.43\pm0.1^{a,2}$	$1.51\pm0.1^{a,1}$	$2.50\pm0.0^{a,1}$	$2.32\pm0.3^{a,1}$	$3.23\pm0.2^{a,1}$	$2.14\pm0.3^{a,1}$	$3.34\pm0.2^{b,1}$	$2.18\pm0.2^{a,1}$
60	$2.09\pm0.1^{a,1}$	$1.99\pm0.3^{a,1}$	$4.24\pm0.5^{a,1}$	$3.26\pm0.4^{a,1}$	$2.42\pm0.1^{a,1}$	$1.81\pm0.1^{a,1}$	$2.49\pm0.2^{a,1}$	$2.57\pm0.5^{a,1}$	$3.31\pm0.4^{a,1}$	$2.19\pm0.3^{a,1}$	$3.06\pm0.3^{b,1}$	$2.61\pm0.3^{a,1}$

F.B: free branching; S.S: single stem. Values represent mean of four to eight replicates (±S.E.). Same alphabet superscripts indicate no significant ($p<0.05$) difference within each column. The comparisons were also made between architectures (between the respective columns) at the corresponding node position, different number superscripts indicate significant difference ($p<0.05$).

Table 2.8 Morphological attribute petiole length (cm) measured in six ecotypes of *E. occidentalis* at nodes 10, 20, 30, 40, 50 and 60 on the main stem of free branching and single stem plants.

Node	Ecotype 15416		Ecotype 13648		Ecotype 15395		Ecotype 13644		Ecotype 13636		Ecotype 13634	
	F.B	S.S	F.B	S.S	F.B	S.S	F.B	S.S	F.B	S.S	F.B	S.S
10	.20±0.1	1.72±0.2	0.90±0.1	1.64±0.1	1.63±0.1	.52±0.3	1.13±0.2	1.67±0.1	1.5±0.2	1.28±0.1	1.55±0.2	1.58±0.2
20	1.72±0.1	2.02±0.2	1.31±0.2	1.84±0.1	1.48±0.2	1.69±0.3	1.23±0.1	2.29±0.2	2.16±0.1	1.99±0.1	1.95±0.1	2.07±0.2
30	1.77±0.1	2.35±0.1	1.44±0.1	1.96±0.2	1.85±0.2	1.94±0.1	1.34±0.1	2.37±0.2	2.3±0.1	2.12±0.1	2.21±0.2	2.63±0.1
40	2.06±0.1	2.42±0.1	1.75±0.2	2.17±0.1	2.08±0.1	2.32±0.1	1.87±0.1	2.81±0.2	2.56±0.1	2.92±0.4	2.75±0.2	2.61±0.3
50	2.2±0.2	2.64±0.3	1.35±0.1	2.15±0.2	2.32±0.1	2.32±0.2	2.25±0.1	2.93±0.2	2.68±0.2	3.01±0.2	2.55±0.1	3.04±0.2
60	2.27±0.1	2.48±0.3	1.61±0.1	1.99±0.2	2.54±0.0	2.39±0.1	2.14±0.0	2.71±0.2	2.25±0.3	2.66±0.2	2.46±0.1	2.86±0.2

F.B: free branching; S.S: single stem. Values represent mean of four to eight replicates (±S.E.).

change in terms of leaf length/maximum width ratio (Table 2.7) were more pronounced in free branching architecture plants than in single stem plants.

However, the significant three-way interaction arose because ecotypes 13644 and 15416 did not display such differences with respect to the architecture treatment (Figure 2.2). Highest ontogeny related leaf morphological change was recorded by ecotype 13648 grown with free branching architecture; the mean values increasing significantly ($p<0.05$) with increase in node number from 3.13 ± 0.5 at node 10 to 5.42 ± 0.5 at 50 (Figure 2.2 panel D). In contrast ecotype 15416 (free branching plants) recorded non-significant increases in length/maximum width ratio with increasing node number from 1.43 ± 0.1 at node 10 to 2.03 ± 0.1 at 50 (Figure 2.2, panel F). Other ecotypes recorded intermediate values (Table 2.7). Highly significant ($p<0.001$) three-way interactions were also found for leaf area and perimeter (Appendix 1, Table 1; Tables 2.2, 2.3).

In contrast, the three-way interaction between ecotype × architecture × node was found to be non-significant ($p > 0.05$) for leaf roundness (Table 2.4), leaf length (Table 2.5) and petiole length (Table 2.8). However, the two-way interactions between ecotype × architecture; ecotype × node and architecture × node were found to be significant for roundness (Figure 2.3A-C). The interaction between ecotype and node showed that the ecotype 13648 stood out from the rest of the ecotypes, consistent with the observation for length/maximum width ratio (Figure 2.3A). The interaction between architecture and node (Figure 2.3B) showed that the leaves of free branching plants started to attain narrow morphology with increasing node number. Leaves of ecotype 13648 were significantly less round in free branching than single stem plants (Figure 2.3C).

Petiole length displayed significant main effects due to ecotype, architecture and node. However, the three-way interaction was non-significant. The two-way interaction chart (Figure 2.4) showed that the single stem plant leaves had longer petioles than their free branching counterparts, but that the effect was more marked in some ecotypes than others (e.g. 13644 and 13648) (Figure 2.4; Table 2.8).

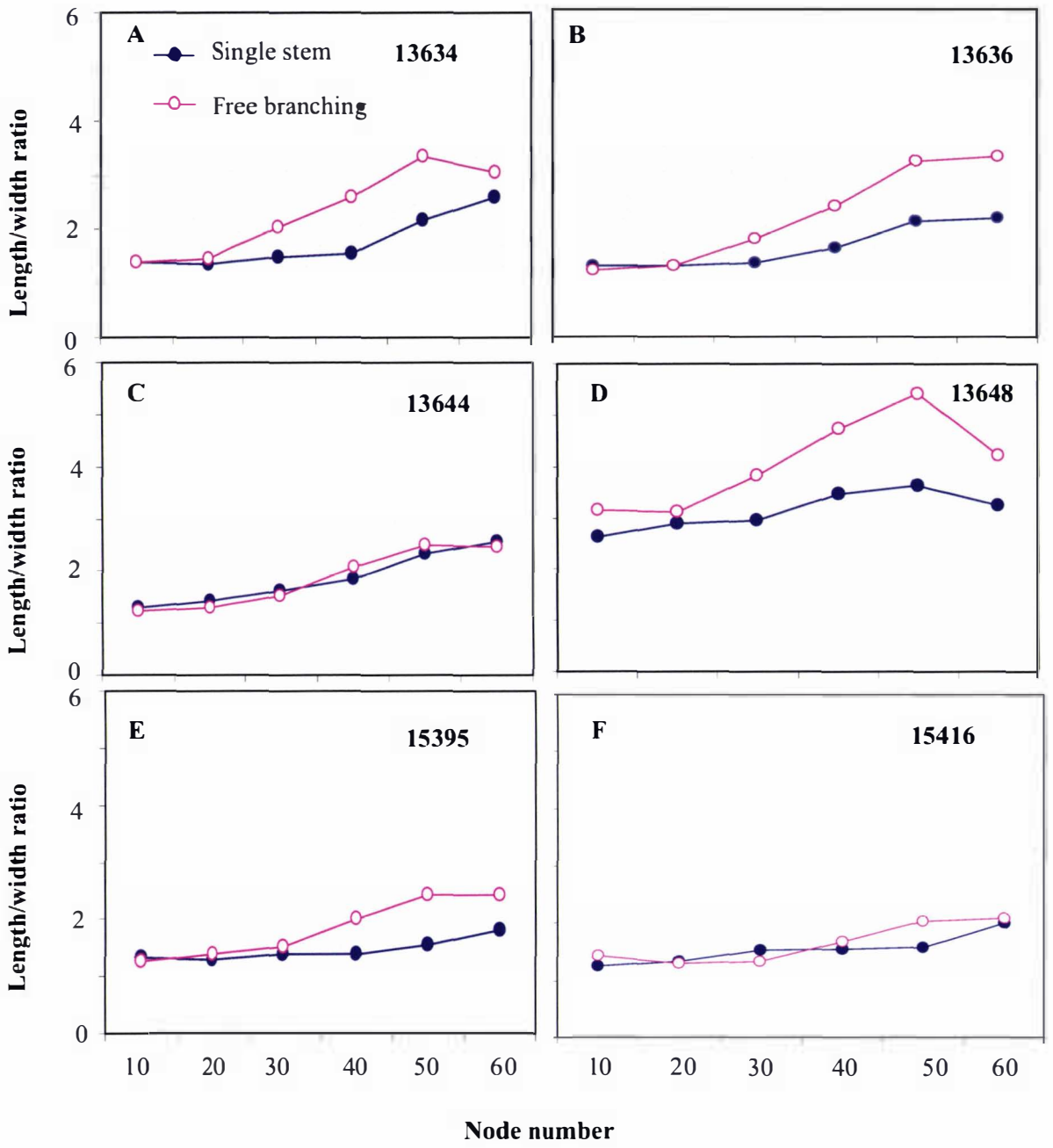

Figure 2.2 Leaf length to maximum width ratio differences between ecotypes of *E. occidentalis* (shown in panels) from node 10 to 60 and their respective architectures (single stem, single stem plants; free branching, free branching plants). Each value represents a mean of four to eight replicates.
Note: Standard errors associated with each of the data points are shown in the Table 2.7.

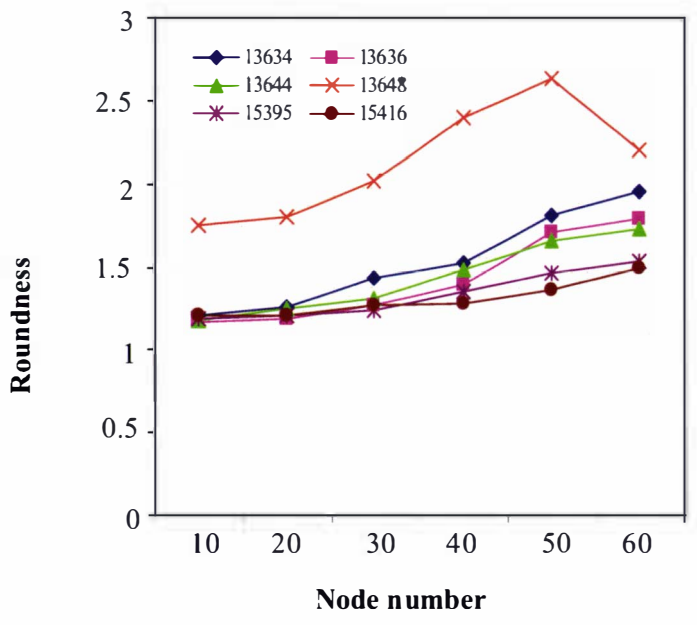

Figure 2.3A Two-way interaction between ecotype and node number for the variable leaf roundness in *E. occidentalis*. Ecotypes identity was shown in the legend to the corresponding number.

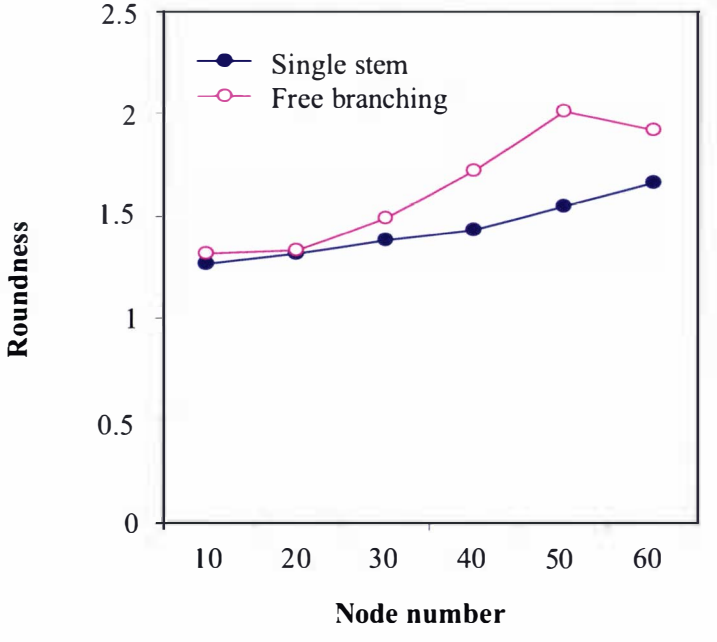

Figure 2.3B Two-way interaction between architecture and node number for the variable leaf roundness of single stem and free branching plants in *E. occidentalis*.

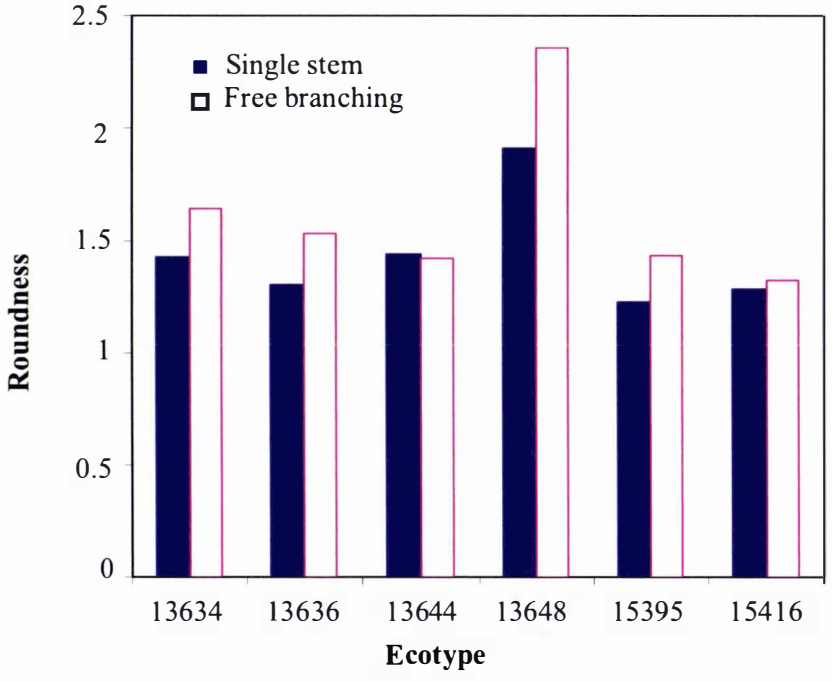

Figure 2.3C Two-way interaction between ecotype and architecture for the variable leaf roundness of single stem and free branching plants in *E. occidentalis*.

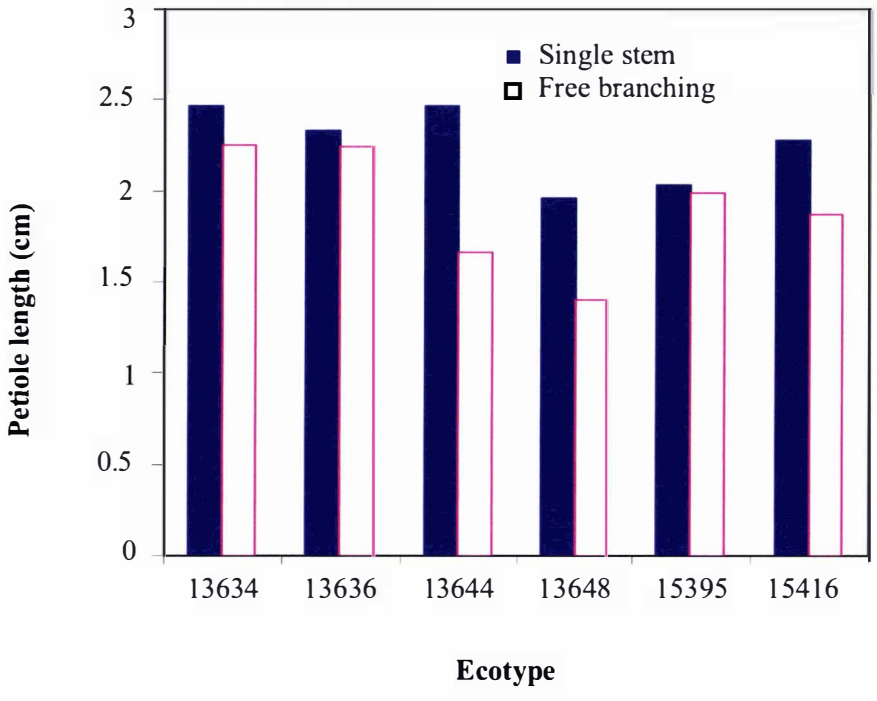

Figure.2.4 Two-way interaction between ecotype and architecture, for the variable petiole length of single stem and free branching plants in *E. occidentalis*.

Canonical discriminant analysis was used to determine the ordinations of leaf morphology attributes, integrating the results for the seven leaf parameters. The gradual change in leaf morphology was depicted clearly by ecotype 13648 grown with free branching architecture. As shown in Figure 2.5 and 2.6, the leaves of ecotype 13648 grown with free branching architecture were positioned away in the ordination hyperspace from the ecotypes displaying lesser changes in leaf morphology (e.g. 15416). This ordination separation lent support to the three-way ANOVA analysis (Appendix 1, Table1).

Based on canonical discriminant analyses (Appendix 2) of all the leaf morphological parameters (seven variables) of the six ecotypes (six classes), ecotype 13648 showed greater squared Mahalanobis distance from the rest of the ecotypes. For example, the distance recorded for ecotype 13648 from the nearest neighbour ecotype (13644) was 36.22. By contrast, the distance of ecotype 13648 from the farthest ecotype (15416) was 64.21. These observed squared Mahalanobis distances to ecotypes were highly significant ($P<0.001$) for 13648, 13644 and 13634. Ecotypes 13636, 15395 and 15416 showed only significant ($p<0.05$) distances. The distance between 15395 and 15416 ecotypes was not significant. The raw canonical coefficients for the first canonical variable (Can1) showed that the classes differed most widely on the linear combination of the centred variables, 0.05 × leaf area -2.50 × length/width ratio -0.21 × perimeter + 0.43 × length + 0.72 × width + 0.95 × petiole + 3.42 × roundness. The proportion of variation explained by the first factor (Can1) was 85% and the second factor (Can 2) a further 7.5% (Figure 2.5). The variables length/width ratio and roundness were the most important in making distinction of ecotype 13648 from the rest of the ecotypes.

Based on canonical discriminant analyses (Appendix 3) of all the leaf morphological parameters (seven variables) of the six ecotypes and the two architectures (12 classes), ecotype 13648 with free branching architecture showed greater squared Mahalanobis distance compared to the rest of the classes. For example, from 13648 of free branching architecture, the distance recorded to the corresponding ecotype with single stem architecture was 37.37. By contrast, the distance between the two architectures was 6.83 for ecotype 13636. However, these observed distances between the architectures were significant for every ecotype ($P<0.001$). The raw canonical coefficients for the first canonical variable Can1 showed that the classes differed most widely on the linear

combination of the centred variables -0.98 × leaf area -1.28 × length/width ratio + 0.14 × length + 0.61 × width + 0.43 × petiole + 0.49 × roundness + 0.83 × perimeter. The proportion of variation explained by the first factor was 66% and the second factor a further 19% (Figure 2.6). The variables length/width ratio and perimeter were the most important in making distinction of the free branching architecture of ecotype 13648 from its single stem counter part and from the rest of the ecotypes.

2.3.2 Flowering

At the end of nine months from sowing (January 2004) inflorescence buds started appearing on the plants. The observations recorded during January 2004 were shown as percentage plants showing flowers (Figure 2.7). The numbers of plants showing floral buds were always greater in free branching plants than in the single stem counterpart of the same ecotype, except for ecotype 15395, which showed no flowering in plants of either architecture. Ecotype 15416 showed minimal flowering (Figure 2.7).

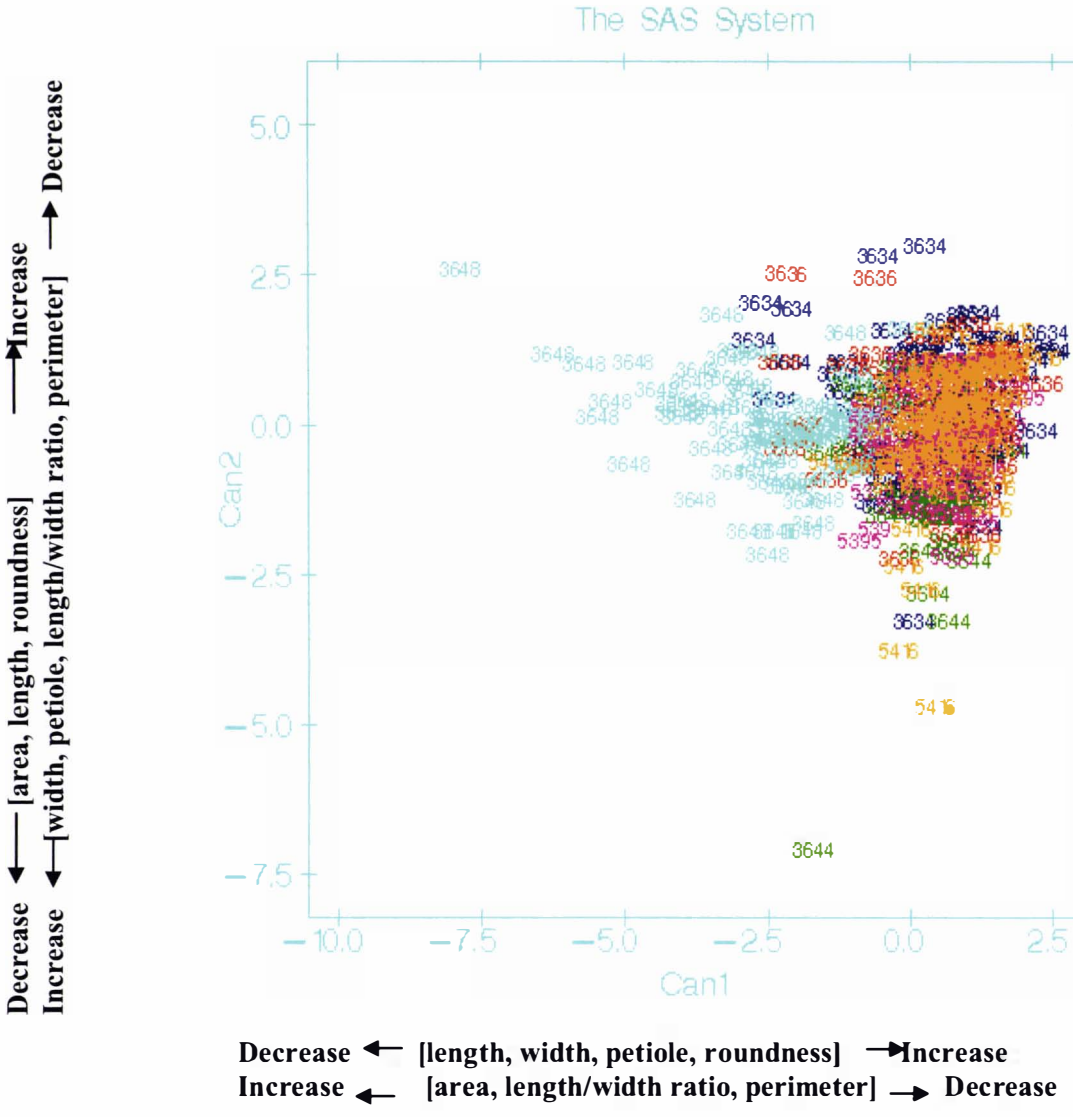

Figure 2.5 Axes Can1 and Can2 of canonical ordinations of morphological data of *E. occidentalis*. Each number represents morphological data ordination for corresponding ecotype (less first common digit).

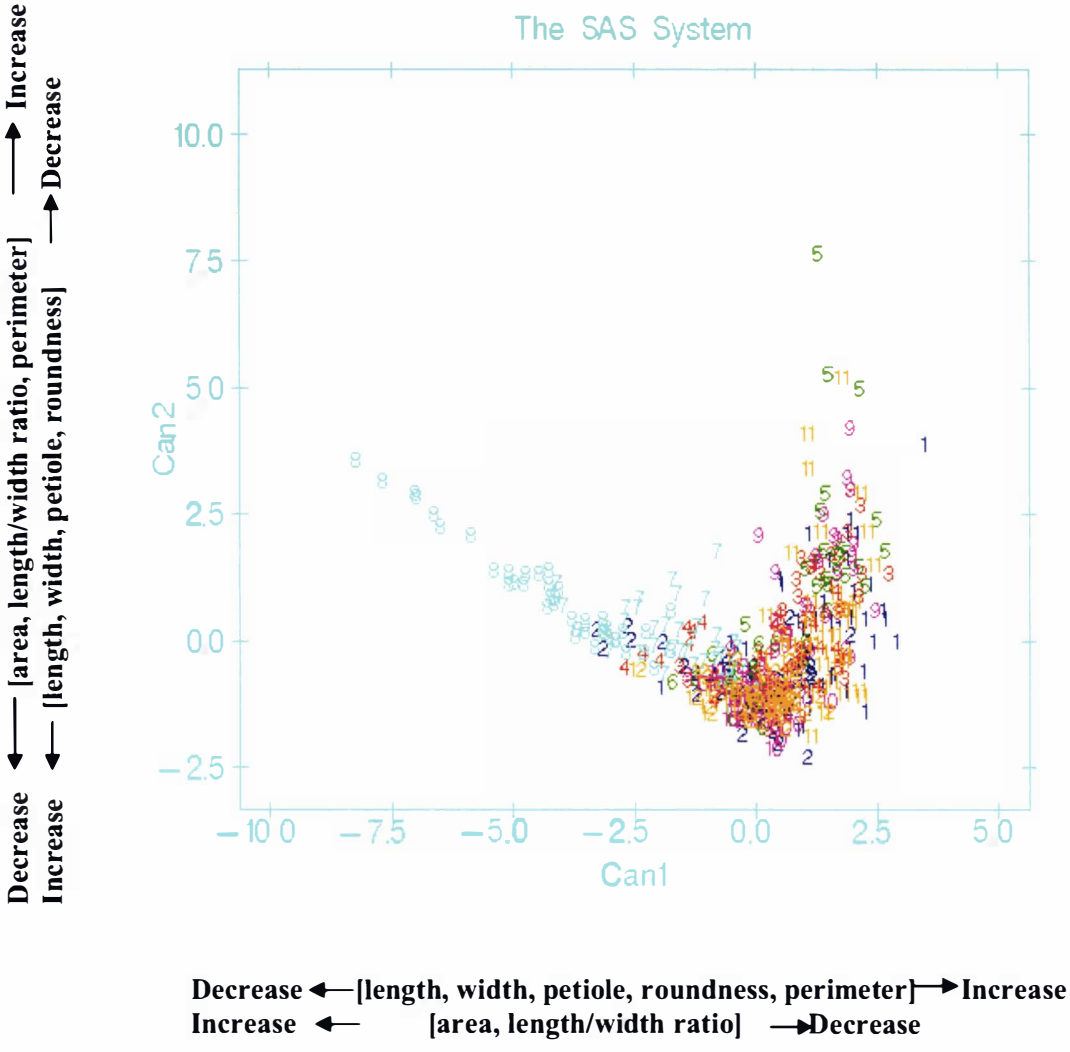

Figure 2.6 Axes Can1 and Can2 of canonical ordinations of morphological data of architecture and ecotype treatments of *E. occidentalis*. Each number represents an ecotype and architecture combination according to, (respectively, single stem and free branching): 1, 2 (13634); 3, 4 (13636); 5, 6 (13644); 7, 8 (13648); 9, 10 (15395); 11, 12 (15416).

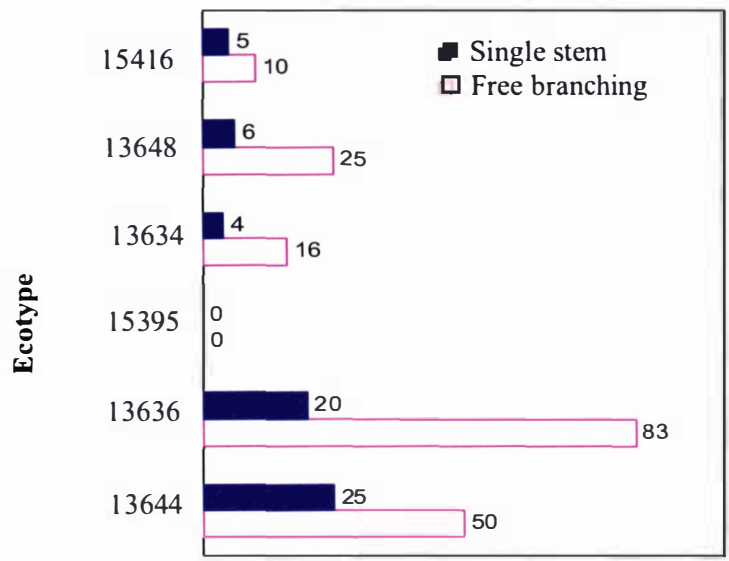

Figure 2.7 Percentage of plants shown at each bar of six ecotypes of *E. occidentalis* that initiated flower buds nine months after sowing when grown with either free branching or single stem architecture.

2.4 Discussion

Leaf morphological attributes were used as a marker of vegetative phase change, and floral bud score was used as a marker of floral transition in six ecotypes of *E. occidentalis*, an early-flowering *Eucalyptus* species from Western Australia.

In *E. occidentalis*, the juvenile leaves are elliptical and ovate in shape and sometimes have undulated margins, whereas the adult leaves are lanceolate and sometimes falcate (Chippendale 1973). To evaluate leaf maturation during shoot development, changes in the leaf length/maximum width ratio and roundness were highly indicative of maturation as the length/width ratio increased as the leaves become more narrow (lanceolate). Similarly, the roundness value increased from close to 1 (full circle) to a higher value indicating a reduction in roundness (leaf narrowing). The rate of vegetative phase change was ecotype specific. For example, ecotype 13648 displayed more rapid leaf morphological changes compared to the rest of the ecotypes tested, producing lanceolate leaves at node 50 on the main stem of free branching plants indicative of this ecotype attaining early maturation.

In an investigation involving two provenances of *Eucalyptus globulus* ssp. *globulus* (Tasmanian and Wilson Promontory), James and Bell (2001) reported that the Wilson Promontory provenance showed a faster transition from juvenile to a transitional phase as compared to the Tasmanian provenance. The Wilson Promontory plants showed adult leaves at node 53. They recorded length/width ratio of 5.57 ± 0.022 in adult leaves of the Tasmanian provenance and 5.28 ± 0.15 in Wilson Promontory leaves as a morphological marker of phase change. Similarly, in this thesis, compared to other ecotypes, ecotype 13648 reached an adult-like stage more rapidly and at node 50 the length/width ratio recorded was 5.42 ± 0.5. This observation indicates that within a species there could be large genetic differences among provenances in the timing of vegetative phase change. Similar observations were recorded in *E. globulus* (Jordan et al., 2000) and *E. nitens* (Dutkowski et al., 2001). Hence phase change is under strong genetic control as differences in the rate of phase change were observed between different provenances when grown under identical conditions.

To demonstrate global differences in phase change pattern due to ecotype and architecture, canonical discriminant analyses were applied to the leaf morphology data. Similar lateral branch removal treatments have previously been shown to accelerate vegetative phase change in woody plants (e.g. Wareing and Frydman, 1976; Clemens et al., 1999). This spatial ordination of canonical discriminant analyses with 12 classes (six ecotypes × two architectures) showed that ecotype 13648 in free branching architecture expressed differences and separated from the rest of the ecotypes and architectures. This was due to rapid progression of this treatment group towards maturation, attaining lanceolate leaf morphology. Such maturation was not observed in the respective single stem counterparts in which acceleration of growth was obtained by removing the axillary buds. This indicates that acceleration of growth in terms of height, by attaining more nodes on a single stem did not promote faster maturation of leaves or phase change in *E. occidentalis*. By contrast, in *Citrus,* acceleration of phase change was observed as a result of increasing growth rate (higher node number) in single stem plants (Snowball et al., 1994). Clemens et al. (1999) also reported that accelerating the growth of the main stem as single stem during the rapid growth phase shortened the juvenile phase in *M. excelsa*.

In the current study, when shoot architecture was modified to produce single stem plants in *E. occidentalis,* vegetative phase change was delayed. The observed delay in the vegetative phase change of the single stem plants of ecotype 13648 plants was not due to any difference in developmental stage or ontogenetic stage as compared to their free branching counterparts. The single stem plants attained a greater number of nodes (to about 80) than the free branching plants (65) on the main stem, at the end of the experiment. Hence, it may be concluded that the architectural modification interfered with the rate of the phase change process. The single stem plants grew taller, but complexity of the crown architecture could have played a more important role than the size (height) of the plants as the free branching plants started to show maturation earlier. This supports the hypothesis that the rate of phase change is controlled primarily by the complexity of shoot architecture.

To initiate floral buds most woody species must first undergo vegetative phase change to attain maturity. This process normally takes several years (Hackett, 1985).

However, some species, such as *E. occidentalis*, are capable of spontaneous precocious flowering (Bolotin, 1975). In this investigation, to determine the effect of accelerating shoot maturity on flowering behaviour, *E. occidentalis* was grown with two architectures (single stem and free branching). At the end of nine months, floral buds started appearing in most of the plants. The percentage of plants starting to flower was higher in free branching plants as compared to their single stem counterparts. Ecotypes that did not display marked phase change characteristics in terms of leaf morphology attributes also flowered, thus expressing neoteny, that is, displaying juvenile leaves while exhibiting reproductive maturity (Figure 2.7). This observation indicates that vegetative phase change is not necessary in order to undergo floral transition.

In the case of ecotype free branching 13648 which showed significant phase change in leaf morphology related characteristics, plants (25%) showed flower buds on their axillary nodes (ranging from position 38 to 47) of the main stem. On the other hand, ecotype 15416 grown with free branching architecture, which displayed lesser leaf morphological changes associated with phase change, showed flowering in fewer plants (10%). No flowering was observed in ecotype 15395 grown with either architecture. Ecotype 13648 showed 6% flowering in single stem plants. Thus, the architectural modification, in spite of causing a delay in vegetative phase change in terms of attaining adult leaf traits in ecotype 13648, did not prevent flowering. Ecotype 15416 had shown relatively less vegetative phase change for leaf morphology attributes, started to display flowering in both architectures. In another investigation using *Eucalyptus risdonii – E. tenuiramis* complex, Wiltshire et al. (1998) demonstrated separate genetic control of the timing of the transition from juvenile to adult foliage and of the onset of flowering. The observations reported in this Chapter further support the hypothesis that the vegetative phase change and floral transition are temporally uncoupled in *E. occidentalis* and these two developmental processes appear to be under separate genetic control.

Chapter 3

Phase change in *Eucalyptus occidentalis* in relation to shoot architecture: physiological study

3.1 Introduction

The morphological studies in Chapter 2 of this thesis revealed that *Eucalyptus occidentalis* ecotype 13648 grown with a free branching architecture attained adult-like shoot phenology earlier compared to the other ecotypes irrespective of architectures. However, it was observed that complexity of shoot architecture had a significant effect on vegetative phase change. In order to analyse phase change in more detail this investigation was extended to measurements of net photosynthesis, leaf anatomy, leaf mass per unit area, and leaf mineral concentration with a view to obtaining additional information to reliably characterise phase change in *E. occidentalis*. Two ecotypes were chosen that had shown contrasting differences (Chapter 2) in leaf morphological attributes as phase change progressed. It was intended to test the hypothesis that the rate of phase change is controlled primarily by the complexity of shoot architecture in *E. occidentalis*. To establish that the differences were not limited by nutrient supply, especially nitrogen, half of the plants were supplied with supplementary fertiliser.

3.2 Materials and Methods

3.2.1 Plant material and treatments

Plants of *Eucalyptus occidentalis* were grown from April 2003 to June 2004 as described in Section 2.2.1. Plants were randomly selected from seedling populations of ecotypes 13648 and 15416 grown with free branching and single stem architectures. These ecotypes had displayed significant differences with respect to several leaf morphological attributes in relation to phase change (Section 2.3.1).

Gas exchange measurements and leaf anatomy observations were carried out starting on 25 January 2004 in 12 plants (2 ecotypes × 2 architectures × 3 plants). Further, gas exchange, leaf mass per unit area, and mineral concentration analyses were carried out in extended treatments [2 ecotypes × 2 architectures × 2 supplementary fertiliser treatments (+/– F) × 4 plants] starting on 18 March 2004. The treatments are shown in Figure 3.1.

To obtain the extended supplementary fertiliser treatments, half of the plants were supplied with a soluble fertiliser (+ F) (N: P: K - 20:4.4:16.6) at the rate of 2.25 g per pot twice a week for 3 weeks. The other half of the plants were not given supplementary fertiliser (– F).

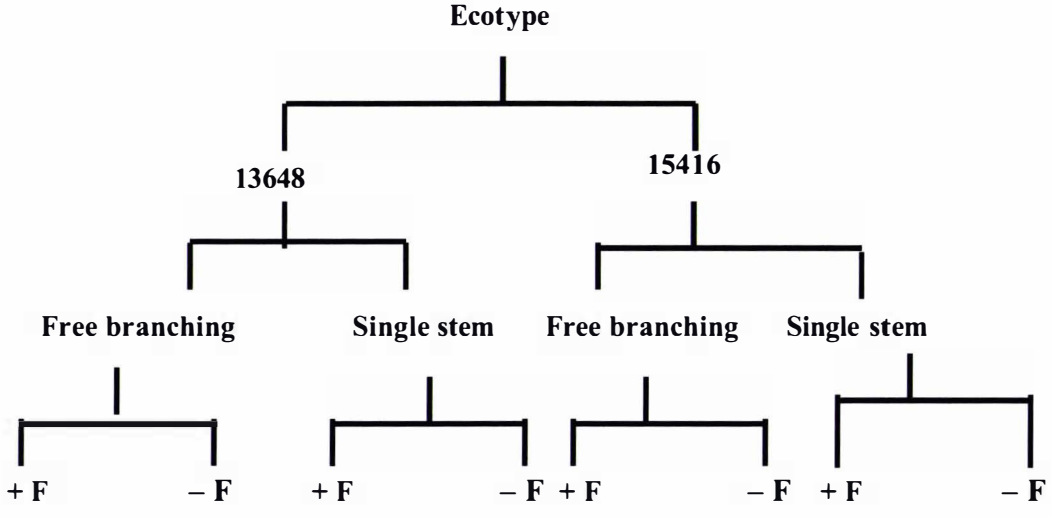

Figure 3.1 Experimental treatments for gas exchange, leaf mass per unit area, and leaf mineral analysis of *E. occidentalis*. + F, supplementary fertiliser; – F, no supplementary fertiliser.

3.2.2 Gas exchange

Three plants were randomly selected from each of the two ecotypes (13648 and 15416) and each architecture type as described in Section 3.2.1 (12 plants in total). Manual CO_2 response curves were obtained between 25 January and 8 February 2004 for leaves at nodes 30, 40, and 50 by plotting net photosynthetic rate (A) versus intercellular CO_2 concentration (C_i). These measurements were taken on the main stem using a LI-6400 portable photosynthesis system (LI-COR Biosciences, Lincoln, N.E., U.S.A.). The measurements were based on differences in CO_2 concentration between sample/leaf and reference chambers. Leaf temperature was maintained at 25 ± 0.5°C and leaf-air vapour pressure deficit (VPD) at 1.5 (± 0.4) kPa for the air entering the leaf chamber. A selected leaf was placed in the leaf chamber where light intensity was provided by the LED system with an internal light source of 6400-02B RedBlue # SI-927 and the photosynthetically active radiation incident on leaf (PARi) was maintained at 1500 μmol quanta m^{-2} s^{-1}. The air flow rate was held at 500 μmol s^{-1}. A range of CO_2 concentrations was obtained using the CO_2 controller by mixing CO_2 free air with known quantities of pure CO_2, and the resulting concentrations were measured using the infrared gas analyser (IRGA). When photosynthesis had stabilised, the initial CO_2 concentration was started at 75 μmol CO_2 mol^{-1}. During the experiment the concentration was increased over 6 - 8 steps to 1000 μmol CO_2 mol^{-1}. For each data point the mean intercellular CO_2 concentration (C_i, μmol mol^{-1}) and the net assimilation rate (A, μmol m^{-2} s^{-1}) were recorded.

Based on A/C_i response curves, biochemically based equations describing the potential limits to photosynthetic capacity were used to estimate the maximum ribulose- 1, 5-bisphosphate carboxylase/oxygenase (Rubisco) activity *in vivo* (V_{cmax}) (von Caemmerer and Farquhar, 1981). From the initial slope of the response of A to C_i and the maximum rate of ribulose- 1, 5-bisphosphate (RUBP) regeneration mediated by electron transport was estimated (J_{max}) from the points above the point of inflection. Computations were carried out using Photosyn Assistant software (version 1.1.2, Dundee Scientific, Dundee, U.K.). The Michaelis-Menten constants for Rubisco carboxylation (K_c) and oxygenation (K_o) were 40.4 Pa and 24.8 kPa, respectively (von Caemmerer, 2000).

After two weeks of supplementary fertiliser application (Section 3.2.1), starting on 1 April 2004, manual CO_2 response curves were obtained as explained earlier in this Section for leaves at nodes 30, 40, and 50 from three randomly selected plants from each treatment (2 ecotypes × 2 architectures × 2 supplementary fertiliser treatments × 3 plants × 3 nodes). The treatments are shown in Figure 3.1. Photosynthetic parameters (V_{cmax} and J_{max}) were estimated as described above.

3.2.3 Leaf anatomy

The leaf opposite to each leaf used for gas exchange measurements (25 January to 8 February) from node 30, 40, and 50 of single stem and free branching plants of ecotypes 13648 and 15416 was harvested immediately after each photosynthesis session. The harvested leaves were placed in FAA (90 ml of 70% ethanol; 5 ml of glacial acetic acid; 5 ml 40% (v/v), formalin) solution and allowed to fix for four days. The leaves were washed with 70% ethanol, dehydrated in a graded ethanol series, and embedded in paraffin wax. Sections (10 - 12 μm) were obtained using an ultra microtome (Leica RM 2145, Leica Microsystems, Wetzlar, Germany), and stained with safranin and fast green with differentiation in picric acid (Johansen, 1940) using standard protocols (Sreekantan, 2002). The sections were viewed under a light microscope (Leica MZ12) and images were captured digitally using a Leica MPS30 camera. Images were processed using Image Pro® PLUS software. From the mid-point of each of two laminar leaf cross transects, measurements were made to determine the number of palisade and total cell layers, leaf thickness and thickness of different cell layers, and intercellular air space as a proportion of the total section area (Sefton et al., 2002). The data were averaged to provide one value for each leaf.

3.2.4 Leaf mass per unit area (LMA)

For LMA analysis, leaves at nodes 30, 40 and 50 on the main stem were collected prior to the supplementary fertiliser application (15 March 2004) as well as at the end of three weeks of supplementary fertiliser application (5 April 2004). On the first occasion, a total of eight plants from each treatment group [(2 ecotypes (13648, 15416) × 2 architectures (free branching, single stem) × 3 (30, 40, 50) node positions)] were sampled including the plants used for gas exchange measurements. On 5 April a total of 3 plants from each treatment group (2 ecotypes × 2 architectures × 2 supplementary

fertiliser treatments × 3 node positions) were sampled including the plants used for gas exchange measurements. Leaf area was measured using a leaf area meter (LI-COR) and dried at 70°C for 48 to 72 h. The dry weight of each leaf was measured and recorded. LMA was calculated as the ratio of leaf dry mass per unit area ($g\ m^{-2}$).

3.2.5 Leaf mineral analysis

The dried leaf samples used for LMA measurements from node 30, 40 and 50 on 15 March 2004 prior to the supplementary fertiliser application and on 5 April after supplementary fertiliser application (as explained in Section 3.2.1 and 3.2.4) were again employed for the determination of mineral concentration. Rarely, when dried leaf samples were too small in quantity (< 0.5 g) for reliable assay, samples collected from the same plant at different nodes (30, 40, and 50) were pooled to obtain desired quantities. Complete mineral analysis (N, P, K, S, Ca, Mg, Na, Fe, Mn, Zn, Cu,and B) was carried out at Hill Laboratories, Hamilton, New Zealand.

3.2.6 Statistical analysis

To assess the effect of ecotype (13648 and 15416), architecture (free branching and single stem), node positions (node 30, 40, and 50), fertiliser (fertiliser supplemented and not supplemented) on gas exchange, LMA, mineral concentrations, and leaf anatomy, two-way or three-way ANOVA using general linear model (SAS). Whenever the main effects and their interaction was statistically significant, pair-wise comparison between means was performed using Tukey's Multiple Comparison Test ($p<0.05$). For gas exchange parameters correlation analyses were used (SAS) to determine the relationships between different attributes.

3.3 Results

3.3.1 Gas exchange

The CO_2 response curves (A/C_i) obtained during January and February 2004 was plotted (Figure 3.2). Irrespective of ecotype, single stem plants showed higher rates of photosynthesis (A) than those of free branching plants at corresponding node positions on the main stem. Single stem plants of ecotype 13648 displayed about a 40 to 50% higher saturated photosynthetic rate (around C_i 800 μmol m^{-1}) than the respective free branching plants.

Three-way ANOVA was carried out for the parameters V_{cmax} and J_{max}. The analysis showed that only the main effect architecture was significant on V_{cmax} ($p<0.0001$); there were no two - or three-way interaction effects between ecotype, architecture and node (Appendix 1, Table 2). The value of V_{cmax} in single stem plants was almost doubled that of free branching plants (113.2 and 69.6 μmol m^{-2} s^{-1}, respectively) (Table 3.1). Similarly J_{max} was affected significantly by architecture ($p<0.0001$), but there were also less significant ($p < 0.05$) main effect of ecotype and the architecture × ecotype interaction (Appendix 1, Table 2). The J_{max} in single stem plants were almost double that of free branching plants (203.2 and 111.8 μmol $m^{-2}s^{-1}$, respectively) (Table 3.1). However, while there was no difference between J_{max} of free branching plants of the two ecotypes, J_{max} of single stem plants was higher in ecotype 13648 than in 15416 (230.4 and 175.8 μmol m^{-2} s^{-1}, respectively). There was a significant correlation (R^2 = 0.96, $p<0.0001$) between V_{cmax} and J_{max} values throughout the experiment (Figure 3.3).

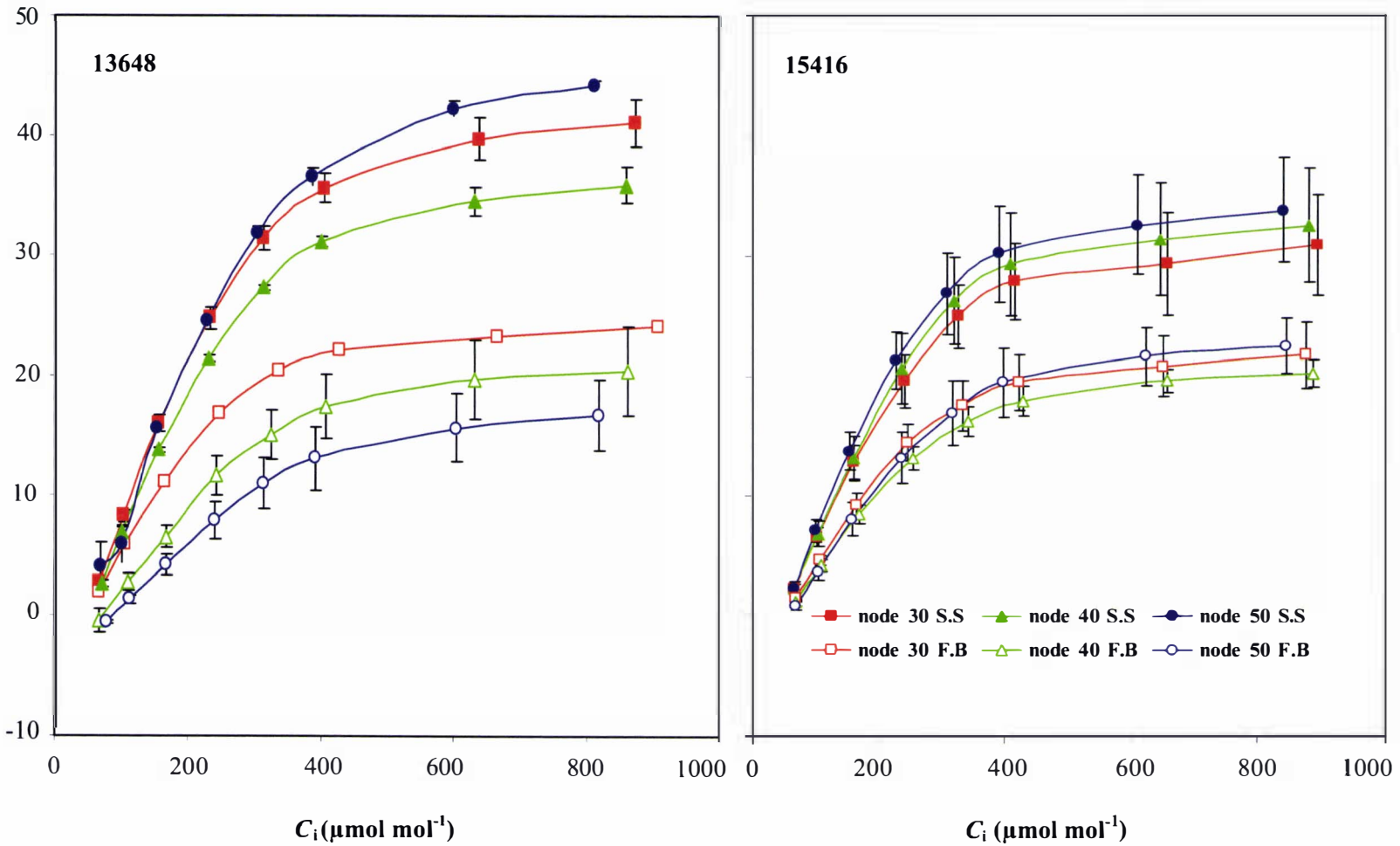

Figure 3.2 The response of net photosynthesis rate (*A*) (mean ± S.E.) to intercellular CO_2 (C_i) in *E. occidentalis* of ecotypes 13648 and 15416. Measurements were carried out at node 30, 40, and 50 on main stem. S.S, single stem plants, and F.B, free branching plants.

Table 3.1 Mean values (± S.E.) of the parameters V_{cmax} (µmol m^{-2} s^{-1}) and J_{max} (µmol m^{-2} s^{-1}) of ecotypes 13648 and 15416 of *E. occidentalis*.

Parameter	Node	Ecotype 13648		Ecotype 15416	
		Free branching	Single stem	Free branching	Single stem
V_{cmax}	30	83.8±0.1	127.0±2.5	73.9±9.3	96.1±9.8
	40	68.8±10.1	111.7±1.8	64.9±5.6	105.1±14.9
	50	52.7±10.6	128.0±6.1	73.5±13.1	111.0±11.0
Mean		68.4	122.2	70.8	104.1
J_{max}	30	124.5±0.3	234.0±12.8	111.9±15.4	162.7±24.0
	40	114.4±21.0	196.7±10.1	103.6±5.3	179.3±30.9
	50	95.9±17.7	260.7±4.9	121.2±16.0	185.3±26.4
Mean		111.3	230.4	112.2	175.8

Parameter values were estimated from CO_2 assimilation curves obtained from gas exchange measurements made during January and February 2004 for leaves at nodes 30, 40, and 50 on the main stem.

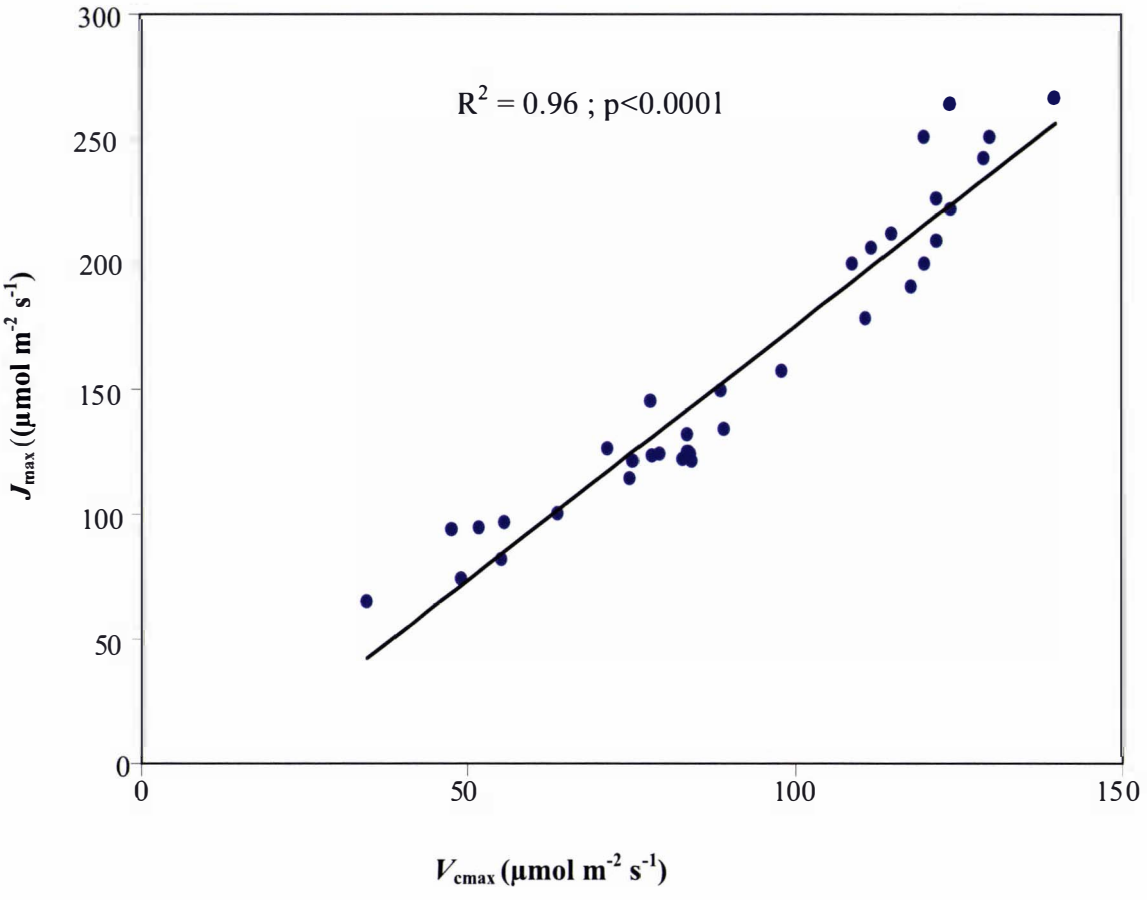

Figure 3.3 Correlation between V_{cmax} and J_{max} parameters in *E. occidentalis* estimated for January and February 2004 gas exchange measurements.

The CO_2 response curves were obtained again at three node positions for the two ecotypes with two architectures treatments during April after half the sampled plants had received a supplementary fertiliser application (Figure 3.4). In line with observations made eight weeks earlier, the leaves of single stem plants showed generally higher rates of photosynthesis (A) than those of free branching plants, irrespective of fertiliser treatment (Figure 3.4) and the single stem plants that were given supplementary fertiliser showed higher saturated photosynthetic rates (around C_i 650 μmol $m^{-1)}$ than the other three treatments. Generally a large drop in A was observed in single stem plants receiving no supplementary fertiliser treatment than free branching counterparts (Figure 3.4B, D), whereas A in single stem plants held steady or increased in response to supplementary fertiliser (Figure 3.4A, C).

Three- or four-way ANOVA for the parameter V_{cmax} showed that the main effect of architecture was highly significant ($p<0.0001$) and ecotype and fertiliser main effects (but not node) were significant ($p<0.05$). There were no significant interaction effects for V_{cmax} (Appendix 1, Table 2). As observed when the first measurements were taken eight weeks earlier, the mean V_{cmax} values obtained for single stem plants were generally higher than those in the corresponding free branching plants (98.2 and 81.2 μmol m^{-2} s^{-1}, respectively) (Table 3.2). Upon supplementary fertiliser treatment, in general there was an increase in mean V_{cmax} values from 84.8 to 94.7 μmol m^{-2} s^{-1}, in no supplementary fertiliser and supplementary fertiliser treatments, respectively (Table 3.2). Ecotype 13648 exhibited higher V_{cmax} (94.6 μmol m^{-2} s^{-1}) than ecotype 15416 (84.8 μmol m^{-2} s^{-1}) (Table 3.2).

The main effects ecotype and architecture, were highly significant on J_{max} ($p<0.0001$). The main effect fertiliser exhibited a significant effect ($p<0.05$). Further, the architecture and fertiliser interaction effect was also significant ($p<0.05$) (Appendix 1, Table 2). Similar to J_{max} estimates made eight weeks earlier, mean values for ecotype 13648 were higher than those of ecotype 15416 (170.0 and 137 μmol m^{-2} s^{-1}, respectively) (Table 3.2).

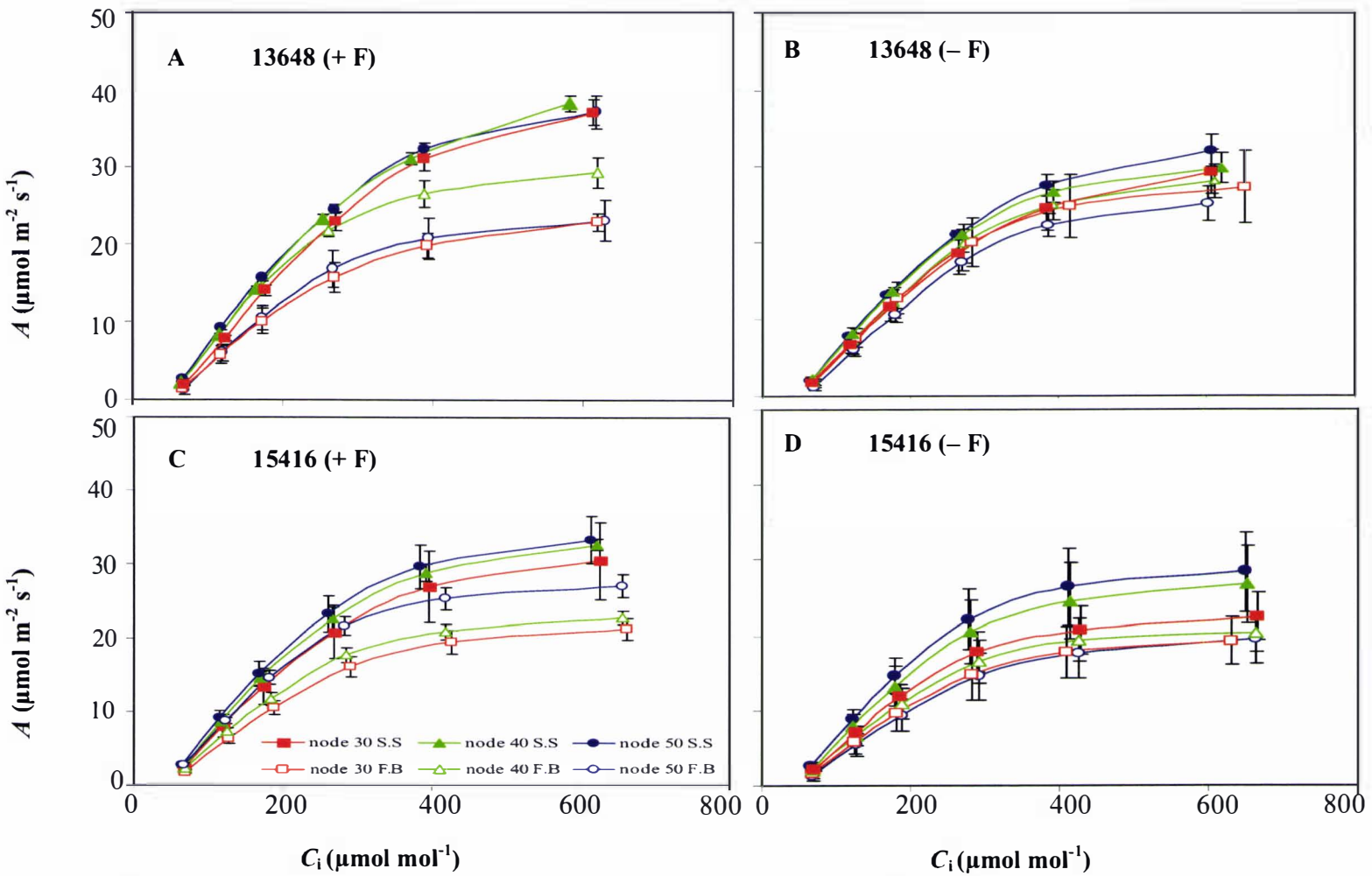

Figure 3.4 The response of photosynthesis (*A*) (mean ± S.E.) to intercellular CO_2 (C_i) in *E. occidentalis*. A, ecotype 13648 with supplementary fertiliser (+ F); B, ecotype 13648 with no supplementary fertiliser (– F); C, ecotype 15416 with supplementary fertiliser (+ F); D, ecotype 15416 with no supplementary fertiliser (– F). Measurements were carried out at node 30, 40, and 50 on main stem. S.S, single stem plants, and F.B, free branching plants.

Table 3.2 Mean values (± S.E.) of the parameters V_{cmax} (µmol m^{-2} s^{-1}) and J_{max} (µmol m^{-2} s^{-1}) for ecotypes 13648 and 15416 of *E. occidentalis* with or without supplementary fertiliser application.

Parameter	Node	Ecotype13648				Ecotype 15416			
		Free branching		Single stem		Free branching		Single stem	
		+ F	– F	+ F	– F	+ F	– F	+ F	– F
V_{cmax}	30	74.7±10.5	88.5±15.0	106.3±5.7	87.5±14.4	69.6±4.4	65.2±13.5	93.3±16.3	78.5±10.8
	40	107.3±1.5	93.7±10.9	108.3±5.8	94.3±2.7	76.3±5.3	70.8±11.9	104.8±10.3	92.6±20.6
	50	83.4±12.0	84.3±3.7	110.7±2.3	96.3±0.9	95.7±7.5	65.2±10.1	105.7±11.1	100.3±19.8
Mean		88.5	88.8	108.4	92.7	80.5	67.1	101.2	90.5
J_{max}	30	121.3±6.1	150.4±29.7	224.7±14.3	163.7±19.2	111.3±8.5	101±17.1	170.7±35.7	119.1±18.9
	40	164.0±13.5	158.3±14.8	228.7±13.1	163.0±15.0	117.7±6.2	107.3±14.8	182.3±5.4	147.4±31.4
	50	127.3±15.0	142.3±11.1	216.7±16.5	179.3±14.8	145.3±9.3	104.9±16.6	186.0±21.5	158.0±36.2
Mean		137.6	150.4	223.3	168.7	124.8	104.4	179.7	141.5

Parameter values were estimated from CO_2 assimilation curves obtained during supplementary fertiliser application (April 2004) gas exchange measurements for leaves at nodes 30, 40, and 50 on the main stem. + F, with supplementary fertiliser; – F, without supplementary fertiliser.

J_{cmax} values obtained for single stem plants were generally higher than those in the corresponding free branching plants (178.3 and 129.3 μmol m^{-2} s^{-1}, respectively) (Table 3.2). Upon supplementary fertiliser treatment, in general, there was an increase in mean J_{cmax} values from 141.2 to 166.3 μmol m^{-2} s^{-1} in no supplementary fertiliser and supplementary fertiliser treatments, respectively (Table 3.2). The interaction effect showed that J_{max} was similar in free branching plants with or without supplemented fertiliser (131.2 and 127.4 μmol m^{-2} s^{-1}, respectively), whereas J_{max} was lower in unfertilised single stem plants (155.0 μmol m^{-2} s^{-1}) than fertilised ones (201.5 μmol m^{-2} s^{-1}). Overall J_{max} was similar in free branching plants in January and March (regardless of fertiliser treatment), but in single stem plants J_{max} had dropped by about 25% from 201.5 to 155.1 μmol m^{-2} s^{-1} from fertilised to no fertilised, respectively. As observed when measurements were made two months earlier there was a highly significant correlation between V_{cmax} and J_{max} (R^2 = 0.88 ; p<0.0001) (Figure 3.5).

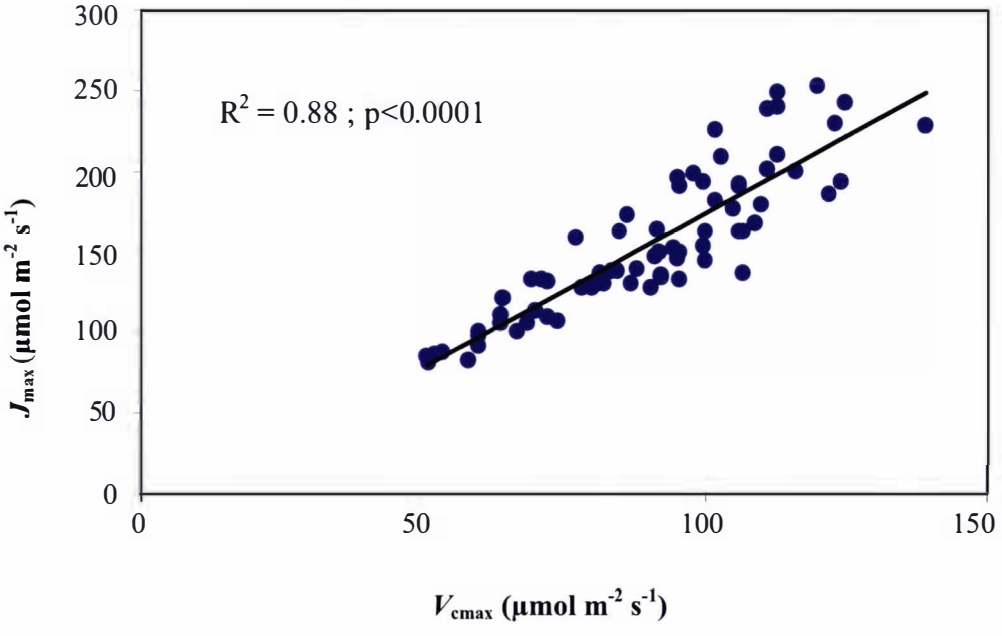

Figure 3.5 Correlation between V_{cmax} and J_{max} parameters in *E. occidentalis* estimated for March and April 2004 gas exchange measurements (+/– supplementary fertiliser application).

3.3.2 Leaf anatomy

Irrespective of ecotype and node position, the leaves of single stem plants were thicker (436.0 μm) and had greater mesophyll thickness (393.4 μm) than those of free branching plants (333.6 and 313.3 μm, respectively) ($p<0.0001$; Table 3.3; Appendix 1, Table 3). Air space was twice as high ($p<0.0001$) in the leaves of single stem plants (11.1 and 20.9 % in free branching and single stem plants, respectively), this effect being more marked in ecotype 13648 (23.3%) than in 15416 (18.4%) (Table 3.3). Similarly, the mean number of cell layers was higher ($p<0.0001$) in leaves of single stem plants than in those of free branching plants (10.1 and 9.6, respectively), this effect being greater in ecotype 15416 (10.6) than in 13648 (9.6) (Table 3.3). Leaves of free branching plants had a significantly greater number ($p<0.0001$) of palisade layers than those of single stem plants (5.1 and 3.6, respectively) (Table 3.3; Appendix 1, Table 3).

The main effect of architecture was not significant ($p<0.05$) for adaxial and abaxial palisade thickness, or for abaxial epidermis thickness. The three-way interaction of ecotype, node and architecture was significant ($p<0.05$) for leaf thickness, mesophyll thickness, abaxial epidermis thickness and palisade thickness suggesting that leaf anatomy had changed differently for the ecotypes in response to architecture during ontogeny (Appendix 1, Table 3). However, no consistent effects of node position or ecotype were evident. In general adaxial epidermal thickness was greater ($p<0.01$) in leaves of single stem plants than free branching plants (22.8 and 20.8 μm, respectively). This effect was found only in ecotype 15416 (24.8 and 21.2 μm for single stem and free branching plants, respectively), and with ecotype 13648 being little affected by architecture (20.7 and 20.5 μm for single stem and free branching plants, respectively).

With regard to the effect of leaf node position, on leaf anatomy (Table 3.3), there was a small but highly significant ($p<0.0001$) increase in cell layer number with increase in node (9.2, 10.0 and 10.3 at nodes 30, 40 and 50, respectively). Ecotype 15416 had small but significantly ($p<0.0001$) more cell layers than ecotype 13648 (10.1 and 9.5, respectively), the ecotypes did not differ consistently at different nodes with respect to cell number. However at node 50 leaves of free branching plants of ecotype 13648 had the lowest leaf thickness, abaxial palisade thickness, abaxial

epidermal thickness and mesophyll thickness (Table 3.3). Typical leaf anatomy at nodes 30, 40 and 50 in ecotypes 13648 and 15416 of *E. occidentalis* grown under two architectures have been shown (Figure 3.6). At node 50 in ecotype 13648 the leaf sections derived from leaves of free branching plants displayed isobilateral characteristics (Figure 3.6A).

3.3.3 Leaf mass per unit area

Only architecture had a significant effect ($p<0.05$) on leaf mass per unit area (LMA) and all interaction effects were non significant (Appendix 1, Table 4). LMA in single stem plants was slightly but significantly higher ($p<0.05$) than that of free branching plants (191.9 and 181.9 g m^{-2}, respectively; Table 3.4). Similarly, when LMA was measured again following the supplementary fertiliser treatment (April 2004), the main effect of architecture showed significance ($p<0.05$). Again single stem plants had slightly higher ($p<0.05$) mean LMA than those of free branching plants (203.0 and 188.3 g m^{-2}, respectively; Table 3.5) although the interaction due to ecotype, fertiliser, and architecture was also significant ($p<0.05$) (Appendix 1, Table 5).

3.3.4 Mineral concentration

Before supplemental fertiliser treatment (March 2004), leaf N concentration was showed significantly affected by ecotype ($p<0.0001$), ontogenetic stage ($p<0.05$) and architecture ($p<0.0001$), with a significant ($p<0.05$) interaction effect between ecotype and architecture (Appendix 1, Table 5). Leaf N concentration was higher in ecotype 13648 than in 15416 (1.43 and 0.96%, respectively). This was most marked in single stem plants than in free branching plants (1.75 and 1.12%, respectively for ecotype 13648, compared to 1.11 and 0.80%, respectively in ecotype 15416). There was a slight increase in leaf N with increasing node position (1.13, 1.14 and 1.33% at node 30, 40 and 50, respectively), although this effect was not observed consistently in the interaction of ecotype, architecture, and node (Table 3.6). In general, higher mineral concentration was observed in leaves of single stem plants than in those of free branching plants, irrespective of the ecotype (Table 3.6). The mean leaf N concentration was 48% higher in single stem plants than in those of free branching plants.

Table 3.3 Leaf anatomical characteristics (mean values ± S.E.) of single stem and free branching plants at different nodes for *E. occidentalis* ecotypes 13648 and 15416.

Ecotype/Characteristic	Node 30		Node 40		Node 50	
	Single stem	Free branching	Single stem	Free branching	Single stem	Free branching
Ecotype 13648						
Number of palisade layers	3.3 ± 0.2	5.0 ± 0.6	3.3 ± 0.4	4.0 ± 0.0	3.3 ± 0.2	5.7 ± 0.5
Number of cell layers	9.7 ± 0.2	9.0 ± 0.0	8.7 ± 0.2	9.3 ± 0.2	10.3 ± 0.2	10.2 ± 0.2
Leaf thickness (μm)	433.0 ± 16.1	345.0 ± 11.1	406.0 ± 24.8	389.8 ± 16.1	472.6 ± 25.6***	304.4 ± 5.7
Mesophyll thickness (μm)	388.8 ± 15.6	303.8 ± 11.1	360.0 ± 23.7	345.3 ± 14.7	432.2 ± 24.0***	267.7 ± 3.4
Adaxial epideimis (μm)	20.6 ± 1.0	18.8 ± 0.7	21.4 ± 1.1	23.0 ± 1.0	20.1 ± 1.4	19.7 ± 0.9
Adaxial palisade (μm)	93.6 ± 14.4	69.8 ± 15.4	81.9 ± 12.5	107.8 ± 11.0	60.4 ± 7.6	66.9 ± 14.3
Abaxial epidermis (μm)	20.3 ± 0.4	19.6 ± 1.0	19.9 ± 1.1	22.7 ± 0.9	21.9 ± 1.0	19.8 ± 1.1
Abaxial palisade (μm)	95.1 ± 16.6	60.1 ± 13.8	80.5 ± 10.1	93.3 ± 4.9	123.3 ± 1.4	77.0 ± 16.6
Airspace (%)	22.1 ± 0.0	11.9 ± 0.0	24.5 ± 0.0	11.9 ± 0.0	23.5 ± 0.0	8.2 ± 0.0
Ecotype 15416						
Number of palisade layers	3.2 ± 0.5	4.7 ± 0.4	3.7 ± 0.2	4.3 ± 0.2	4.7 ± 0.8	7.0 ± 0.4
Number of cell layers	9.7 ± 0.2	9.3 ± 0.2	11.2 ± 0.4	10.0 ± 0.0	11.0 ± 0.4	9.7 ± 0.2
Leaf thickness (μm)	416.7 ± 5.0	344.9 ± 16.3	459.1 ± 7.7*	361.1 ± 4.0	428.2 ± 34.9	376.9 ± 22.6
Mesophyll thickness (μm)	375.8 ± 6.4	307.8 ± 15.3	419.3 ± 5.8*	321.7 ± 4.8	384.4 ± 34.3	334.5 ± 21.2
Adaxial epideimis (μm)	26.9 ± 0.8	20.3 ± 2.1	23.8 ± 1.0	21.7 ± 0.9	23.8 ± 2.2	21.6 ± 1.0
Adaxial palisade (μm)	110.2 ± 15.9	121.0 ± 9.0	111.5 ± 20.1	109.2 ± 7.8	103.9 ± 15.6	164.4 ± 6.4
Abaxial epidermis (μm)	22.1 ± 0.6	21.5 ± 1.4	23.2 ± 0.5	21.21 ± 1.1	21.0 ± 0.9	22.1 ± 1.3
Abaxial palisade (μm)	67.8 ± 11.6	83.4 ± 13.4	79.6 ± 8.3	73.5 ± 5.55	97.3 ± 19.3	137.5 ± 5.7
Airspace (%)	19.9 ± 0.0	9.2 ± 0.0	21.0 ± 0.0	16.3 ± 0.0	14.5 ± 0.0	0.9.1 ± 0.0

*Pair-wise comparison of means of corresponding nodes of each architecture ($p<0.05$), *** ($p<0.0001$)

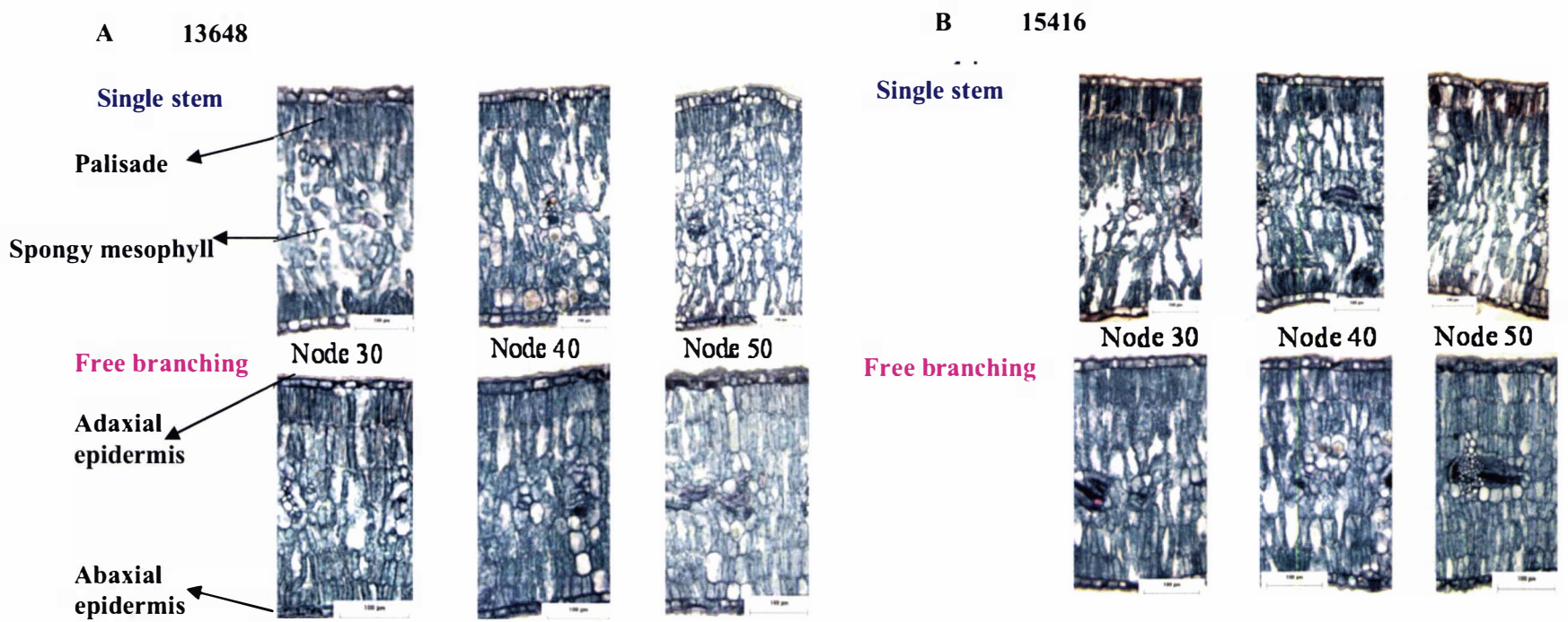

Figure 3.6 Photomicrographs of traverse sections of representative single stem and free branching leaves of *E. occidentalis* ecotype 13648 and 15416 at node 30, 40 and 50 on the main stem. Each section has incorporated scale size bar of 100 µm. For more details on section preparations please refer to Section 3.2.3.

Similarly, the other minerals P, K, S, Ca, Mg, Na, Fe, Mn, Zn, Cu and B were 50, 12, 56, 48, 42, 52, 16, 36, 20, 54, and 27% higher than in free branching concentration, respectively (Table 3.6). While P concentration was also higher in the leaves of single stem plants than those of free branching counterparts (0.45 and 0.33%, respectively). P value decreased consistently with increasing node position, an effect most marked in single stem plants (0.64, 0.44 and 0.24% for node 30, 40 and 50, respectively for single stem plants; 0.44, 0.25, 0.22% for node 30, 40, and 50, respectively for free branching plants) (Table 3.6).

In the second set of leaves analysed with or without supplemental fertiliser treatment (April 2004), leaf N concentration responded to the main effects of architecture ($p<0.0001$) and fertiliser ($p<0.05$) but not ecotype (Appendix 1, Table 6). However, there was no significant interaction effect between ecotype, architecture, and fertiliser. As observed in the previous experiment, leaf N concentration was about 44% higher in single stem plants than in free branching plants. In general, higher mineral concentration was observed in leaves of single stem plants than in those of free branching plants, irrespective of the ecotype, (1.63 and 1.14, respectively) (Table 3.7).

Table 3.4 Leaf mass per unit area (g m^{-2}), of leaves of free branching and single stem plants for two ecotypes of *E. occidentalis* prior to supplementary fertiliser application (15 March 2004).

Ecotype	Free branching	Single stem
13648	179.5	188.8
15416	184.4	194.9

Table 3.5 Leaf mass per unit area (g m^{-2}), of leaves of free branching and single stem plants for two ecotypes of *E. occidentalis* following supplementary fertiliser treatment to half of the plants (5 April 2004).

Ecotype	Free branching		Single stem	
	+ F	– F	+ F	– F
13648	200.7	182.1	201.5	210.7
15416	187.0	182.6	181.3	218.5

+ F, with supplementary fertiliser; – F, without supplementary fertiliser.

Table 3.6 Mean values (± S.E.) of leaf mineral concentration of single stem and free branching plants of *E. occidentalis* at different nodes prior to supplementary fertiliser application.

Mineral	Node	13648 Free branching	13648 Single stem	15416 Free branching	15416 Single stem
N (%)	30	1.00 ± 0.06	1.80 ± 0.58	0.73 ± 0.30	1.00 ± 0.06
	40	0.93 ± 0.03	1.77 ± 0.09	0.80 ± 0.06	1.07 ± 0.12
	50	1.48 ± 0.18	1.70 ± 0.06	0.87 ± 0.07	1.27 ± 0.13
P (%)	30	0.54 ± 0.09	0.90± 0.02	0.33 ± 0.01	0.48 ± 0.06
	40	0.28 ± 0.01	0.58 ± 0.05	0.22 ± 0.01	0.29 ± 0.03
	50	0.32 ± 0.08	0.28 ± 0.03	0.13 ± 0.01	0.19 ± 0.05
K (%)	30	1.23 ± 0.12	1.53 ± 0.12	0.97 ± 0.03	1.27 ± 0.08
	40	1.27 ± 0.13	1.57 ± 0.09	1.17 ± 0.12	1.20 ± 0.12
	50	1.30 ± 0.00	1.27 ± 0.03	1.37 ± 0.15	1.37 ± 0.12
S (%)	30	0.12 ± 0.00	0.19 ± 0.01	0.09 ± 0.00	0.11 ± 0.01
	40	0.16 ± 0.01	0.24 ± 0.01	0.09 ± 0.00	0.13 ± 0.00
	50	0.13 ± 0.02	0.27 ± 0.02	0.11 ± 0.01	0.15 ± 0.01
Ca (%)	30	1.01 ± 0.11	1.63 ± 0.08	0.98 ± 0.10	1.23 ± 0.11
	40	0.98 ± 0.09	1.38 ± 0.05	0.93 ± 0.10	1.24 ± 0.10
	50	0.83 ± 0.08	1.31 ± 0.10	0.80 ± 0.03	1.42 ± 0.09
Mg (%)	30	0.21 ± 0.04	0.30 ± 0.01	0.23 ± 0.02	0.25 ± 0.02
	40	0.24 ± 0.02	0.32 ± 0.01	0.25 ± 0.03	0.33 ± 0.01
	50	0.20 ± 0.02	0.34± 0.03	0.24 ± 0.01	0.39 ± 0.04
Na (%)	30	0.14 ± 0.01	0.29 ± 0.02	0.12 ± 0.01	0.13 ± 0.01
	40	0.10 ± 0.01	0.19 ± 0.02	0.09 ± 0.01	0.11 ± 0.01
	50	0.1 ± 0.0	0.13 ± 0.02	0.07 ± 0.00	0.10 ± 0.01
Fe ($mg.kg^{-1}$)	30	27.67 ± 2.03	39.00 ± 4.04	20.00 ± 0.58	23.00 ± 2.65
	40	34.00 ± 7.37	32.67 ± 1.45	18.00 ± 1.15	19.33 ± 2.60

	50	28.33 ± 4.37	44.33 ± 7.06	28.00 ± 5.77	23.00 ± 1.00
Mn ($mg.kg^{-1}$)	30	146.70 ± 12.00	246.70 ± 37.10	173.33 ± 14.50	203.30 ± 16.70
	40	126.70 ± 12.00	156.70 ± 23.30	166.70 ± 16.70	223.30 ± 17.60
	50	99.30 ± 6.40	130.00 ± 11.50	120.0 0± 0.00	173.33 ± 3.33
Zn ($mg.kg^{-1}$)	30	25.67 ± 3.84	34.67 ± 4.18	25.67 ± 4.26	33.33 ± 2.67
	40	23.67 ± 1.76	23.67 ± 0.88	20.33 ± 0.33	24.33 ± 2.03
	50	25.00 ± 1.53	31.33 ± 2.19	21.00 ± 1.53	21.67 ± 2.60
Cu ($mg.kg^{-1}$)	30	3.00 ± 0.57	7.00 ± 0.57	2.00 ± 0.00	2.67 ± 0.33
	40	5.00 ± 0.00	7.67 ± 1.20	2.67 ± 0.33	3.00 ± 0.58
	50	7.00 ± 1.15	12.33 ± 2.67	4.33 ± 0.88	4.33 ± 0.33
B ($mg.kg^{-1}$)	30	24.67 ± 2.33	32.33 ± 4.91	25.67±0.33	32.00 ± 1.73
	40	20.33 ± 1.86	23.00 ± 5.29	20.33±2.85	24.00± 1.15
	50	15.00 ± 0.57	23.67 ± 0.88	16.33±0.88	20.00 ± 2.00

Table 3.7 Mean values (± S.E.) of leaf mineral concentration of single stem and free branching plants of *E. occidentalis* following supplementary fertiliser treatment to half of the plants.

Mineral	Supplementary Fertiliser	Ecotype 13648		Ecotype 15416	
		Free branching	Single stem	Free branching	Single stem
N (%)	+ F	1.40 ± 0.18	1.92 ± 0.12	1.12 ± 0.15	1.70 ± 0.23
	– F	1.03 ± 0.08	1.72 ± 0.08	1.00 ± 0.17	1.18 ± 0.08
P (%)	+ F	0.36 ± 0.03	0.50 ± 0.08	0.27 ± 0.05	0.28 ± 0.05
	– F	0.41 ± 0.06	0.43 ± 0.08	0.20 ± 0.03	0.37 ± 0.07
K (%)	+ F	1.26 ± 0.12	1.15 ± 0.11	1.27 ± 0.09	1.26 ± 0.04
	– F	1.28 ± 0.11	1.20 ± 0.14	1.15 ± 0.10	1.26 ± 0.10
S (%)	+ F	0.14 ± 0.01	0.26 ± 0.02	0.11 ± 0.01	0.17 ± 0.01
	– F	0.12 ± 0.01	0.21 ± 0.01	0.11 ± 0.01	0.12 ± 0.01
Ca (%)	+ F	1.11 ± 0.08	1.59 ± 0.13	1.24 ± 0.19	1.41 ± 0.21
	– F	0.98 ± 0.10	1.43 ± 0.05	1.04 ± 0.19	1.90 ± 0.19
Mg (%)	+ F	0.23 ± 0.01	0.34 ± 0.05	0.31 ± 0.04	0.34 ± 0.03
	– F	0.22 ± 0.02	0.37 ± 0.02	0.26 ± 0.03	0.46 ± 0.05
Na (%)	+ F	0.12 ± 0.00	0.19 ± 0.04	0.09 ± 0.00	0.13 ± 0.01
	– F	0.11 ± 0.01	0.13 ± 0.03	0.11 ± 0.01	0.11 ± 0.01
Fe ($mg.kg^{-1}$)	+ F	92.70 ± 58.00	39.83 ± 3.26	27.33 ± 3.73	35.00 ± 4.91
	– F	26.0 ± 1.46	36.50 ± 1.84	30.17 ± 9.44	27.00 ± 1.75
Mn ($mg.kg^{-1}$)	+ F	176.70 ± 29.10	138.30 ± 24.40	216.7 ± 29.30	201.70±23.40
	– F	135.00 ± 12.30	134.70 ± 20.80	198.3 ± 29.00	225.0 ± 14.30
Zn ($mg.kg^{-1}$)	+ F	27.33± 2.60	41.17± 4.11	32.00 ± 5.19	30.67 ± 2.19
	– F	25.33 ± 2.58	28.00 ± 1.93	23.00 ± 4.50	32.00± 3.15
Cu ($mg.kg^{-1}$)	+ F	5.33 ± 0.89	12.50 ± 2.83	3.50 ± 0.72	5.67 ± 1.17
	– F	4.50 ± 0.67	10.83 ± 1.54	4.50 ± 0.85	3.83 ± 0.65
B ($mg.kg^{-1}$)	+ F	26.67 ± 6.44	28.83 ± 2.70	26.83 ± 2.09	26.33 ± 2.63
	– F	21.17 ± 2.87	35.83 ± 9.51	21.83 ± 2.64	29.33 ± 1.50

+ F, with supplementary fertiliser; – F,without supplementary fertiliser.

The supplementary fertiliser treatments had higher leaf N (1.53%) than the no supplementary fertiliser treatments (Table 3.7), and the difference was significant ($p<0.05$) (Appendix 1, Table 6). The main effects ecotype, and architecture were highly significant for S ($p<0.0001$) and significant for fertiliser, and ecotype and architecture interactions ($p<0.05$). In 13648 ecotype single stem plants contained 80.77% higher S than free branching plants. Similarly, in ecotype 15416, the single stem plants had 31.82% higher S than the free branching counter parts. Single stem plants recorded higher Ca (44.85%), Na (30.23%), Mg (48.04%), Mn (43.95%) and B (24.68%) than free branching plants (Table 3.7). For minerals Fe and Zn, the three-way interaction of ecotype, architecture and fertiliser was significant ($p<0.05$) (Appendix 1, Table 6).

3.4 Discussion

The characterisation of phase change was extended by measuring traits including gas exchange, leaf anatomy, LMA, and mineral concentration in *E. occidentalis* in relation to shoot architecture. Ecotypes 13648 and 15416, which showed significant differences in leaf morphology during shoot development, were analysed in detail. In *Eucalyptus globulus*, James and Bell (2001) reported that leaf morphology changes during phase change were associated with changes in leaf anatomy and gas exchange parameters. In *Sequoia sempervirens* (coastal redwood), higher photosynthetic rates, nitrogen content and respiration rates were observed in juvenile shoots, which was consistent with the more vigorous and rapid growth phase (Huang et al., 2003). Similarly in *Hedera helix,* developmental anatomy was correlated with gross morphological differences between juvenile and adult forms (Stein and Fosket, 1969).

3.4.1 Gas exchange

Photosynthetic rates have been observed to increase, decrease or not change during development at the whole plant level (Bond, 2000; Thomas and Winner, 2002). However, there are relatively few data comparing adult versus juvenile foliage on the same plant. In *Hedera helix*, lower to higher photosynthesis was recorded from juvenile to adult leaves, respectively (Bauer and Bauer, 1980), whereas in *M. excelsa* photosynthesis was higher in juvenile foliage than in adult leaves (Kubien et al., 2007). In *E. occidentalis* the observed differences of photosynthesis in single stem and free

branching plants at the corresponding nodes on the main stem showed that shoot architecture manipulation has contributed to changes in photosynthetic rates. In *E. occidentalis*, higher photosynthetic rates were observed in single stem plants as compared to the respective free branching plants. The single stem plants displayed a more juvenile appearance and the observed higher photosynthetic rates were similar to those observed in *M. excelsa* juvenile leaves (Kubien et al., 2007).

The higher levels of photosynthesis in single stem plants contributed to higher estimated Rubisco capacity (V_{cmax}) and a higher rate of maximum electron transport (J_{max}). These estimates V_{cmax} and J_{max} provided a measure of the activity of Rubisco and RUBP regeneration, respectively, within the leaves analysed. These mathematical models have been developed to simulate leaf photosynthesis and were based on mechanisms of diffusion of CO_2 to the chloroplast and enzyme kinetics (von Caemmerer, 2000). The adult-like leaf morphology (lanceolate leaves) observed in free branching plants of ecotype 13648 at node 50 (Section 2.3) recorded lower V_{cmax} and J_{max} values than single stem plants at the corresponding node. These results suggest that changes in leaf traits due to phase change contributed to lower rates of photosynthesis. In *M. excelsa* both V_{cmax} and J_{max} declined during ontogeny and the lower V_{cmax} and J_{max} were considered one of the characteristics of adult leaves (Henriod, 2001).

V_{cmax} is the maximum capacity for RuBP carboxylation and is a function of leaf nitrogen content. Many studies have reported tight correlations between leaf N and V_{cmax} (e.g. Warren, 2004). The decline in V_{cmax} and J_{max} estimates observed in free branching plants of *E. occidentalis* was unlikely to be related to declining N availability. This was established when the differences in gas exchange measurements between the single stem and free branching plants did not change even after supplementary fertiliser treatment (Table 3.2). This indicates that the nitrogen allocation to Rubisco is more efficient in single stem plants as compared to free branching plants, and this allocation could be independent of the N supplementation. Thus, manipulation of shoot growth as single stem and free branching resulted in changes in gas exchange parameters as well as differences in attaining adult shoot phenology.

3.4.2 Leaf anatomy

The rates of phase change as observed by changes of leaf anatomical attributes were significantly different in single stem and free branching plants. Further, these changes were progressive rather than abrupt. Anatomical changes due to ontogenetic stage (node 30, 40 and 50) were clearly observed in free branching plants of ecotype 13648. The major changes in leaf anatomy of free branching plants were increased cell layers, and a concomitant reduction in the proportion of intercellular air space. Single stem plants of ecotypes 13648 and 15416, showed similar numbers of cell layers but the differentiation with free branching counterparts was with regard to the number of palisade layers and the proportion of intercellular space. Sefton et al. (2002) reported a mean value of 3.7 palisade layers in 10-week-old *E. occidentalis* plants. In another investigation, in *E. globulus* ssp. *globulus* the palisade layers increased from one to three as the leaves progressed from the juvenile to the adult phase through a transitional phase (James et al., 1999). Further, in *E. occidentalis* ecotype 13648, the numbers of palisade layers in single stem plants were similar between node 30 and 50, showing juvenile appearance. By contrast, 13648 free branching plants displayed increasing numbers of palisade layers from node 30 to 50 showing adult-like leaf anatomy.

Observations of leaf anatomy showed that phase change was delayed in single stem plants as compared to free branching plants. In this study, the observed mean leaf thickness and mesophyll thickness did not increase gradually from juvenile to adult through a transitional phase. This may be due to the internal variation between the anatomy of transitional phase leaves. Changes in phase specific traits are not always completely correlated, with transitional leaves having characteristics of more than one phase (Lawson and Poethig, 1995; Bongard-Pierce et al., 1996). Leaf thickness was significantly greater in leaves from single stem plants as compared to their respective free branching counterparts, irrespective of the ecotype. The increase in leaf thickness was not due to an increase in cell layers but due to an increase in mesophyll thickness and air space area. Differences in tissue density arise from variations in internal anatomy that determine the volume of intercellular air space (Koike, 1988), the amount of cuticle, and the thickness of the cell walls (Witkowski and Lamont, 1991).

Thus, leaf anatomy measurements, especially the greater air space area, was correlated to higher rates of photosynthesis in single stem plants. The path taken by CO_2 to reach

sites of carboxylation involves many barriers. Aalto and Juurola (2002) suggested that CO_2 diffuses across a boundary layer in the air above the foliage surface, through a stomatal opening, and across intercellular air spaces in the sub-stomatal cavity and then enter the surface of mesophyll cells and finally diffuses within the cell to the chloroplast membrane, and from there to the sites of carboxylation. Hence, greater air space facilitates more CO_2 diffusion, and in turn greater photosynthesis. Ecotype 13648 free branching plants at node 50 showed lesser air space area and isobilateral leaf anatomy with a greater number of palisade layers on both adaxial and abaxial sides of the leaves, and therefore showed adult-like anatomy and concomitant reduction in photosynthesis.

3.4.3 Leaf mass per unit area and mineral concentrations

Leaf dry mass per unit area, appears to be a key attribute representing the trade-off between resource acquisition and the constraints imposed by leaf structure, herbivore resistance and the mitigation of water loss (Dijkstra, 1990). The LMA was slightly higher in single stem plants ($p<0.05$) in both supplementary fertiliser as well as no fertiliser treatments indicating that nutrient limitation was not a significant factor affecting LMA in the current experiments. In *Eucalyptus grandis* seedlings, Grassi et al. (2002) showed that the nitrogen supplementation decreased LMA.

Differences in leaf mineral concentrations were observed between single stem and free branching plants indicating that the architecture manipulations influenced the leaf mineral concentrations. P levels at node 50 of free branching plants were slightly higher than the corresponding single stem plants. It was reported that P fertiliser significantly reduced the length of the juvenile vegetative phase, and N, in contrast to P, promoted flowering (Williams et al., 2004).

To summarise vegetative phase change in *E. occidentalis*, the visible leaf morphology changes in free branching plants of ecotype 13648 (Chapter 2) was correlated with lower photosynthetic rates, isobilateral organisation of palisade mesophyll, and less air space area. In contrast, the single stem plants of *E. occidentalis* retained the more juvenile characteristics of higher photosynthetic rates, and dorsiventral leaf anatomy. Lateral branch removal treatments have previously been shown to accelerate vegetative phase change in *M. excelsa* (Clemens et al., 1999), and in *Citrus* (Snowball et al., 1994). In contrast to the above studies, in this thesis, *E. occidentalis* single stem plants showed

delayed vegetative phase change compared to the corresponding free branching plants in terms of leaf parameters. Hence complexity of shoot architecture has contributed to the rate of phase change more than size (height) of the plant. The observations reported in this Chapter support the hypothesis that in *E. occidentalis* the rate of phase change is controlled primarily by the complexity of shoot architecture.

.

Chapter 4

Floral transition in *Eucalyptus occidentalis* in relation to shoot architecture: molecular study

4.1 Introduction

The floral transition is the developmental turning point from the vegetative to the reproductive stage. The morphological and physiological studies (Chapters 2 and 3) revealed that the rate of phase change was controlled primarily by the complexity of shoot architecture in *E. occidentalis* and that the phase change and floral transition could be temporally uncoupled. These two developmental processes appear to be under separate genetic control.

The meristem identity genes are the final players in the pathway to flowering (Blazquez et al., 2001). As the floral transition is controlled by the meristem identity genes, this work was extended to isolate homologues of the *Arabidopsis* meristem identity genes *LFY*, *AP1* and *TFL1*, from *E. occidentalis*. Further, the expression of these genes was monitored during the floral transition using quantitative real-time PCR in single stem and free branching plants. Based on the earlier leaf morphology and physiological results and our current understanding regarding the meristem identity genes, it was hypothesised that there would be (i) a higher level of expression of the shoot identity or inflorescence meristem identity gene *TFL1*, in single stem plants, and (ii) a higher level of expression of the floral meristem identity genes, *LFY* and *AP1*, in free branching plants because the free branching plants of ecotype 13648 attained adult-like shoot phenology earlier compared to their corresponding single stem counterparts and to the rest of the ecotypes.

4.2 Materials and Methods

4.2.1 Plant material

Seed of *E. occidentalis* ecotype 13648 was sown and the seedlings transplanted and grown in greenhouses as described in Section 2.2.1. Buds were collected at regular intervals from December 2003 to May 2004 from both free branching and single stem plants. Axillary buds were collected from the node immediately below the apical bud as shown in Figure 4.1. One bud per plant with a total of approximately 13-15 buds were pooled for each architure treatment and two samples were obtained for each collection date. The opposite bud of each bud sampled for gene expression studies was tagged at the time of bud collection and visual observations were carried out after three or four days (finally confirmed after the bud break) of each bud sample collected to determine the fate of the parallel bud as vegetative or floral, and also the potential number of floral buds present in each sample.

4.2.2 Total RNA extraction

Two RNA extraction methods were used. For initial isolation of genes from *Eucalyptus*, a modified hot borate method described by Wilkins and Smart (1996) was used. For gene expression studies the RNeasy plant mini kit (QIAGEN GmbH, Hilden, Germany) was used. For both methods RNase-free components were essential and it was done by baking all glassware at 180°C for 6 h; all plastic-ware was soaked in 3% (v/v) hydrogen peroxide for 1 h and rinsed with milli Q water and autoclaved in aluminium foil; all mortar and pestles were wrapped in aluminium foil and autoclaved; and all solutions were treated with DEPC @ 1 ml/l.

4.2.2.1 Hot borate RNA extraction

The hot borate extraction (XT) buffer was prepared by adding:

- 0.2 M Na borate decahydrated (borax)
- 30 mM EDTA
- 2% (w/v) SDS
- 10 mM dithiotrietol (DTT)
- 1% Nonidet P-40 (NP-40)
- 2% (w/v) polyvinylpyrrolidone (PVP)

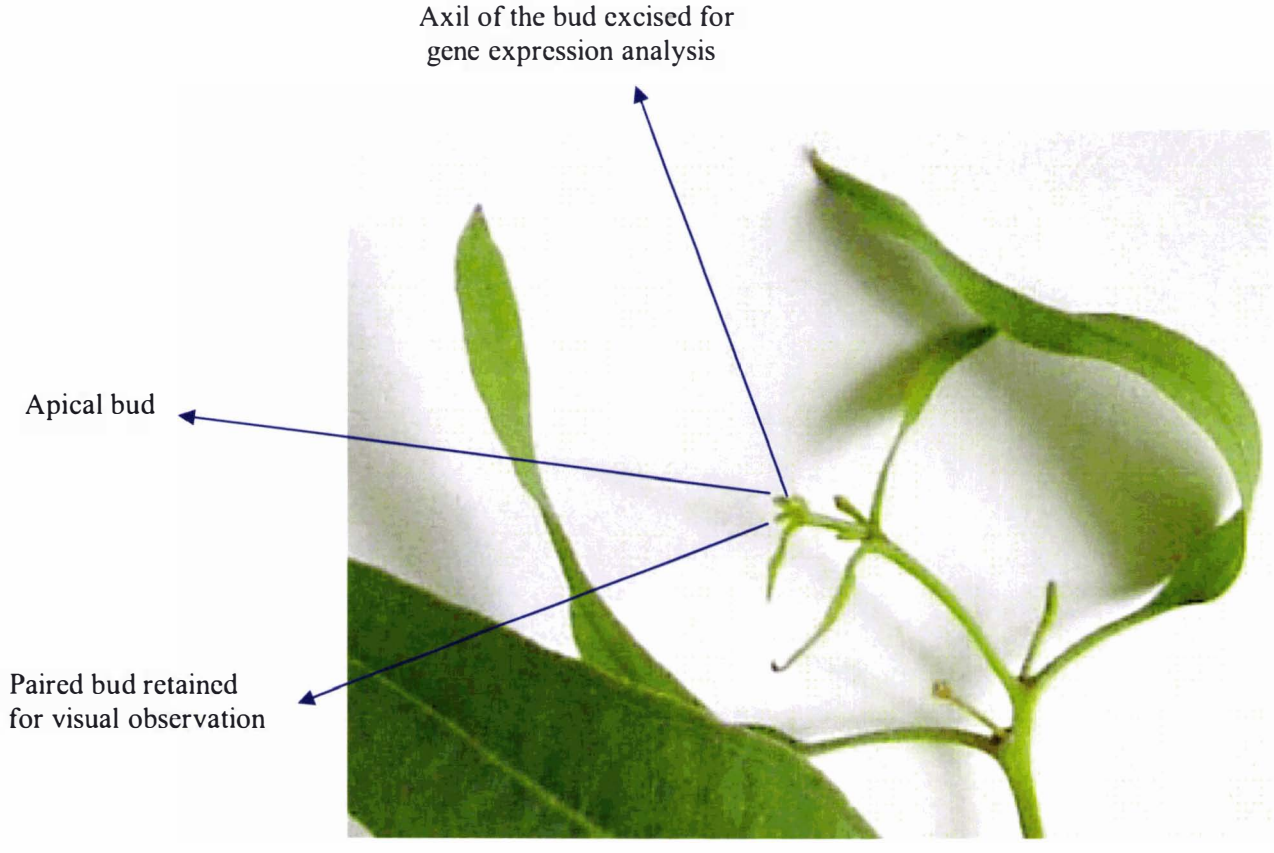

Figure 4.1 Typical example showing sites of bud collection for meristem identity gene expression analysis. Axillary bud was excised from the position shown above. The paired axillary bud was retained for visual examination to determine if the bud was floral or vegetative.

All the chemicals were dissolved in RNase-free, pre-warmed milli-Q water, the pH was adjusted to 9 with 2 M NaOH, and the stock solution was autoclaved. DTT, PVP, NP-40 were added just before the time of extraction.

Aliquots (1 g) of frozen (-80°C) plant tissue were deep frozen in liquid nitrogen and ground to a powder using a mortar and pestle. The finely ground powder was transferred into a cold Oak Ridge tube and chilled in liquid nitrogen. The XT buffer was heated to 80°C in an Oak Ridge tube. The cold powder was transferred to 5 ml of hot buffer and vortex was done for 30 s, 105.5 µl of proteinase K (20 mg ml^{-1} in water) was added, and the mixture was incubated at 42°C for 1.5 h with gentle swirling and mixing every 10 min. After that, 400 µl of 2 M KCl was added and the extraction mix incubated on ice for 30 min with gentle and horizontal swirling. Cellular debris and denatured proteins were pelleted by centrifugation at 26,000 × g for 20 min at 4°C, and the aqueous supernatant transferred to a fresh tube. RNA was precipitated at 4°C overnight by the addition of a 1/3 volume of 8 M LiCl (to a final concentration of 2 M LiCl), after which the precipitate was pelleted by centrifugation at 26,000 × g for 30 min at 4°C. The supernatant was decanted and discarded.

The pellet was gently dispersed and washed four times in 4 ml of ice cold 2 M LiCl. The samples each time were centrifuged at 12,000 × g for 10 min at 4°C. The supernatant was decanted and discarded. After the final wash the pellet was suspended in 2 ml of 10 mM Tris-HCl (pH 7.5), by warming to room temperature and followed by a gentle vortex. The insoluble materials were pelleted by centrifuging at 12000 × g for 10 min at 4°C. The supernatant was carefully pipetted to another glass Corex tube and 1/10 volume 2 M potassium acetate (pH 5.5) was added, and incubated for 15 min on ice. Centrifugation was followed at 12,000 × g at 4°C for 10 min to remove polysaccharides and insoluble material. The supernatant was transferred to a clean 15 ml Corex tube and RNA was precipitated by adding 2.5 × volume of 100% ethanol and left overnight at -20°C. RNA was pelleted on the next day, by centrifuging for 30 min at 9,000 × g at 4°C. The supernatant containing ethanol was discarded. The RNA pellet was gently washed with 2 ml cold 70% ethanol and centrifuged at 9800 × g for 5 min at 4°C. The supernatant was removed carefully and also residual ethanol was removed under vacuum. The pellet was re-suspended in 200 µl RNase-free water and transferred

to a 1.5 ml tube. The RNA was quantified and stored in aliquots at -20°C. Small aliquots were run on gel to visualise the sharpness of 18S and 25S bands (Section 4.2.7).

4.2.2.2 QIAGEN RNA extraction

A frozen bud sample (20-40 mg) sample was ground in liquid nitrogen. The sample was transferred to 1.5 ml tube. By following the instructions of the manufacturer (QIAGEN), the following method was used. Before starting the extraction 10 µl β-mercaptoethanol was added to 450 ml (RLT) lysis buffer (supplied by the manufacturer), which contained guanidine and isothiocyanate buffer. The frozen ground tissue was added to the lysis buffer and vortex was done vigorously. The lysate was pipetted directly onto a QIAshredder spin column, placed in 2 ml collection tube and was centrifuged for 2 min at 14,000 rpm. Supernatant of the flow-through fraction was carefully transferred to a new micro centrifuge tube without disturbing the cell-debris pellet in the collection tube. Ethanol (96-100%) of 0.5 volumes was added to the cleared lysate and mixed immediately by pipetting. The sample was applied to an RNeasy mini column, placed in a 2 ml collection tube, the tube gently closed and centrifuged for 15 s at 10,000 rpm. The flow-through was discarded. DNase treatment was done at this stage as described by the manufacturer (QIAGEN). After washing with RW1 buffer (supplied by the manufacturer) the RNeasy column was transferred into a new 2 ml collection tube. RPE buffer (supplied by the manufacturer) of 500 µl was pipetted onto the RNeasy column and centrifuged for 15 s at 10,000 rpm, to wash the column. The flow-through was discarded. The second wash with RPE was done and centrifuged for 2 min at 10,000 rpm to dry the RNeasy silica-gel membrane. To eliminate any chance of buffer RPE carryover, RNeasy column was placed in a new 2 ml collection tube and centrifuged at 14,000 rpm for 1 min. The RNeasy column was transferred to a new 1.5 ml collection tube to elute. RNase free water (40 µl) was pipetted directly onto the RNeasy silica gel membrane, and centrifuged for 1 min at 10,000 rpm to elute. RNA quality and quantity was measured using the Nano Drop spectrophotometer (NanoDrop Technologies Inc, Wilmington, D.E., U.S.A).

4.2.3 Genomic DNA isolation

Genomic DNA was isolated from seedling leaves of *E. occidentalis* by adapting the method of McKinnon et al. (1999). About 10 g tissue was ground to a powder under liquid nitrogen using a mortar and pestle, then added to ice cold extraction buffer [3.2% (w/v) sorbitol, 5% (w/v) polyethylene glycol 600, 0.05% (w/v) bovine serum albumin, 0.05% (w/v) spermine, 0.05% (w/v) spermidine, 4% (w/v) polyvinyl pyrrolidone 40, 0.05% (v/v) 2-mercaptoethanol, 15 mM EDTA, 50 mM Tris, pH 8.0]. The homogenate was filtered once through muslin, centrifuged (2000 × g, 5 min) and the pellet retained and suspended in 4 ml wash buffer [6.4% (w/v) sorbitol, 2-mercaptoethanol, 25 mM EDTA, 50 mM Tris, pH 8.0]. To the suspension, 1 ml of NaCl (5 M), 0.8 ml of 8.6% hexadecyltrimethylammonium bromide (0.7 M), and 1.6 ml of 5% (w/v) N-laurylsarcosine were added in order and with mixing. The suspension was incubated for 15 min at ambient temperature and then transferred to a 55°C water bath for 15 min. The solution was extracted twice with 8 ml chloroform:isoamyl alcohol (24:1), with mixing times of 30 and 5 min, respectively, for the first and second extractions. The aqueous phase was separated from the organic phase by centrifugation (2,000 × g, 8 min). DNA was precipitated by addition of 6 ml ice cold isopropanol and collected by centrifugation (2,000 × g, 5 min). The pellet was washed in 1 ml of 50% isopraponol and 0.3 M ammonium acetate mixture for 30 min. The supernatant was removed after centrifugation. The pellet was air dried and re-suspended in TE buffer (10 mM Tris, 1 mM EDTA, pH 7.4) containing RNase (10 µg/ml) and incubated at 37°C for 1 h. DNA was re-precipitated with ethanol and 0.22 mM ammonium acetate, collected by spooling. The spooled fluffy DNA was washed in 70% ethanol and stored at -20°C in TE buffer pH 7.4 for further analyses.

4.2.4 Quantification of total nucleic acids

The quality and quantity were obtained by considering the A_{230}, A_{260}, A_{280}, and A_{320} values of 1/50 and 1/100 dilutions (1 A_{260} = 40 ug RNA ml^{-1}) using an Ultraspec 3000 UV/visible spectrophotometer (Pharmacia Biotech Ltd, Cambridge, U.K.). An A_{230} nm : A_{260} nm : A_{280} nm of 1:2:1 indicated good quality preparation.

4.2.5 Reverse transcription reaction (RT)

Two methods of RT were used for cDNA synthesis. For initial isolations cDNA was prepared using the following methods:

Method 1

One μg RNA, 1 μl oligo dT primer and RNase free sterile water were added to a 1.5 ml reaction tube to make the final volume to 10 μl. This solution was incubated at 65°C for 10 min, in a water bath. A reaction mix was prepared on ice as follows:

5 x buffer	4 μl
100 mM DTT	2 μl
10 mM dNTP mix	2 μl
RNase inhibiter (40 U μl^{-1}) (Roche)*	1 μl
Expand Reverse Transcriptase (Roche)	1 μl

*(Roche Diagnostics GmbH, Penzberg, Germany)

The reaction mix was added to the reaction tube (final volume of 20 μl) and incubated at 42°C for 60 min. After the cDNA synthesis, the reaction was cooled on ice, and stored at -20°C until the PCR reaction.

Method 2

RT reactions were performed by using ThermoScript™ RT-PCR system (Invitrogen Corporation, Carlsbad, CA, USA). In a 1.5 ml reaction tube, 8 μl RNA (around 250 ng), was added. One μl 50 μM Oligo $(dT)_{20}$, 1 μl random primer, and 2 μl 10 mM dNTP mix were added to the RNA. Incubation was carried out at 65°C for 5 min and placed on ice (to denature RNA and primer). Master reaction mix was prepared as follows:

5 × cDNA synthesis buffer	4 μl (was vortexed for 5 s, prior to use)
0.1 M DTT	1 μl
RNaseOUT™ (40 U/μl)	1 μl
DEPC treated water	1 μl
ThermoScript™ RT (15 units/μl)	1 μl

The master reaction mix (8 μl) was added to the reaction tube on ice. The sample was transferred to a thermal cycler, preheated to the cDNA synthesis temperature and incubated for 10 min at 25°C, followed by 40 min at 55°C. The reaction was terminated

by incubating for 5 min at 85°C. 1 µl RNase H was added and incubated for 20 min at 37°C. The prepared cDNA reaction was stored at -20°C for further analysis.

4.2.6 Polymerase chain reaction (PCR)

For amplifying either genomic DNA or cDNA the following reaction mix was used:

10 × Taq buffer	2.0 µl
dNTPs (2 mM)	2.5 µl
25 mM $MgCl_2$	1.0 µl
Primers (10 pmol/µl)	1.0 µl each
cDNA (5-fold diluted)	2.0 µl
Taq DNA polymerase (5 U/µl)	0.2 µl
Water	10.3 µl

The PCR (Thermo Fisher Scientific Inc, M.A., U.S.A) was carried out to synthesise the second cDNA strand using 2 µl (0 to 5-fold) diluted RT reaction. For second round PCR's 2 µl of first round PCR product was used as template. The PCR program was 94°C, 4 min (1 cycle); 94°C, 30 s; 50°C, 30 s; 72°C, 60 s (30 cycles); 72°C, 3 min (1 cycle) and final cooling to 4°C.

4.2.7 Agarose gel electrophoresis and band purification

DNA fragments were separated on 2% agarose gels in 1 × TBE buffer and were run at 100v for 1 h. DNA markers (Invitrogen) were used to estimate the fragment size. After electrophoresis, the gel was stained with ethidium bromide (0.5% (v/v) 10 mg/ml stock solution) and then transferred onto a UV- transilluminator (UVP Inc, San Gabriel, C.A, U.S.A) for photography. The PCR products of appropriate sized bands were cut out of the agarose gel after electrophoresis and purified by using QIAquick® PCR purification kit (QIAGEN) by following the manufacturer's instruction.

4.2.8 Isolation of the partial homologues of meristem identity genes

Partial homologue sequences of meristem identity genes *LEAFY, APETALA1* and *TERMINAL FLOWER1* were isolated by RT-PCR or PCR from either cDNA or genomic DNA from *E. occidentalis* with degenerate primers or specific primers. *LFY* was isolated by the degenerate primers which were designed from conserved regions of *LFY* by McKenzie et al. (1997). To obtain a longer intron-spanning sequence of *LFY*

another *Eucalyptus* specific forward primer described for *E. globulus* was used (Southerton et al., 1998). *TFL1* was isolated by using the primers designed by Sreekantan et al. (2004). *AP1* was isolated by primers which were designed by using the publicly available GenBank sequence of *E. globulus*. The primer sequences are given in Table 4.1. The PCR reactions (50 µl) were run in double wells on 1-2% agarose gels. The correct size bands were cut and gels purified as described in Section 4.2.7. Quantification of DNA for sequencing was done using High DNA Mass Ladder (Invitrogen). The resulting sequences were compared with GenBank sequences.

Table 4.1 Primers used for isolating meristem identity genes.

Gene	Sequence (5′ → 3′)	Reference
LFY	Forward GCGAATTCTTCACCACYACHGCYGARCG	McKenzie et al. (1997)
	Reverse CGGAGATGACAACCTTCTTAG	
	Forward AGGAGCTCGACGACATGATGAACT	Southerton et al. (1998)
TFL1	Forward GGTTATGACAGACCCAGATGT	Sreekantan et al. (2004)
	Reverse CCAACCTGTGGATACCAATG	
AP1	Forward AACCGACAAATCACCTTC	this study
	Reverse CAGAAGTTCCCTTTTATGTC	

4.2.9 Reference genes

Reference genes *α-TUBULIN, 18S RNA, GAPDH,* and *β-ACTIN* were isolated from cDNA by RT-PCR to test the suitability of reference genes for relative quantification of meristem gene expression. The primer sequences were given in Table 4.2. The genes were amplified using cDNA generated from total RNA derived from *E. occidentalis* and the PCR product obtained was gel purified and sequenced and the sequence was compared with GenBank sequences.

4.2.10 Sequencing of isolated meristem identity and reference genes

The required amount of each purified PCR product was pipetted into a 1.5 ml tube with 2 µl BigDye™ Terminator version 3.1 dye (Applied Biosystems, Foster City, C.A., U.S.A) and 3 µl of 5 × sequencing buffer (Applied Biosystems). Primer, either reverse

or forward of 3.2 µl was added (the same primers used for isolation) with a ten-fold dilution to a final concentration of 1 pmol μl^{-1}. Milli-Q water was added to make the final reaction volume to 20 µl. The sequencing was carried out at the Allan Wilson Centre Genome Service, Massey University, Palmerston North, New Zealand, using the ABI.3730 DNA Analyzer (Applied Biosystems).

Table 4.2 Primers used for isolating reference genes.

Gene	Sequence (5′ → 3′)	Reference
α-*TUBULIN*	Forward TCGTTTCGCAGGTCATTT Reverse CAACAACATCAACAGCCAAT	Diaz et al. (1996)
18S RNA	Forward CTCAACGGGGACGGCGGGC Reverse GAGCATCGCACTCTTGTTC	McKinnon et al. (2004)
GAPDH	Forward TAGCCATTTCCAGAACCCTCG Reverse CGGAGATGACAACCTTCTTAG	Brill and Watson (2004)
β-ACTIN	Forward GCGAATTCTTCACCACYACHGCYGARCG Reverse GCGGATCCCCRATCCARACACTGTAYTTCC	Sreekantan (2002)

4.2.11 Sequence verification

Both forward and reverse sequences of the DNA strands were obtained by using both forward and reverse primers in separate reactions. Two to four independent sequences were obtained for each strand of every isolated putative gene. Manual checking of the raw DNA sequence data was done first and compared with electropherograms. The sequence was analysed using the biological sequence alignment editor, BioEdit (Ibis Biosciences, Carlsbad, C.A., U.S.A) to improve the quality and reliability of the data. The sequences of each target gene were aligned using the multiple sequence alignment programme Clustal X (Thompson et al., 1997) and a consensus sequence was obtained for further analysis.

Each edited cDNA sequence was translated in all three reading frames by using the Primer Premier programme (version 5.0) to verify and obtained the right gene homologue from each specific target gene. Both cDNA and protein sequences were searched against the GenBank database at the National Centre for Biotechnology Information (NCBI) (http:/www.ncbi.nlm.nih.gov/BLAST) using the BLAST search programme (Altschul et al., 1990). For each confirmed meristem identity gene (*LFY*, *AP1*, and *TFL1*), the structure of the isolated gene fragment (exon/intron splice sites) and its relative position either in *Eucalyptus* (*ELF*) or *Arabidopsis* (*AP1* and *TFL1*) gene was deduced by comparing its sequence with the GenBank cDNA sequence and genomic sequence.

4.2.12 Phylogenetic analysis

For phylogenetic analysis, 15 homologous sequences were obtained from GenBank that comprised phylogenically diverse as well as related species. All the sequences including the *E. occidentalis* isolates were aligned using Clustal X programme (version 1.8, Thompson et al., 1997). Phylogenetic trees were constructed by using the neighbour joining method (Saitou and Nei, 1987) using the same program or using TreeView, or TreeView program in conjunction with BLAST (version 2.2.15) program. The graphic tree representation was given by TreeView software version 1.6.1 (Page, 1996). All analyses were performed with 1000 bootstrap replicates.

4.2.13 Southern analysis

The procedure was based upon the method described by Southern (1975). Southern analysis was performed on the restriction digested genomic DNA of *E. occidentalis* using non-radioactive probes prepared from the purified PCR products amplified with *LFY*, *AP1* and *TFL1* specific primers.

4.2.13.1 Electrophoresis of DNA digests and blotting

Eucalyptus occidentalis genomic DNA (10 µg) was digested with either *EcoR1* or *BamH1* for analysing each of the three gene homologues (*LFY*, *AP1*, *TFL1*). The digested DNA was loaded onto a 1% (w/v) agarose gel and electrophoresis was carried out overnight by applying current at 1v/cm of gel. The gel was transferred into depurination solution (250 mM HCl) and incubated for 10 min with gentle agitation.

The depurination solution was discarded and the gel rinsed with distilled water. The gel was transferred to denaturation solution (1.5 M NaCl and 0.5 M NaOH) and incubated for 20 min with gentle agitation. Denaturation solution was again discarded and the gel rinsed with distilled water. The gel was covered with neutralising solution (1.5 M NaOH and 0.5 M Tris HCl, pH 7.5) and gently agitated for 30 min. The neutralisation solution was discarded and the gel subjected to overnight capillary blotting to transfer DNA onto Hybond-N+ nylon membrane following the manufacturer's instructions (Amersham Biosciences, Priscotaway, N.J., U.S.A). The following day the membrane was rinsed in 2 × SSC and the DNA fixed by UV cross linking.

4.2.13.2 Probe preparation

The *E. occidentalis* genomic DNA was subjected to PCR using *LFY* or *AP1* or *TFL1* specific primers. The resulting PCR product was purified using QIAGEN PCR purification kit (QIAGEN) and following the manufacturer's instructions. Labelling of probe was carried out using Gene Images random prime labelling kit (Amesham Biosciences). Briefly, 20 µl of diluted purified DNA (3 ng/µl) was denatured by heating in a boiling water bath for 5 min and kept on ice. The labelling reaction mix (50 µl) was prepared by combining nucleotide mix (10 µl), primer (5 µl), denatured DNA (as required) and Klenow fragment (5 units/µl). The reaction mix was incubated at 37°C for 1 h. The reaction was stopped by adding EDTA to 20 mM final concentration. The probes were stored in the dark at -20°C.

4.2.13.3 Hybridisation and detection of non-radioactive probes

For overnight hybridisations, the membranes were placed in hybridisation tubes and hybridisation buffer was added [5 × SSC, 0.1% (w/v) SDS, 5% (w/v) dextran sulphate and 20-fold dilution of liquid block (supplied by the manufacturer)]. The membranes were pre-hybridised with gentle rotation at 60°C for 1 h. Labelled probe was denatured by placing in a boiling water bath for 5 min and added to the hybridisation solution at a concentration of 10 ng/ml. The incubation was continued overnight. The following day, the hybridisation buffer was removed from the tubes and the membranes were washed with 1 × SSC, 0.1% (w/v) SDS at 60°C with rotation for 15 min. The second washing was done using 0.5 × SSC, 0.1% (w/v) SDS under the same conditions used for the first wash. The third wash was repeated as for the second wash. The membranes were

soaked in liquid blocking agent and the detection of labelled probes was performed using Gene Images CDP-Star detection module following the manufacturer's instructions (Amersham Biosciences).

4.2.14 Temporal expression of meristem identity genes

Quantification of meristem identity genes was carried out by real-time quantitative RT-PCR using a LightCycler™ 2.0 instrument (Roche).

4.2.14.1 Primers used for quantification of meristem identity genes

For real-time PCR quantification, the primers were designed by spanning an intron and to give a product size less than 290 bp. Primer Premier (version 5.0, Premier Biosoft International, Palo Alto, C.A., U.S.A) was used to design suitable primers for meristem identity genes and reference gene (Table 4.3).

Table 4.3 Primers used for real-time quantitative RT-PCR.

Gene	Sequence (5′ → 3′)
LFY	Forward AGGAGGAAGTGGAGGAGATGAGGA
	Reverse AGGCGTAGCAGTGGACGTAGTG
AP1	Forward CCTTGACTCACCTGTTGTT
	Reverse CAGAAGTTCCCTTTTATGTC
TFL1	The same primers as used for isolation (Table 4.1)
α-*TUBULIN*	Forward GTATCAACTACCAGCCGCCCACA
	Reverse ACTCGTCACCCTCATCAT

4.2.14.2 Quantitative real-time PCR assay

The FastStart DNA Master SYBR® Green I (Roche Dagnostics) kit was used for carrying out PCR reactions. The reaction was performed in glass capillaries in 20 µl reaction volume. Each reaction mixture was prepared by combining 2.0 µl of 10-20 fold diluted cDNA template, a final concentration of 3.0 mM $MgCl_2$, primers at 0.5 µM each final concentration, 2.0 µl of FastStart DNA Master SYBR® Green I (Roche) and sterile distilled water to make-up to 20 µl volume. The thermal cycling conditions were carried out at an initial denaturation temperature of 95°C for 10 min followed by 45 cycles at 95°C for 10 s, 55°C for 10 s, 72°C for 15 s, and 80-84°C for 1 s. During

thermal cycling the SYBR Green signal was acquired during each cycle at 80-84°C to detect and quantify the fluorescence at a temperature above the denaturation of primer dimers by using a slope of 20°C s^{-1}. At the end of thermal cycling a melting curve was generated using the program, one cycle at 95°C for 0 s, and 50°C for 40 s using a slope of 20°C s^{-1}, followed by 95°C for 0 s using a slope of 0.05°C s^{-1}. The SYBR Green signal was acquired continuously during the melting curve program. Finally the instrument was cooled to 40°C for 1 min before stopping.

4.2.14.3 Optimisation of real-time PCR conditions

To obtain efficient amplification of cDNA (RT reaction), template dilution and $MgCl_2$ concentration were optimised. The RT reaction was used as a series of dilutions (1:10, 1:20, 1:40, 1: 50, 1:80 and 1:100) and three levels of $MgCl_2$ (2, 3 and 4 mM). Four sets of primers specific to *E. occidentalis LFY*, *AP1, TFL1* and *α-TUBULIN* were used in the reactions. The real-time PCR mix and run conditions were the same as described in Section 4.2.14.2.

4.2.14.4 Selection of reference gene for relative quantification

The reference gene for relative quantification was selected based on its reproducibility and uniformity in amplification reactions in RT-PCR with randomly selected experimental bud samples. Four reference genes *α-TUBULIN, 18S RNA, GAPDH,* and *β-ACTIN* were tested. The PCR reactions were performed with cDNA templates derived from five bud samples. The PCR reaction conditions were carried out as described in section 4.2.6. The reference gene primers used were described in Section 4.2.9. Further, the selected reference gene was subjected to real-time PCR quantification of cDNA derived from five randomly selected bud samples. The protocol of real-time PCR was that described in Section 4.2.14.2.

4.2.14.5 Calculation of PCR efficiencies

The PCR efficiencies for target and reference genes were calculated to determine the amplification efficiency of each of the target and reference genes. This was performed by generating standard curves for each gene. Standard curves were generated by the first strand cDNA with serial dilutions of 10, 100, 1,000, 10,000 and 100,000 folds as template. Two to three replicates were taken for each dilution. Real-time quantitative PCR was performed as described in Section 4.2.14.2. A standard curve was obtained

for each gene by plotting the log concentration of the initial DNA on the x-axis and the crossing point (Cp) in cycles on the y-axis: the higher the crossing point,the lower the initial concentration of DNA. The slope of the standard curve was referred to as the efficiency of the curve and was calculated by the LightCycler™ software (version 4.0, Roche) by using the formula

$$E = 10^{(1/slope)}$$

An efficiency of 2.0 indicated a "perfect" PCR amplification with every cycle doubling the quantity of DNA template.

4.2.14.6 Relative quantification of meristem identity genes

The quantification analysis was performed with an amplification program using LightCycler™ 2.0 software version 4.0 (Roche). Relative quantification analysis compares two ratios: the ratio of the target DNA sequence to a reference DNA sequence (e.g.α-*TUBULIN*) in an unknown sample, is compared with the ratio of the same two sequences in a standard sample called a calibrator (in the current experiments vegetative buds were used). In every PCR run, two sets (of 12 samples each) were loaded, one set with the reference gene primers and the other with target gene primers so that the same cDNA template was shared by both target and reference genes. In addition, three replicates of one calibrator sample were included for both target and reference genes to normalise the results. The calibrator contains typical proportions of the target and reference sequences. A negative control or no template control was also included in each run. At the end of each run, relative gene expression was calculated in each sample. The result of a relative quantification analysis was, therefore, expressed as a normalised ratio:

$$\text{Normalised ratio} = \frac{\dfrac{\text{concentration target (sample)}}{\text{concentration reference (sample)}}}{\dfrac{\text{concentration target (calibrator)}}{\text{concentration reference (calibrator)}}}$$

4.3 Results

4.3.1 Meristem identity gene isolation and analysis

4.3.1.1 *LEAFY* (*LFY*)

A partial *LFY* homologue sequence was isolated from *E. occidentalis* using total RNA as well as from genomic DNA employing degenerate (McKenzie et al., 1997) and specific primers (Southerton et al., 1998). By using degenerate primers, a 270 bp (Figure 4.2A) product was obtained from cDNA and by using one specific forward primer and degenerate reverse primer a more than 1000 bp product was obtained from genomic DNA (Figure 4.2B). The putative *LFY,* PCR products were sequenced and from multiple alignments of numerous sequences, a verified 270 bp and 525 bp of product sequences were obtained from cDNA and genomic DNA, respectively. The sequences are given below.

Putative *E. occidentalis LFY* sequence obtained from cDNA:

TGACGAACCAGGTGTTCAGGTACGCGAAGAAGGCGGGAGCAAGCTACATA
AACAAGCCGAAGATGAGGCACTATGTCCACTGCTACGCCCTGCACTGCCTG
GACGAGCACGCCTCCAACGCCCTTCGCAAGAGCTTCAAGGAGCGCGGGGAG
AACGTCGGCGCCTGGAGGCAAGCCTGTTACCACCCCCTGGTCACCATCGCC
GGCCGCAGGGCCGGCTGGGACATCGACGCCATCTTCAATGCCCACCCCCGC
CTCTGCATCTGGTATGTCCC

Putative *E. occidentalis LFY* sequence from genomic DNA:

GGGAGCACCCCTTCATAGTGACGAAGCCCGGGGAGGTGGCGCGTGGGAAG
AAGACCGCCCTGGACTACCTTTTCCTTTTTTAGGACCAGTGCCGGGACTTCT
TCTTCCAATTCCATTCCTTGGCCAAGGAGCGGGGCGAGGAATACCCCACCA
AGGTCCTCCCCCTTTCTTCTTTTTATAGTCTTTCGATACAATCAAACTTCTTC
GAACGTACCCAAGCACGGATCATTCAAACAAGAAGACGATGCAGGTGACG
AACCAGGTGTTCAGGTACGCGAAGAAGGCGGGAGCAAGCTACATAAACAA
GCCGAAGATGAGGCACTACGTCCACTGCTACGCCCTGCACTGCCTGGACGA
GCACGCCTCCAACGCCCTTCGCAAGAGCTTCAAGGAGCGCGGGGAGAACGT
CGGCGCCTGGAGGCAAGCCTGTTACCACCCCCTGGTCACCATCGCCGGCCGCAG
GGCCGGCTGGGACATCGACGCCATCTTCAATGCCCACCCCCGCCTCTGCATCTGGT
ATGTCCC

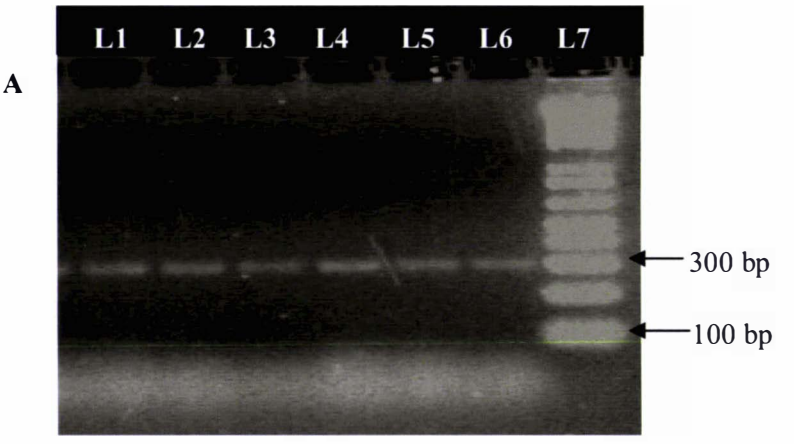

Figure 4.2A Isolation of partial homologue of *LFY* (270 bp) from *E. occidentalis*.
RT-PCR generated cDNA fragments using degenerate primers to amplify putative *LFY*. PCR products were separated by electrophoresis on a 2% (w/v) agarose gel and visualised with ethidium bromide. The relative sizes of the DNA ladder are indicated on the right. L1 to L6: First round RT-PCR product; L7: 1 Kb Plus DNA ladder.

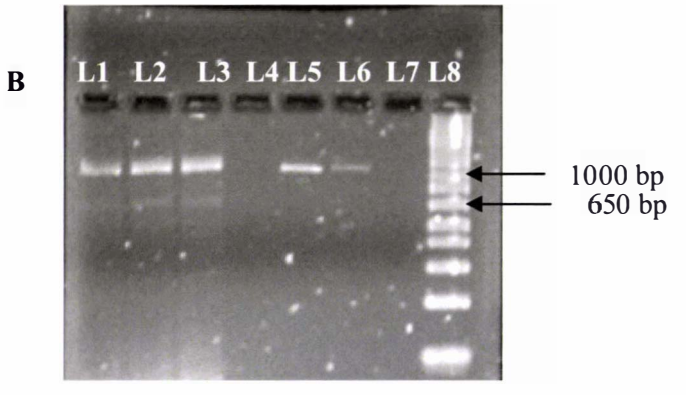

Figure 4.2B Isolation of partial homologue of *LFY* (1000 bp) from *E. occidentalis*.
PCR generated DNA fragments using specific forward primer and degenerate reverse primer to amplify putative *LFY*. PCR products were separated by electrophoresis on a 1% (w/v) agarose gel and visualised with ethidium bromide. The relative sizes of the DNA ladder are indicated on the right. L1 to L3, L5 and L6: First round PCR product; L8: 1 Kb Plus DNA ladder; L4 and L7 were empty:

The identities of these sequences were confirmed by comparing the sequences with GenBank sequences. The confirmed putative *LFY* sequence was given the name *EOLFY*. Conceptual translation of the ORFs of the combined cDNA and genomic DNA sequences yielded an amino acid sequence with 92 amino acids which is given below:

TNQVFRYAKKAGASYINKPKMRHYVHCYALHCLDEHASN ALRKSFKER
GENVGAWRQACYHPLV TIAGRRAGWDIDAIFNAHPRLCIWYVPT

The EOLFY protein sequence was compared with GenBank sequences using BLAST. The sequence showed typical characteristic of *Arabidopsis* LEAFY and *Antirrhinum* FLORICAULA, which displayed the Pfam PFO1698 FLO/LFY protein domain. This protein domain family consists of various plant development proteins which were homologues of FLO/LFY proteins. Mutations in the sequences of these proteins affect flower and leaf development.

The 92 amino acid fragment EOLFY matched to conserved regions of LFY protein. Highest similarity was shared by LFY protein derived from *Eucalyptus globulus* (100%) followed by *Eucalyptus grandis* (98%) and *Metrosideros excelsa* (98%). When the EOLFY protein sequence was compared to other genera, the LFY protein sequences derived from *Lycopersicon* and *Citrus* shared 90% sequence similarity, whereas *Vitis*, *Populus* and *Petunia* showed 89% similarity. *Arabidopsis* displayed 86% similarity. The sequence alignment with various LFY-like proteins in GenBank is displayed in Figure 4.3. The *E. occidentalis* and other Myrtaceae species showed single or double amino acid polymorphism when compared to *Arabidopsis thaliana.* At position 365 and 366, *Arabidopsis* showed arginine and alanine, which were substituted by lysine and serine in *Eucalyptus.* Similarly at postions 382, 387, 392, and 408 single amino acid polymorphisms were observed which were found to be conserved in the Myrtaceae.

A phylogenetic tree was constructed using the isolated EOLFY protein fragment and LFY-like protein sequences derived from GenBank. As observed in Figure 4.4, the Myrtaceae family members *Eucalyptus*, *Metrosideros* and *Syzygium* clustered together. The possible structure of the *EOLFY* gene fragment was deduced by aligning with the *Eucalyptus LFY* sequences derived from the GenBank (GenBank accession number AF034806 and AY 640314). *E. globulus LFY* (GenBank accession number AF034806)

gene structure appears as three exons and two introns and is typical of *Arabidopsis LFY*. The *EOLFY* fragment sequence incorporated the second intron, with 165 bp at the end of exon 2, and continued with intron 2 and to the exon 3 sequence (Figure 4.5).

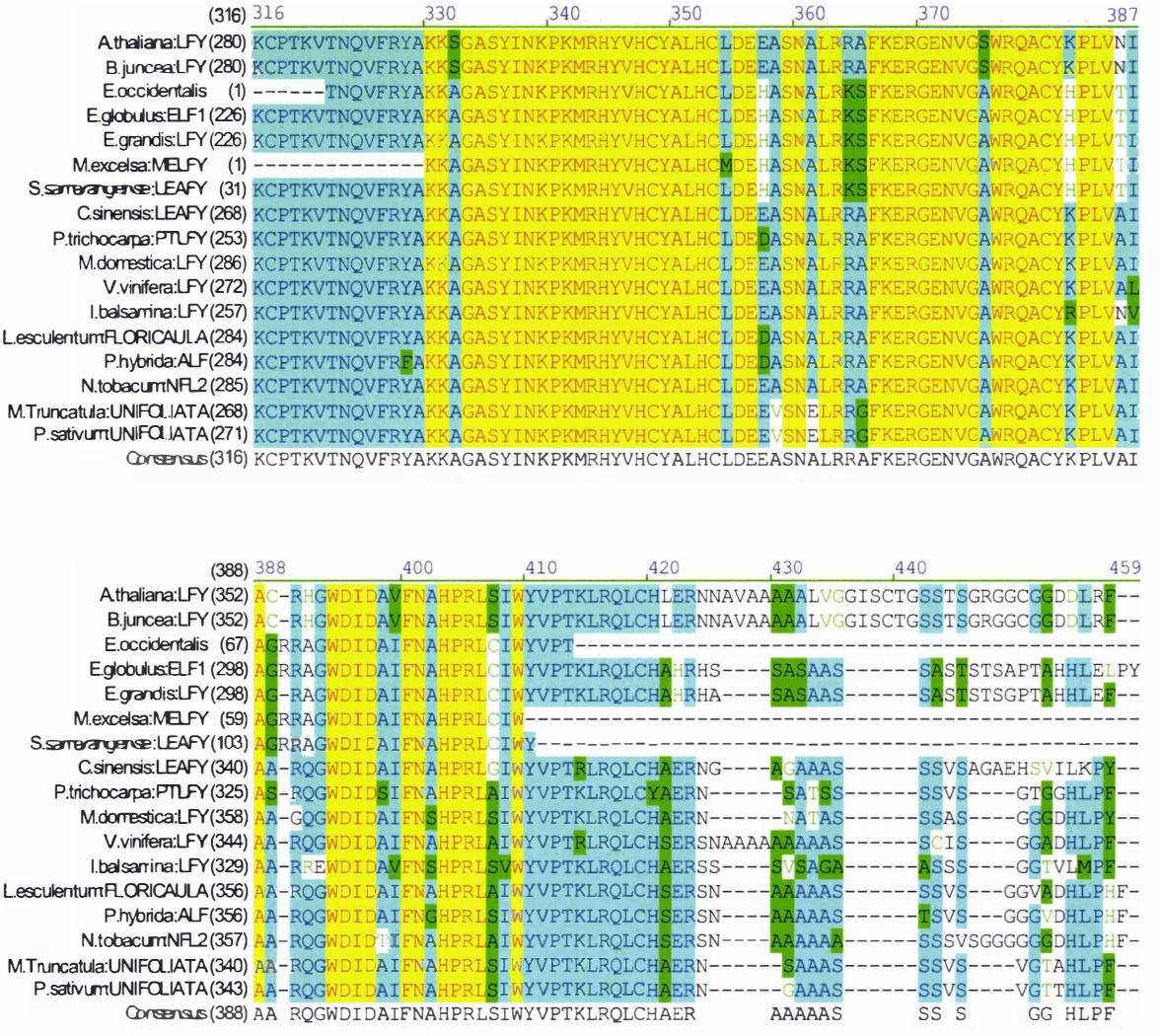

Figure 4.3 Comparison of the amino acid sequence of EOLFY with LFY-like protein sequences from GenBank. Yellow refers conserved regions and blue refers species specific variation.

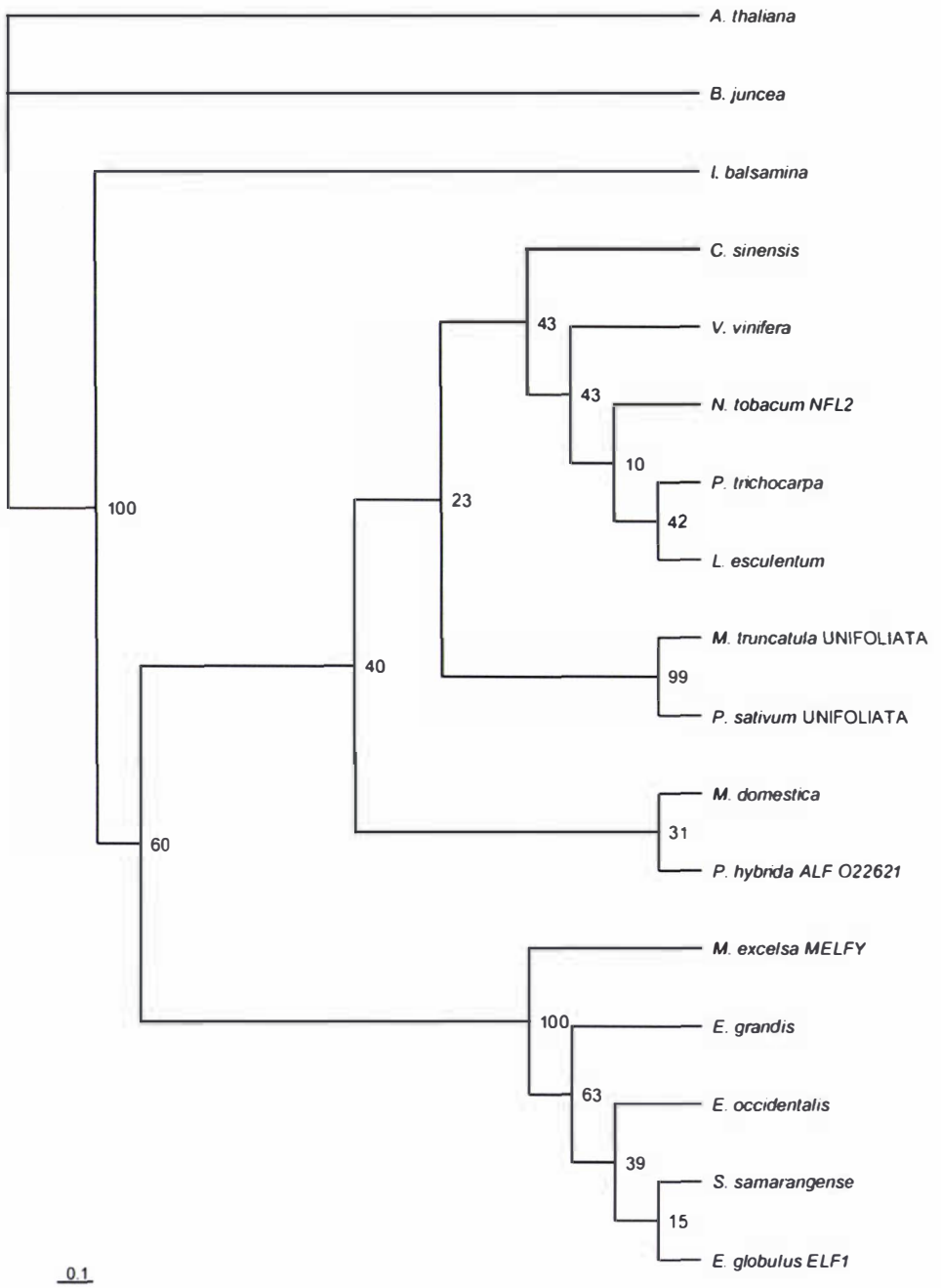

Figure 4.4 Phylogenetic relationships of some *LFY* homologues derived from plants from a wide range of angiosperm species using the neighbour joining method and TreeView software.

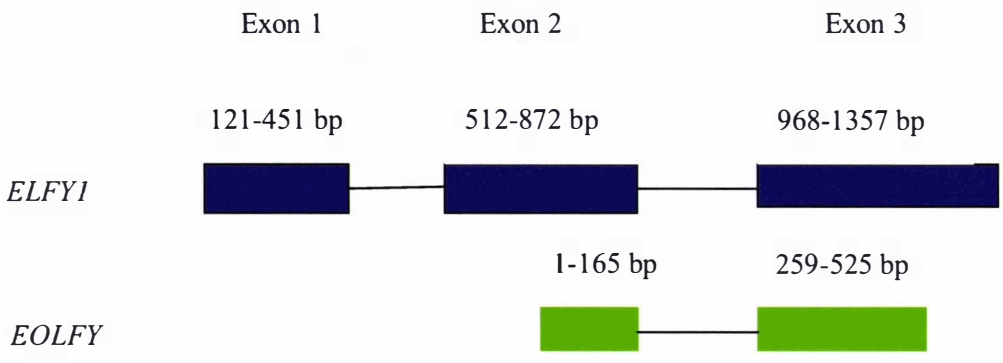

Figure 4.5 Deduced gene structure of *EOLFY* sequence
Based on GenBank derived *E. globulus* (*ELFY1)* sequence (Accession no: AF034806) the putative structure of *EOLFY* fragment was analysed and found to incorporate the second intron.

4.3.1.2 *TERMINAL FLOWER1* (*TFL1*)

A partial *TFL1* homologue was isolated from cDNA of *E. occidentalis* by using *M. excelsa* primers and PCR (Sreekantan et al., 2004). A product of approximately 170 bp was obtained (Figure 4.6). The putative *TFL1* RT-PCR product was sequenced and multiple alignments of more sequencing reactions and a verified 170 bp of product sequence was obtained. The sequence is given below.

Putative *E. occidentalis TFL1* sequence obtained from cDNA:

GATATCAGCCCCATGTTGGTTATGACAGACCCAGATGTGCCTGGTCCTAGTG
ATCCATATCTAAGGGAGCACTTGCACTGGATGGTGACGGACATCCCGGGCA
CAACAGATGCCACATTTGGAAAGAAGGTGGTGGAGTACGAGATGCCGAGG
CCCAACATTGGTATCCACAGGTTCGAACTGATGGCCACGGTTCG

The identity of these sequences was confirmed by comparing with GenBank sequences. The confirmed putative *TFL1* sequence was given the name *EOTFL1*. Conceptual translation of the ORFs of this cDNA sequence yielded an amino acid sequence with 60 amino acids, which is given below:

LVMTDPDVPGPSDPYLREHLHWMVTDIPGTTDATFGKKVVEYEMPRPNIGIHR
FELMATV

The protein sequence was compared with GenBank sequences using BLAST. The sequence showed typical characteristics of TFL1 and CEN homologues. The protein consisted of Pfam profile PFO 1161, phosphatidylethanolamine binding domain also known as Raf-1 kinase inhibitor protein (RKIP). The other TFL1 orthologues, CEN in *Antirrhinum*, and SELF PRUNING (SP) in tomato, also belonged to RKIP protein domain. The highest similarity was shared by TFL1-like protein derived from *M. collina* (100%) followed by *M. excelsa* (98%). When compared with EOTFL1 protein sequence, the TFL1 protein sequences derived from *Lycopersicon* and *Citrus* shared 85 and 88% sequence similarity, whereas *Vitis* and *Populus* showed 87 and 90% similarity, respectively. *Arabidopsis* displayed 83% similarity.

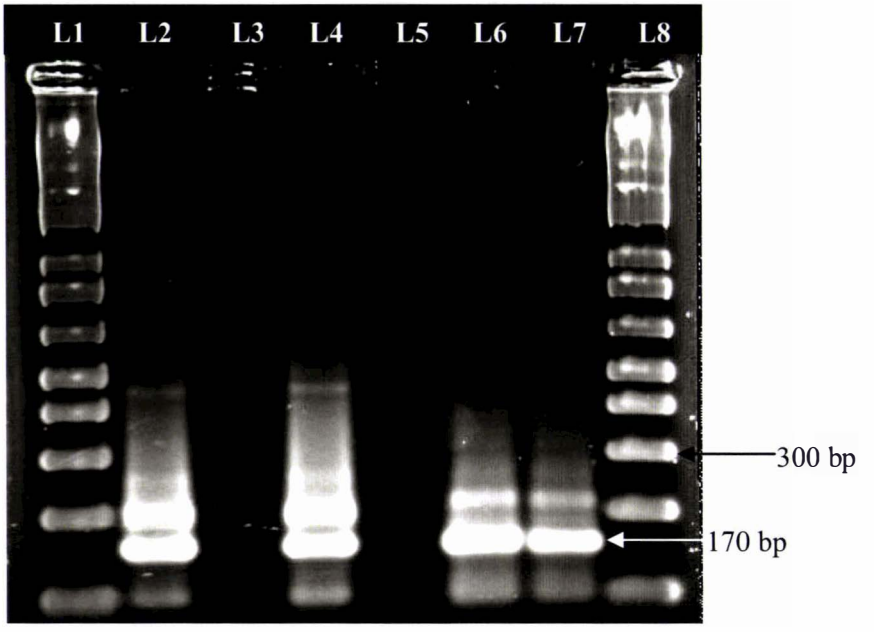

Figure 4.6 Isolation of partial homologue of *TFL1* (170 bp) from *E. occidentalis*

RT-PCR generated cDNA fragments using *M. excelsa* primers to amplify putative *TFL1*. PCR products were separated by electrophoresis on a 2% (w/v) agarose gel and visualised with ethidium bromide. The relative sizes of the DNA ladder and product are indicated on the right. L1 and L8: 1 Kb Plus DNA ladder; L2, L4, L6 and L7: second round RT-PCR product; L3 and L5 were empty.

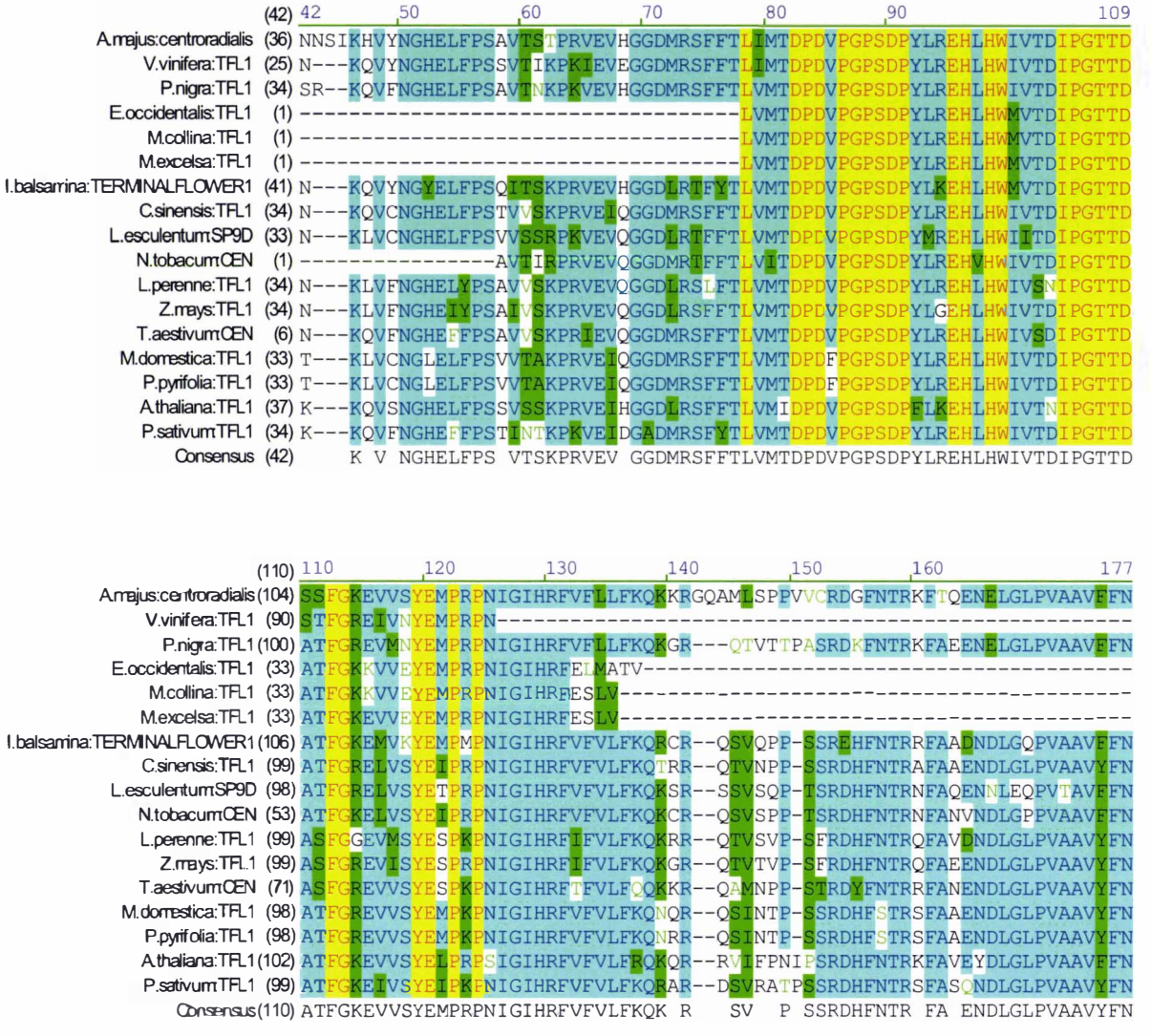

Figure 4.7 Comparison of the amino acid sequence of EOTFL1 with TFL1-like protein sequences from GenBank. Yellow refers the conserved regions and blue refers species specific variation.

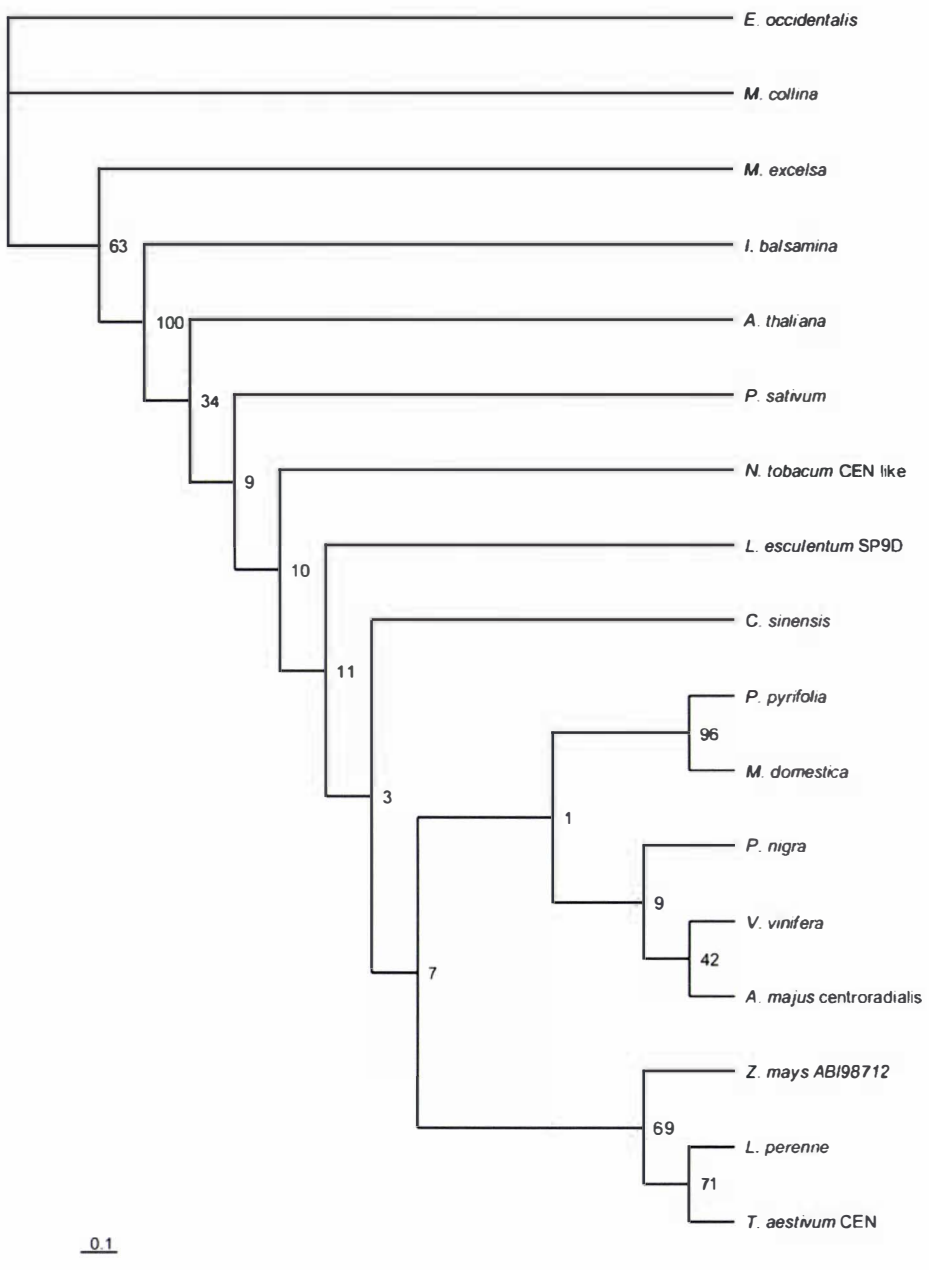

Figure 4.8 Phylogenetic relationships of some *TFL1* homologues derived from plants from a wide range of angiosperms using the neighbour joining method and TreeView software.

The sequence alignment with various CEN or TFL1-like proteins in GenBank is displayed in Figure 4.7. The Myrtaceae family members showed single amino acid polymorphisms at positions 115 (lysine replacing arginine) and 133 (glutamic acid replacing valine). A phylogenetic tree was constructed using the isolated EOTFL1 protein fragment and TFL1-like protein sequences derived from GenBank. As observed in Figure 4.8, the Myrtaceae family members *Eucalyptus* and *Metrosideros* clustered together. The *EOTFL1* gene structure was deduced by aligning with the *Arabidopsis TFL1* gene structure based on The Arabidopsis Information Resource (TAIR) (Accession no: AT5G03840). The putative structure of the *EOTFL1* fragment was analysed and it incorporated introns one to three (Figure 4.9).

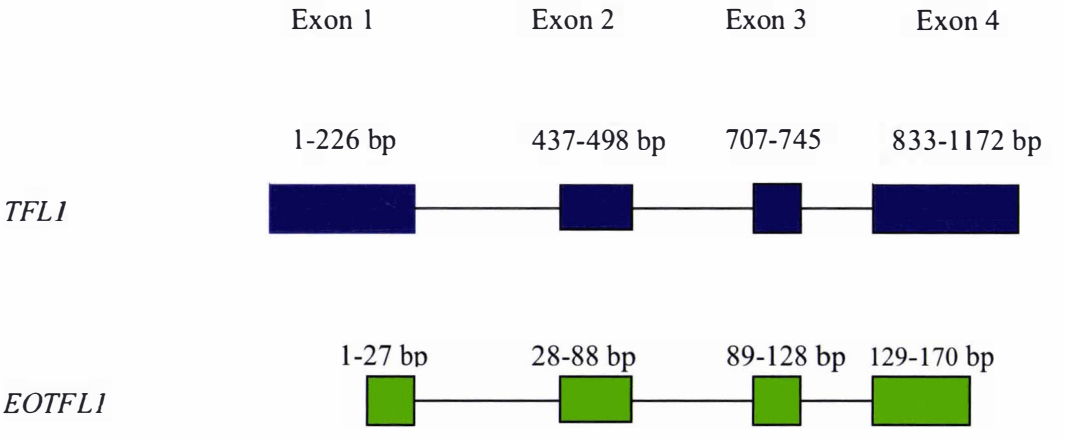

Figure 4.9 Deduced gene structure of the *EOTFL1* sequence (Derived from the *Arabidopsis* Information Resource, TAIR).

4.3.1.3 *APETALA1* (*AP1*)

A partial *AP1* homologue was isolated from cDNA of *E. occidentalis* by RT-PCR by using specific primers. A product of approximately 650 bp was obtained (Figure 4.10). The putative *AP1* RT-PCR product was sequenced and after multiple alignments of more sequencing reactions, a verified 540 bp of product sequence was obtained. The sequence is given below.

Putative *E. occidentalis AP1* sequence obtained from cDNA:

TCCGTACTCTGCGACGCCGAGGTCGCCCTCATCATCTTCTCCGCCAAGGGCA
AGCTCTCGAGTACTCCACCGATTCCTGCATGGAGAGAATTCTCGAACGCTAT
GAAAGATACTCATTGCGGAGCACCAAGTTCTTGCAAGTGAGACGGAATCGA
TTGGTAGCTGGACTTTGGAGCTGCTAAGCTCAAGGCCAGACTTGAAGTTTTA
CACAGAAATTATAGGCATTTCATGGGAAAGATCTTGATTCTTTGAGTCTCAA
GGACCTCCAAAATTTGGAGCAGCAACTGGAGTCTGCTCTTAAACACATAAG
ATCGAGAAAGAATCAGCTCATGCATGAATCAATCTCAGCGCTTCAGAAAAA
GGATAGGGCATTGCAGGAGCAAAACAACCTGCTTACAAAGAAAGTAAAGG
AGAAGGAGAGGGCACTAGCACAGCAAGCTCAGTGGGAGCAGCAAGACCAT
GCCCTTGACTCACCTGTTGTTCTACCCCACTACTTGCCATCTCTCGACACCAA
TGGCTCTTATCAAGCGAGACA

The identity of this sequence was confirmed by comparing with GenBank sequences. The confirmed putative *AP1* sequence was given the name *EOAP1*. Conceptual translation of the ORFs of this cDNA sequence yielded an amino acid sequence with 179 amino acids which is given below:

SVLCDAEVALIIFSAKGKLFEYSTDSCMERILERYERYSYAEHQVLASETESIGS
WTLEHAKLKARLEVLHRNYRHFMGKDLDSLSLKDLQNLEQQLESALKHIRSRK
NQLMHESISALQKKDRALQEQNNLLTKKVKEKERALAQQAQWEQQDHALDSP
VVLPHYLPSLDTNGSYQAR

When this sequence was compared with GenBank sequences using BLAST, the sequence showed typical characteristics of *AP1* homologue with characteristic MADS-box domain and K box domain. The EOAP1 sequence started in the middle of the MADS-box domain. The highest similarity was shared by AP1-like protein derived from *E. globulus* (98%) followed by *Betula pendula* (88%) and *Vitis vinifera* (87%). When compared with EOAP1 protein sequence, the AP1 protein sequences derived from *Lycopersicon* and *Citrus* shared 86 and 80% sequence similarity, whereas *Populus* showed 81% and *Antirrhinum* displayed 88% similarity. With *E. globulus AP2* 81% similarity was obtained indicating that the isolated gene was the homologue of *AP1*. The sequence alignment with various AP1-like proteins in GenBank is displayed in

Figure 4.11. At the position 254 in the protein sequence (Fig 4.11) which is in the middle of MADS-box domain, there is a glutamic acid and at position 262 alanine in EOAP1 which matched to the EAP1 sequence. Whereas, in the same positions in EAP2 an aspartic acid and a threonine were recorded. Similarly in the middle of the K-box region in EOAP1 the aminoacids at positions 329 to 332 were tyrosine, arginine, histidine and phenylalanine, which matched to EAP1. In the case of EAP2, the amino acids at these positions were glutamine, lysine, asparagines, and leucine, respectively (Fig 4.11).

A phylogenetic tree was constructed using the isolated EOAP1 protein fragment and AP1- like protein sequences derived from GenBank. As observed in Figure 4.12, *E. occidentalis* AP1 protein showed close similarity with *E. globulus* AP1 and less similarity (81%) to AP2. The *EOAP1* gene structure was deduced by aligning with the *Arabidopsis AP1* gene structure (TAIR accession no AT1G 69120) and, based on the gene structure, the *EOAP1* sequence incorporated introns one to seven (Figure 4.13).

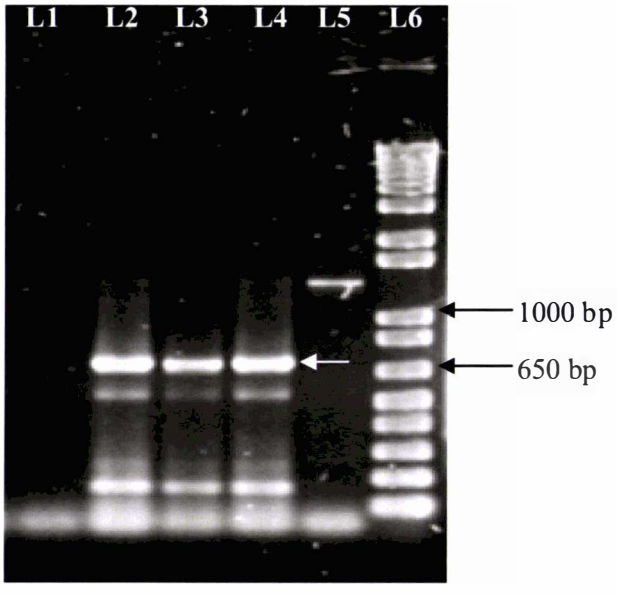

Figure 4.10 Isolation of partial homologue of *AP1* (650 bp) from *E. occidentalis*. RT-PCR generated cDNA fragments using specific primers to amplify putative *AP1*. PCR products were separated by electrophoresis on a 0.8% (w/v) agarose gel and visualised with ethidium bromide. The relative sizes of the DNA ladder are indicated on the right. L2 – L4: First round RT-PCR product; L6: 1 Kb Plus DNA ladder; L5: genomic DNA product; L1: template negative control.

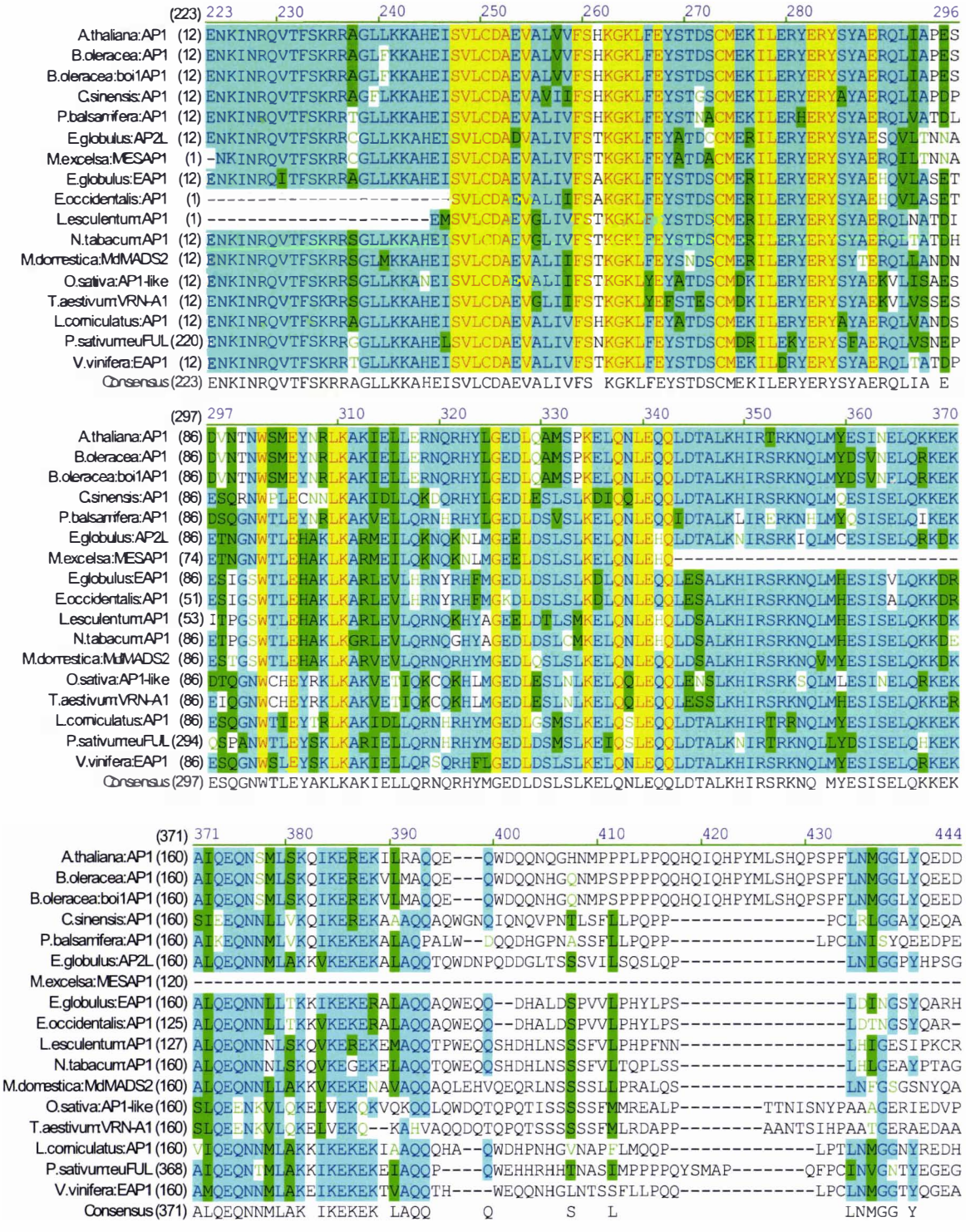

Figure 4.11 Comparison of amino acid sequence of EOAP1 with AP1-like protein sequences from GenBank. Yellow refers the conserved regions and blue refers species specific variation.

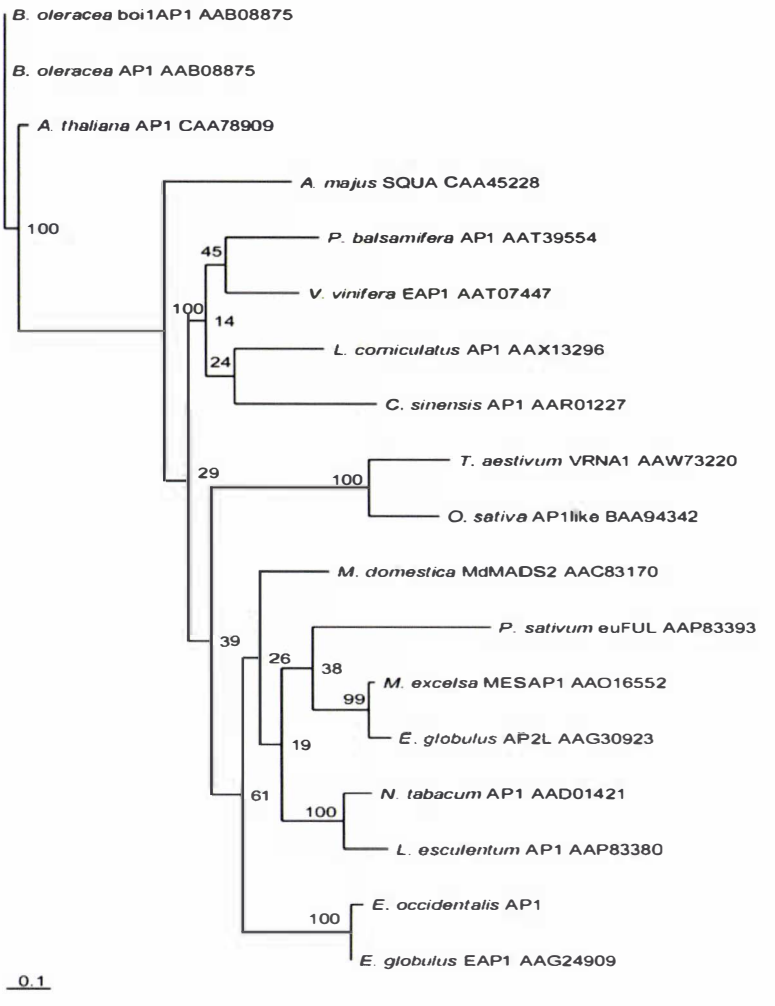

Figure 4.12 Phylogenetic relationship of some *AP1* homologues derived from plants from a wide range of angiosperms using neighbour joining method and TreeView software.

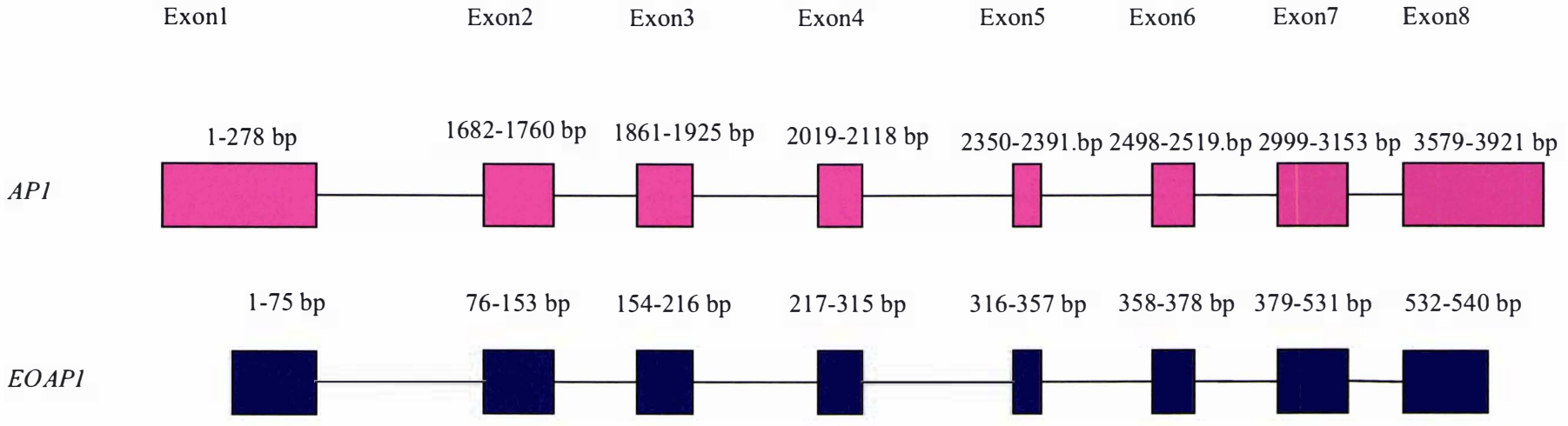

Figure 4.13 Deduced gene structure of the *EOAP1* sequence.
Based on The *Arabidopsis* Information Resource (TAIR), *A. thaliana* (*AP1)* sequence (Accession no: AT1G69120), the putative structure of *EOAP1* fragment was derived which incorporated introns one to seven.

4.3.2 Isolation and identification of reference genes

For quantification of meristem identity gene expression, the reference genes indicated below were isolated from *E. occidentalis*. The primer designs were based on the *Eucalyptus* sequences available in the GenBank database.

4.3.2.1 α-*TUBULIN*

A partial α-*TUBULIN* homologue was isolated from cDNA of *E.occidentalis* by RT-PCR by using specific primers. A product of approximately 650 bp was obtained (Figure 4.14). The putative α-*TUBULIN* RT-PCR product was sequenced and by multiple alignments of more sequencing reactions, a verified 480 bp of product sequence was obtained. The sequence is given below:

Putative *E. occidentalis* α-*TUBULIN* sequence obtained from cDNA:

TGGCTGAGATCACCAACAGCGCTTTCGAGCCATCCTCTATGATGGCCAAGTGCG
ACCCTCGCCATGGGAAATACATGGCATGCTGCCTCATGTACCGTGGTGATGTGG
TGCCCAAGGACGTGAACGCAGCTGTGGCAACCATCAAGACCAAGCGCACCATCC
AGTTCGTCGACTGGTGCCCCACCGGATTCAAGTGCGGTATCAACTACCAGCCGC
CCACAGTTGTCCCTGGAGGCGACCTCGCCAAGGTCCAGAGGGCTGTGTGCATGA
TCTCCAACTCAACCAGCGTTGCTGAGGTCTTCTCGCGCATTGACCACAAGTTCGA
TCTGATGTATGCCAAGCGTGCCTTTGTGCACTGGTACGTGGGTGAGGGTATGGA
GGAGGGTGAGTTCTCTGAGGCTCGGGAGGATCTCGCTGCCCTCGAGAAGGATTA
TGAGGAGGTTGGTGCAGAGTTGGCTGAGGGCGAGGATGATGAGGGTGACG

The identity of the sequence was confirmed by comparing with available GenBank sequences using BLAST programme.

4.3.2.2 *GAPDH*

A partial *GAPDH* homologue was isolated from cDNA of *E.occidentalis* by RT-PCR by using specific primers. A product of approximately 380 bp was obtained (Figure 4.14). The putative *GAPDH* RT-PCR product was sequenced and by multiple alignments of more sequencing reactions, a verified 320 bp of product sequence was obtained. The sequence is given below:

Putative *E. occidentalis GAPDH* sequence obtained from cDNA:

GCCATGGGGAAGGTCAAGATCGGAATCAACGGTTTCGGAAGGATCGGTC
GTTTGGTCGCTGCCATGGGAAATACATGGCATGCTGCCTCATGTACCGTG
GTGATGTGGTGCCCAAGGACGACCGACTACATGACGTACATGTTCAAGT
ACGACAGTGTCCACGGACAGTGGAAGCATAACGAGCTCAAGGTCAAGGA
CACCAAGACGCTTCTCTTCGGCGAGAAGGAGGTCTCCGTTTTTGGCATCA
GGAACCCCGAGGAGATTCCATGGGGCGAGACTGGAGCTGAGTTCATCGT
GGAATCTACCGGTGTCTTCACCGACAAGGAAAA

The identity of the sequence was confirmed by comparing with available GenBank sequences using BLAST programme

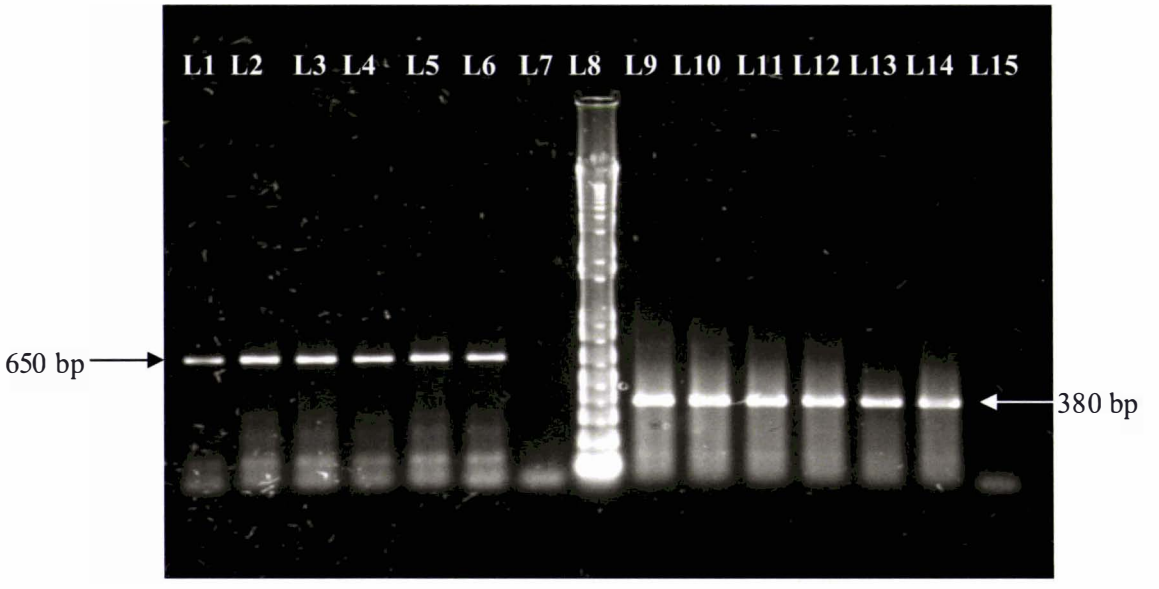

Figure 4.14 Isolation of partial homologue of α-*TUBULIN* (650 bp) and *GAPDH* (380 bp) from *E. occidentalis*.
RT-PCR generated cDNA fragments using specific primers to amplify putative α-*TUBULIN* and *GAPDH*. PCR products were separated by electrophoresis on a 1.5% (w/v) agarose gel and visualised with ethidium bromide. The relative sizes of the products are indicated on the right and left. L1 – L6: First round RT-PCR product of α-*TUBULIN*; L8: 1 Kb Plus DNA ladder; L9-14: First round RT-PCR product of *GAPDH*; L7, L15: template negative controls.

4.3.2.3 *18S RNA*

A partial *18S RNA* homologue was isolated from cDNA of *E. occidentalis* by RT-PCR by using specific primers. A product of approximately 180 bp was obtained (Figure 4.15). The putative *18S RNA* RT-PCR product was sequenced and by multiple alignments of more sequencing reactions, a verified 180 bp of product sequence was obtained. The sequence is given below:

Putative *E. occidentalis 18S RNA* sequence obtained from cDNA:

AACTCAACGGGGACGGCGGGCACAGCCCGACGTCCCTCTCGACGCCGAG
GATCCGGCTCGGGCTCCTTAGGGCGCTCGGTCTTTGTCCTCGGCGGCACA
ACGAACCCCGGCGCGGAATGCGCCAAGGAACTTGAACAAGAGTGCGATG
CTCCCGCCGCCCCATACACGGTGCGCGCGCGG

The identity of the sequence was confirmed by comparing with available GenBank sequences using BLAST programme

4.3.2.4 *β-ACTIN*

A partial *β-ACTIN* homologue was isolated from cDNA of *E. occidentalis* by RT-PCR by using degenerate primers. A product of approximately 450 bp was obtained (Figure 4.16). The putative *β-ACTIN* RT-PCR product was sequenced and by multiple alignments of more sequencing reactions, a verified 335 bp was obtained. The sequence is given below:

Putative *E. occidentalis β-ACTIN* sequence obtained from cDNA:

GCTCTTCTGTCGAGAAAAACTATGAGCTGCCTGATGGACAAGTCATCACA
ATCGGGGCTGAGAGATTCCGTTGCCCAGAAGTCCTCTTCCAGCCATCATT
GATTGGAATGGAAGCTGCTGGAATTCATGAAACCACCTACAACTCCATCA
TGAAGTGTGATGTGGATATCAGGAAGGATCTTTATGGCAATATTGTGCTT
AGTGGTGGTTCCACTATGTTCCCTGGTATTGCAGACAGGATGAGCAAGGA
GATTACTGCTCTTGCTCCAAGCAGCATGAAGATYAAGGTGGTTGCACCSC
CAGAGAGGAAATACAGTGTCTGGATTGGGGATCCG

The identity of the sequence was confirmed by comparing with available GenBank sequences using BLAST programme

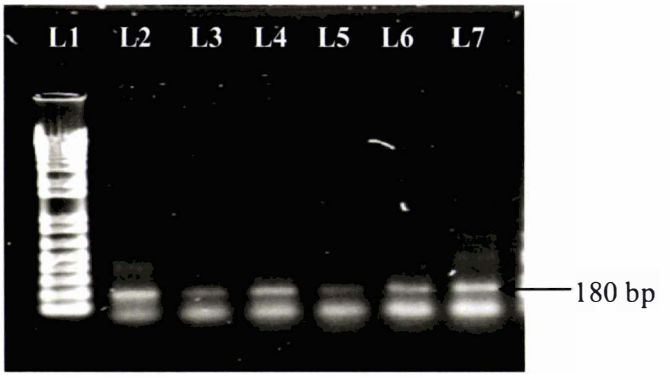

Figure 4.15 Isolation of partial homologue of *18S RNA* (180 bp) from *E. occidentalis*. RT-PCR generated cDNA fragments using specific primers to amplify putative *18S RNA*. PCR products were separated by electrophoresis on a 2% (w/v) agarose gel and visualised with ethidium bromide. The relative size of the product is indicated on the left. L1 – 1 Kb Plus DNA ladder; L2-L7: First round RT-PCR product of *18S RNA*.

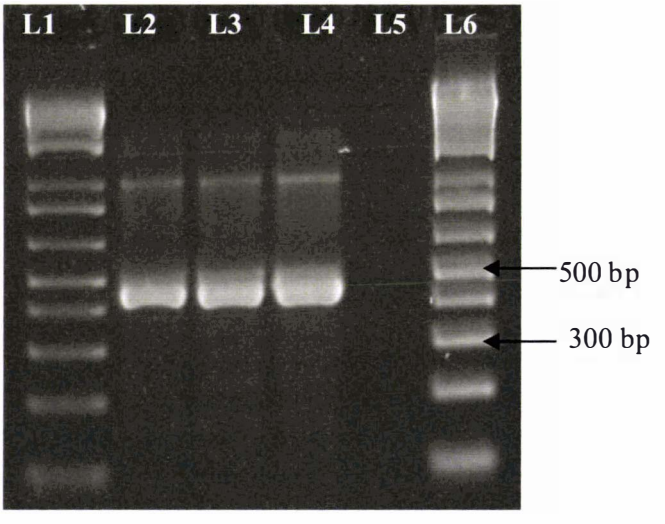

Figure 4.16 Isolation of partial homologue of *β-ACTIN* (450 bp) from *E. occidentalis*. RT-PCR generated cDNA fragments using specific primers to amplify putative *β-ACTIN*. PCR products were separated by electrophoresis on a 1.5% (w/v) agarose gel and visualised with ethidium bromide. The relative sizes of the DNA ladder are indicated on the left. L1 and L6: 1 KbPlus DNA ladder; L2-LL4: First round RT-PCR product of *β-ACTIN*; L5 was empty

4.3.3 Southern analysis

Southern analysis showed two bands (one small and one large) when the blot was probed with the *EOLFY* fragment (Figure 4.17 A); three bands (two weak and one strong) were observed when the blot was probed with *EOTFL1* fragment (Figure 4.17 B). The *EOAP1* probe fragment yielded one single band (Figure 4.17 C).

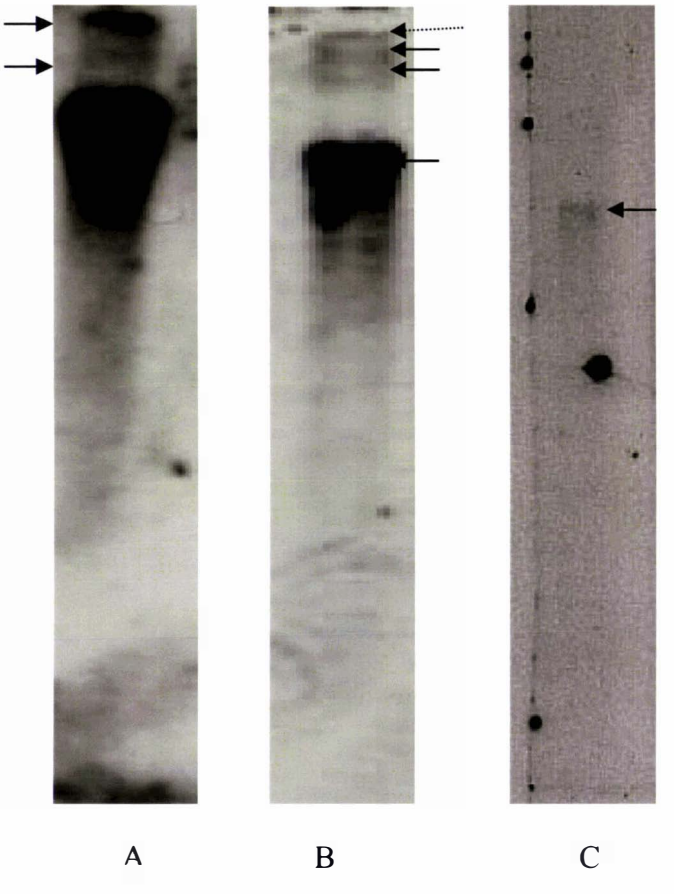

Figure 4.17 Southern analysis of *E. occidentalis* genomic DNA after restriction digestion.
A: Restriction digestion with *EcoR1* and probed with *EOLFY*.
B: Restriction digestion with *Bam H1* and probed with *EOTFL1*.
C: Restriction digestion with *EcoR1* and probed with *EOAP1*
The membrane was washed after probing with high stringency washes (1 × SSC, 0.1% (w/v) SDS at 60°C) to remove non-specific binding. Black arrows indicate the gene band and dotted arrow is a pencil mark.

4.3.4 Temporal expression of meristem identity genes using qRT-PCR during growth and development in response to shoot architectural modification

The expression of *EOLFY*, *EOAP1*, and *EOTFL1* from *E. occidentalis* was analysed in response to shoot architecture manipulation involving the single stem and free branching plants described in Section 2.2.1

4.3.4.1 Total RNA extraction from bud samples

Due to low sample size (20-40 mg) the RNA extraction protocols needed strict optimisation. Total RNA isolated using a RNase Plant Minikit (QIAGEN) was generally of good quality, with a 260/280 ratio of 1.8 to 2.0 in elution buffer. However, it was difficult to get consistent yields. Ethanol precipitation after elution yielded just enough good quality RNA for further analyses. The Nano drop RNA yield measurements ranged from 50 to 800 ng/µl, and with a total yield of 2 to 32 µg in the samples.

The integrity and size distribution of total purified RNA was checked by gel electrophoresis. The respective ribosomal bands appeared as sharp bands on the stained gels (Figure 4.18). 25S ribosomal RNA bands presented with an intensity approximately twice that of the 18S bands. On-column DNase treatment was critical to ensure that the RNA was free from genomic DNA.

4.3.4.2 Reference gene validation by RT-PCR

To select suitable reference genes that could be amplified reproducibly from the bud samples, five randomly selected bud samples were used to produce cDNA using RT-PCR. The amplification product of *18S RNA* and *α-TUBULIN* are shown in Figure 4.19. *α-TUBULIN,* but not *18S RNA*, gave reproducible and uniform results. Amplification of *β-ACTIN* occurred in only three out of five samples tested (Figure 4.20A). The amplification of *GAPDH* in bud samples was poor and not reproducible (Figure 4.20B). Consequently, among the reference genes tested, *α-TUBULIN* was selected as the most suitable gene for the relative quantification experiments.

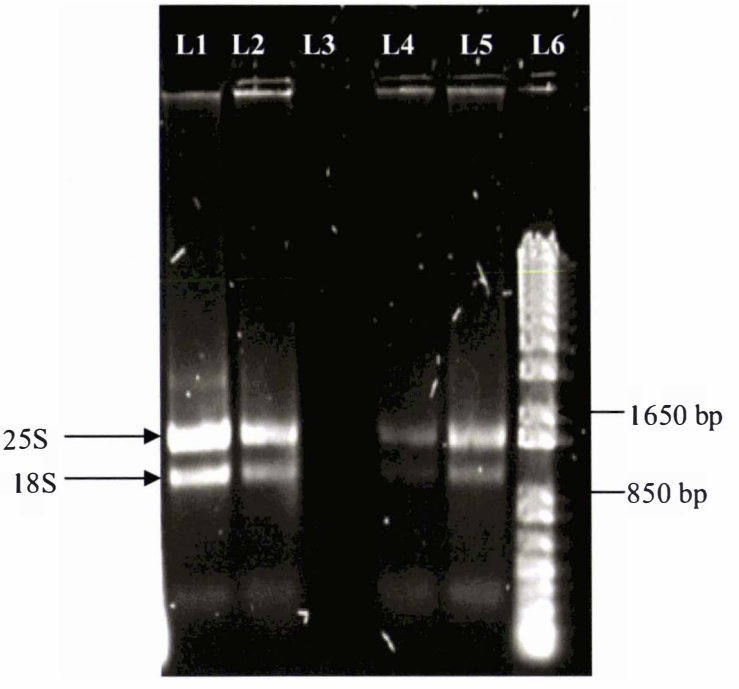

Figure 4.18 Example of total RNA (RNA integrity) used for gene expression assays.

RNA was isolated using RNeasy mini kit (QIAGEN) and 5 µl of total RNA eluate was loaded in each well of 1% agarose gel and electrophoresis was carried out. Relative sizes of the DNA ladder are indicated on the left and the identity of the RNA bands is indicated on the right. L1, L2, L4 and L5, total RNA isolations from random bud samples; L6, 1 Kb Plus DNA ladder; L3, empty.

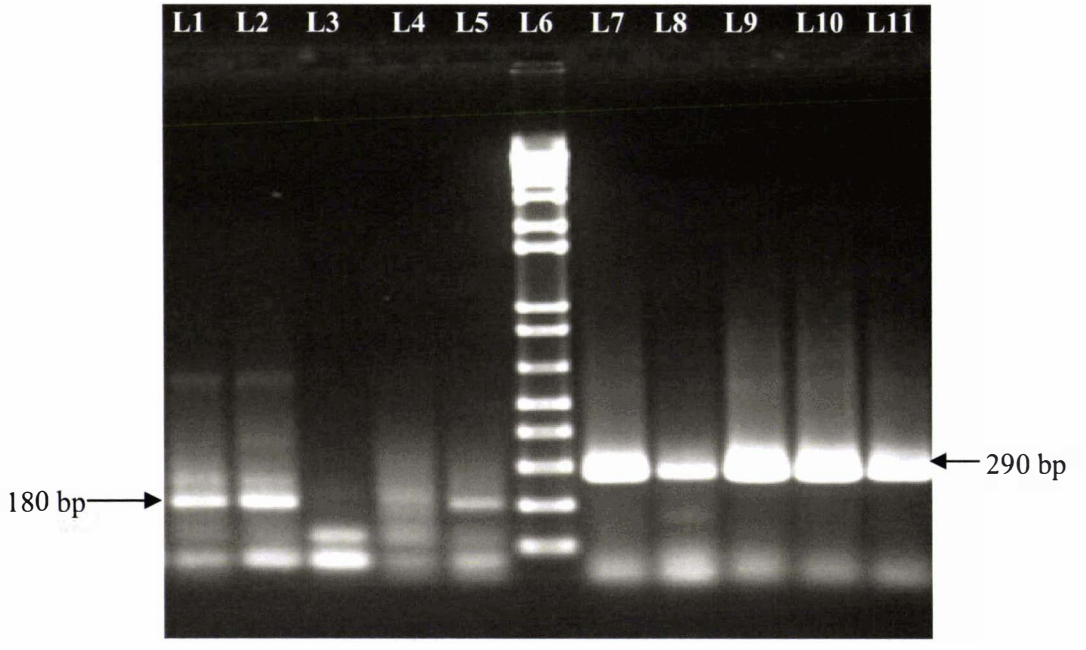

Figure 4.19 Expression of potential reference genes *18S RNA* and *α-TUBULIN* in random bud samples of *E. occidentalis*.
RT-PCR generated reference gene products were separated by electrophoresis on a 2% (w/v) agarose gel and visualised with ethidium bromide. The size of the *18S RNA* is indicated on the left and *α-TUBULIN* on the right. L1 – L5, First round RT-PCR product of *18S RNA* in five bud samples; L6, 1 Kb Plus DNA ladder
L7-L11: First round RT-PCR product of *α-TUBULIN* in five bud samples.

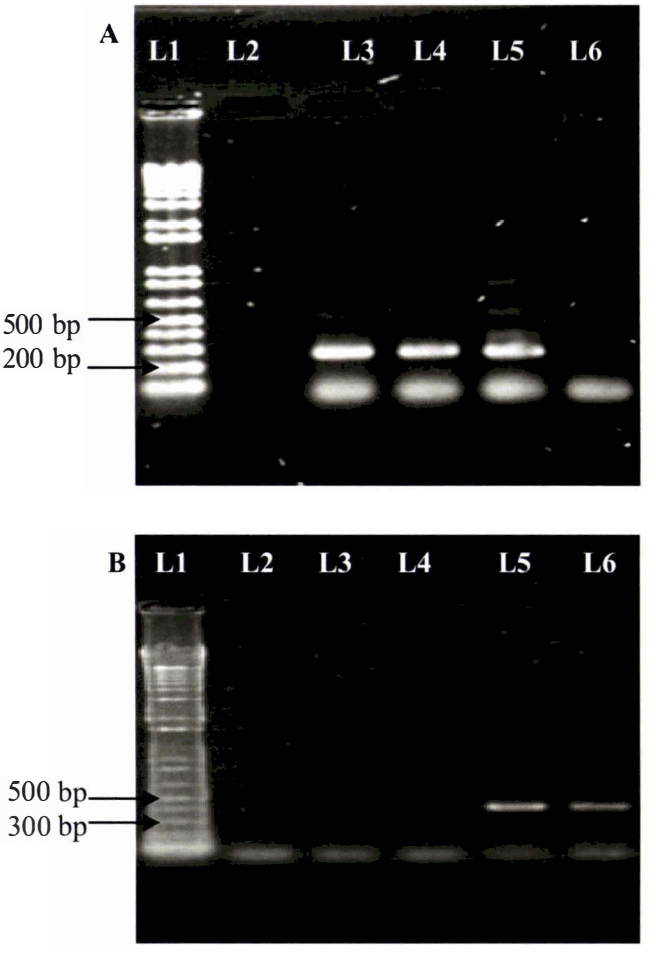

Figure 4.20A and B Expression of potential reference genes *β-ACTIN* and *GAPDH*, respectively in random bud samples of *E. occidentalis*. RT-PCR generated reference gene products were separated by electrophoresis on a 1.5% (w/v) agarose gel and visualised with ethidium bromide. Panel A, L2 – L6, first round RT-PCR product of *β-ACTIN* in five bud samples. Panel B, L2-L6, first round RT-PCR product of *GAPDH* in five bud samples. Panel A&B, L1, 1 Kb Plus DNA ladder

4.3.4.3 Real time PCR optimisation: determination of template and $MgCl_2$ concentration

In this experiment the cDNA template and $MgCl_2$ concentration were optimised. The Table 4.4 shows the Cp values derived from the amplification reactions conducted at various template dilutions and $MgCl_2$ concentrations. Figure 21A-D depicts the amplification curves used to generate these Cp values. The difference in amplification curves (Cp values) for each meristem identity and reference gene was observed from a single bud sample template. These results indicated that a $MgCl_2$ concentration at 3mM gave the lower Cp values (29.00 to 33.70) indicating better efficiency in amplification. The template dilutions at 10 and 20-fold were found to be more suitable when compared to other dilutions tested. Further, to make the gene expression comparisons more accurate, the sizes of the PCR products of the genes (*EOLFY*, *EOAP1*, *EOTFL1* and *α-TUBULIN*) to be compared were kept similar (170 to 290 bp).

Table 4.4 Optimisation of real time PCR with cDNA derived after RT reaction for template dilution and $MgCl_2$ concentrations.

Template dilution (fold)	$MgCl_2$ (mM)	Cp values			
		LEAFY	*AP1*	*TFL1*	*α-TUBULIN*
10	2	30.42	33.80	30.46	31.46
20	2	30.79	33.64	30.60	31.45
40	2	30.83	34.11	NA	32.83
50	2	29.16	34.10	31.10	32.24
80	2	30.62	34.00	NA	31.59
100	2	30.48	34.03	30.91	32.65
10	3	29.24	31.88	28.83	29.19
20	3	29.22	31.99	29.00	29.29
40	3	29.61	32.24	29.55	29.61
50	3	29.68	32.90	29.84	29.49
80	3	29.65	32.69	29.26	30.71
100	3	30.15	33.70	29.64	29.42
10	4	30.76	35.73	33.39	33.85
20	4	31.08	35.98	33.06	34.17
40	4	31.63	35.67	33.58	33.44
50	4	30.81	35.29	34.61	33.69
80	4	30.76	34.58	34.17	33.48
100	4	NA	36.30	34.10	NA

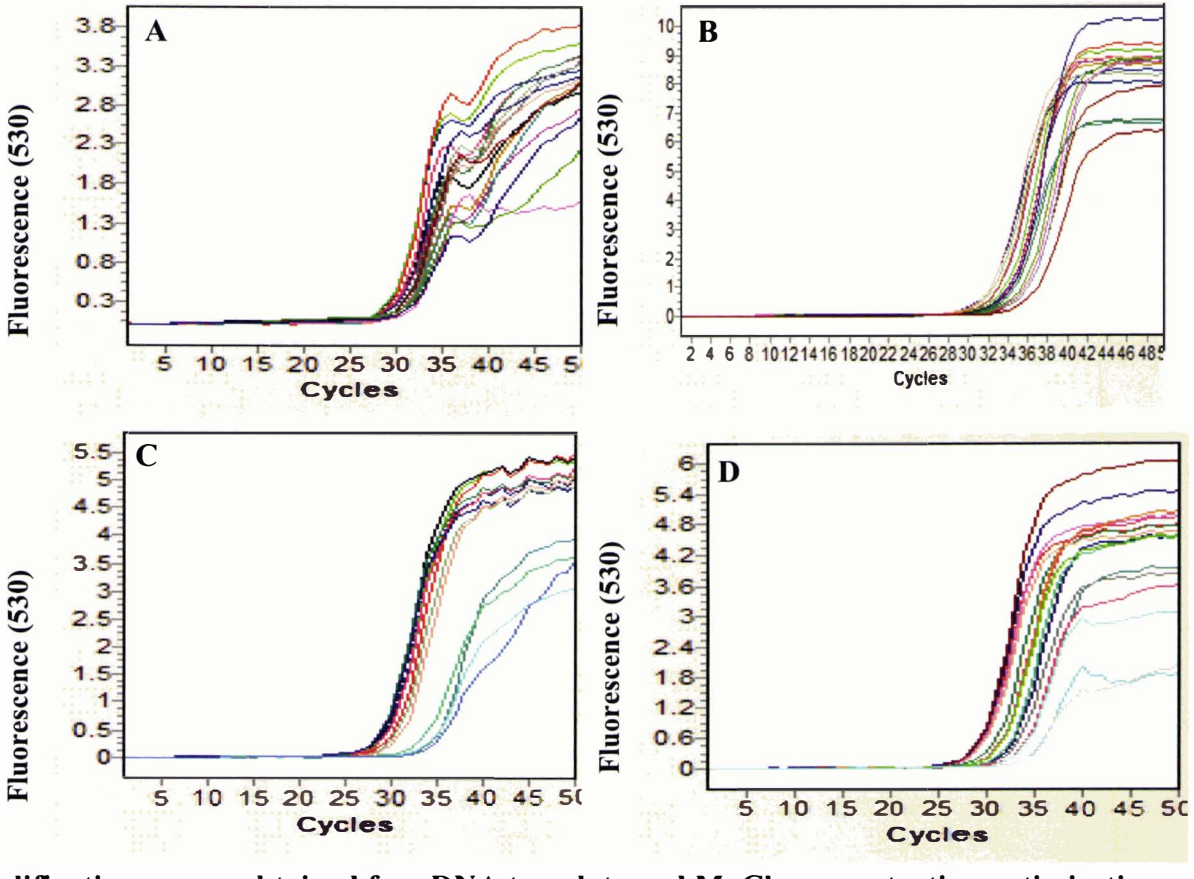

Figure 4.21 Amplification curves obtained for cDNA template and $MgCl_2$ concentration optimisation assay. (*A*)*EOLFY,* (*B*) *EOAP1,* (C) *EOTFL1,* (D) *α-TUBULIN.* cDNA derived from a bud sample was diluted to give 10, 20, 40, 50, 80 and 100 fold dilution and mixed in combination with 3 levels (2, 3, and 4 mM) of $MgCl_2$ concentration. Displayed are the differences in amplification curves (Cp values) for each meristem identity and reference gene.

4.3.4.4 Performance of *α-TUBULIN* in LightCycler™ experiments

To test the amplification performance of α-*TUBULIN* in five randomly selected bud samples, and also to demonstrate any variability between samples, real-time PCR was performed. The amplification curves are shown in Figure 4.22. The mean Cp value was 23.29 ± 0.24 (S.E.) indicating relatively uniform performance across the samples.

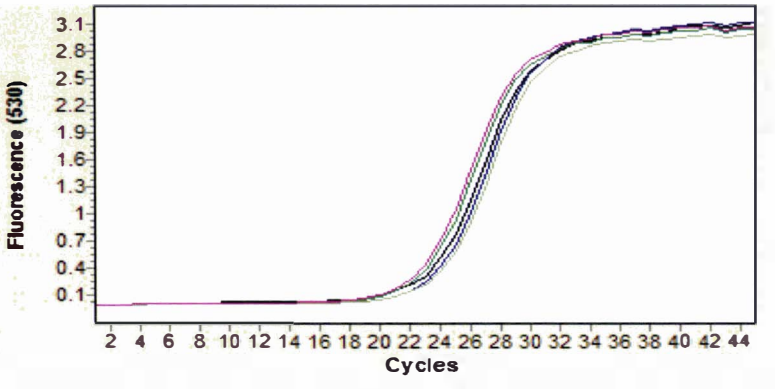

Figure 4.22 Amplification performance of *α-TUBULIN* in five randomly selected bud samples. The template cDNA (15-fold dilution) was used in combination with 3 mM $MgCl_2$ concentration. The Cp values were 23.4, 22.8, 23.7, 23.8 and 22.6 with a mean of 23.29 ± 0.24.

4.3.4.5 PCR amplification efficiency determination

To enable accurate comparison when performing the relative quantification experiments, PCR efficiency values for the target and reference genes must be specified. Accuracy of the results from a relative quantification depends on the PCR efficiency of both target and reference genes. A standard curve, based on serial dilutions of an external standard (one of the RT reactions), was used to determine the efficiency of the PCR for both target and reference genes.

The PCR efficiency values were determined by generating a standard curve between starting cDNA concentrations and corresponding Cp values of serial dilutions. Figure 4.23A - C shows the standard curves generated for the meristem identity genes *EOLFY*,

EOAP1 and *EOTFL1,* and Figure 4.23D shows the standard curve generated for the reference gene α-*TUBULIN.* These plots were linear and showed that the efficiency was constant over the concentration range studied. The PCR efficiency values were 1.704, 1.999, 1.755, and 2.120, respectively. Generally accepted range of PCR efficiency is 1.7 to 2.0 (Pfaffl et al., 2002). The error value is a measure of the accuracy of the quantification result based on the standard curve and acceptable value <0.2 (Anon., 2005).

4.3.4.6 Melting curve analysis

The melting curve analysis was carried out to identify characteristic melting profiles in a PCR product through T_m calling (LightCycler Software 4.0). A graph of melting behaviour [plot of the first negative derivative (-dF/dT) of the fluorescence vs. temperature] reveals that pure, homogeneous PCR product produces a single, sharply defined melting curve with a narrow peak. In contrast, primer dimers melt at relatively low temperatures and have broader peaks. The temperature at which the DNA strands separate or melt when heated can vary, depending on the sequence length and GC content. Even a single base difference can be detected using melting curves (Nitsche et al. 2006). The Figures 4.24A to D show the typical melting peaks of genes used in this study. The melting peaks for *EOLFY*, *EOAP1 EOTFL1* and α-*TUBULIN* were 89.5, 86.5 86.1°C, and 89.0°C, respectively, which indicated homogeneous PCR products in gene quantification experiments. The sizes of the PCR products from the bud samples were verified by electrophoresis through agarose gels, which yielded the expected sizes: a product of 270 bp for *EOLFY,* 190 bp for *EOAP1*, 170 bp for *EOTFL1*, and 290 bp for α-*TUBULIN* (Figure 4.24A.1 to D.1).

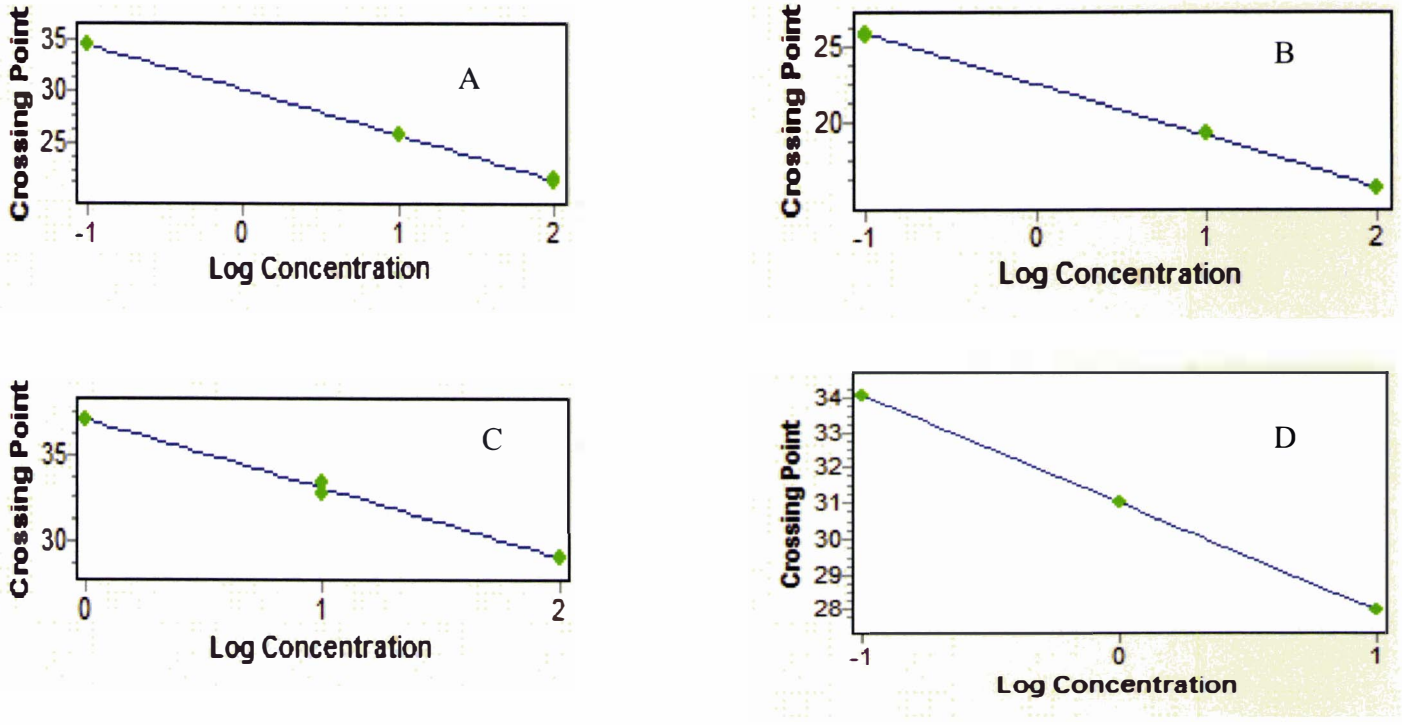

Figure 4.23 Standard curves showing the starting cDNA log concentration verses Cp values in PCR amplification programme.

A: Standard curve of *EOLFY* meristem identity gene; the PCR efficiency was 1.704 with an error of 0.000.
B: Standard curve of *EOAP1* meristem identity gene; the PCR efficiency was 1.999 with an error of 0.049.
C: Standard curve of *EOTFL1* meristem identity gene; the PCR efficiency was 1.755 with an error of 0.010.
D: Standard curve of *α-TUBULIN* reference gene; the PCR efficiency was 2.120 with an error of 0.005.

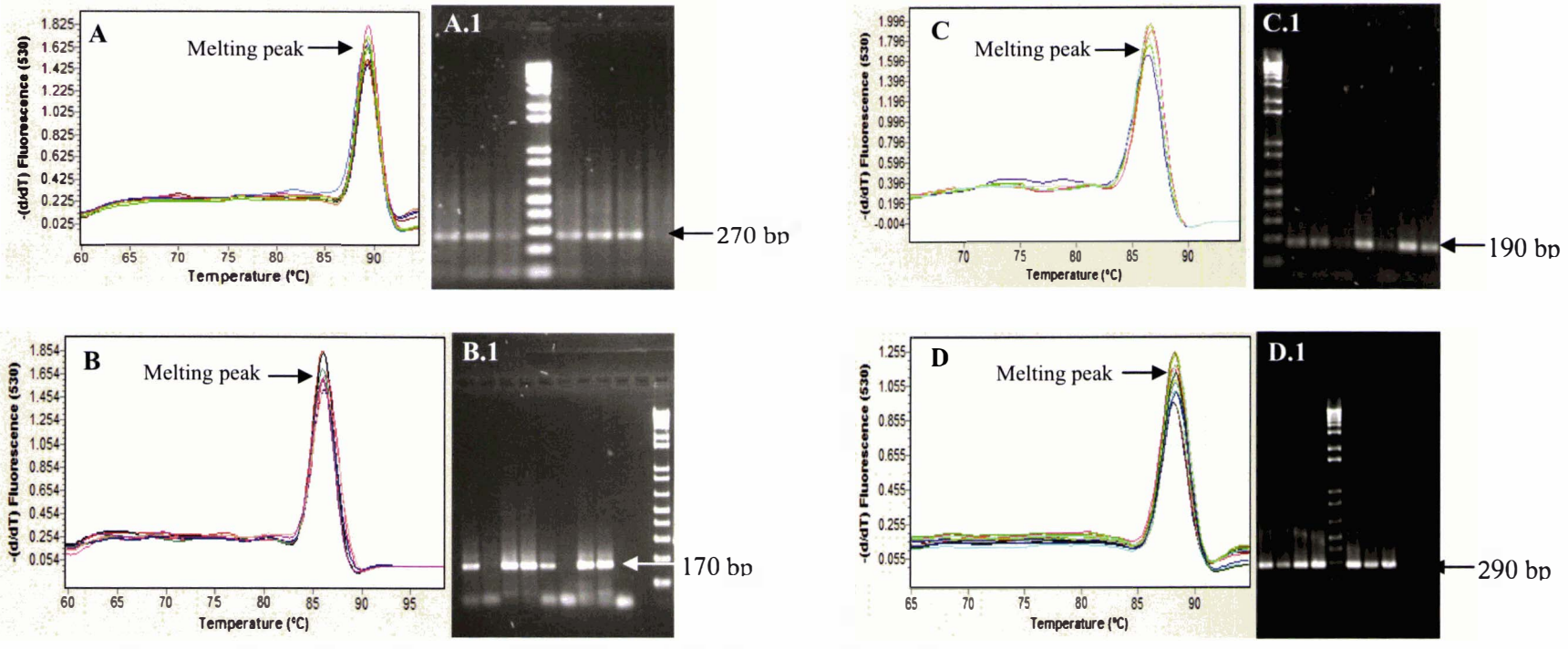

Figure 4.24 Melting curve analysis of meristem identity and reference genes.
(A) Typical melting peak (89.5°C) of *EOLFY* amplicon produced during amplification of cDNA using qRT-PCR.
(A.1) Agarose (2%) gel showing about 270 bp product of *EOLFY* corresponding to the melting peak.
(B) Typical melting peak (86.5°C) of *EOAP1* amplicon produced during amplification of cDNA using qRT-PCR.
(B.1) Agarose (2%) gel showing about 190 bp product of *EOAP1* corresponding to the melting peak.
(C) Typical melting peak (86.1°C) of *EOTFL1* amplicon produced during amplification of cDNA using qRT-PCR.
(C.1) Agarose gel (2%) showing about 170 bp product of *EOTFL1*corresponding to the melting peak.
(D) Typical melting peak (89°C) of *α-TUBULIN* amplicon produced during amplification of cDNA using qRT-PCR.
(D.1) Agarose gel (2%) showing about 290 bp product of *α-TUBULIN* corresponding to the melting peak.

4.3.4.7 Meristem identity gene expression in relation to architectural manipulation and flowering in *E. occidentalis*

In this experiment, the relative quantification of *EOLFY*, *EOAP1,* and *EOTFL1* expression using *α-TUBULIN* as the reference gene is described. The gene expression levels were compared between the genes as well as between developmental stages, and between buds from plants with single stem and free branching architectures. The axillary buds were collected from nodes 36 to 65 in free branching plants and 45 to 80 in single stem plants from just below the apical bud on the main stem at regular intervals between mid-summer to autumn.

As described in Chapter 2, the free branching plants showed faster phase change in terms of leaf morphological characteristics when compared to single stem plants. The single stem plants showed rapid growth and achieved greater node numbers when compared to the main stem of the free branching plants. The free branching plants started showing floral buds in late December at an average node position of 39, and by late February 60% plants were showing floral buds at an average node number of 51 (Figure 4.25). By contrast the single stem plants started showing floral buds when the average node number was 53 (mid January) and the number of flower bearing plants reached a peak of 60% by mid April at an average node number 78 (Figure 4.25).

The relative expression levels of *EOLFY*, *EOAP1*, and *EOTFL1* showed differences attributable to architectural modification (Figure 4.26 A and B). Increased levels of expression of *EOAP1* (relative to α-*TUBULIN*) were displayed at nodes 38 to 56 in free branching plants but not until node 78 in single stem plants. *EOLFY* expression levels were higher than *EOTFL1* all through floral transition. The expression ratios of floral meristem identity genes, *LFY* and *AP1*, compared to the shoot identity gene, *EOTFL1*, are depicted in Figure 4.27 A and B. The ratio of *EOLFY* to *EOTFL1* in free branching plants was higher as compared to the ratios observed in single stem plants during December and January (Figure 4.27A). In addition, the ratios of *EOAP1* to *EOTFL1* were higher in free branching plants as compared to ratios observed in single stem plants and displayed a significant increase from February to April (Figure 4.27B). Elevated *EOAP1* expression levels correlated with percentage floral score when the paired axillary buds were examined (Figure 4.25). As the flowering peak was delayed in single stem plants (node 64 to 78) as a result of architectural modification, the peak

level of *EOAP1* expression also shifted (node 56 to 78). However, the leaves were still either juvenile (single stem plants) or in a transitional state (free branching plants) when the flowering started, as described in Chapter 2.

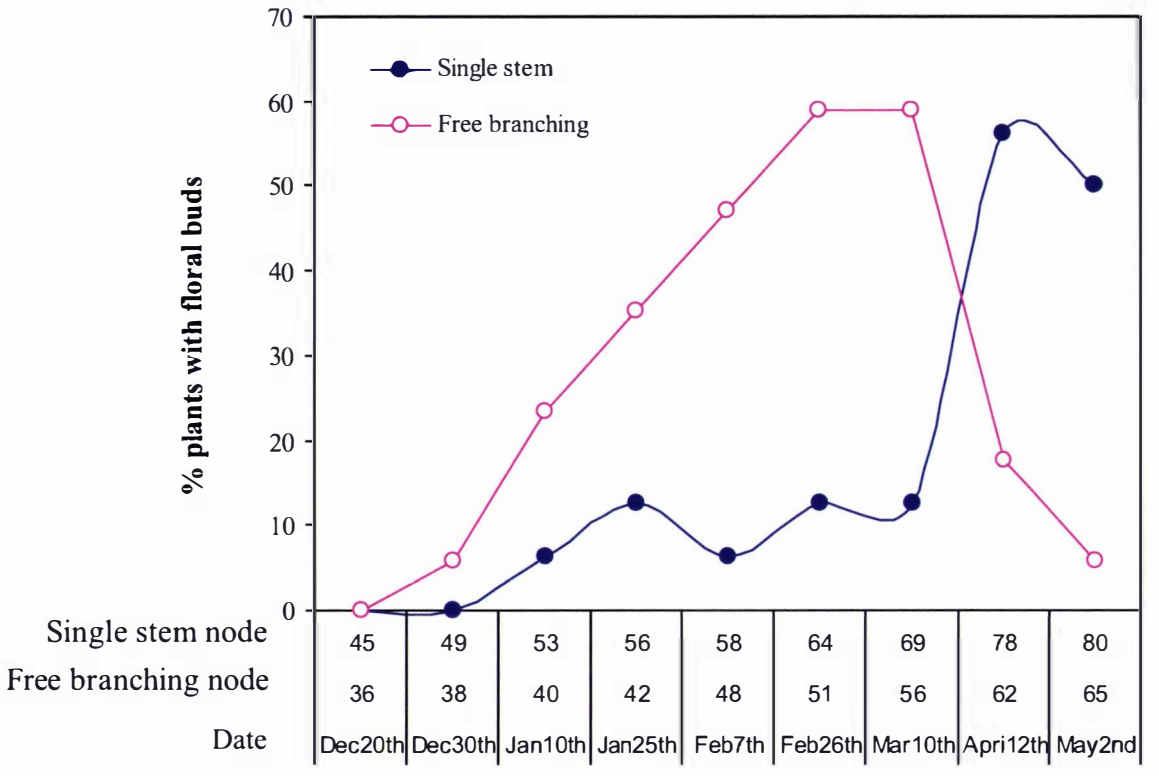

Figure 4.25 Percent floral score of paired axillary buds.
The buds were collected from nodes 36 to 65 in free branching plants and 45 to 80 in single stem plants from just below the apical bud on the main stem at regular intervals between mid-summer to autumn.

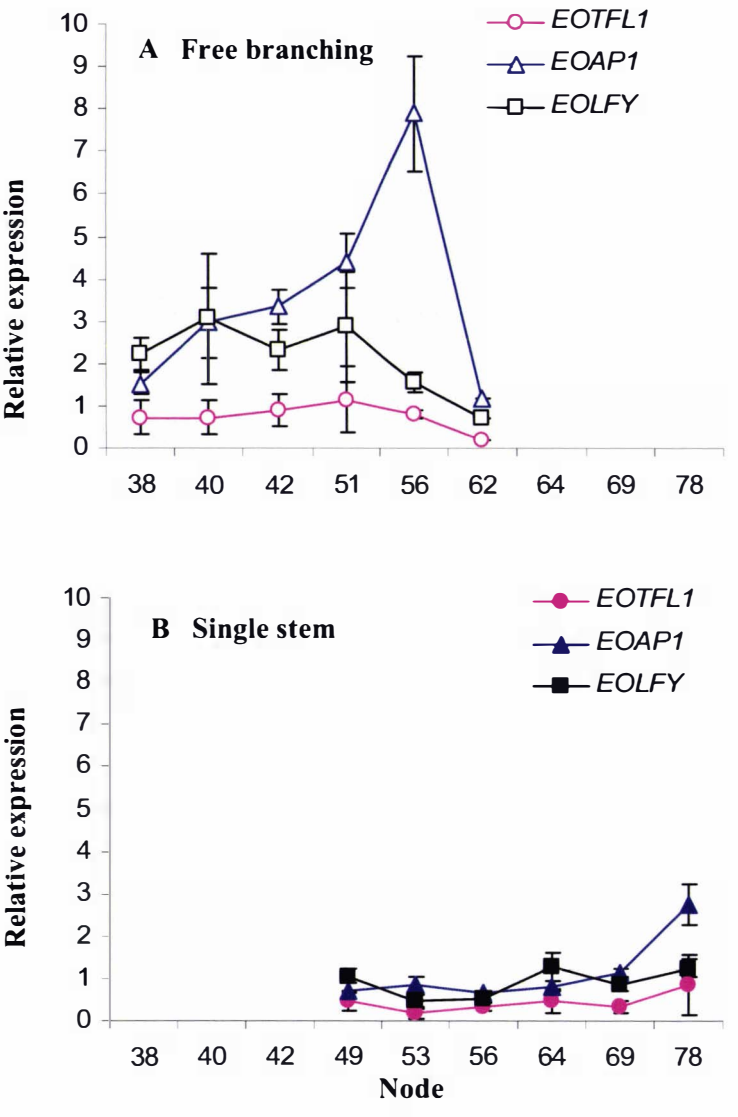

Figure 4.26 Expression of meristem identity genes (*EOLFY*, *EOTFL 1* and *EOAP 1)* in (A) free branching and (B) single stem plants.

The expression patterns of partial homologues of the meristem identity genes during development of branched and single stemmed plants were analysed by qRT-PCR using axillary buds. For relative quantification *β-TUBULIN* was used as the reference gene. Each gene expression value represents at least three replicates (± S.E).

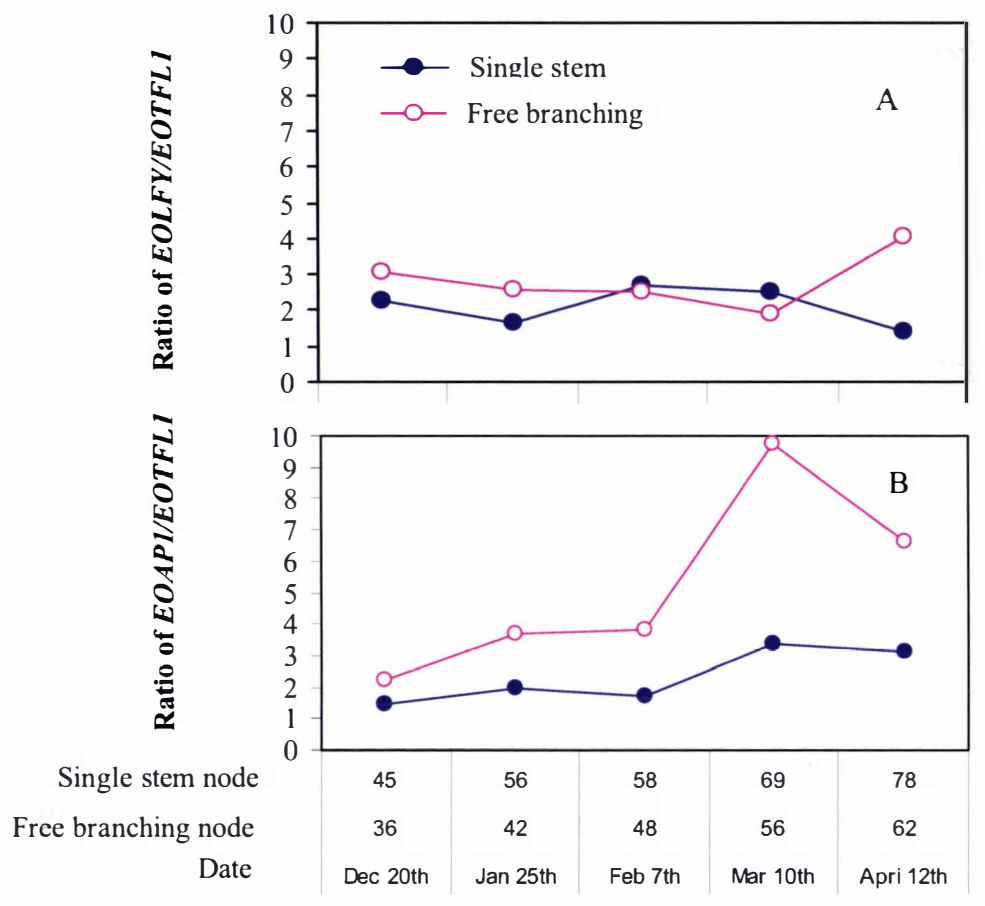

Figure 4.27 The ratios of expression of floral meristem identity genes *EOLFY* (A) *EOAP1* (B) as compared to shoot identity gene *EOTFL1*.

4.4 Discussion

4.4.1 Identification of partial homologues of meristem identity genes

In this study partial homologues of *LFY, AP1* and *TFL1* in *E. occidentalis* were isolated. The respective mRNA and deduced protein sequences were compared with GenBank sequences. The combined evidence obtained by BLAST searches against the GenBank sequence comparisons, alignments and the construction of phylogenetic trees confirmed the identity of the isolated genes as homologues of *LFY/FLO*, *AP1/SQUA*, and *TFL1/CEN* from *Arabidopsis* and *Antirrhinum*, respectively. The isolated sequences were given the names *EOLFY*, *EOAP1*, and *EOTFL1*.

The presence of the floral meristem identity gene, *LFY*, had already been shown in *Eucalyptus* species by earlier workers (Southerton et al., 1998; Dornelas et al., 2004). The isolated putative *EOLFY* fragment showed high sequence similarity to *E. globulus* (*ELF1*). Phylogenetic analysis involving sequences derived from closely related and unrelated species have shown that the sequences share significant similarity with the homologues of other *Eucalyptus* species and within the Myrtaceae family. This was consistent with their taxonomic relationship since they all belong to the family Myrtaceae. In *Eucalyptus globulus*, Southerton et al. (1998) identified two *LFY* equivalents from the genomic DNA of this species, one of which appeared to be a pseudogene as there was only one expressed gene copy. In *E. occidentalis* it is also proposed that there are two copies of the *EOLFY* gene as two bands were obtained in Southern analysis. Real-time RT-PCR melting curve analysis yielded only a single peak indicating that the second copy obtained in the Southern analysis appears to be a pseudogene. Southerton et al. (1998) reported that the duplication was probably a general phenomenon within the genus *Eucalyptus*, and the authors suggested that *Eucalyptus* might have experienced an ancient genome duplication and many of their genes might be expected to be present in at least two copies. There are no *LFY*-related genes in the *Arabidopsis* genome and the DNA-binding protein encoded by *LFY* is unrelated to other classes of transcription factors (Weigel et al., 1992; Parcy et al., 1998). In contrast to angiosperms, in *Pinus, NEEDLY* (*NLY*) and *PRFLL* were reported as representing two divergent *Pinus radiata LFY* homologues (Mellerowicz et al., 1998; Mouradov et al., 1998). *LFY* homologues have generally been identified as a single

copy gene in diploid plant species, such as *Arabidopsis* (Weigel et al., 1992), *Antirrhinum* (Coen et al., 1990), tomato (Molinero-Rosales et al., 1999), *Oryza sativa* (Kyozuka et al., 1998) and grapevine (Carmona et al., 2002). In maloid plants two different *LFY* homologues were reported and Esumi et al. (2005) suggested that this could be due to the polyploidy origin of the Maloideae.

The presence of the floral meristem identity gene *AP1* has also been shown in *Eucalyptus* species by earlier workers (Kyozuka et al., 1997). In contrast to *LFY*, *AP1* belongs to the family of MADS-box genes, many of which encode transcription factors regulating different aspects of flower development (Mandel et al., 1992). The isolated EOAP1 protein showed 98% similarity to EAP1 and 82% similarity to EAP2 proteins. The isolated EOAP1 contained the MADS-box domain and K-box domain which are involved in DNA binding and protein dimerisation, respectively (Schwarz-Sommer et al., 1992; Davies et al., 1996). Kyozuka et al. (1997) suggested that *EcoR1* digested genomic DNA yielded a single band when probed with *EAP1*, but two bands when probed with *EAP2*. With regard to *EOAP1,* the Southern blot results (Figure 4.17C) agree with those of Kyozuka et al. (1997) showing a single band on the *EcoR1* digested DNA blot using an *EOAP1* fragment as the probe. Considering the results from this Southern analysis, the BLAST search, the protein alignment and the phylogeny, it is considered that *EOAP1* is an *AP1* equivalent and not equivalent to the *AP2* of *E. globulus*. In *E. globulus*, both these genes were found to be expressed predominantly in flower buds with slightly different expression levels during flower development. *EAP1* was expressed at all stages of floral morphogenesis whereas *EAP2* was expressed more predominantly in young flower buds (Kyozuka et al., 1997).

Collins and Campbell (2001) isolated three *TFL1*-like genes from *Eucalyptus*, all of which showed a high level of identity with *TFL1*. However, no *Eucalyptus TFL1* sequence is available in the GenBank. More recently, Dornelas and Rodriguez (2005) reported the presence of *TFL1* homologous expressed sequence tags (EST) in *Eucalyptus* spp. while data mining the FORESTS database. In this study, a partial homologue of *TFL1* was isolated from *E. occidentalis*. The identity was confirmed by comparing the cDNA and the deduced amino acid sequences with known GenBank TFL1-like sequences. EOTFL1 contains a phosphatidylethanolamine binding protein domain which has the potential to interact with a variety of signalling pathways (Pnueli

et al., 2001). Phylogenetic analysis showed that the corresponding cDNA and deduced protein sequence share distinct similarity with other *TFL1*- or *CEN*- like proteins derived from members of the Myrtaceae. The Southern analysis indicated that one strong and two weaker hybridisations occurred when hybridised with the *EOTFL1* fragment suggesting that one, or at least one, *EOTFL1* homologue exists in *E. occidentalis*. However, it was beyond the aim of this study to confirm the copy number of this gene. In this study, Southern analysis was carried out to identify homologues in the genome, and to validate the cDNA fragments as suitable probes for gene expression analysis. Results from the structures of *EOLFY*, *EOAP1* and *EOTFL1* showing exon-intron boundaries also confirmed that the meristem identity genes were conserved across a broad taxonomic range. These finding substantiate the presence of floral and inflorescence meristem identity genes in *E. occidentalis*.

4.4.2 Optimisation and advantages of the real-time qRT-PCR assay

Optimisation of qRT-PCR parameters was essential for reproducible results of biological samples. For quantification of the expression of meristem identity genes, cDNA was generated from bud samples using Thermoscript™ (Invitogen) enzyme (Section 4.2.5). The high reaction temperature used facilitated good and consistent yields. The RNase H used at the end of the reaction removed all RNA-DNA hybrids, improving the efficiency of the cDNA. Relative quantification methodology compensated for the variations in the initial sample amount, variations in nucleic acid recovery, possible RNA degradation of sample material, differences in sample and/or nucleic acid quality, variations in sample loading/pipetting errors and variations in cDNA synthesis efficiency. It was found that the selection of α-*TUBULIN* as a reference gene for gene quantification was a good choice. It was selected after comparing with the semi-quantitative expression levels (RT-PCR) of other reference genes (*18S RNA*, *β-ACTIN* and *GAPDH*) in randomly selected bud samples (Figures 4.19 & 4.20).

The real-time qRT-PCR technique used in this thesis enabled confirmation of the existence of the homologues of the floral meristem identity genes (*LFY* and *AP1*) and inflorescence meristem identity gene (*TFL1*) in buds of *E. occidentalis* as well as measurement of changes in gene expression and the degree of change over time,

developmental stage, and architectural treatment. Previously, gene expression was measured using northern analysis. However, quantitative real-time PCR has many advantages over northern blotting. The first advantage is the obvious one of time. In general, any northern blot experiment takes three days to two weeks and it depends upon the target transcript abundance, whereas qRT-PCR takes a few hours and it requires only nanogram quantities of RNA. In the current experiments, due to the very small sample size, this method of quantification had a distinct advantage over northerns as it required only micrograms of RNA and no radioactive probes. Further, northern blots require methods such as densitometry or fluorimaging to determine the abundance of an individual transcript, whereas qRT-PCR data are related in terms of numbers, allowing easy analysis of fold changes in an experiment. Both of these methods depend on control genes to normalise data from sample to sample.

4.4.3 Gene expression in architecturally manipulated plants

In this study, to investigate the differences in the pattern of meristem identity gene expression between single stem and free branching plants during phase change and floral transition, the expression of *EOLFY*, *EOTFL1*, and *EOAP1* was followed using qRT-PCR. The central mechanism of the *Arabidopsis* and *Antirrhinum* model is that the positive regulators of floral meristem commitment, *LFY* and *FLO* (Weigel et al., 1992), act with *AP1* and *SQUA* (Mandel et al., 1992) to promote the conversion of meristems to a floral state. *TFL1* and *CEN* (Bradley et al., 1996) act in opposition to this process and allow meristems to remain indeterminate, promoting an inflorescence state. All these genes are expressed strongly during inflorescence development in *Arabidopsis* with *TFL1* highest in the centre of the apex, and floral meristem genes expressing on its periphery (Bradley et al., 1997).

A difference in the timing of peak levels of expression of the floral meristem identity genes, *EOLFY* and *EOAP1*, in free branching plants compared to single stem plants was observed (Figure 4.26). This suggests that shoot architecture manipulation delayed the peak expression of these genes in single stem plants. This observation was positively correlated with the number of floral buds. Similar results were reported in *Citrus* wherein the expression of both *CsLFY* and *CsAP1* were positively correlated with the propensity to flower (Pillitteri et al., 2004).

The induction of flowering was shown to depend on the relative expression of *MdTFL1* and *AFL1* in apple and it was also suggested that *MdTFL1* was involved in maintaining the vegetative phase in apple (Kotoda and Wada, 2005). In *Eucalyptus*, *ETCL* genes shared functions with *TFL1* and were reported to have the ability to delay vegetative to reproductive transition considerably (Collins and Campbell, 2001). In addition, juvenile plants expressed more *TFL1* than adult plants in *Citrus* and expression of the *TFL1* homologue was positively correlated with juvenility (Pillitteri et al., 2004). In contrast to *Citrus sinensis*, in this study *E occidentalis* displayed low levels of *EOTFL1* in both single stem (showing juvenile leaf morphology) and free branching plants (showing transitional to adult leaf morphology) during the sampling period (Figure 4.26). It could be predicted that lower levels of *EOTFL1* in both juvenile and adult-like plants have a bearing on the precocious flowering and exhibition of neoteny in this species. This phenomenon occurred irrespective of architecture manipulation and it could be further hypothesised that it is under strong genetic control. In some species of *Eucalyptus* there is no quantitative association between timing of vegetative phase change and of first flowering. Even though flowering usually follows vegetative phase change, Jordan et al. (1999) suggested that first flowering was unlikely to be conditional on vegetative phase change.

Further, Pillitteri et al. (2004) suggested that the absolute amount of *LFY* and *TFL1* transcript accumulation is less important than the ratio of *LFY*: *TFL1* in determining meristem fate. A higher ratio results in shortening of the vegetative phase and production of floral meristems (Ratcliffe et al., 1999). However, the ratio of expression of *EOLFY* to *EOTFL1* confirmed that there was no significant difference between trends observed in single stem and free branching plants during the sampling period, which could again reinforce the precocious nature of this species (Figure 4.27A). There was a higher *EOAP1*: *EOTFL1* ratio in free branching plants as compared to single stem plants especially during March (Figure 4.27B), and hence appearance of floral buds earlier in free branching plants than single stem plants. However, higher levels of *EOAP1*started to become evident during April (Figure 4.26B), and elevated *EOAP1* levels were correlated with flowering score in both the architecture treatments (Figure 4.25).

The terminal inflorescence of *E. occidentalis* may be dependent upon a floral inductive pathway that uses an integration system different from *EOLFY*, and the most likely candidate is the *EOAP1* pathway. Ordidge et al. (2005) suggested similar mechanisms in *Impatiens balsamina*. The *AP1* homologue (*IMP-SQUA*) in *Impatiens* is up-regulated on transfer to inductive conditions, and expression of *IMP-SQUA* stops during the reversion process (Pouteau et al., 1997), suggesting an involvement in the control of terminal flowering and the requirement for a leaf-derived signal. In *Arabidopsis* the perception of a daylength signal leads to the activation of *CO* (Suarez-Lopez et al., 2001). In turn *CO* is involved in the up-regulation of *FT* (Kardailsky et al., 1999; Kobayashi et al., 1999; Samach et al., 2000), which is suggested to promote flowering via *AP1* rather than *LFY* (Ruiz-Garcia et al., 1997; Nilsson et al., 1998). Thus, it could be speculated that in *E. occidentalis* the daylength pathway could be the contributing pathway for floral transition by a leaf-derived signal. This could be operating directly from *FT* to *AP1* rather than through *LFY* as depicted in Figure 1.2 and hence higher levels of *EOAP1* were observed compared to the *EOLFY* during the floral transition.

Based on these results, the hypothesis that *EOTFL1* will be expressed more in single stem plants compared to their free branching counterparts, has not been supported. However, the second part of the hypothesis that *EOLFY* and *EOAP1* will be expressed at higher levels in free branching plants has been supported.

Chapter 5

Effect of environment and shoot architecture on floral transition and gene expression in *Eucalyptus occidentalis*

5.1 Introduction

Eucalyptus occidentalis ecotype 13648 expressed significant differences in the timing of vegetative phase change and floral transition in response to architectural modifications (Chapters 2 to 4). This was further investigated by growing single stem and free branching plants in greenhouses maintained under different environmental conditions which were effectively either warm long days or ambient temperature and daylength.

Based on the information available on floral induction in *Eucalyptus* and other members of the Myrtaceae and the data obtained in Chapters 2 to 4, it was anticipated that a long photoperiod would promote floral induction in *E. occidentalis*, but that the complexity of shoot architecture would have an over-riding effect on floral induction. It was expected that under inductive environmental conditions (long days) together with shoot complexity, the floral meristem identity genes *EOLFY* and *EOAP1* would be up-regulated. In Chapter 4 it had already been established that flowering was considerably delayed by single stem architecture. In this Chapter single stem plants were allowed to branch after 45 nodes to establish if flowering would commence once complexity was obtained. A similar treatment was also applied to *M. excelsa* (Chapter 6).

5.2 Materials and Methods

5.2.1 Plant material

Seeds of *Eucalyptus occidentalis* of the ecotype 13648 were obtained from the Australian Tree Seed Centre, CSIRO, Australia. Seeds were germinated at room temperature during January/ February 2005 and seedlings were transferred to small pots

and finally to 10 l pots. The potting medium was prepared as described in Section 2.2.1. Plants were grown in greenhouses at the Massey University Plant Growth Unit (Palmerston North), New Zealand.

In this experiment, two environmental conditions were applied. Temperature and photoperiod were controlled in one greenhouse (Warm/LD) with a warm temperature regime (24/17°C) (day/night) and maintenance of a 16 h photoperiod. Photoperiod was extended using 100 W incandescent lamps (10 μmol m^{-2} s^{-1}). In the second greenhouse (Ambient), conditions reflected the ambient temperature and ambient photoperiod. Mean ambient day/night temperatures during mid-winter were 13/8°C rising to 25/17°C in mid-summer. Photoperiod declined to 9 h at mid-winter and rose to 16 h in mid-summer. All plants were watered twice daily to container capacity using an automatic irrigation system.

The plants were subjected to two architectural treatments: half the plants were grown to obtain the single stem architecture by repeatedly removing the axillary buds when the plants were 300 mm tall and there after the reminder were not pruned to obtain the free branching architecture, as described in Section 2.2.1. During flowering, care was taken to retain floral buds on single stem plants as well as maintaining the single stem architecture. However, the single stem plants were allowed to branch freely at nodes distal to node 45 on the main stem to attain complexity in the crown at higher node positions. This treatment is termed in this thesis as single stem-free branching (SsFb). Typical plant architectures are shown in Figure 5.1. Forty replicate plants for each treatment (Warm/LD free branching, Warm/LD SsFb, Ambient free branching and Ambient SsFb) were maintained for 16 months (from January/February 2005 to May 2006).

5.2.2 Plant growth and flowering

During January 2006, 12 months after sowing plant growth and flowering measurements were made across the four treatments (two environments and two architectures). These measurements included the total number of nodes on the main stem, and the first floral node on the main stem, the total number of branches per plant, the number of floral branches, the average number of floral buds per branch and the ratio between floral branches to total branches. The observations were recorded in 15

randomly selected plants of the 40 replicates per treatment. Mean and standard error were calculated for each parameter.

5.2.3 Bud collections

Axillary buds were collected from the node just below the apical bud as demonstrated in Figure 4.1, from 40 plants in each of the four experimental treatments from August 2005 to May 2006 at regular intervals for the analysis of expression of selected meristem identity genes. Twelve samples were obtained for each treatment between nodes 16 and 60 in free branching plants and between 16 and 77 in SsFb plants from the Warm/LD greenhouse. Further samples were obtained between nodes 15 and 58 in free branching plants and between15 and 69 in SsFb plants from the Ambient greenhouse. Bud removal for sampling did not influence the branching architecture in free branching plants as shown in Figure 5.3. Visual observation of the parallel-paired bud was carried out for each bud sample collected to determine the potential number of floral buds present in each sample as described in Section 4.2.1. Total number of floral buds was converted to percentage number and termed as percent floral score in each sampling.

5.2.4 Statistical analysis

Statistical analysis was carried out by using SAS as recorded in Section 2.2.4 for morphological observations.

5.2.5 Temporal expression of meristem identity genes

5.2.5.1 Total RNA extractions

Total RNA was extracted from the 48 bud samples by using a QIAGEN RNeasy plant mini kit as described in Section 4.2.2. Each bud sample was extracted twice to increase the efficiency of the total RNA obtained.

5.2.5.2 cDNA preparations

cDNA was prepared from the 48 bud samples by using ThermoScript™ (Invitrogen) as described in Section 4.2.5. A total of 144 cDNA preparations were obtained including three replicates for each bud sample.

5.2.5.3 Quantification of *EOLFY*, *EOAP1* and *EOTFL1*

Quantification was carried out by using real-time PCR. The methodology was carried out as described in Section 4.2.14.

Figure 5.1 *Eucalyptus occidentalis* ecotype 13648 plants grown with free branching (A) and single stem-free branching architectures (B).

5.3 Results

5.3.1 Plant growth and flowering

Measurements were carried out in SsFb plants (after allowing free branching) and free branching plants of *E. occidentalis* grown in the Warm/LD and Ambient conditions. To measure the growth performance of these plants, the total number of nodes on the main stem was measured and the mean values were plotted. The statistical analysis using ANOVA showed that the main effect, architecture, was highly significant ($p<0.0001$). Further, a significant ($p< 0.05$) interaction between environment and architecture was also observed (Appendix 1, Table 7). Overall there were more nodes on the main stem of SsFb plants than on the free branching plants irrespective of environment: SsFb plants under Warm/LD conditions attained the most nodes (Figure 5.2A).

To estimate the density of flowering, the average number of floral buds per branch was calculated. The main effects, environment and architecture, and the interaction of environment and architecture were highly significant ($p<0.0001$) (Appendix 1, Table 7) with the most dense flowering occuring on SsFb plants under the Warm/LD environment (Figure 5.2B). For the node number to first floral bud measurements (Figure 5.2C), the effect of architecture was highly significant ($p <0.0001$) (Appendix 1, Table 8). There was no interaction effect.

Further, to estimate the extent of flowering, the ratio between number of flowering branches and total number of branches was calculated. The main effects were significant, with architecture being highly significant ($p<0.0001$) and environment significant ($p<0.05$) (Appendix 1, Table 7). The SsFb plants under the Warm/LD environment showed the highest ratio (0.95) compared to other treatments (Figure 5.2D).

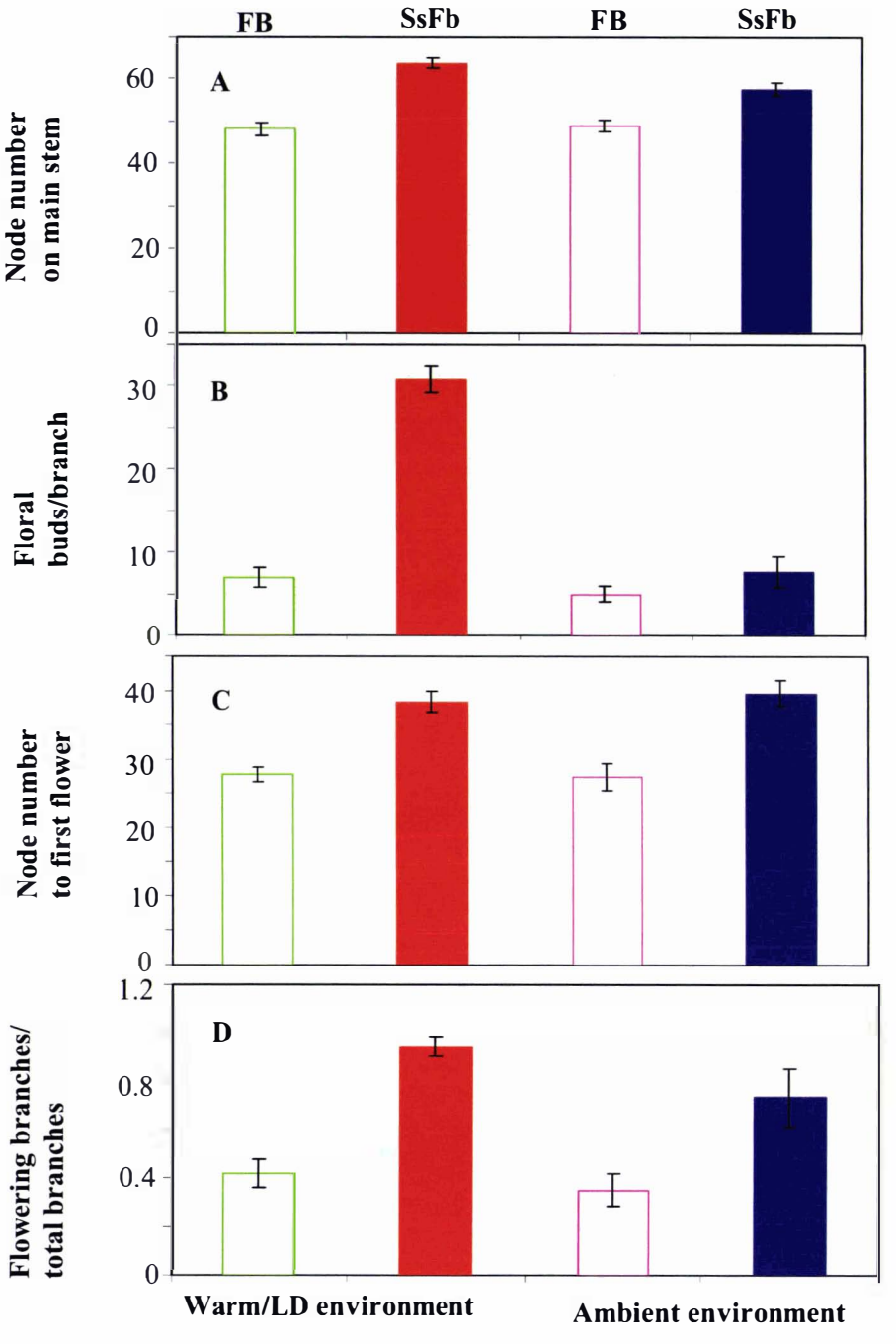

Figure 5.2A-D Plant growth and flowering pattern in *E. occidentalis* grown in Warm/long day and Ambient treatments. Please refer to Section 5.2.1 for details of treatments. A, Total node number on main stem; B, Average number of floral buds per branch displayed by plants; C, First flowering node on the main stem; D, The ratio between flowering branches to total number of branches. FB: free branching plants, SsFb: single stem-free branching plants. Each bar represents at least 15 replicates ± S.E. Measurements were carried out during January 2006 after allowing free branching in SsFb plants.

5.3.2 Floral score and meristem identity gene expression

5.3.2.1 Floral score

The percent floral scores of paired axillary buds in *E. occidentalis* grown under different environmental and architectural conditions are depicted in Figure 5.3. In Ambient conditions free branching plants first showed floral buds at node 26 reaching a maximum floral bud score by node 42. The SsFb counterparts displayed floral buds at node 38, reaching maximum floral bud score after node 61. The free branching plants grown under Warm/LD first showed floral buds at node 24 and reaching maximum flowering by node 39 (Figure 5.3). By contrast, Warm/LD SsFb plants first showed floral buds at node 39 reaching maximum flowering after node 64. In general, irrespective of environmental condition, free branching plants reached maximum flowering some 20 nodes earlier than SsFb plants, displaying the overriding effect of architecture (Figure 5.3).

5.3.2.2 Expression of meristem identity genes

The observed relative expression levels of the meristem identity genes *EOAP1, EOLFY,* and *EOTFL1* from plants from the four treatments were plotted (Figures 5.4 and 5.5). During the gene expression study from (August 2005 to May 2006), plant growth as height was greater in SsFb plants in both environments compared to their corresponding free branching counterparts. Consequently, the 12 buds collected from each treatment were from slightly different nodes as described in Section 5.2.3. SsFb plants were allowed to branch freely at nodes distal to node 45 to attain complexity to crown at higher node positions and to investigate the effect of shoot complexity on expression of floral meristem identity genes (*EOLFY* and *EOAP1*).

Generally there was a similar pattern of gene expression observed in buds from both Warm/LD and Ambient environments. The main differences observed were between architectures. An over-riding effect of architecture similar to the observations made on nodes to first floral bud in both environments was observed (Figures 5.4 and 5.5). Irrespective of the treatment, *EOLFY* levels were higher than *EOTFL1* and *EOAP1* at nodes 15 and 16 in both Ambient and Warm/LD conditions, respectively (Figures 5.4 and 5.5). As development progressed, differences in flowering and, in turn, differences in meristem identity gene expression were observed between architectures. As flowering started, as observed through the paired bud observations (Figure 5.3), *EOLFY*

and *EOAP1* levels started to increase (Figures 5.4 and 5.5). These floral meristem identity genes showed an expression pattern that was positively correlated with the flowering pattern depicted in Figure 5.3 in all four treatments. However, a second spell of elevated levels of *EOAP1* was also observed in free branching plants at nodes 40 to 48.

In Warm/LD conditions, the free branching plants showed an increase in *EOLFY* expression at node 24 and *EOAP1* expression at node 31 (Figure 5.4A), which was earlier than in the corresponding SsFb plants (node 39, Figure 5.4B). By node 34, *EOLFY* was at its maximum and *EOAP1* showed its highest peak at node 48 in free branching plants (Figure 5.4A), whereas the peak expression of *EOLFY* occurred at node 44 and at node 60 for *EOAP1* in SsFb plants (Figure 5.4B). Expression levels of *EOTFL1* were low in most of the samples during the study period. However, expression of this gene started to increase at node 58 in free branching plants and at node 72 in SsFb plants (Figure 5.4 lower panels) by which time the appearance of floral buds had decreased (Figure 5.3).

In Ambient conditions, the gene expression pattern was similar to that observed in Warm/LD conditions (Figure 5.5A and B). In free branching plants *EOLFY* expression started to increase at node 15 and *EOAP1* at node 24(Figure 5.5A). In the corresponding SsFb plants expression of *EOLFY* and *EOAP1* also increased (Figure 5.5B). By node 42 *EOLFY* was at its maximum, *EOAP1* showed this peaks of expression at nodes 40 and node 44 in free branching plants (Figure 5.5A). In SsFb plants peak expression occurred at node 48 for *EOLFY* and at node 52 for *EOAP1* (Figure 5.5B). Expression levels of *EOTFL1* were at base level in most of the samples during the study period as observed in Warm/LD conditions.

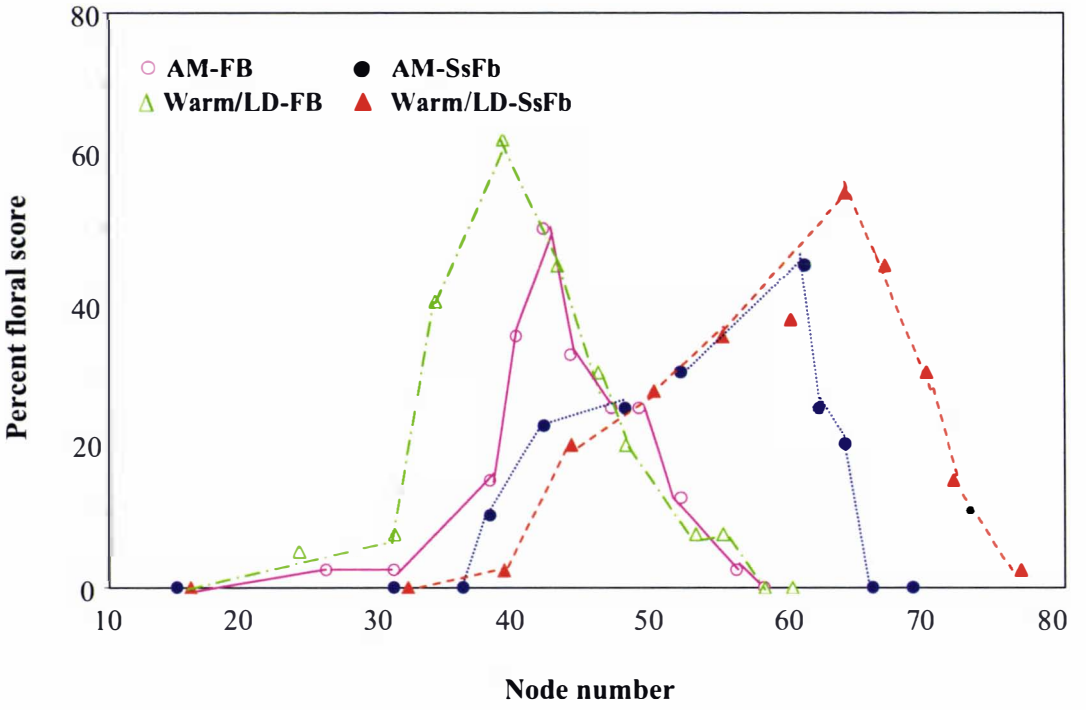

Figure 5.3 Percent floral scores of paired axillary buds on plants grown in different environments with different architectures. AM-FB, free branching plants grown in Ambient conditions; AM-SsFb, SsFb plants grown in Ambient conditions; Warm/LD-FB, free branching plants grown in Warm/LD condition; Warm/LD-SsFb, SsFb plants grown in Warm/LD condition.

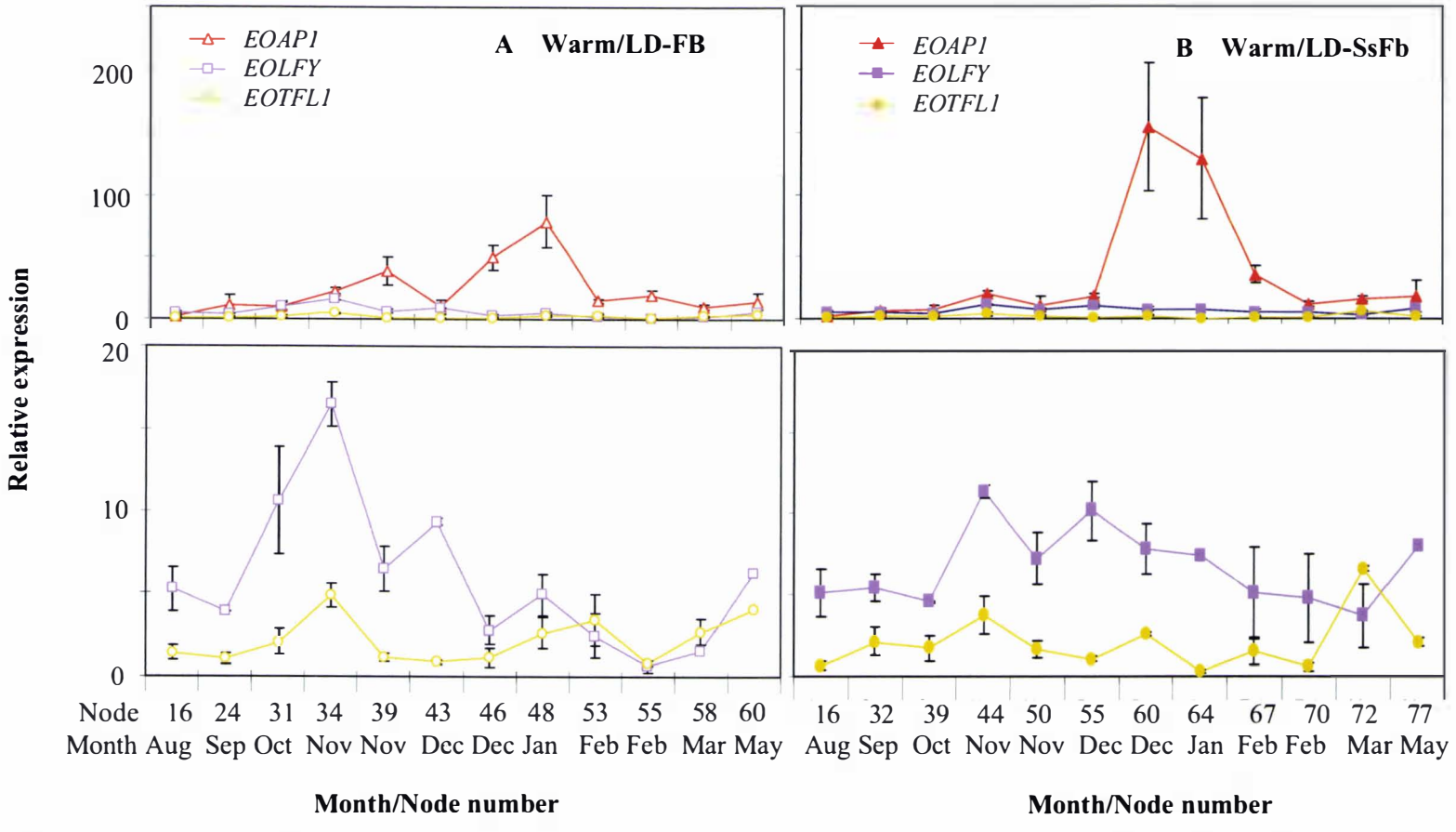

Figure 5.4 Relative quantification of meristem identity gene expression in plants grown under Warm/LD conditions with different shoot architecture. A, Warm/LD-FB, free branching plants grown under Warm/LD environment, the lower panel shows the same data on an expanded scale for *EOLFY* and *EOTFL1*; B, SsFb plants grown under Warm/LD environment, the lower panel shows the same data on an expanded scale for *EOLFY* and *EOTFL1*. Each gene expression value represents at least three replicates (± S.E.).

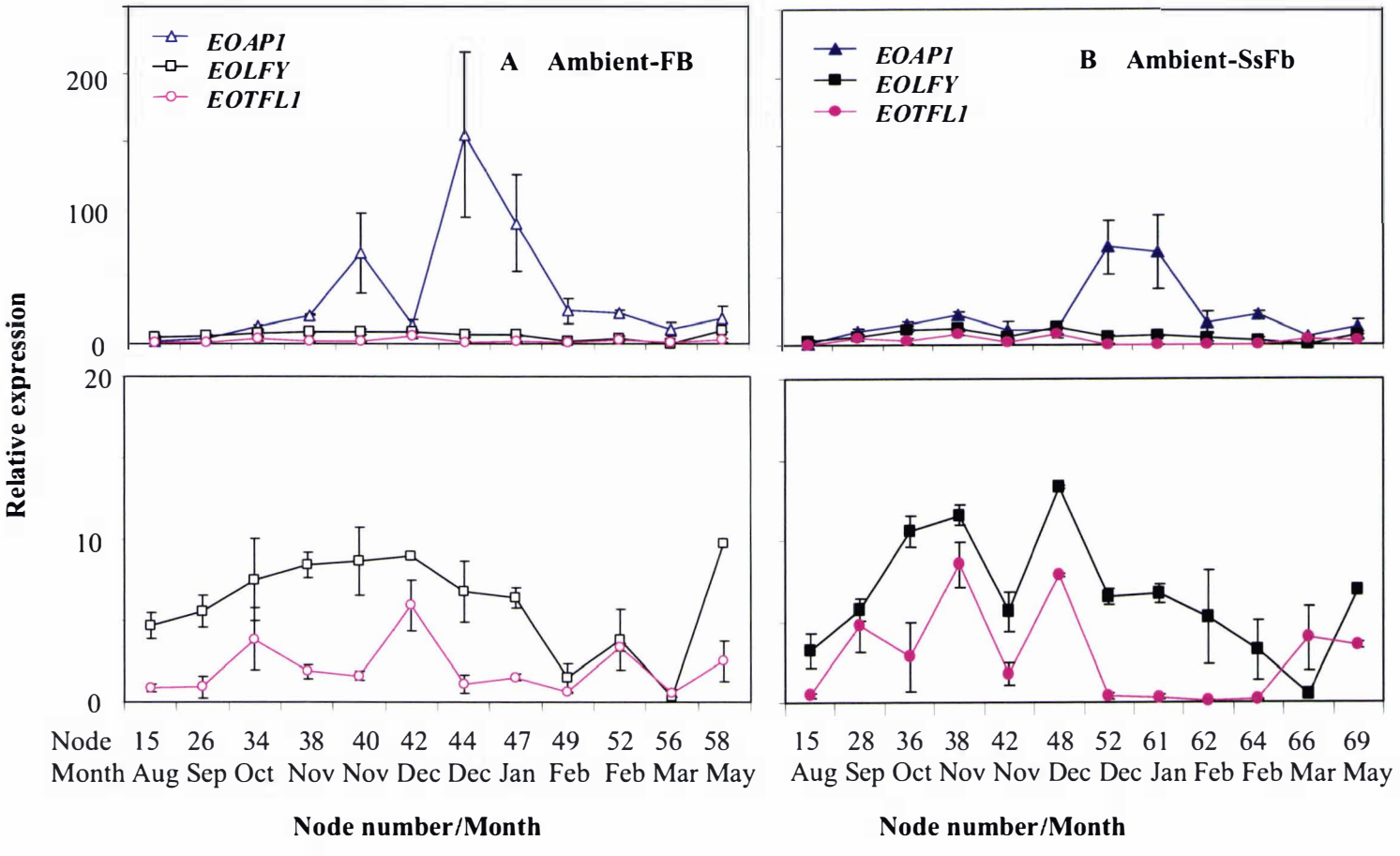

Figure 5.5 Relative quantification of meristem identity gene expression in plants grown under Ambient conditions with different shoot architecture. A, Ambient-FB, free branching plants grown under Ambient environment, the lower panel shows the same data on an expanded scale for *EOLFY* and *EOTFL1*; B, SsFb plants grown under Ambient environment, the lower panel shows the same data on an expanded scale for *EOLFY* and *EOTFL1*. Each gene expression value represents at least three replicates (± S.E.).

5.4 Discussion

The effect of environment (Warm/LD and Ambient) and shoot architecture on floral transition and expression of meristem identity genes in *E. occidentalis* was monitored. The over-riding effect of increased shoot complexity on the first node to flower indicates that architecture had a more significant effect on promoting the floral transition in this species than either of the environmental parameters. The single stem-free branching (SsFb) plants grew taller and faster than free branching plants. The appearance of first floral buds at earlier nodes on free branching plants than their corresponding SsFb plants in both the environments indicate that growth in terms of shoot complexity rather than height has contributed to the rate of floral transition in this species as described in Chapter 4. In addition, more floral branches were obtained when the SsFb plants were allowed to branch freely at nodes distal to node 45. These observations showed that the complexity of crown architecture has a significant role in flowering in *E. occidentalis*, supporting the suggestions by Sismilich et al. (2002) that juvenile plants and plantlets of *M. excelsa* must attain a certain size and/or structural complexity before passing to the adult state.

In an earlier investigation, Bolotin (1975) used four ecotypes (Acre, Gilat, Kattaning and Ongerup) of *E. occidentalis* to demonstrate the effect of long day conditions (16 h photoperiod) on flowering. Out of four ecotypes, Gilat and Acre showed 68% and 51% flowering at the end of 21 weeks. None of the control seedlings raised under natural daylengths (15 h photoperiod) initiated floral buds during that time. The day temperatures adopted by the author were 21± 5°C and the night temperatures were 15± 5°in both long day and control environments (Bolotin, 1975). In this thesis, Warm/LD floral observations support the above study. However, plants displayed floral buds in the Ambient environment also. This could be due to cool mid-winter day/night temperatures (13/8 °C) and short days (9 h photoperiod) followed by increases in day/night temperature(25/17°C) and daylength (16 h) during mid-summer in the Ambient greenhouse. Moncur (1992) suggested that under natural environments, floral buds of many *Eucalyptus* species develop during stem elongation which is active in spring when temperature, daylength and solar radiation are increasing following the less favourable growing conditions of winter. The present study suggests that flowering in

Warm/LD environment plants might be independent of temperature effect as a result of longer daylength. On the other hand, flowering in Ambient environment plants might be as a result of a combination of temperature and endogenous factors (a period of moderate stress followed by favourable conditions). A combination of lower temperatures and short photoperiods are also important for floral induction in a number of temperate and tropical species within Myrtaceae (Henriod, 2001). The observation that there were more floral buds per branch in *E. occidentalis* Warm/LD SsFb plants after being allowed to branch freely as compared to free branching plants showed that complexity of shoot architecture along with Warm/LD conditions together synergistically promoted a greater number of floral buds per branch.

The lower levels of *EOTFL1* expression in all four treatments leads to the suggestion that this could have contributed to the precocious flowering of this species as observed in Chapter 4. Southerton (2007) suggested that competence to flower early is a general characteristic of *E. occidentalis*. In *Citrus TFL* (*CsTFL*), Pillitteri et al. (2004) reported higher levels of *CsTFL* accumulation in juvenile stem tissue as compared to adult tissue.

An increase in expression of the floral meristem identity gene, *EOLFY* occurred prior to the marked increase of *EOAP1*. Not unexpectedly there was a positive correlation between increased expression of *EOAP1* and percent floral score supporting the use of *EOAP1* as a marker of floral transition (Hempel et al., 1997). Increased expression of both genes supports their involvement in the vegetative to reproductive transition. Irrespective of environment, free branching plants showed an earlier increase in *EOAP1* expression as compared to SsFb plants demonstrating that shoot architecture manipulation contributed to changes in floral meristem identity gene expression patterns and, in turn, floral transition. Further, floral marker *EOAP1* expression was up-regulated in SsFb plants along with the production of higher number of floral buds after node 45 during which the shoot architecture changed from single stem to free branching. This again supports the suggestion that shoot complexity has a significant role in enhancing the floral transition.

Thus, the higher levels of *EOAP1* are correlated with shoot complexity in both architecture treatments (free branching and SsFb plants). From the present study, it could be speculated that shoot complexity in free branching and SsFb plants after

allowing free branching and more leaf area. This could lead to more leaf derived signal and in turn to more *EOAP1* in floral buds. Pouteau et al. (1997) reported that the *AP1* homologue (*IMP-SQUA*) in *Impatiens* was up-regulated on transfer to inductive conditions and expression of *IMP-SQUA* stopped during the reversion process. The authors suggested an involvement of *IMP-SQUA* in the control of terminal flowering and the requirement for a leaf-derived signal (Pouteau et al., 1997). Similarly, Ordidge et al. (2005) hypothesised that in *Impatiens,* the terminal inflorescence may be dependent upon a floral inductive pathway which uses a different integration system to *IbLFY*, the most likely candidate being the *AP1* pathway through *FT* integration shown in Figure1.1. Higher levels of *EOAP1* than *EOLFY* during the floral transition lend support to the existence of the *FT* to *AP1* pathway in this species.

The results demonstrate that the Warm/LD environment enhanced the growth of free branching and SsFb plants in terms of mean node number achieved compared to the Ambient environment. Further, the earliest floral buds were observed in both the environments with concomitant elevated levels of *EOAP1* demonstrating floral induction has taken place in the longer photoperiod as well as ambient photoperiods. The hypothesis that long day treatment will promote flowering together with increased expression of floral meristem identity genes faster than the Ambient environment has not been supported completely. The anticipation that complexity of shoot architecture has an important role in floral transition has been supported, as an over-riding effect of architecture was observed in both environments. In addition, when the SsFb plants were allowed to branch freely at node 45, again the over-riding effect of shoot complexity was observed.

Chapter 6

Effect of environment and shoot architecture on gene expression in relation to phase change and floral transition in *Metrosideros excelsa*

6.1 Introduction

In this Chapter, the effect of environment, shoot architecture manipulation and meristem identity gene expression studies were extended to *Metrosideros excelsa*. *Metrosideros excelsa* exhibits the following major differences in relation to phase change and floral transition compared to *E. occidentalis*:

- *M. excelsa* takes a longer time to flower, and passes through a homoblastic vegetative phase change.
- The inflorescence terminates with a vegetative bud not a terminal flower.
- An inflorescence reversion mechanism exists in which an inflorescence meristem reverses to vegetative development.

It has been demonstrated that rapid plant growth with respect to height by growing plants with single stem architecture accelerated the rate of vegetative phase change (Clemens et al., 1999). It was expected that both size (height) and complexity of branching would affect the attainment of reproductive competence in *M. excelsa,* as it has been suggested that reproductive competence was a consequence of the plant reaching a certain degree of branching complexity (Clemens et al., 2002; Sismilich et al., 2003).

The current genetic models for flowering (involving the inflorescence and floral meristem identity genes *TFL1, LFY* and *AP1* from the annual plants *Arabidopsis* and *Antirrhinum*) have been shown to apply to *M. excelsa* (Sreekantan et al., 2004). The present study was carried out to determine whether different environmental and shoot architecture treatments led to differences in expression of key meristem identity genes. The hypothesis that floral inductive environmental treatments as determined by Henriod

et al., (2000) would promote higher expression levels of the floral meristem identity genes *MEL* and *MESAP1*, has been tested.

6.2 Materials and Methods

6.2.1 Plant material and growth conditions

Seedlings of approximately five node stage of *Metrosideros excelsa* were transplanted to10 l pots containing commercial potting soil supplemented with slow-release fertiliser in June 2003. All axillary buds were removed at the time of transplanting and thereafter when they appeared in order to maintain the single stem architecture shown previously to accelerate vegetative phase change (Clemens et al. 1999). Single stem plants were allowed to branching freely distal to node 50 to attain complexity in the crown. These plants are referred to below as single stem-free branching (SsFb) plants. For a further 20 plants, axillary buds were not removed allowing free branching from the beginning. These plants are referred as free branching.

Plants were grown in a greenhouse under natural illumination at the Massey University Plant Growth Unit (Palmerston North, New Zealand, latitude 40° 37′S longitude 175° 61′E). Plants were watered daily and fertilised monthly during the summer, and as needed for the remainder of the year. The experimental population consisted of 20 plants. From June 2003 to June 2004 the plants were grown under Ambient daylength in a temperature controlled greenhouse (25/15°C) (day/night). From June 2004 to mid-January 2005, the period preceeding the inductive treatments, all the plants were grown under Ambient daylength and temperature conditions. For convenience, the period of plant growth from June 2003 to mid-January 2005 is referred to below as the first growing season.

In mid-January 2005, 10 SsFb plants (which were allowed free branching distal to node 50 on the main stem) and 10 free branching plants were transferred to a Warm long day (Warm/LD) greenhouse. Temperature and photoperiod were applied in Warm/LD greenhouse as warm temperature regime (24/17°C) (day/night) and maintenance of 16 hour photoperiod. Photoperiod was increased using 100 W incandescent lights (10 μmol m^{-2} s^{-1}). Another equal set of plants was transferred to a greenhouse maintained at

Ambient photoperiod and temperature (Ambient) conditions, except that heating was provided to avoid frosts. Mean Ambient day/night temperatures during mid-winter were 13/8 °C rising to 25/17°C in mid-summer. Ambient photoperiod declined through mid-winter to 9 h, and extended to 16 h in mid-summer. Plants were maintained in the two different environments until November 2005. For convenience the period of the plant growth from mid-January 2005 to November 2005 is referred to below as the second growing season.

6.2.2 Leaf anatomy

Leaves for anatomical observations were collected from SsFb plants in the first growing season. To examine leaf anatomy, juvenile (node 20), transitional (nodes 40 and 55), and adult (node 75) leaves were removed and cut into small rectangular pieces, avoiding the midrib; one leaf of each stage was sampled from each of five different plants. Dr David Kubien measured the stomatal density of leaves by making impressions of both surfaces with clear acrylic nail polish by sampling one leaf from each of five different plants. Impressions were mounted on a microscope slide, and the number of stomata was counted in a 0.145 mm^2 field of view. I sampled the leaves for anatomical measurements which were opposite to those used for stomatal density determination. Excised leaf pieces were fixed for four days in FAA (18: 1 : 1 [v /v /v] 70% ethanol, glacial acetic acid, 40% [w /v] formalin). The processing of fixed specimens, microscopy and image processing was done as described in Section 3.2.3. From each leaf, two sections were used to determine the thickness of different cell layers (upper and lower epidermis, palisade and spongy mesophyll) and the proportion of intercellular air space area. The data from each section were averaged to provide one estimate for the corresponding leaf.

6.2.3 Bud collection and cymule scale scar count

During the second growing season, the distal axillary buds were collected on three occasions, quarterly (30 March, 16 June, and 21 September 2005) for analysis of meristem identity gene expression. For analysis of gene expression, distal axillary buds were excised and immediately transferred into liquid nitrogen, then stored at -80°C. In October 2005, the cymule scale scars (scars left by deciduous scales subtending cymules in the inflorescence Figure 6.1) were counted for each plant at the distal end of

branches from each treatment. A total of eight cymule scale scar counts /plant and in all the plants of four treatments was measured. Buds with 2-3 pairs of scale scars (4-6 scars) were regarded as vegetative (Henriod et al., 2001).

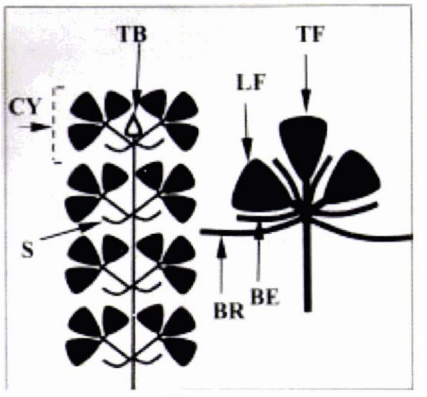

Figure 6.1 Schematic diagram of the inflorescence and one cymule of *M. excelsa* (Sreekantan et al., 2001). BE, deciduous bracteoles subtending lateral flowers; BR, one of a pair of deciduous bracts subtending each group of three flowers; CY, one of a number of three-flowered cymules that terminate secondary axes in the inflorescence; LF, lateral flower; S, scale subtending each cymule; TB, terminal bud to the primary axis; TF, terminal flower.

6.2.4 Statistical analysis

Two-way ANOVA was performed to determine the effect of environment and architecture and their interaction on cymule scale scar counts. Statistical analyses were carried out using SAS (version 9) as recorded in Section 2.2.4.

6.2.5 Total RNA extractions

Total RNA was extracted from bud samples by using QIAGEN RNeasy plant mini kit as described for *Eucalyptus* in Section 4.2.2.2. Two sets of extractions were carried out for each bud sample to increase the efficiency of total RNA obtained. A total of 24 extractions were carried out from two environments, two architectures, three sampling times and two replicates.

6.2.6 cDNA preparations

cDNA was prepared from all samples by using ThermoScript™ (Invitrogen) as described in Section 4.2.5. Three replicate cDNA preparations were carried out for each bud sample collection of each treatment and a total of 36 were obtained.

6.2.7 Isolation and quantification of *MEL*, *MESAP1* and *METFL1*

The partial homologues of *LFY* (*MEL*), *AP1* (*MESAP1*) and *TFL1* (*METFL1*) were isolated by Sreekantan (2002). Quantification was carried out by using real-time PCR. The methodology was carried out as described in Section 4.2.14. The reference gene, *β-ACTIN* was used for relative quantification. The primers used for quantification are shown in Table 6.1.

Table 6.1 Primers used for real-time quantitative RT-PCR of *Metrosideros excelsa*.

Gene	Sequence (5′ → 3′)
MEL	Forward Primer: 5′AGGAGGAAGTGGAGGAGATGAGGA 3′ Reverse Primer: 5′AGGCGTAGCAGTGGACGTAGTG 3′
MESAP1	Forward Primer: 5′CAAGCTTGAAGAGGATAGA 3′ Reverse Primer: 5′GCTTAAGAGCAGTATCAAGCTG 3′
METFL1	Forward Primer: 5′GGTTATGACAGACCCAGATGT 3′ Reverse Primer: 5′CGAACCTGTGGATACCAATG 3′
β-ACTIN	Forward Primer: 5′GCGAATTCTTCACCACYACHGCYGARCG 3′ Reverse Primer: 5′GCGGATCCCCRATCCARACACTGTAYTTCC 3′

6.3 Results

6.3.1 Leaf anatomy

The typical anatomy of leaves at nodes 20, 40 and 55 and 75 in juvenile, transitional and adult leaves from SsFb plants is shown in Figure 6.2. In contrast to the transverse sections at nodes 20 and 40, the traverse sections of leaves sampled at nodes 55 and 75 displayed adaxial epidermal hairs. On a similar note, the thickness of the abaxial and adaxial epidermis significantly ($p<0.05$) increased at nodes 55 and 75 as compared to leaves sampled at nodes 20 and 40 (Table 6.2). The depth of the palisade and mesophyll started to increase from juvenile to mature leaves from nodes 20 to 75 and the differences were statistically significant ($p<0.01$). The proportion of air space per unit area also showed an increasing trend up to node 55 and then dropped, but the differences were not significant (Table 6.2).

6.3.2 Bud scale scar counts

To understand the floral pattern in Ambient and Warm/LD environments of SsFb and free branching plants, the bud scale scar numbers were counted and plotted (Figure 6.3). The greatest number of bud scale scar pairs at the distal node was observed in SsFb plants grown in Ambient greenhouse. These plants had significantly ($p<0.001$) more bud scale scars than Ambient free branching plants. SsFb plants grown under Warm/LD had marginally more bud scale scars than corresponding free branching plants ($p<0.05$) (Appendix 1, Table 8), although the effect was not as marked as in Ambient conditions.

6.3.3 Quantification of meristem identity genes

Relative quantification of the expression of meristem identity genes showed a consistently low level of expression of *METFL1*, *MEL* and *MESAP1* in buds derived from plants grown under three of the treatment combinations (Ambient free branching, Warm/LD SsFb and Warm/LD free branching) (Figure 6.4). Only in Ambient SsFb plants during March were higher levels of *MESAP1* and *MEL* and, to a lesser extent, *METFL1* observed. In these plants, *MEL* levels were higher than *MESAP1* and *METFL1*. During June, the expression levels of all three genes dropped. In September, *MEL* levels started to increase as did *MESAP1*. The *METFL1* level was lower than

MELFY and *MESAP1*. In the other three treatments, in general no consistent pattern in gene expression was observed above base levels.

The ratios of *MEL* to *METFL1* and *MESAP1* to *METFL1* showed that there was a difference in meristem identity gene expression in buds from free branching and SsFb plants (Figure 6.5). The *MEL* to *METFL1* ratio was higher as compared to *MESAP1* to *METFL1* ratios in Ambient SsFb plants. SsFb plants grown under Warm/LD started with a high *MELFY* to *METFL1* ratio, but in June and September the values were low. In Ambient free branching plants, during September the ratio of *MESAP1* to *METFL1* was higher as compared to corresponding SsFb plants, but this trend was not observed with *MEL* to *METFL1* ratio. In Warm/LD SsFb and free branching plants, very low levels of *MESAP1* to *METFL1* ratios were observed.

Table 6.2 Anatomical parameters of *Metrosideros excelsa* leaves collected from SsFb plants. [1, 2]

Node	Palisade depth (μm)	Spongy depth (μm)	Air space (%)	Epidermis (μm) abaxial	adaxial
20	$123^{a} \pm 6.4$	$144^{a} \pm 3.9$	$9.9^{a} \pm 2.0$	$19^{a} \pm 0.4$	$18^{a} \pm 0.8$
40	$148^{a} \pm 8.9$	$130^{a} \pm 6.7$	$9.9^{a} \pm 3.0$	$13^{a} \pm 0.8$	$15^{a} \pm 0.7$
55	$263^{b} \pm 25.6$	$221^{b} \pm 11.3$	$14.6^{a} \pm 0.4$	$33^{b} \pm 0.7$	$38^{b} \pm 1.5$
75	$258^{b} \pm 12.3$	$212^{b} \pm 12.8$	$10.6^{a} \pm 1.3$	$38^{b} \pm 3.0$	$31^{b} \pm 2.5$

[1]Each value represents the mean (± S.E.) of leaves from five different plants. Values with different superscripts in the same column are significantly different ($p<0.05$, Tukey).

[2]These data are published in Kubien et al. (2007).

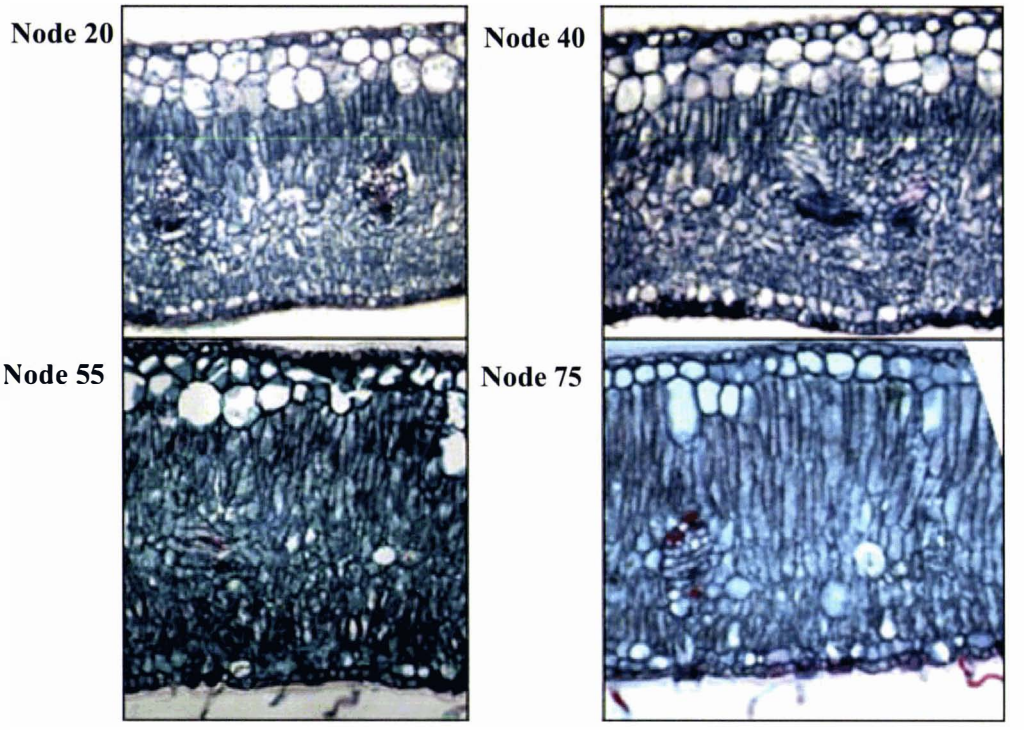

Figure 6.2 Typical leaf sections (200 X) of *M. excelsa* at node 20, 40, 55 and 75 on the main stem of SsFb plants. While preparing sections the midrib was avoided. For more details on section preparations please refer to Section 6.2.2.

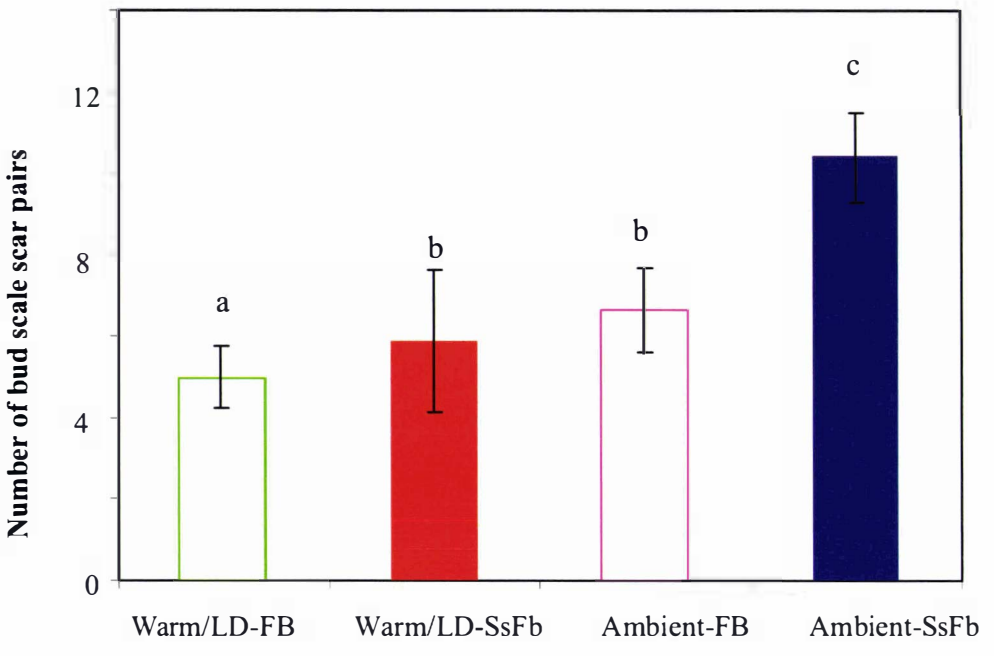

Figure 6.3 Number of bud scale scar pairs at distal ends of branches of plants grown under different environments with architecture modification. Warm/LD-FB, Warm long day free branching plants; Warm/LD-SsFb, Warm long day single stem-free branching plants; Ambient-FB, Ambient free branching plants; Ambient-SsFb, Ambient single stem-free branching plants. Bars with different letters are significantly different ($p<0.05$).

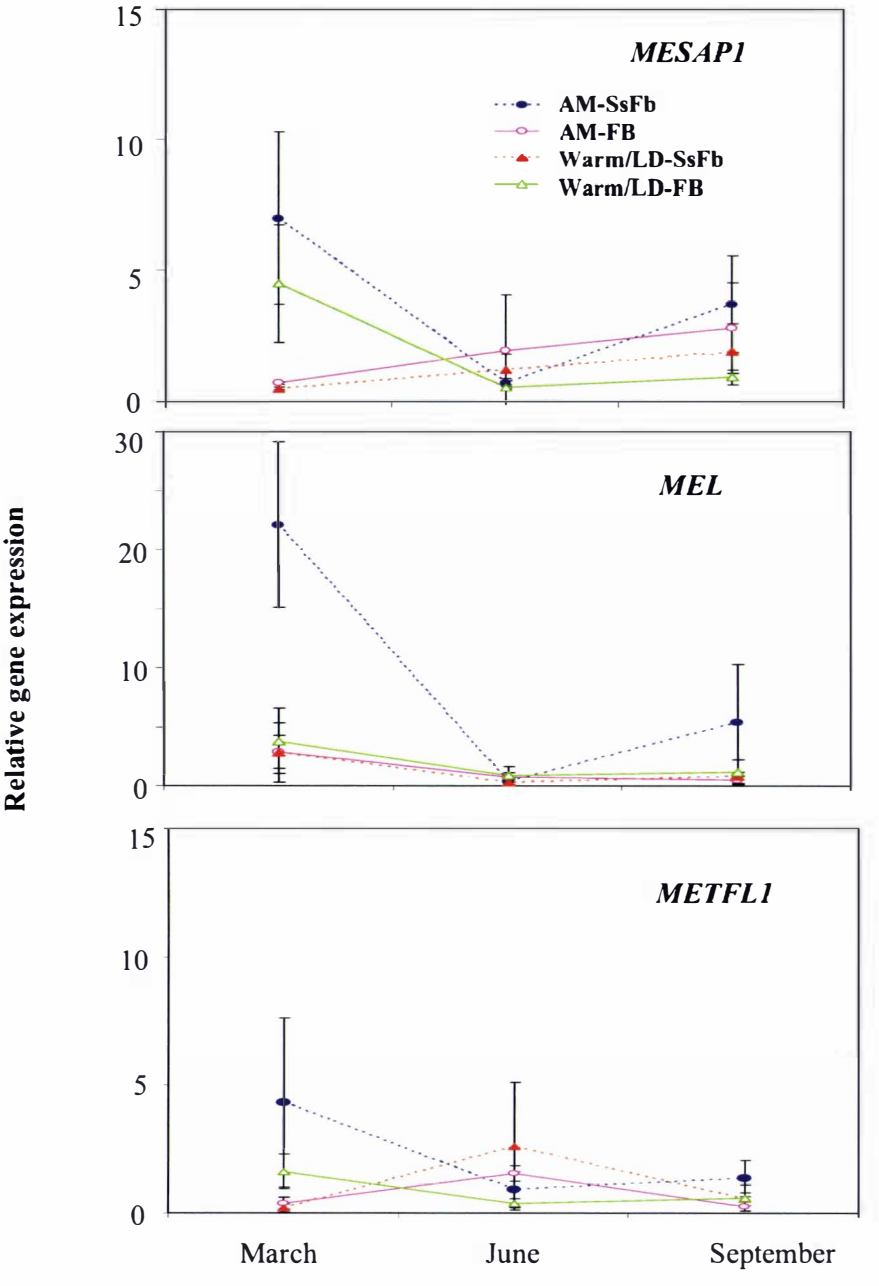

Figure 6.4 Relative quantification of meristem identity gene expression on three occasions in *M. excelsa* plants grown under different environmental and architecture treatments. AM-FB, Ambient free branching plants; AM-SsFb, Ambient single stem-free branching plants; Warm/LD-FB, Warm/LD free branching plants; Warm/LD-SsFb, Warm/LD single stem-free branching plants; Each gene expression value represents at least three replicates (± S.E.).

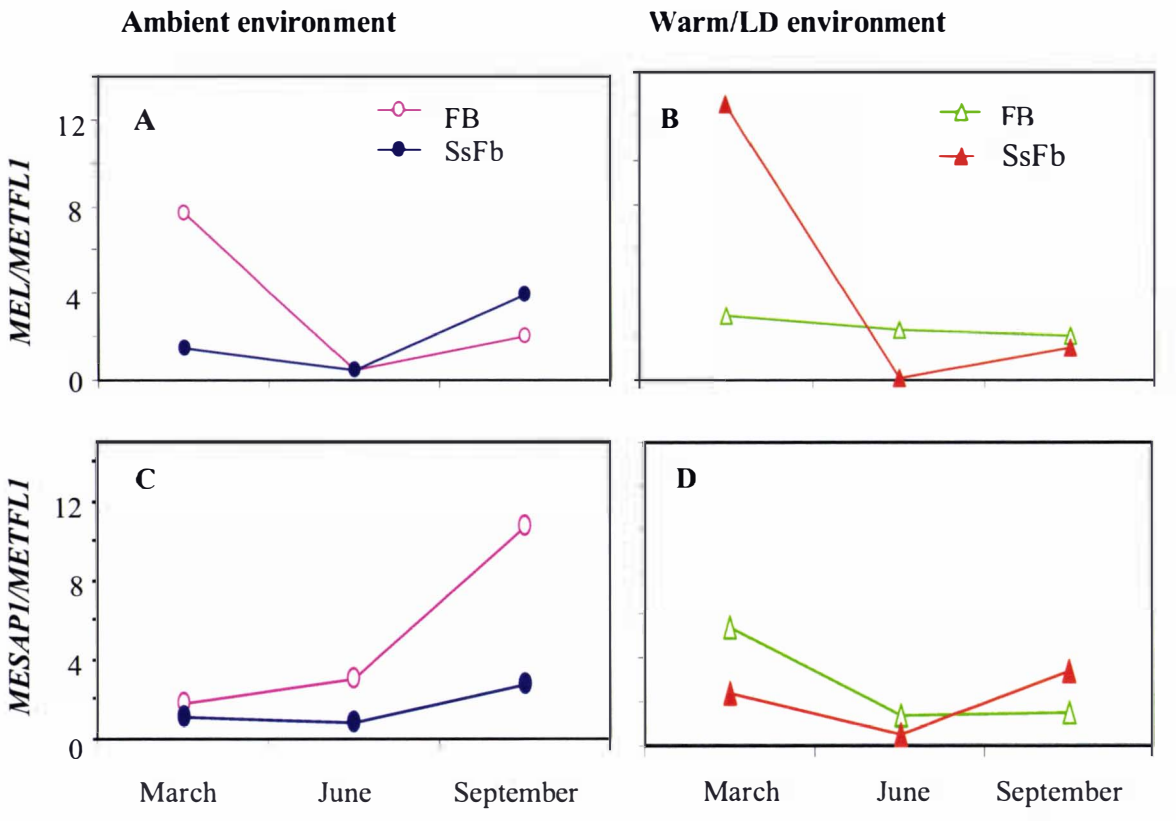

Figure 6.5 A-D Plots showing the expression ratios of *MEL/METFL1* and *MESAP1/METFL1* on three occasions in plants grown under Ambient and Warm/LD environments with architecture modification. A, *MEL/METFL1* ratio in Ambient environment; B, *MEL/METFL1* ratio in Warm/LD environment; C, *MESAP1/METFL1* ratio in Ambient environment; *MESAP1/METFL1* ratio in Warm/LD environment; FB, free branching plants and SsFb, single stem-free branching plants.

6.4 Discussion

6.4.1 Leaf anatomy

Earlier studies showed homoblastic behaviour of *M. excelsa* during phase change using several optical and dimensional leaf parameters and reported that adult leaves had more mealiness or whiteness and roundness than the juvenile leaves (Clemens et al., 1999). In this thesis the detailed anatomical measurements showed that adult leaves resembled sun leaves by having deeper palisade and spongy mesophyll layers than juvenile or transitional foliage (Figure 6.2; Kubien et al., 2007). The increase in the depth of the mesophyll layer in adult leaves as compared to juvenile may serve to reduce the penetration of light through the leaf and hence prevent high light-induced damage (Kubien et al., 2007). There was an increase in the size of the abaxial and adaxial epidermis from juvenile to adult leaves. These epidermal changes were coincident with changes in leaf pubescence. The leaf pubescence began to appear on foliage produced at nodes 30-35, but fully pubescent foliage was produced at around node 55. These anatomical observations support the suggestion that there is a smooth transition from juvenile to adult foliage in *M. excelsa* with the eventual attainment of fully pubescent adult leaves. In addition, this study confirms the earlier observations that single stem architectural modification accelerates phase change in terms of leaf anatomy as well as morphology (Clemens et al., 1999).

6.4.2 Floral transition and expression of meristem identity genes

During the study period, no flowers were observed on *M. excelsa* plants, irrespective of environmental or architectural treatment, indicating that these factors alone were not sufficient to cause flowering in *M. excelsa*. Numbers of cymule scale scar pairs were counted as evidence of inflorescence formation and reflected the number of cymules that had developed in the resting buds at the distal end of branches. While studying bud size and flowering in *Metrosideros*, Henriod et al. (2000) considered that the presence of two to three pairs of bud scar pairs on resting distal buds as indicative of a vegetative state, more than three pairs of scars as indicative of the floral state. Single stem-free branching (SsFb) plants grown under Ambient conditions showed more pairs of bud scale scars indicating that floral initiation had occurred over the previous winter. However, flowers had not developed due to inflorescence reversion, a mechanism

previously considered to occur in *M. excelsa* (Sreekantan et al., 2001). Sreekantan et al. (2001) suggested that this might be a result of not receiving a sufficiently strong inductive signal from the leaf subtending the inflorescence or from the scale leaves protecting the resting terminal bud. In addition, endogenous factors such as an over-riding effect of leaf development and terminal shoot expansion might have contributed to the incomplete floral development. Such incomplete floral developmental cycles were recorded in *M. excelsa* trees studied over two seasons (Sreekantan et al., 2001).

Manipulation of temperature and/or photoperiod has been successful in promoting flowering in *Eucalyptus* (Bolotin, 1975; Moncur, 1992), *Hypocalymma* (Day et al., 1994), *Pimelea* (King et al., 1996), and *Hardenbergia* (King, 1998). By contrast, in *M. excelsa* Ambient daylength /Ambient temperature conditions and not Warm/LD conditions produced a higher proportion of buds with potential inflorescences based on bud scale scar data. Cymules apparently did not differentiate due to unsuitable conditions. The inductive effect of ambient winter conditions (shortdays and cold temperatures) in *M. excelsa* was also reported by Henriod et al. (2000). These authors also showed that Ambient daylength in winter, but warm winter conditions could result in fewer flowers reaching anthesis.

The gene expression studies in *M. excelsa* showed that, during inflorescence meristem initiation in March (autumn), the Ambient SsFb plants recorded higher levels of *MEL* and *MESAP1* showing floral determination and floral commitment in this treatment. By contrast, in single stem plants of *E. occidentalis* showed delayed *EOLFY* and *EOAP1* response (Chapter 4). Bud scale scars data shows a greater degree of floral development to be associated with elevated levels of *MEL* and *MESAP1*. *METFL1* levels were also moderate in this treatment showing the importance of inflorescence meristem identity genes during March (inflorescence meristem initiation). There was a significant drop in gene expression levels during June which was also reported by Sreekantan et al. (2004). These findings of Ambient SsFb plants support the bimodal pattern of meristem identity gene expression during floral transition of *M. excelsa.*

The expression of *MEL* and *MESAP1* started to increase in September in Ambient SsFb plants, but the levels were apparently not sufficient for the continuation of floral

development or inflorescence reversion could have played a role and no flowers were formed. This low level of *MEL* expression may be insufficient either to activate or to repress the *M. excelsa* homologues of *AG* or *AGL24*. It was reported that these genes have a role in floral meristem determinacy in *Arabidopsis*, and that a low level of *LFY* expression is key to a number of instances of reversion (Tooke et al., 2005).

The free branching plants in either Ambient or Warm/LD environments displayed a base level of *MEL* and *MESAP1* expression, showing that no floral transition had happened in these plants. Hence Ambient SsFb plants as compared to free branching plants had contributed to the rate of floral transition in *M. excelsa* plants. The SsFb plants in Warm/LD environment have shown lower levels of floral meristem identity gene expression and no bimodal pattern of gene expression as compared to their Ambient environment counterparts. Hence environment has a significant role in the floral transition in *M. excelsa*. Based on these results, in *M. excelsa*, the hypothesis that floral inductive environmental treatments such as Ambient temperature and Ambient photoperiod, promote higher expression levels of floral meristem identity genes *MEL* and *MESAP1*, has been supported.

The successful method of shortening the juvenile period (accelerating phase change) was achieved by growing the *M. excelsa* plants with single stem architecture and it was proposed that this occurred because of greater linear distance between roots and shoot apex (Clemens et al., 1999). In *M. excelsa* under an inductive Ambient environment, SsFb architectural modification (plants displayed adult foliage) influenced the rate of floral transition although floral buds did not fully develop. These observations support the suggestion that both height and complexity of branching would affect the attainment of reproductive competence in *M. excelsa,* as reported by Clemens et al. (2002) and Sismilich et al. (2003) and reinforces the observation that in *M. excelsa* vegetative phase change and the floral transition process appear to be co-ordinated and floral transition appears dependent on phase change.

Chapter 7
Final Discussion

According to Poethig (1990), the shoot apex of higher plants passes through three distinct phases during its post-embryonic development: a juvenile vegetative phase, an adult vegetative phase and a reproductive phase. Lawson and Poethig (1995) suggested that these developmental phases may be regulated independently of each other, or they may be co-ordinatedly expressed, with the expression of one phase dependent on the manifestation of the other. In this thesis, morphological, physiological, and molecular studies were carried out in *E. occidentalis* and *M. excelsa* to investigate the progress and regulation of phase change and the floral transition.

In *M. excelsa* phase change has been characterised by several optical and dimensional leaf parameters (Clemens et al., 1999) and gas exchange measurements (Kubien et al., 2007). Leaf anatomical measurements made during this thesis also showed a smooth transition from juvenile to adult foliage in architecturally manipulated single stem plants. These morphological and anatomical studies indicate that phase change in *M. excelsa* is accelerated in single stem plants, suggesting that plant height (i.e. a greater distance between the shoot apex and roots) accelerates phase change in this species as concluded by Clemens et al. (1999). However, both height and complexity of branching would appear to be involved in the attainment of reproductive competence in *M. excelsa,* supporting the mathematical studies that indicated that reproductive competence was a consequence of the plant reaching a certain degree of branching complexity (Clemens et al., 2002; Sismilich et al., 2003).

Inflorescence development occurs in distal axillary buds in *M. excelsa* (Sreekantan et al., 2001) and, generally, *M. excelsa* takes several years for seedlings and over three years for plantlets rejuvenated by micropropagation to flower (Clemens et al., 1999). Henriod et al. (2000) suggested that *M. excelsa* responded as a facultative short day plant with maximum flowering exhibited after a 15 week cool (mean 15°C) short day (10 h) inductive treatment. During the period of this study, *M. excelsa* did not produce

flowers that reached anthesis. However, floral initiation occurred as determined by the number of bud scale scar pairs reflecting inflorescence formation in single stem plants allowed to branch freely (SsFb) grown under Ambient conditions. However, in completely free branching plants grown under the same conditions there was no evidence that floral initiation had occurred. Moreover, phase change, as expressed in leaf morphological characters, occurred in SsFb plants before they were allowed to branch, and this did not occur in free branching plants. It appears that phase change and floral transition are accelerated only when height and complexity are combined in SsFb plants in *M. excelsa.* In addition, Warm/LD SsFb plants of *M. excelsa,* which were displaying adult foliage, did not show any inflorescence initiation. This suggests that an inductive environment is also playing a role in floral transition in *M. excelsa.*

In stark contrast, in *E. occidentalis*, increased shoot complexity rather than height has contributed the significant dominant effect on the rate of phase change. Ecotype 13648 grown as free branching plants attained lanceolate leaf morphology, isobilateral leaf anatomy, and lower photosynthetic rates earlier than single stem plants.

Moreover, floral transition occurred irrespective of shoot architecture and ecotype (except ecotype 15395) in *E. occidentalis* showing independent regulation of developmental phases. Flowering was observed on shoots showing either juvenile or transitional leaf attributes in plants grown with either single stem or free branching architecture. These observations confirm that attaining adult shoot phenology is not necessarily a requirement for vegetative to reproductive transition. Independent regulation of vegetative and reproductive transition was observed in *E. risdonni* and *E. tenuiramis* and the authors suggested that these phases were under separate genetic control (Wiltshire et al., 1998). Lawson and Poethig (1995) suggested that independent regulation would allow greater plasticity of interactions between phases and new structures, or adaptive traits could be produced by novel overlaps between programmes that were previously separated.

Further, in this thesis, *E. occidentalis* displayed neoteny and precocious flowering. Bolotin (1975) and Southerton (2007) also observed precocious flowering in this *Eucalyptus* species. In contrast, *M. excelsa* exhibited a longer time to flower and passed through a long homoblastic vegetative phase change (Clemens et al., 1999).

Inflorescence reversion reported by Sreekantan et al. (2001) in *M. excelsa* was also recorded in this thesis as observed by the number of cymule scale scars. As a consequence the shoot apical meristem reverts to vegetative development, which provides a mechanism for ensuring a polycarpic perennial life-history in this species (Sreekantan et al., 2001).

Irrespective of environmental conditions, *E. occidentalis* showed an over-riding effect of shoot architecture on rate of floral transition. It would appear that free branching plants of *M. excelsa* which had not attained adult shoot phenology could not respond to floral inductive treatment. This indicates that attaining adult shoot phenology appears to be necessary for floral transition and that developmental phases are regulated co-ordinately in *M. excelsa*. *Eucalyptus occidentalis* exhibited neoteny and dissociation between phase change and floral transition, whereas *M. excelsa* exhibited homoblasty, and sequential phase change and floral transition.

As discussed in Chapter 4, the isolated gene sequences of *EOLFY*, *EOAP1* and *EOTFL1* are the homologues of *Arabidopsis LFY*, *AP1* and *TFL1*, respectively. Shoot architectural manipulation of free branching and single stem plants affected the timing in peak expression of *EOLFY* and *EOAP1* during ontogeny in *E. occidentalis*. Increased expression of *EOLFY* and *EOAP1* was observed earlier in free branching plants, which correlated with changes taking place in the morphological and physiological characteristics. By contrast, in *M. excelsa*, only the Ambient SsFb plants recorded elevated levels of *MEL* and *MESAP1* and only during inflorescence meristem initiation (during March).

Eucalyptus occidentalis displayed lower relative expression levels (less than one fold) of *EOTFL1* as compared to *EOLFY* and *EOAP1* in both single stem (showing juvenile leaf morphology) and free branching plants (showing transitional to adult leaf morphology) during the sampling period. This suggests that lower levels of *EOTFL1* are perhaps contributing to precocious flowering of this species. In contrast with *E. occidentalis*, the relative expression levels of *METFL1* relative to *MEL* and *MESAP1* in *M. excelsa* were higher (ranging approximately from one to eight-fold).

EOAP1 was found to be a reliable marker of floral commitment in *E. occidentalis*. However, in *M. excelsa* no such conclusions could be reached for *MESAP1* as flowering did not occur during the study period, possibly as a result of inflorescence reversion. In *E. occidentalis*, it could be speculated that the photoperiod pathway is independent of *LFY* (Figure 1.1).

In *M. excelsa*, *MEL* and *MESAP1* expression indicated that floral determination in Ambient SsFb plants had occurred in those buds sampled during March (autumn) but possibly due to, or as a consequence of, inflorescence reversion, significant increases in the expression of *MEL* or *MESAP1* were not observed in the buds collected in September (spring). In contrast to *E. occidentalis,* higher levels of *MEL* than *MESAP1* during the floral transition leads to the suggestion that flowering may have occurred via the up-regulation of *LFY* in *M. excelsa* (Figure 1.1). *LFY* is known to regulate the transcription of *AP1*, *AP3*, and *AG* and gives floral identity to the shoot apical meristem (Busch et al., 1999; Wagner et al., 1999; Lamb et al., 2002).

Thus, this study has brought out the importance of shoot architecture in relation to phase change and floral transition in *E. occidentalis* and shown that complexity of architecture contributes to both phase change and floral transition and that these are under strong genetic control. But for *M. excelsa* phase change was accelerated in response to growth in height and floral transition responded to branching complexity. Environmental signals were also playing an important role for floral induction in *M. excelsa*. However, this study is still at an early stage, at the molecular level.

In conclusion, the objectives as initially stated in this thesis and in fulfilment of the sub-contract of Massey University to the Crop & Food Research Institute were addressed and achieved successfully. The current thesis, provides a deeper understanding of the mechanisms underlying phase change and the floral transition in relation to shoot architecture in *E. occidentalis,* which in turn enhances our understanding of phase change mechanisms in *M. excelsa.*

Appendix 1

Table 1 p-values generated using three-way ANOVA of leaf morphology attributes in *E. occidentalis.*

Parameter/ Treatment	Ecotype (E)	Node (N)	Architecture (A)	E*N	E*A	N*A	E*N*A
Leaf area	***	***	***	*	***	***	**
Leaf perimeter	***	***	***	NS	***	***	**
Leaf roundness	***	***	***	**	***	***	NS
Leaf length	***	***	***	*	***	**	NS
Leaf width	***	***	***	**	**	**	*
Leaf length/width	***	***	***	***	*	***	***
Petiole length	***	***	***	NS	***	NS	NS

*** $p<0.0001$; **$p<0.001$; *$p<0.05$; NS = non-significant

Table 2 p-values generated using either three-way or four-way ANOVA of gas exchange estimates V_{cmax} and J_{max} in *E. occidentalis*.

Experiment	Parameter	Ecotype (E)	Architecture (A)	Fertiliser (F)	Node (N)	E*A	E*F	E*N	A*F	A*N	F*N	E*A*F	E*A*N	E*F*N	A*F*N	E*A*F*N
Before fertiliser treatment	$V_{c\,max}$	NS	***	-	NS	NS	-	NS	-	NS	-	-	NS	-	-	-
	J_{max}	*	***	-	NS	*	-	NS	-	NS	-	-	NS	-	-	-
Following supplementary fertiliser treatment	$V_{c\,max}$	*	***	*	NS	NS	NS	NS	NS	NS	NS	NS	NS	NS	NS	NS
	J_{max}	***	***	*	NS	NS	NS	NS	*	NS	NS	NS	NS	NS	NS	NS

*** p<0.0001; **p<0.001; *p<0.05

Table 3 p-values derived from three-way ANOVA of leaf anatomy characteristics in *E. occidentalis*.

Parameter	Ecotype (E)	Node (N)	Architecture (A)	E*N	E*A	N*A	E*N*A
Number of palisade layers	NS	***	***	*	NS	*	NS
Number of cell layers	***	***	**	***	*	NS	NS
Leaf thickness	NS	NS	***	NS	NS	NS	*
Mesophyll thickness	NS	NS	***	NS	NS	NS	*
Adaxial epidermis thickness	**	NS	*	NS	*	NS	NS
Adaxial palisade thickness	***	NS	NS	*	NS	NS	NS
Abaxial epidermis thickness	NS	NS	NS	NS	NS	NS	*
Abaxial palisade thickness	NS	**	NS	NS	*	NS	*
Air space (%)	NS	NS	***	NS	*	NS	NS

*** $p<0.0001$; **$p<0.001$; *$p<0.05$; NS, non-significant

Table 4 p-values obtained after three-way or four-way ANOVA of LMA (g m^{-2}) data in *E. occidentalis*.

Experiment	Ecotype (E)	Architecture (A)	Fertiliser (F)	Node (N)	E*A	E*F	E*N	A*F	A*N	F*N	E*A*F	E*A*N	E*F*N	A*F*N	E*A*F*N
Before supplementary fertiliser treatment	NS	*	-	NS	NS	-	NS	-	NS	-	-	NS	-	-	-
Followig supplementary fertiliser treatment	NS	*	NS	NS	NS	NS	NS	NS	NS	NS	*	NS	NS	NS	NS

*p<0.05; NS, non-significant

Table 5 p-values obtained after three-way ANOVA for *E. occidentalis* leaf mineral concentrations analysed before supplemental fertiliser treatment in March 2004.

Mineral	Ecotype (E)	Architecture (A)	Node (N)	E*A	E*N	A*N	E*A*N
N	***	***	*	*	NS	NS	*
P	***	***	***	NS	*	*	*
K	*	*	NS	NS	*	NS	NS
S	***	***	**	***	NS	*	NS
Ca	NS	***	*	NS	NS	NS	NS
Mg	NS	***	*	NS	NS	*	NS
Na	***	***	***	***	*	*	*
Fe	***	NS	NS	NS	NS	NS	NS
Mn	*	***	***	NS	NS	NS	NS
Zn	NS	*	*	NS	NS	NS	NS
Cu	***	**	***	*	NS	NS	NS
B	NS	**	***	NS	NS	NS	NS

*** $p<0.0001$; **$p<0.001$; *$p<0.05$; NS, non-significant

Table 6 p-values obtained after ANOVA for *E .occidentalis* leaf mineral concentrations after supplemental fertiliser treatment in April 2004.

Mineral	Ecotype (E)	Architecture (A)	Fertiliser (F)	E*A	E*F	A*F	E*A*F
N	NS	***	*	NS	NS	NS	NS
P	*	NS	NS	NS	NS	NS	NS
K	NS	NS	NS	NS	NS	NS	NS
S	***	***	*	*	NS	NS	NS
Ca	NS	***	NS	NS	NS	NS	NS
Mg	NS	***	NS	NS	NS	NS	NS
Na	NS	*	NS	NS	NS	NS	NS
Fe	*	NS	*	NS	*	NS	*
Mn	**	NS	NS	NS	NS	NS	NS
Zn	NS	*	*	NS	NS	NS	*
Cu	**	**	NS	*	NS	NS	NS
B	NS	NS	NS	NS	NS	NS	NS

*** $p<0.0001$; ** $p<0.001$; * $p<0.05$; NS, non-significant

Table 7 p-values derived from ANOVA of morphological parameters of environmental and architectural treatments

Parameter	Environment	Architecture	Environ × Archi
Flowering node	NS	***	NS
Total nodes	NS	***	*
Buds per branch	***	***	***
Flowering branches/total branches	*	***	NS

*** p<0.0001; **p<0.001; *p<0.05; NS, non-significant

Table 8 p-values derived from ANOVA of bud scale scars of environmental and architectural treatments of *M. excelsa*

Parameter	Environment	Architecture	Environ × Archi
Bud scale scars	***	***	***

*** p<0.0001.

Appendix 2

The SAS System 20:23 Thursday, September 8, 2005 31

The CANDISC Procedure

Observations	468	DF Total	467
Variables	7	DF Within Classes	462
Classes	6	DF Between Classes	5

Class Level Information

eco	Variable Name	Frequency	Weight	Proportion
3634	_3634	96	96.0000	0.205128
3636	_3636	72	72.0000	0.153846
3644	_3644	48	48.0000	0.102564
3648	_3648	84	84.0000	0.179487
5395	_5395	72	72.0000	0.153846
5416	_5416	96	96.0000	0.205128

The SAS System 20:23 Thursday, September 8, 2005 32

The CANDISC Procedure

Pairwise Squared Distances Between Groups

$$D^2(i|j) = (\bar{X}_i - \bar{X}_j)' \, COV^{-1} \, (\bar{X}_i - \bar{X}_j)$$

Squared Distance to eco

From eco	3634	3636	3644	3648	5395	5416
3634	0	0.57770	1.65858	9.02834	0.70590	0.69564
3636	0.57770	0	1.26274	7.87077	0.47018	0.54532
3644	1.65858	1.26274	0	8.40893	1.09114	1.52779
3648	9.02834	7.87077	8.40893	0	9.16218	10.16385
5395	0.70590	0.47018	1.09114	9.16218	0	0.06143
5416	0.69564	0.54532	1.52779	10.16385	0.06143	0

F Statistics, NDF=7, DDF=456 for Squared Distance to eco

From eco	3634	3636	3644	3648	5395	5416
3634	0	3.35135	7.48361	57.03095	4.09507	4.70818
3636	3.35135	0	5.12781	43.02583	2.38669	3.16355
3644	7.48361	5.12781	0	36.21699	4.43095	6.89350
3648	57.03095	43.02583	36.21699	0	50.08539	64.20387
5395	4.09507	2.38669	4.43095	50.08539	0	0.35638
5416	4.70818	3.16355	6.89350	64.20387	0.35638	0

Prob > Mahalanobis Distance for Squared Distance to eco

From eco	3634	3636	3644	3648	5395	5416
3634	1.0000	0.0017	<.0001	<.0001	0.0002	<.0001
3636	0.0017	1.0000	<.0001	<.0001	0.0209	0.0028
3644	<.0001	<.0001	1.0000	<.0001	<.0001	<.0001
3648	<.0001	<.0001	<.0001	1.0000	<.0001	<.0001
5395	0.0002	0.0209	<.0001	<.0001	1.0000	0.9270
5416	<.0001	0.0028	<.0001	<.0001	0.9270	1.0000

The SAS System 20:23 Thursday, September 8, 2005 33

The CANDISC Procedure

Univariate Test Statistics

F Statistics, Num DF=5, Den DF=462

Variable	Label	Total Standard Deviation	Pooled Standard Deviation	Between Standard Deviation	R-Square	R-Square / (1-RSq)	F Value	Pr > F
Area	Area	20.3445	18.1317	10.3036	0.2142	0.2726	25.19	<.0001
Length	Length	2.6673	2.5720	0.8263	0.0801	0.0871	8.05	<.0001
Width	Width	2.1106	1.7047	1.3754	0.3546	0.5495	50.77	<.0001

Petiole	Petiole	0.6463	0.6079	0.2497	0.1247	0.1424	13.16	<.0001
Lwratio	Lwratio	1.0781	0.8167	0.7757	0.4323	0.7614	70.35	<.0001
Roundness	Roundness	0.4915	0.3980	0.3187	0.3511	0.5410	49.99	<.0001
Perimeter	Perimeter	6.4593	5.9355	2.8681	0.1647	0.1971	18.21	<.0001

Average R-Square

Unweighted	0.2459516
Weighted by Variance	0.2096298

Multivariate Statistics and F Approximations

S=5 M=0.5 N=227

Statistic	Value	F Value	Num DF	Den DF	Pr > F
Wilks' Lambda	0.34469521	15.81	35	1920.6	<.0001
Pillai's Trace	0.78216371	12.19	35	2300	<.0001
Hotelling-Lawley Trace	1.55593660	20.21	35	1285.3	<.0001
Roy's Greatest Root	1.32457755	87.04	7	460	<.0001

NOTE: F Statistic for Roy's Greatest Root is an upper bound.

The CANDISC Procedure

	Canonical Correlation	Adjusted Canonical Correlation	Approximate Standard Error	Squared Canonical Correlation
1	0.754860	0.748878	0.019907	0.569814
2	0.320645	0.280577	0.041517	0.102813
3	0.273289	0.263864	0.042818	0.074687
4	0.184466	0.175929	0.044700	0.034028
5	0.028659	-.042828	0.046236	0.000821

Test of H0: The canonical correlations in the current row and all that follow are zero

Eigenvalues of Inv(E)*H = CanRsq/(1-CanRsq)

Eigenvalue	Difference	Proportion	Cumulative	Likelihood Ratio	Approximate F Value	Num DF	Den DF	Pr > F
1	1.3246	1.2100	0.8513	0.8513	0.34469521	15.81	35	1920.6	<.0001
2	0.1146	0.0339	0.0737	0.9250	0.80127074	4.36	24	1595.5	<.0001
3	0.0807	0.0455	0.0519	0.9768	0.89309248	3.53	15	1264.7	<.0001
4	0.0352	0.0344	0.0226	0.9995	0.96517877	2.05	8	918	0.0380
5	0.0008	0.0005	1.0000	0.99917866	0.13	3	460	0.9447

The CANDISC Procedure

Total Canonical Structure

Variable	Label	Can1	Can2	Can3	Can4	Can5
Area	Area	0.545279	-0.550342	0.295250	-0.457615	0.098169
Length	Length	0.203292	-0.393840	0.676957	-0.431685	-0.314740
Width	Width	0.762541	-0.436707	0.052418	-0.318451	0.223887
Petiole	Petiole	0.372040	0.361072	0.575632	-0.471695	-0.308162
Lwratio	Lwratio	-0.857117	0.251449	0.308059	0.033627	-0.193709
Roundness	Roundness	-0.763267	0.248293	0.391343	0.196431	-0.187286
Perimeter	Perimeter	0.445480	-0.463351	0.555515	-0.435252	-0.069768

Between Canonical Structure

Variable	Label	Can1	Can2	Can3	Can4	Can5
Area	Area	0.889343	-0.381277	0.174340	-0.182390	0.006079
Length	Length	0.542059	-0.446071	0.653496	-0.281283	-0.031862
Width	Width	0.966584	-0.235139	0.024055	-0.098644	0.010775

Petiole	Petiole	0.795378	0.327895	0.445538	-0.246431	-0.025013
Lwratio	Lwratio	-0.984076	0.122630	0.128049	0.009435	-0.008444
Roundness	Roundness	-0.972391	0.134365	0.180500	0.061154	-0.009059
Perimeter	Perimeter	0.828724	-0.366142	0.374139	-0.197867	-0.004928

Pooled Within Canonical Structure

Variable	Label	Can1	Can2	Can3	Can4	Can5
Area	Area	0.403453	-0.588058	0.320391	-0.507374	0.110699
Length	Length	0.139024	-0.388958	0.678963	-0.442374	-0.328031
Width	Width	0.622570	-0.514906	0.062766	-0.389602	0.278579
Petiole	Petiole	0.260814	0.365552	0.591839	-0.495516	-0.329242
Lwratio	Lwratio	-0.746102	0.316097	0.393285	0.043863	-0.256982
Roundness	Roundness	-0.621453	0.291951	0.467311	0.239660	-0.232397
Perimeter	Perimeter	0.319686	-0.480196	0.584665	-0.468047	-0.076304

The CANDISC Procedure

Total-Sample Standardized Canonical Coefficients

Variable	Label	Can1	Can2	Can3	Can4	Can5
Area	Area	-0.94532677	-2.38317073	0.38113433	0.84756470	0.01890882
Length	Length	1.13592858	-1.68250701	-4.47428279	0.22227137	-8.03914012
Width	Width	1.50983091	1.16672546	-4.28750097	-1.31962235	-3.58008113
Petiole	Petiole	0.61100241	1.02270206	0.29782072	-0.34908636	-0.02635150
Lwratio	Lwratio	-2.69010763	1.25336811	-1.90454469	-4.78266578	1.12085482
Roundness	Roundness	1.68004240	-0.74161212	1.34918065	4.22181535	-1.00175175
Perimeter	Perimeter	-1.34917091	1.97451598	7.31283228	-0.55701895	10.23580067

Pooled Within-Class Standardized Canonical Coefficients

Variable	Label	Can1	Can2	Can3	Can4	Can5
Area	Area	-0.842507166	-2.123962290	0.339679795	0.755378302	0.016852176
Length	Length	1.095337450	-1.622384521	-4.314399341	0.214328751	-7.751870519
Width	Width	1.219463319	0.942343207	-3.462937554	-1.065835276	-2.891567249
Petiole	Petiole	0.574732937	0.961993853	0.280141906	-0.328364381	-0.024787256
Lwratio	Lwratio	-2.037873991	0.949481072	-1.442775762	-3.623078155	0.849096466
Roundness	Roundness	1.360673073	-0.600634626	1.092706819	3.419265171	-0.811322760
Perimeter	Perimeter	-1.239760605	1.814393654	6.719802013	-0.511847793	9.405733822

Raw Canonical Coefficients

Variable	Label	Can1	Can2	Can3	Can4	Can5
Area	Area	-0.046465874	-0.117140563	0.018733987	0.041660551	0.000929430
Length	Length	0.425872589	-0.630791082	-1.677459687	0.083332073	-3.013965390

Width	Width	0.715342936	0.552782971	-2.031375506	-0.625224001	-1.696206990
Petiole	Petiole	0.945415842	1.582446681	0.460823765	-0.540148073	-0.040774180
Lwratio	Lwratio	-2.495131067	1.162525127	-1.766505016	-4.436022493	1.039616277
Roundness	Roundness	3.418368536	-1.508952110	2.745166845	8.590093171	-2.038256101
Perimeter	Perimeter	-0.208871436	0.305684022	1.132133647	-0.086234700	1.584652005

Class Means on Canonical Variables

eco	Can1	Can2	Can3	Can4	Can5
3634	0.524866406	0.393067946	0.388429990	0.117881648	0.002098938
3636	0.341681554	0.081930054	0.005681635	-0.430602852	0.003926771
3644	0.296703573	-0.871454983	0.374597617	0.033535475	-0.011953895
3648	-2.424670977	0.035211824	-0.050730509	0.030550891	-0.002067880
5395	0.588627658	-0.114508254	-0.275791052	0.106701365	0.055801202
5416	0.750637002	0.036282849	-0.328757541	0.081544700	-0.03910857

Appendix 3

The SAS System 20:23 Thursday, September 8, 2005 37

The CANDISC Procedure

Observations	468	DF Total	467
Variables	7	DF Within Classes	456
Classes	12	DF Between Classes	11

Class Level Information

archi	Variable Name	Frequency	Weight	Proportion
1	_1	48	48.0000	0.102564
2	_2	48	48.0000	0.102564
3	_3	36	36.0000	0.076923
4	_4	36	36.0000	0.076923
5	_5	24	24.0000	0.051282
6	_6	24	24.0000	0.051282
7	_7	42	42.0000	0.089744
8	_8	42	42.0000	0.089744
9	_9	36	36.0000	0.076923
10	_10	36	36.0000	0.076923
11	_11	48	48.0000	0.102564
12	_12	48	48.0000	0.102564

The SAS System 20:23 Thursday, September 8, 2005 38

The CANDISC Procedure

Pairwise Squared Distances Between Groups

$$D^2(i|j) = (\bar{X}_i - \bar{X}_j)' \, COV^{-1} \, (\bar{X}_i - \bar{X}_j)$$

Squared Distance to archi

From archi	1	2	3	4	5	6	7	8
1	0	3.23287	0.80790	2.81306	5.00140	3.95780	9.95116	30.60950
2	3.23287	0	4.14562	0.65005	12.13512	1.42411	4.61539	19.01991
3	0.80790	4.14562	0	2.69330	3.78389	3.91534	9.27603	27.91615
4	2.81306	0.65005	2.69330	0	10.51170	1.43601	3.60362	19.18975
5	5.00140	12.13512	3.78389	10.51170	0	11.33483	15.30443	35.36687
6	3.95780	1.42411	3.91534	1.43601	11.33483	0	4.59337	19.66457
7	9.95116	4.61539	9.27603	3.60362	15.30443	4.59337	0	12.62201
8	30.60950	19.01991	27.91615	19.18975	35.36687	19.66457	12.62201	0
9	1.57604	5.43143	0.40312	3.73692	3.98161	4.06940	10.17614	27.38161
10	4.09729	0.75661	4.68925	1.56774	13.56069	0.91944	6.86077	22.11193
11	0.80958	3.82203	0.30933	2.75904	5.29057	3.42272	10.39183	29.29974
12	3.47315	0.93222	3.71762	1.24616	12.43708	0.59153	6.68756	21.98146

From archi	9	10	11	12
1	1.57604	4.09729	0.80958	3.47315
2	5.43143	0.75661	3.82203	0.93222
3	0.40312	4.68925	0.30933	3.71762
4	3.73692	1.56774	2.75904	1.24616
5	3.98161	13.56069	5.29057	12.43708
6	4.06940	0.91944	3.42272	0.59153
7	10.17614	6.86077	10.39183	6.68756
8	27.38161	22.11193	29.29974	21.98146
9	0	5.71764	0.73848	4.29811
10	5.71764	0	3.70501	0.25048
11	0.73848	3.70501	0	2.99347

12	4.29811	0.25048	2.99347	0

The CANDISC Procedure

F Statistics, NDF=7, DDF=450 for Squared Distance to archi

From archi	1	2	3	4	5	6	7	8
1	0	10.93828	2.34300	8.15818	11.28136	8.92738	31.42470	96.66158
2	10.93828	0	12.02274	1.88523	27.37245	3.21229	14.57492	60.06287
3	2.34300	12.02274	0	6.83449	7.68158	7.94843	25.34947	76.28908
4	8.15818	1.88523	6.83449	0	21.33953	2.91520	9.84794	52.44161
5	11.28136	27.37245	7.68158	21.33953	0	19.17547	32.95212	76.14877
6	8.92738	3.21229	7.94843	2.91520	19.17547	0	9.89003	42.33998
7	31.42470	14.57492	25.34947	9.84794	32.95212	9.89003	0	37.36779
8	96.66158	60.06287	76.28908	52.44161	76.14877	42.33998	37.36779	0
9	4.57069	15.75172	1.02297	9.48279	8.08296	8.26119	27.80928	74.82830
10	11.88257	2.19426	11.89941	3.97828	27.52923	1.86652	18.74906	60.42735
11	2.73917	12.93169	0.89709	8.00152	11.93362	7.72042	32.81630	92.52550
12	11.75127	3.15414	10.78149	3.61400	28.05357	1.33428	21.11860	69.41512

From archi	9	10	11	12
1	4.57069	11.88257	2.73917	11.75127
2	15.75172	2.19426	12.93169	3.15414
3	1.02297	11.89941	0.89709	10.78149
4	9.48279	3.97828	8.00152	3.61400
5	8.08296	27.52923	11.93362	28.05357
6	8.26119	1.86652	7.72042	1.33428
7	27.80928	18.74906	32.81630	21.11860
8	74.82830	60.42735	92.52550	69.41512
9	0	14.50904	2.14168	12.46498
10	14.50904	0	10.74492	0.72642
11	2.14168	10.74492	0	10.12829
12	12.46498	0.72642	10.12829	0

The CANDISC Procedure

Prob > Mahalanobis Distance for Squared Distance to archi

From archi	1	2	3	4	5	6	7	8
1	1.0000	<.0001	0.0234	<.0001	<.0001	<.0001	<.0001	<.0001
2	<.0001	1.0000	<.0001	0.0702	<.0001	0.0025	<.0001	<.0001
3	0.0234	<.0001	1.0000	<.0001	<.0001	<.0001	<.0001	<.0001
4	<.0001	0.0702	<.0001	1.0000	<.0001	0.0054	<.0001	<.0001
5	<.0001	<.0001	<.0001	<.0001	1.0000	<.0001	<.0001	<.0001
6	<.0001	0.0025	<.0001	0.0054	<.0001	1.0000	<.0001	<.0001
7	<.0001	<.0001	<.0001	<.0001	<.0001	<.0001	1.0000	<.0001
8	<.0001	<.0001	<.0001	<.0001	<.0001	<.0001	<.0001	1.0000
9	<.0001	<.0001	0.4141	<.0001	<.0001	<.0001	<.0001	<.0001
10	<.0001	0.0337	<.0001	0.0003	<.0001	0.0733	<.0001	<.0001

11	0.0086	<.0001	0.5085	<.0001	<.0001	<.0001	<.0001
12	<.0001	0.0029	<.0001	0.0008	<.0001	0.2321	<.0001

From archi	9	10	11	12
1	<.0001	<.0001	0.0086	<.0001
2	<.0001	0.0337	<.0001	0.0029
3	0.4141	<.0001	0.5085	<.0001
4	<.0001	0.0003	<.0001	0.0008
5	<.0001	<.0001	<.0001	<.0001
6	<.0001	0.0733	<.0001	0.2321
7	<.0001	<.0001	<.0001	<.0001
8	<.0001	<.0001	<.0001	<.0001
9	1.0000	<.0001	0.0383	<.0001
10	<.0001	1.0000	<.0001	0.6497
11	0.0383	<.0001	1.0000	<.0001
12	<.0001	0.6497	<.0001	1.0000

The CANDISC Procedure

Univariate Test Statistics

F Statistics, Num DF=11, Den DF=456

Variable	Label	Total Standard Deviation	Pooled Standard Deviation	Between Standard Deviation	R-Square	R-Square / (1-RSq)	F Value	Pr > F
Area	Area	20.3445	13.3968	16.1181	0.5766	1.3618	56.45	<.0001
Length	Length	2.6673	2.1496	1.6832	0.3658	0.5768	23.91	<.0001
Width	Width	2.1106	1.3229	1.7290	0.6164	1.6071	66.62	<.0001
Petiole	Petiole	0.6463	0.5758	0.3199	0.2250	0.2904	12.04	<.0001
Lwratio	Lwratio	1.0781	0.7752	0.7916	0.4952	0.9810	40.67	<.0001
Roundness	Roundness	0.4915	0.3810	0.3296	0.4132	0.7040	29.18	<.0001
Perimeter	Perimeter	6.4593	4.5145	4.8740	0.5230	1.0966	45.46	<.0001

Average R-Square

Unweighted	0.4593239
Weighted by Variance	0.568416

Multivariate Statistics and F Approximations

S=7 M=1.5 N=224

Statistic	Value	F Value	Num DF	Den DF	Pr > F
Wilks' Lambda	0.10724841	15.85	77	2704	<.0001
Pillai's Trace	1.55563696	11.84	77	3192	<.0001
Hotelling-Lawley Trace	3.62816207	21.13	77	1845.5	<.0001
Roy's Greatest Root	2.40617357	99.75	11	456	<.0001

NOTE: F Statistic for Roy's Greatest Root is an upper bound.

The CANDISC Procedure

	Canonical Correlation	Adjusted Canonical Correlation	Approximate Standard Error	Squared Canonical Correlation
1	0.840485	0.834280	0.013585	0.706415
2	0.642824	0.628276	0.027153	0.413222
3	0.473179	0.451453	0.035914	0.223898
4	0.306119	.	0.041938	0.093709
5	0.278553	.	0.042684	0.077592
6	0.165888	.	0.045001	0.027519
7	0.115245	.	0.045660	0.013281

Eigenvalues of Inv(E)*H = CanRsq/(1-CanRsq)

	Eigenvalue	Difference	Proportion	Cumulative	Test of H0: The canonical correlations in the current row and all that follow are zero: Likelihood Ratio	Approximate F Value	Num DF	Den DF	Pr > F
1	2.4062	1.7020	0.6632	0.6632	0.10724841	15.85	77	2704	<.0001
2	0.7042	0.4157	0.1941	0.8573	0.36530669	8.36	60	2368	<.0001
3	0.2885	0.1851	0.0795	0.9368	0.62256405	5.03	45	2025	<.0001
4	0.1034	0.0193	0.0285	0.9653	0.80216801	3.22	32	1672.2	<.0001
5	0.0841	0.0558	0.0232	0.9885	0.88511094	2.70	21	1304.2	<.0001
6	0.0283	0.0148	0.0078	0.9963	0.95956520	1.58	12	910	0.0914
7	0.0135		0.0037	1.0000	0.98671867	1.23	5	456	0.2950

The CANDISC Procedure

Total Canonical Structure

Variable	Label	Can1	Can2	Can3	Can4
Area	Area	0.757980	0.641951	0.004151	-0.035523
Length	Length	0.496093	0.541743	0.527961	0.238558
Width	Width	0.877146	0.383823	-0.190361	-0.187378
Petiole	Petiole	0.464861	0.082192	0.245447	0.693771
Lwratio	Lwratio	-0.792516	0.194110	0.299382	0.388421
Roundness	Roundness	-0.718666	0.171794	0.231952	0.482248
Perimeter	Perimeter	0.713371	0.581667	0.311299	0.120430

Total Canonical Structure

Variable	Can5	Can6	Can7
Area	0.014513	-0.103991	0.032576
Length	-0.088162	-0.234172	0.249288
Width	0.084253	0.047165	0.051217
Petiole	0.300106	-0.381245	-0.013227
Lwratio	0.085169	-0.050907	0.289645
Roundness	-0.014871	0.043259	0.406877
Perimeter	-0.022695	-0.082415	0.184521

Between Canonical Structure

Variable	Label	Can1	Can2	Can3	Can4
Area	Area	0.838978	0.543447	0.002587	-0.014321
Length	Length	0.689391	0.575781	0.413047	0.120742
Width	Width	0.938987	0.314253	-0.114726	-0.073058
Petiole	Petiole	0.823636	0.111380	0.244830	0.447702
Lwratio	Lwratio	-0.946549	0.177314	0.201306	0.168966
Roundness	Roundness	-0.939728	0.171808	0.170753	0.229671
Perimeter	Perimeter	0.829047	0.517011	0.203674	0.050975

Between Canonical Structure

Variable	Can5	Can6	Can7
Area	0.005324	-0.022718	0.004944

Length	-0.040604	-0.064228	0.047500
Width	0.029892	0.009965	0.007518
Petiole	0.176224	-0.133322	-0.003213
Lwratio	0.033713	-0.012000	0.047434
Roundness	-0.006445	0.011164	0.072951
Perimeter	-0.008741	-0.018904	0.029404

The CANDISC Procedure

Pooled Within Canonical Structure

Variable	Label	Can1	Can2	Can3	Can4
Area	Area	0.631173	0.755724	0.005620	-0.051972
Length	Length	0.337536	0.521099	0.584051	0.285180
Width	Width	0.767393	0.474730	-0.270780	-0.288026
Petiole	Petiole	0.286119	0.071520	0.245625	0.750251
Lwratio	Lwratio	-0.604393	0.209280	0.371219	0.520453
Roundness	Roundness	-0.508312	0.171783	0.266744	0.599296
Perimeter	Perimeter	0.559680	0.645162	0.397095	0.166007

Pooled Within Canonical Structure

Variable	Can5	Can6	Can7
Area	0.021422	-0.157601	0.049730
Length	-0.106325	-0.289979	0.310949
Width	0.130654	0.075101	0.082147
Petiole	0.327411	-0.427073	-0.014925
Lwratio	0.115130	-0.070658	0.404955
Roundness	-0.018645	0.055687	0.527590
Perimeter	-0.031561	-0.117681	0.265400

The CANDISC Procedure

Total-Sample Standardized Canonical Coefficients

Variable	Label	Can1	Can2	Can3	Can4
Area	Area	-1.49264792	3.24556815	-2.82337886	1.41588650
Length	Length	0.17294902	-2.15342640	-1.53152429	-2.71370740
Width	Width	0.97290288	-2.09394197	-1.36424954	-2.74228956
Petiole	Petiole	0.47488925	-0.38531475	-0.26238798	0.98363734
Lwratio	Lwratio	-1.77644547	1.07851293	2.17368741	-2.62410543
Roundness	Roundness	0.63484670	-0.27269001	-2.74335437	2.54279261
Perimeter	Perimeter	1.18250001	1.79822555	5.56455445	2.76006005

Total-Sample Standardized Canonical Coefficients

Variable	Can5	Can6	Can7
Area	-3.06402950	-1.85152789	-2.58856624
Length	-1.57613989	-7.29123621	5.43852541
Width	3.27343277	-2.99605599	5.85580127
Petiole	0.62841193	-0.30371440	-0.34740549
Lwratio	5.36195877	-0.25976288	0.03596538
Roundness	-3.88614020	0.23779926	1.48154560
Perimeter	1.95912401	10.87057308	-6.47292401

Pooled Within-Class Standardized Canonical Coefficients

Variable	Label	Can1	Can2	Can3	Can4

Area	Area	-0.982900079	2.137187973	-1.859178748	0.932353122
Length	Length	0.139381113	-1.735464966	-1.234268677	-2.187000268
Width	Width	0.609770510	-1.312385937	-0.855048485	-1.718740212
Petiole	Petiole	0.423069323	-0.343269196	-0.233756199	0.876302814
Lwratio	Lwratio	-1.277271423	0.775455124	1.562889974	-1.886742339
Roundness	Roundness	0.492161604	-0.211401516	-2.126771214	1.971286750
Perimeter	Perimeter	0.826455710	1.256789648	3.889097468	1.929021027

Pooled Within-Class Standardized Canonical Coefficients

Variable	Can5	Can6	Can7
Area	-2.017645814	-1.219220474	-1.704555989
Length	-1.270224776	-5.876070339	4.382954673
Width	2.051636197	-1.877789266	3.670145283
Petiole	0.559839603	-0.270573082	-0.309496598
Lwratio	3.855269887	-0.186770552	0.025859256
Roundness	-3.012709985	0.184352636	1.148560526
Perimeter	1.369242460	7.597502841	-4.523961909

The CANDISC Procedure

Raw Canonical Coefficients

Variable	Label	Can1	Can2	Can3	Can4
Area	Area	-0.073368482	0.159530191	-0.138778219	0.069595409
Length	Length	0.064840562	-0.807344137	-0.574185938	-1.017399878
Width	Width	0.460951753	-0.992088971	-0.646367922	-1.299269643
Petiole	Petiole	0.734805319	-0.596204966	-0.405997999	1.522001086
Lwratio	Lwratio	-1.647690306	1.000343285	2.016140511	-2.433912640
Roundness	Roundness	1.291717390	-0.554840142	-5.581880708	5.173799329
Perimeter	Perimeter	0.183068338	0.278391678	0.861474607	0.427297759

Raw Canonical Coefficients

Variable	Can5	Can6	Can7
Area	-0.150606978	-0.091008595	-0.127236418
Length	-0.590912836	-2.733567678	2.038965250
Width	1.550920035	-1.419501663	2.774420659
Petiole	0.972353928	-0.469943173	-0.537547240
Lwratio	4.973328851	-0.240935499	0.033358646
Roundness	-7.907097685	0.483848200	3.014488725
Perimeter	0.303301118	1.682924080	-1.002103532

Class Means on Canonical Variables

archi	Can1	Can2	Can3	Can4
1	1.299277252	0.156646241	0.051512947	0.478613085
2	-0.189342001	-0.794764018	0.071690303	0.521213043
3	1.117638163	0.599056734	-0.097492978	-0.078232870
4	-0.078774611	-0.429743830	0.287517897	0.062420010
5	1.562259539	2.078775712	0.386296809	0.220003357
6	-0.101021502	-0.647223880	0.008834754	-0.559271560
7	-1.415227904	-0.003132273	1.449053475	-0.238922370
8	-4.116384283	0.913123810	-0.640008839	0.106898746
9	1.066790742	0.819189722	-0.340444804	-0.466354627
10	0.061014361	-1.173395408	-0.295993182	0.010115584
11	1.229340281	0.232533188	-0.350556861	-0.128938784
12	0.145264620	-0.967764335	-0.343316427	-0.231693644

Class Means on Canonical Variables

archi	Can5	Can6	Can7
1	0.122045827	0.295058814	0.061736414

2	-0.024984592	0.010093991	-0.019852436
3	0.243438754	-0.161664689	-0.091781960
4	0.427683037	-0.164205278	-0.130435019

The CANDISC Procedure

Class Means on Canonical Variables

archi	Can5	Can6	Can7
5	-0.792664262	-0.152678298	-0.085030246
6	-0.388534485	0.253518381	0.158261443
7	0.057843787	0.004065642	0.044044693
8	0.017648117	0.014748692	0.016953332
9	0.215030577	0.214570361	-0.084242852
10	-0.352542889	-0.183770735	0.076503097
11	0.214724921	-0.190750660	0.215187041
12	-0.187449308	0.040018026	-0.174592339

References

Aalto T, Juurola E (2002) A three-dimensional model of CO_2 transport in airspaces and mesophyll cells of a silver birch leaf. Plant Cell & Environment **25:** 1399–1409

Abe M, Kobayashi Y, Yamamoto S, Daimon Y, Yamaguchi A, Ikeda Y, Ichinoki H, Notaguchi M, Goto K, Araki T (2005) FD, a bZIP protein mediating signals from the floral pathway integrator *FT* at the shoot apex. Science **309:** 1052-1056

Alabadi D, Oyama T, Yanovsky MJ, Harmon FG, Mas P, Kay SA (2001) Reciprocal regulation between *TOC1* and *LHY/CCA1* within the *Arabidopsis* circadian clock. Science **293:** 880-3

Aldwinckle HS (1975) Flowering of apple seedlings 16–20 months after germination. Horticultural Science **10:** 124–126

Altschul SF, Gish W, Miller W, Myers EW, Lipmanl DJ (1990) Basic local alignment search tool. Journal of Molecular Biology **21:** 403-10

Alvarez J, Guli CL, Yu XH Smyth DR (1992) *TERMINAL FLOWER*: a gene affecting inflorescence development in *Arabidopsis thaliana.* Plant Journal **2:** 103-116

Amasino RM (1996) Control of flowering time in plants. Current Opinion in Genetics and Development **6:** 482-487

An H, Roussot C, Suarez-Lopez P (2004) CONSTANS acts in the phloem to regulate a systemic signal that induces photoperiodic flowering of *Arabidopsis.* Development **131:** 3615–3626

Anonymous (2003) Agriculture Statistics Published by Statistics New Zealand Te Tari Tatau Wellington, New Zealand Catalogue Number 71.001 ISSN 0110 4624

Anonymous (2005) LightCycler® 2.0 Instrument operators Manual Version 2.0 Software version 4.05. Roche Diagnostics GmbH, Mannhein, Germany

Apple M, Tiekotter K, Snow M, Young J, Soeldner A, Phillips D, Tingey D, Bond BJ (2002) Needle anatomy changes with increasing tree age in Douglas-fir. Tree Physiology **22:** 129-36

Araki T (2001) Transition from vegetative to reproductive phase. Current Opinion in Plant Biology **4:** 63-68

Atkinson IAE (1992) A method for measuring branch divergence and interlacing in woody plants. Department of Science and Industrial Research Division. Land Resources Technical Record **86:** 1–18

Bassiri A, Irish EE, Poethig RS (1992) Heterochronic effects of *Teopod 2* on the

growth and photosensetivity of the maize shoot. The Plant Cell **4:** 497-504

Battey NH, Tooke F (2002) Molecular control and variation in the floral transition. Current Opinion in Plant Biology **5:** 62-68

Bauer H, Bauer U (1980) Photosynthesis in leaves of the juvenile and adult phase of ivy (*Hedera helix*). Physiologia Plantarum **49:** 366–372

Bernier G (1988) The control of floral evocation and morphogenesis. Annual Review of Plant Physiology and Molecular Biology **39:** 175-219

Blazquez MA, Ferrandiz C, Madueno F, Parcy F (2006) How floral meristems are built. Plant Molecular Biology **60:** 855-70

Blazquez MA, Green R, Nilsson O, Sussman MR, Weigel D (1998) Gibberellins promote flowering of *Arabidopsis* by activating the *LEAFY* promoter. Plant Cell **10:** 791-800

Blazquez MA, Koornneef M, Putterill J (2001) Flowering time**:** genes that regulate the floral transition. EMBO reports **2:** 1078-1082

Blazquez MA, Soowal LN, Lee I, Weigel D (1997) *LEAFY* expression and flower initiation in *Arabidopsis*. Development **124:** 3835-3844

Blazquez MA, Trenor M, Weigel D (2002) Independent control of gibberellin biosynthesis and flowering time by the circadian clock in *Arabidopsis*. Plant Physiology **130:** 1770-1775

Blazquez MA, Weigel D (2000) Integration of floral induction signals in *Arabidopsis*. Nature **404:** 889-892

Boardman NK (1977) Comparative photosynthesis of sun and shade plants. Annual Review of Plant Physiology **28:** 155-177

Bollman KM, Aukerman MJ, Park MY, Hunter C, Berardini TZ, Poethig RS (2003) *HASTY*, the *Arabidopsis* ortholog of exportin 5/MSN5, regulates phase change and morphogenesis. Development **130:** 1493-1504

Bolotin M (1975) Photoperiodic Induction of precocious flowering in a Woody Species *Eucalyptus occidentalis* Endl. Botanical Gazette, **136:** 358-365

Bomblies K, Wang RL, Ambrose BA, Schmidt RJ, Meeley RB, Doebley J (2003) Duplicate *FLORICAULA/LEAFY* homologs *ZFL1* and *ZFL2* control inflorescence architecture and flower patterning in maize. Development **130:** 2385-95

Bond BJ (2000) Age related changes in photosynthesis of woody plants. Trends in Plant Science **5:** 349-353

Bongard-Pierce DK, Evans MMS, Poethig RS (1996) Heteroblastic features of leaf anatomy in maize and their genetic regulation. International Journal of Plant

157: 331-340

Borchert R, Tomlinson PB (1984) Architecture and crown geometry in *Tabebuia rosea* (Bignoniaceae). American Journal of Botany **71:** 958–969

Borner R, Kampmann G, Chandler J, Gleissner R, Wisman E (2000) A MADS domain gene involved in the transition to flowering in *Arabidopsis.* Plant Journal **24:** 591–99

Bowman JL, Alvarez J, Weigel D, Meyerowitz EM, Smyth DR (1993) Control of flower development in *Arabidopsis thaliana* by *APETALA1* and interacting genes. Development **119:** 721-743

Bradley D, Carpenter R, Copsey L, Vincent C Rothstein S, Coen E (1996) Control of inflorescence architecture in *Antirrhinum.* Nature **379:** 791-797

Bradley D, Ratcliffe O, Vincent C, Carpenter R, Coen E (1997) Inflorescence commitment and archtecture in *Arabidopsis.* Science **275:** 80-83

Brill EM, Watson JM (2004) Ectopic expression of *Eucalyptus grandis SVP* orthologue alters the flowering time of *Arabidopsis thaliana.* Functional Plant Biology **31:** 217-224

Brink RA (1962) Phase change in higher plants and somatic cell heredity. The Quarterly Review of Biology **37:** 1-22

Browne RD (1995) Maturation and rejuvenation in Jack pine (*Pinus banksiana* Lamb)**:** Aspects of shoot morphology, anatomy and adventitious rooting of cuttings. Ph. D dissertation, University of Saskatchewan, Sascatoon, Canada

Burd CG, Dreyfuss G (1994) Conserved structures and diversity of functions of RNA-binding proteins. Science **265:** 615-21

Busch MA, Bomblies K, Weigel D (1999) Activation of a floral homeotic gene in *Arabidopsis.* Science **285:** 585-7

Calonje M, Cubas P, Martinez-Zapater JM, Carmona MJ (2004) Floral meristem identity genes are expressed during tendril development in grapevine. Plant Physiology **135:** 1491-501

Carlsbecker A, Tandre K, Johanson U, Englund M, Engström P (2004) The MADS-box gene *DAL1* is a potential mediator of the juvenile-to-adult transition in Norway spruce (*Picea abies).* The Plant Journal **40:** 546–557

Carmona MJ, Calonje M, Martinez-Zapater JM (2007) The *FT/TFL1* gene family in grapevine. Plant Molecular Biology **63:** 637-50

Carmona MJ, Cubas P, Martinez-Zapter JM (2002) *VFL*, the grapevine *FLORICAULA/LEAFY* ortholog, is expressed in meristematic regions independently of their fate. Plant Physiology **130:** 68-77

Carr SM, Irish VF (1997) Floral homeotic gene expression defines developmental arrest stages in *Brassica oleracea* L. vars. *botrytis* and *italica*. Planta **201:** 179-88

Chippendale G M (1973) *Eucalyptus* of the Western Australian gold fields. Department of Primary Industry, Australian Govt Publishing Service, pp 47-48

Chiurugwi T, Pouteau S, Nicholls D, Tooke F, Ordidge M, Battey N (2007) Floral meristem indeterminacy depends on flower position and is facilitated by acarpellate gynoecium development in *Impatiens balsamina*. The New Phytologist **173:** 79-90

Ciannamea S, Kaufmann K, Frau M, Tonaco IA, Petersen K, Nielsen KK, Angenent GC, Immink RG (2006) Protein interactions of MADS box transcription factors involved in flowering in *Lolium perenne*. Journal of Experimental Botany **57:** 3419-31

Clark SE, Williams RW, Meyerowitz EM (1997) The *CLAVATA1* gene encodes a putative receptor kinase that controls shoot and floral meristem size in *Arabidopsis*. Cell **89:** 575-585

Clarke JH, Dean C (1994) Mapping *FRI*, a locus controlling flowering time and vernalization response in *Arabidopsis thaliana*. Mol Gen Genet **242:** 81-89

Clemens J, Henroid R, Sismilich M, Sreekantan L Jameson PE (2002) Mini review of Research Activity – A woody perennial perspective of flowering. Flowering News Letter **33:** 17-22

Clemens J, Henriod RE, Bailey DG, Jameson PE (1999). Vegetative phase change in *Metrosideros*: shoot and root restriction. Plant Growth Regulation **28:** 207-214

Cockayne L (1912) Observations concerning evolution derived from ecological studies in New Zealand. Transactions and Proceedings of the New Zealand Institute **44:** 1-50

Coen ES, Romero JM, Doyle S, Elliott R, Murphy G, Carpenter R (1990) *FLORICAULA*: a homeotic gene required for flower development in *Antirrhinum majus*. Cell **63:** 1311-1322

Collins AJ, Campbell MM (2001) Maturation-related genes from Eucalyptus. 77th Annual Report, Oxford Forestry Institute, pp 14

Conway LJ, Poethig RS (1993) Heterochrony in plant development. Semin Dev Biol **4:** 65-72

Corbesier L, Coupland G (2006) The quest for florigen: a review of recent progress. Journal of Experimental Botany **57:** 3395–3403

Cseke LJ, Podila GK (2004) MADS-box genes in dioecious aspen II: a review of MADS-box genes from trees and their potential in forest biotechnology. Physiology and Molecular Biology of Plants **10:** 7–28

Davies B, Egea-Cortines M, de Andrade Silva E, Saedler H, Sommer H (1996) Multiple interactions amongst floral homeotic MADS-box proteins. EMBO J **15:** 4330-4343

Davis LJ (1991) Early induction of flowering in kiwifruit seedlings. Acta Horticulturae **297:** 231-235

Dawson JW (1968) The vegetative buds of the New Zealand species of *Metrosideros.* New Zealand Journal of Botany **6:** 240-242

Day JS, Gould KS, Jameson PE (1997) Vegetative architecture or *Elaeocarpus hookerianus.* Periodic growth patterns in divaricating juveniles. Annals of Botany **79:** 407-416

Day JS, Loveys BR, Aspinall D (1994) Environmental control of flowering of *Boronia megastigma* (Rutaceae) and *Hypocalymma amgustifolium* (Myrtaceae). Australian Journal of Botany **42:** 219-229

Day ME, Greenwood MS, White AS (2001) Age-related changes in foliar morphology and physiology in red spruce, and their influence on declining photosynthetic rates and productivity with tree age. Tree Physiology **21:** 1195–1204

Devlin PF (2002) Signs of the time: environmental input to the circadian clock. Journal of Experimental Botany **53:** 1535-50

Diaz EC, Martin F, Tagu D (1996) *Eucalypt* alpha-tubulin: cDNA cloning and increased level of transcripts in ectomycorrhizal root system. Plant Molecular Biology **31:** 905-10

Dijkstra P (1990) Causes and differences in specific leaf area. In Causes and consequences of variation in growth rate and productivity of higher plants. SPB (eds Lambers H, Cambridge ML, Konings H, Pons TL) Academic Publishing, The Hague, The Netherlands

Dornelas MC, Neves do Amaral WA, Rodriguez APM (2004) *EgLFY*, the *Eucalyptus grandis* homolog of the *Arabidopsis* gene *LEAFY* is expressed in reproductive and vegetative tissues. Brazilian Journal of Plant Physiology **16:** 105-114

Dornelas MC, Rodriguez APM (2005) The rubber tree (*Hevea brasiliensis* Muell. Arg.) homologue of the *LEAFY/FLORICAULA* gene is preferentially expressed in both male and female floral meristems. Journal of Experimental Botany **56:** 1965–1974

Dornelas MC, Rodriguez APM (2006) The tropical cedar tree (*Cedrela fissilis* Vell., Meliaceae) homolog of the *Arabidopsis LEAFY* gene is expressed in reproductive tissues and can complement *Arabidopsis* leafy mutants. Planta **223:** 306–314

Dutkowski GW, Potts BM, Williams DR, Kube PD, McArthur C (2001) Geographic

genetic variation in Central Victorian *Eucalyptus nitens.* In Developing the Eucalypt of the Future 10-15 September, Valdivia, Chile pp 39

Eckardt NA (2007) Phloem-borne FT signals flowering in Cucurbits. The Plant Cell **19:** 1435–1438

Elo A, Lemmetyinen J, Turunen ML, Tikka L, Sopanen T (1996) Three MADS box genes homologous to *SQUAMOSA* and *APETALA1* have different expression patterns in silver birch (*Betula pendula* Roth). NCBI sequence submission Accession X99655

Eriksson ME, Millar AJ (2003) The circadian clock: a plant's best friend in a spinning world. Plant Physiology **132:** 732-8

Esumi T, Tao R, Yonemori K (2005) Isolation of *LEAFY* and *TERMINAL FLOWER 1* hologues from six fruit tree species in the subfamily Maloideae of the Rosaceae. Sexual Plant Reproduction **17:** 277-287

Evans J (1999) Leaf anatomy enables more equal access to light and CO_2 between chloroplasts. New Phytologist **143:** 93-104

Evans LT (1971) Flower induction and the florigen concept. Annual Review of Plant Physiology and Plant Molecular Biology **22:** 365-394

Evans MM, Passas HJ, Poethig RS (1994) Heterochronic effects of *glossy15* mutations on epidermal cell identity in maize. Development **120:** 1971-81

Evans, MM, Barton MK (1997) Genetics of angiosperm shoot apical meristem development. Annual Review of Plant Physiology and Plant Molecular Biology **48:** 673-701

Fortanier EJ, Jonkers H (1976) Juvenility and maturity of plants as influenced by their ontogenetic and physiological aging. Acta Horticulturae **56:** 37-44

Foucher F, Morin J, Courtiade J, Cadioux S, Ellis N, Banfield MJ, Rameau C (2003) *DETERMINATE* and *LATE FLOWERING* are two *TERMINAL FLOWER1/CENTRORADIALIS* homologs that control two distinct phases of flower initiation and development in Pea. The Plant Cell **15:** 2742-2754

Frydman VM, Wareing PF (1973) Phase change in *Hedira helix*, Gibberellin like substances in the two growth phases. Journal of Experimental Botany **24:** 1131-1138

Gendall AR, Levy YY, Wilson A, Dean C (2001) The *VERNALIZATION 2* gene mediates the epigenetic regulation of vernalization in *Arabidopsis.* Cell **107:** 525-35

Goebel K (1900) Organography of plants. In General organography (English transilation by I.B. Balfour) Reprinted by Hafner, New York pp 707

Gould KS (1993) Leaf heteroblasty in *Pseudopanax crassifolius*: Functional

significance of leaf morphology and anatomy. Annals of Botany **71:** 61-70

Grassi G, Meir P, Cromer R, Tompkins D, Jarvis PG (2002) Photosynthetic parameters in seedlings of *Eucalyptus grandis* as affected by rate of nitrogen supply. Plant Cell and Environment **25:** 1677-1688

Greenwood MS (1992) Theoretical aspects of juvenility and maturation. In "A Symposium in IUFRO'S Centennial Year", Bordeaux-France

Greenwood MS (1995) Juvenility and maturation in conifers: current concepts. Tree Physiology **15:** 433-438

Greenwood MS, Hopper CA, Hutchison KW (1989) Maturation in larch. I. Effect of age on shoot growth, foliar characteristic and DNA methylation. Plant Physiology **90:** 406-412

Greenwood MS, Schmidtling RC (1981) Regulation of catkin production. U. S. Department of Agricultural and Forestry Services. Agricultural Handbook **587:** 20-6

Griffin AR, Whiteman P, Rudge T, Burgess IP, Moncur M (1993) Effect of paclobutrazol on flower-bud production and vegetative growth in two species of *Eucalyptus*. Canadian Journal of Forestry Research **23:** 640–647

Grulke NE, Miller PR (1994) Changes in gas exchange characteristics during the life span of giant sequoia: implications for response to current and future concentrations atmospheric ozone. Tree Physiology **14:** 659-668

Hackett WP (1976) Control of phase change in woody plants. Acta Horticulturae **56:** 143-154

Hackett WP (1985) Juvenility, maturation and rejuvenation in woody plants. Horticultural Reviews **7:** 109-155

Hackett WP, Murry JR (1997) Approaches to understanding maturation or phase change. Biotechnology of Ornamental Plants CAB International (pub), Wallingford, UK, pp 73-86

Hackett WP, Murry JR, Smith A (1992) Control of maturation in woody species. *In* "Mass production technology of genetically improved fast growing forest tree species synthesis" AFOCEL, Paris, France, pp 45-50

Hasan O, Reid JB (1995) Reduction of generation time in *Eucalyptus globulus.* Plant Growth Regulation **17:** 53–60

Haughn GW, Schultz EA, Martinez-Zapater JM (1995) The regulation of flowering in *Arabidopsis thaliana* meristems, morphogenesis and mutants. Canadian Journal of Botany **73:** 959-981

Hayama R, Coupland G (2003) Shedding light on the circadian clock and the photoperiodic control of flowering. Current Opinon of Plant Biology **6:** 13-9

Hempel FD, Weigel D, Mandel MA, Ditta G, Zambryski PC, Feldman LJ, Yanofsky MF (1997) Floral determination and expression of floral regulatory genes in Arabidopsis. Development **124:** 3845-3853

Henriod RE, Jameson PE, Clemens J (2000) Effects of photoperiod, temperature, and bud size on flowering in *Metrosideros excelsa* (Myrtaceae). Journal of Horticultural Science and Biotechnology **75:** 55-61

Henriod R E (2001) Phase change, flowering and post-harvest characteristics of *Metrosideros excelsa* (Myrtaceae). Ph.D thesis. IMBS, Massey University, Palmerston North

Hepworth SR, Valverde F, Ravenscroft D, Mouradov A, Coupland G (2002) Antagonistic regulation of flowering-time gene *SOC1* by *CONSTANS* and *FLC* via separate promoter motifs. EMBO J **21:** 4327–37

Hill KD, Johnson LAS (1995) Systematic studies in the eucalypts – 7 A revision of the bloodwoods, genus *Corymbia* (Myrtaceae). Telopea **6:** 173–505

Hofer J, Turner L, Hellens R, Ambrose M, Matthews P, Michael A, Ellis N (1997) *UNIFOLIATA* regulates leaf and flower morphogenesis in pea. Current Biology **7:** 581–587

Huang L-C, Weng JH, Wang CH, Kuo CI, Shieh YJ (2003) Photosynthetic potentials of *in vitro*-grown juvenile, adult, and rejuvenated *Sequoia sempervirens* (D. Don) Endl. Shoots. Botanical bulletin of Academia Sinica **44:** 31-35

Huijser P, Klein J, Lonning, WE, Meijer H, Saedler H, Sommer H (1992) Bracteomania, an inflorescence anomaly, is caused by the loss of function of the MADS-box gene, *SQUAMOSA*, in *Antirrhinum majus*. EMBO **J 11:** 1239-1249

Hutchison KW, Sherman CD, Smith SS, Singer PB, Greenwood MS (1990) Maturation in Larch II Effects of age on photosynthesis and gene expression in developing foliage. Plant Physiology **94:** 1308-1315

IBIS World reports (2006) Nursery and Floriculture Production in the U.S. Sep-29-2006. http://www.ibisworld.com/industry

Jacobs MR (1955) Growth habits of the eucalypts. Forestry and Timber Bureau, Canberra, Australia

James SA, Bell DT (2001) Leaf morphological and anatomical characteristics of heteroblastic *Eucalyptus globulus* ssp. *globulus* (Myrtaceae). Australian Journal of Botany **49:** 259-269

James SA, Smith WK, Vogelmann TC (1999). Ontogenetic differences in mesophyll structure and chlorophyll distribution in *Eucalyptus globules* ssp. *globules*. American Journal of Botany **86:** 198-207

Jensen CS, Salchert K, Nielsen KK (2001) A *TERMINAL FLOWER1*-like gene from perennial ryegrass involved in floral transition and axillary meristem identity. Plant Physiology **125:** 1517-1528

Johansen DA (1940) Plant microtechnique. McGraw-Hill, London, pp 523

Johnson ED (1926) A comparison of the juvenile and adult leaves of *Eucalyptus globulus*. New Phytologist **26:** 202–212

Jones CS (1999) An essay on juvenility, phase change, and heteroblasty in seed plants. International Journal of Plant Science **160:** S105-S111

Jordan GJ, Potts BM, Chalmers P, Wiltshire RJE (2000) Quantitative genetic evidence that the timing of vegetative phase change in *Eucalyptus globulus* ssp. *globulus* is an adaptive trait. Austtralian Journal of Botany **48:** 561–567

Jordan GJ, Potts BM, Wiltshire RJE (1999) Strong, independent, quantitative genetic control of the timing of vegetative phase change and first flowering in *Eucalyptus globulus* ssp. *globulus* (Tasmanian Blue Gum). Heredity **83:** 179-187

Kardailsky I, Shukla VK, Ahn JH, Dagenais N, Christensen SK, Nguyen JT, Chory J, Harrison MJ, Weigel D (1999) Activation tagging of the floral inducer *FT*. Science **286:** 1962–1965

Kazumi A, Satoh N, Sasaki H, Satoh H, Nagato Y (2002) A rice heterochronic mutant, *mori1*, is defective in the juvenile-adult phase change. Development **129:** 265-273

Kelly D (1994) Towards a numerical definition for divaricate (interlaced small-leaved) shrubs. New Zealand Journal of Botany **32:** 509–518

Kerstetter R.A, Poethig RS (1998) The specification of leaf identity during shoot development. Annual review of cell and developmental biology **14:** 373-398

Kester DE (1976) The relationship of juvenility to plant propogation. Combined Proceedings International Plant Propagators Society **26:** 71-84

King RW (1998) Dual control of flower initiation, and development by temperature and photoperiod in *Hardenbergia violaceae*. Australian Journal of Botany **46:** 65-74

King RW, Moritz T, Evans LT, Martin J, Andersen CH, Blundell C, Kardailsky I, Chandler PM (2006) Regulation of flowering in the long day grass, *Lolium temulentum* by gibberellins and the gene *FLOWERING LOCUS T* (*FT*). Plant Physiology **141:** 498–507

King RW, Pate JS, Johnston J (1996) Ectopic differences in the flowering of *Pimelea ferruginea* (Thymelaeaceae), in response to cool temperatures. Australian Journal of Botany **44:** 47-55

Kobayashi Y, Kaya H, Goto K, Iwabuchi M, Araki T (1999) A pair of related genes with antagonistic roles in mediating flowering signals. Science **286:** 1960–1962

Koike T (1988) Leaf structure and photosynthetic performance as related to the forest succession of deciduous broad-leaved trees. Plant Species Biology **3:** 77–87

Kolb TE, Stone JE (2000) Differences in leaf gas exchange and water relations among species and tree sizes in an Arizona pine-oak forest. Tree Physiology **20:** 1-12

Komeda Y (2004) Genetic regulation of time to flower in *Arabidopsis thaliana.* Annual Reviews of Plant Biology **55:** 521-35

Koornneef M, Alonso-Blanco C, Blankestijn-de Vries H, Hanhart CJ, Peters AJM (1998b) Genetic interactions among late flowering mutants of *Arabidopsis.* Genetics **148:** 885-892

Koornneef M, Alonso-Blanco C, Peters AJM, Soppe W (1998a) Genetic control of flowering time in *Arabidopsis.* Annual Reviews of Plant Physiology and Plant Molecular Biology **49:** 345-370

Koornneef M, Hanhart CJ, Van Der Veen JH (1991) A genetic and physiological analysis of late flowering mutants in *Arabidopsis thaliana.* Molecular and general genetics **229:** 57-66

Kotake T, Takada S, Nakahigashi K, Ohto M, Goto K (2003) *Arabidopsis TERMINAL FLOWER 2* gene encodes a heterochromatin protein 1 homolog and represses both *FLOWERING LOCUS T* to regulate flowering time and several floral homeotic genes. Plant Cell Physiology **44:** 555-64

Kotoda N, Iwanami H, Takahashi S, Abe K (2006) Antisense expression of *MdTFL1*, a *TFL1*-like gene, reduces the juvenile phase in apple. Journal of American Society for Horticultural Science **131:** 74–81

Kotoda N, Wada M, Kusaba S, Kano-Murakami Y, Masuda T, Soejima J (2002) Overexpression of *MdMADS5*, an *APETALA*-like gene of apple, causes early flowering in transgenic *Arabidopsis.* Plant Science **162:** 679-687.

Kotoda N, Wada M (2005*) MdTFL1*, a *TFL1*-like gene of apple, retards the transition from the vegetative to reproductive phase in transgenic *Arabidopsis.* Plant Science **168:** 95–104

Kruger EL, Volin JC (2006) Re-examining the empirical relation between plant growth and leaf photosynthesis. Functional Plant Biology **33:** 421-26

Kubien DS, Jaya E, Clemens J (2007) Differences in the structure and gas exchange physiology of juvenile and adult leaves in *Metrosideros excelsa.* International Journal of Plant Science **168:** 563-570

Kull O, Koppel A (1987) Net photosynthetic response to light intensity of shoots from different crown positions and age in *Picea abies* (L.) Karst. Scandinavian Journal of

Forest Research **23:** 450-456

Kyozuka J, Harcourt R, Peacock WJ, Dennis ES (1997) *Eucalyptus* has functional equivalents of the *Arabidopsis AP1* gene. Plant Molecular Biology **35:** 573-84

Kyozuka J, Konishi S, Nemoto K, Izawa T, Shimamoto K (1998) Down-regulation of *RFL*, the *FLO/LFY* homolog of rice, accompanied with panicle branch initiation. Proceedings of National Academy of Science USA **95:** 1979-82

Kyozuka SKJ (2002) Rice as a model for comparative genomics of plants. Annual Review of Plant Biology **53:** 399-419

Lamb RS, Hill TA, Tan QK, Irish V F (2002) Regulation of *APETALA3* floral homeotic gene expression by meristem identity genes. Development **129:** 2079-86

Lang A (1952) Physiology of flowering. Annual Reviews of Plant Physiology 3**:** 265-306

Larsson AS, Landberg K, Meeks-WagnerD (1998) The *TERMINAL FLOWER2* (*TFL2*) gene controls the reproductive transition and meristem identity in *Arabidopsis thaliana*. Genetics **149:** 597–605

Lawson JR, Poethig RS (1995) Shoot development in plants**:** time for a change. Trends in Genetics **11:** 263-268

Lee H, Suh SS, Park E, Cho E, Ahn JH (2000) *AGAMOUS-LIKE 20* MADS domain protein integrates floral inductive pathways in *Arabidopsis*. Genes and Development **14:** 2366–76

Lee I, Aukerman MJ, Gore SL, Lohman KN, Michaels SD, Weaver LM, John MC, Feldmann KA, Amasino RM (1994b) Isolation of *LUMINIDEPENDENCE***:** A gene involved in the control of flowering time in *Arabidopsis*. Plant Cell **6:** 75-83

Lee I, Michaels SD, Masshardt AS, Amasino RM (1994a) The late flowering phenotype of *FRIGIDA* and mutations in *LUMINIDEPENDENCE* is suppressed in the Landsberg erecta strain of *Arabidopsis*. Plant Journal **6:** 903-909

Levy Y, Dean C (1998) The transition to flowering. Plant Cell **10:** 1973-1989

Levy YY, Mesnage S, Mylne JS, Gendall AR, Dean C (2002) Multiple roles of *Arabidopsis VRN1* in vernalization and flowering time control. Science **297:** 243-6

Liljegren SJ, Gustafson-Brown C, Pinyopich A, Ditta GS, Yanofsky MF (1999) Interactions among *APETALA1*, *LEAFY*, and *TERMINAL FLOWER1* specify meristem fate. Plant Cell **11:** 1007–1018

Lin MK, Belange H, Lee YJ, Varkonyi-Gasic E, Taoka KI, Miura E, Xoconostle-Cazares B, Gendler K, Jorgensen RA, Phinney B, Lough TJ, Lucas WJ (2007) FLOWERING LOCUS T protein may act as the long-distance florigenic signal in the cucurbits. Plant Cell **19:** 1488–1506

Longman KA, Nasr TAA, Wareing PF (1965) Gravimorphism in trees: The effect of gravity on flowering. Annals of botany **115:** 459–473

Longman KA, Wareing PF (1959) Early induction of flowering in birch seedlings. Nature **184:** 2037–2038

Lovatt CJ, Pillitteri LJ, Walling LL (2004) Isolation and characterization of *LEAFY* and *APETALA1* homologues from *Citrus sinensis* L. Osbeck 'Washington'. Journal of the American Society for Horticultural Science **129:** 846-856

Lovett-Doust J (1989) Plant reproductive strategies and resource allocation. Trends in Ecology and Evolution **4:** 230–234

Macknight R, Bancroft I, Page T, Lister C, Schmidt R, Love K, Westphal L, MurphyG, Sherson S, Cobbett C, Dean C (1997) *FCA*, a gene controlling flowering time in *Arabidopsis*, encodes a protein containing RNA-binding domains. Cell **89:** 737–745

Mandel MA, Gustafson-Brown C, Savidge B, Yanofsky MF (1992) Molecular characterization of the *Arabidopsis* floral homeotic gene *APETALA1*. Nature **360:** 273–277

Mandel MA, Yanofsky M (1995) A gene triggering flower formation in *Arabidopsis*. Nature **377:** 522–524

Mckenzie MJ, Veit B, Walton EF, Jameson PE, Clemens J (1997) A *LEAFY*-like DNA isolated from *Metrosideros excelsa*. GenBank Accession No AF007869

McKinnon GE, Steane DE, Potts BM, Vaillancourt RE (1999) Incongruence between chloroplast and species phylogenies in *Eucalyptus* subgenus *Monocalyptus* (Myrtaceae). American Journal of Botany **86:** 1038-1046

McKinnonGE, Vaillancourt RE, Steane DA, Potts BM (2004) The rare silver gum *Eucalyptus cordata* is leaving its trace in the organellar gene pool of *Eucalyptus globulus*. Molecular Ecology **13:** 3751-3762

Mediavilla S, Escudero A (2003) Photosynthetic capacity, integrated over the lifetime of a leaf, is predicted to be independent of leaf longevity in some tree species. New Phytologist **159:** 203-211

Meilan R (1997) Floral induction in woody angiosperms. New Forests **14:** 179–202

Mellerowicz EJ, Horgan K, Walden A, Coker A, Walter C (1998) *PRFLL*: a *Pinus radiata* homologue of *FLORICAULA* and *LEAFY* is expressed in buds containing vegetative and undifferentiated male cone primordia. Planta **206:** 619–629.

Michaels SD, Amasino RM (2000) Memories of winter: Vernalisation and competence of flower. Plant Cell and Environment **23:** 1145-1153

Mimida N, Goto K, Kobayashi Y, Araki T, Ahn JH, Weigel D, Murata M, Motoyoshi F, Sakamoto W (2001) Functional divergence of the *TFL1*-like gene family in *Arabidopsis* revealed by characterisation of a novel homologue. Genes to Cells **6:** 327-336

Molinero-Rosales N, Jamilena M, Zurita S, Gomez P, Capel J, Lozano R (1999) *FALSIFLORA*, the tomato orthologue of *FLORICAULA* and *LEAFY*, controls flowering time and floral meristem identity. Plant Journal **20:** 685-93

Moncur MW (1992) Effect of low temperature on floral induction of *Eucalyptus lansdowneana* subsp. l*ansdowneana.* Australian Journal of Botany **40:** 157–167

Moncur MW, Hasan O (1994) Floral induction in *Eucalyptus nitens.* Tree Physiology **14:** 1303–1312

Monteuuis O (1991) Rejuvenation of a 100-year-old *Sequoiadendron giganteum* through in vitro meristem culture I. Organogenic and morphological arguments. Physiologia Plantarum **81:** 111-115

Moon J, Suh SS, Lee H, Choi KR, Hong CB, Paek NC, Kim SG, Lee I (2003) The *SOC1* MADS-box gene integrates vernalization and gibberellin signals for flowering in *Arabidopsis.* Plant Journal **35:** 613–623

Moose SP, Sisco PH (1994) *GLOSSY15* controls the epidermal juvenile-to-adult phase transition in maize. The Plant Cell **6:** 1343-1355

Morel JB, Godon C, Mourrain P, Beclin C, Boutet S, Feuerbach F, Proux F, Vaucheret H (2002) Fertile hypomorphic ARGONAUTE (ago1) mutants impaired in post-transcriptional gene silencing and virus resistance. Plant Cell **14:** 629-639.

Mouradov A, Cremer F, Coupland G (2002) Control of flowering time: interacting pathways as a basis for diversity. Plant Cell **14:** S111-30

Mouradov A, Glassic T, Hamdorf B, Murphy L, Fowler B, Marla S, Teasdale RD (1998) *NEEDLY*, a *Pinus radiata* orthologue of *FLORICAULA/LEAFY* genes, expressed in both reproductive and vegetative meristems. Proceedings of National Academy of Science USA **95:** 6537-6542

Murai K, Miyamae M, Kato H, Takumi S, Ogihara Y (2003) *WAP1*, a wheat *APETALA1* homolog, plays a central role in the phase transition from vegetative to reproductive growth. Plant Cell Physiology **44:** 1255–1265

Murphy G, Sherson S, Cobbett C, Dean C (1997) *FCA*, a gene controlling flowering time in *Arabidopsis*, encodes a protein containing RNA-binding domains. Cell **89:** 737-45

Murry JR, Smith AG, Hackett WP (1994) Differential dihydroflavonol reductase transcription and anthocyanin pigmentation in the juvenile and mature phases of ivy (*Hedera helix* L.). Planta **194:** 102-109

Nakagawa M, Shimamoto K, Kyozuka J (2002) Overexpression of *RCN1* and *RCN2*, rice *TERMINAL FLOWER1/CENTRORADIALIS* homologs, confers delay of phase transition and altered panicle morphology in rice. Plant Journal **29:** 743-50

Navarro L, Roistacher CN, Murashige T (1975) Improvement of shoot tip grafting *in vitro* grown virus-free *Citrus*. Journal of American Society for Horticultural Science **100:** 471-479

Nilsson O, Lee I, Blazquez MA, Weigel D (1998) Flowering-time genes modulate the response to *LEAFY* activity. Genetics **150:** 403-10

Nitsche A, Buttner M, Wilhelm S, Pauli G, Meyer H (2006) Real-time PCR detection of parapoxvirus DNA. Clinical chemistry **52:** 316-9

Oliphant JL (1990) Juvenility and maturity of woody species in New Zealand. *In* Plant Aging: Basic and Applied Approaches. Plenum Press, New York, pp 37-42

Olszewski N, Sun T, Gubler F (2002) Gibberellin signalling: Biosynthesis, catabolism and response pathways. Plant Cell **14:** S61-S80

Ordidge M, Chiurugwi T, Tooke F, Battey NH (2005) *LEAFY*, *TERMINAL FLOWER1* and *AGAMOUS* are functionally conserved but do not regulate terminal flowering and floral determinacy in *Impatiens balsamina*. The Plant Journal **44:** 985-1000

Orkwiszewski JA, Poethig RS (2000) Phase identity of the maize leaf is determined after leaf initiation. Proceedings of National Academy for Sciences USA **97:** 10631-6

Page T, Macknight R, Yang C, Dean C (1999) Genetic interactions of the *Arabidopsis* flowering time gene, *FCA*, with genes regulating floral initiation. Plant Journal **17:** 231-239

Parcy F, Nilsson O, Busch, MA, Lee L, Weigel D (1998) A genetic frame work for floral patterning. Nature **395:** 561-566

Pena L, Martín-Trillo M, Juárez J, Pina JA, Navarro L, Martínez-Zapater JM (2001) Constitutive expression of *Arabidopsis LEAFY* or *APETALA1* genes in citrus reduces their generation time. Nature Biotechnology **19**: 263-267

Pfaffl MW, Horgan GW, Dempfle L (2002) Relative expression software tool (REST) for group-wise comparison and statistical analysis of relative expression results in real-time PCR. Nucleic Acids Research **30:** 36

Pillitteri LJ, Lovatt CJ, Walling LL (2004) Isolation and characterization of a *TERMINAL FLOWER* homolog and its correlation with juvenility in *Citrus*. Plant Physiology **135:** 1540-51

Pnueli L, Gutfinger T, Hareven D, Ben-Naim O, Ron N, Adir N, Lifschitz E (2001) Tomato SP-interacting proteins define a conserved signalling system that regulates

shoot architecture and flowering. Plant Cell **13:** 2687-2702

Poethig RS (1988a) Heterochronic mutations affecting shoot development in maize. Genetics **119:** 959-973

Poethig RS (1988b) A non-cell-autonomous mutation regulating juvenility in maize. Nature **336:** 82-83

Poethig RS (1990) Phase change and regulation of shoot morphogenesis in plants. Science **250:** 923-930

Poethig RS (2003) Phase change and the regulation of developmental timing in plants. Science **301:** 334-436

Poethig RS (2007) ms403 the regulation of vegetative phase change by miRNAs and ta-siRNAs. International Plant Growth Substances Association, 19th Annual meeting Puerto Vallarta, Mexico

Potts BM, Wiltshire RJE (1997) Eucalypt genetics and genecology *In* J Wiliams, J Woinarski, eds, Eucalypt Ecology: Individuals to Ecosystems, Cambridge University Press, Cambridge, pp 56-91

Pouteau S, Nicholls D, Tooke F, Coen E, Battey N (1997) The induction and maintenance of flowering in *Impatiens*. Development **124:** 3343–3351

Preston K (1999) Can plasticity compensate for architectural constraints on reproduction? Patterns of seed production and carbohydrate translocation in *Perilla frutescens*. Journal of Ecology **87:** 697–712

Putterill J, Laurie R, Macknight R (2004) It's time to flower: the genetic control of flowering time. Bioessays **26:** 363-73

Pyankov VI, Black CC, Jr Artyusheva EG, Voznesenskaya EV, Ku MSB, Edwards GE (1999) Features of photosynthesis in *Haloxylon* species of Chenopodiaceae that are dominant plants in Central Asian deserts. Plant and Cell Physiology **40:** 125–134

Ratcliffe OJ, Amaya I, Vincent CA, Rothstein S, Carpenter R, Coen ES, Bradley DJ (1998) A common mechanism controls the life cycle and architecture of plants. Development **125:** 1609-1615

Ratcliffe OJ, Bradley DJ, Coen ES (1999) Separation of shoot and floral identity in *Arabidopsis*. Development **126:** 1109-1120

Rogler CE, Hackett WP (1975) Phase change in *Hedera helix*: Induction of the mature to juvenile phase change by gibberellin. Physiologia Plantarum **43:** 141-147

Rottmann WH, Meilan R, Sheppard LA, Brunner AM, Skinner JS, Ma C, Cheng S, Jouanin L, Pilate G, Strauss SH (2000) Diverse effects of overexpression of *LEAFY* and *PTLF*, a poplar (*Populus*) homolog of *LEAFY/FLORICAULA*, in

transgenic poplar and *Arabidopsis*. Plant Journal **22:**235-45

Ruiz-García L, Madueño F, Wilkinson M, Haughn G, Salinas J, Martínez-Zapater JM (1997) Different roles of flowering-time genes in the activation of floral initiation genes in *Arabidopsis*. Plant Cell **9:** 1921-1934

Sablowski R (2007) Flowering and determinacy in *Arabidopsis*. Journal of Experimental Botany **58**: 899-907

Sachs RM, Hackett WP (1983) Source-sink relationships in flowering. *In* Strategies of Plant Reproduction. Meudt, W.J (ed), Allanheld, Osmun, Granada, pp 263-272

Samach A, Coupland G (2000) Time measurement and the control of flowering in plants. Bioessays **22:** 38-47

Samach A, Onouchi H, Gold SE, Ditta GS, Schwarz-Sommer Z, Yanofsky MF, Coupland G (2000) Distinct roles of *CONSTANS* target genes in reproductive development of *Arabidopsis*. Science **288:** 1613-1616

Saitou N, Nei M (1987) The neighbour joining method: a new method for reconstructing phylogenetic trees. Molecular Biology Evolution **4:** 406-425

Sarnowski TJ, Swiezewski S, Pawlikowska K, Kaczanowski S, Jerzmanowski A (2002) *AtSWI3B*, an *Arabidopsis* homolog of *SWI3*, a core subunit of yeast Swi/Snf chromatin remodeling complex, interacts with *FCA*, a regulator of flowering time. Nucleic Acids Research **30:** 3412-21

Schomburg FM, Patton DA, Meinke DW, Amasino RM (2001) *FPA*, a gene involved in floral induction in *Arabidopsis*, encodes a protein containing RNA-recognition motifs. Plant Cell **13:** 1427-36

Schwarz-Sommer Z, Hue I. Huijser R, Flor RJ, Hansen R, Tetens E, Lonnig W, Saedler H, Sommer H (1992) Characterization of the *Antirrhinu*m floral homeotic MADS-box gene deficiencies: evidence for DNA binding and autoregulation of its persistent expression throughout flower development. EMBO J **11:** 251-263

Scurfield G, Moore CWE (1958) Effects of Gibberellic acid on species of *Eucalyptus*. Nature **181:** 1276-1277

Sefton, CA, Montagu, KD, Atwell, BJ, Conroy JP (2002) Anatomical variation in juvenile *Eucalyptus* leaves accounts for differences in specific leaf area and CO_2 assimilation rate. Australian Journal of Botany **50:** 301-310

Shannon S, Meeks-Wagner DR (1991) A mutation in the *Arabidopsis TFL1* gene affects inflorescence meristem development. Plant Cell **3:** 877-892

Sheldon CC, Burn JE, Perez PP, Metzger J, Edwards JA, Peacock WJ, Dennis ES (1999) The *FLF* MADS box gene: A repressor of flowering in *Arabidopsis* regulated by vernalization and methylation. Plant Cell **11:** 445-458

SheldonCC, Rouse DT, Finnigan EJ, Peacock WJ, Dennis ES (2000) The molecular basis of vernalization: The central role of *FLOWERING LOCUS C* (*FLC*). Proceedings of National Academy of Sciences USA **97:** 3753-3758

Simons AM, Johnston MO (2000) Plasticity and the genetics of reproductive behaviour in the monocarpic perennial, *Lobelia inflata* (Indian tobacco). Heredity **85:** 356-365

Simpson GG, Gendall AR, Dean C (1999) When to switch to flowering. Annual review of cell and developmental biology **15:** 519-550

Sismilich M (2001) Quantitative markers of phase change and modelling the size and complexity of trees. PhD thesis IMBS, Massey University, Palmerston North

Sismilich M, Henriod RE, Jameson PE, Clemens J (2003) Changes in carbon isotope composition during vegetative phase change in a woody perennial plant. Plant Growth Regulation **39:** 33-40

Sismilich M, Menzies MI, Gandar PW, Jameson PE, Clemens J (2003) Development of a mathematical method for classifying and comparing tree architecture using parameters from a topological model of a trifurcating botanical tree. Journal of Theoretical Biology **220:** 371–391

Snowball AM, Warrington IJ, Halligan EA, Mullins MG (1994) Phase change in citrus: The effects of main stem node number, branch habit and paclobutrazol application on flowering in citrus seedlings. Journal of Horticultural Science **69:** 149–160

Song J (2005) Genetic diversity and flowering in *Clianthus* and New Zealand *Sophor*a (Fabaceae). PhD thesis IMBS, Massey University, Palmerston North

Southern EM (1975) Detection of specific sequences among DNA fragments separated by gel electrophoresis. Journal of Molecular Biology **98:** 503-515

Southerton SG (2007) Early flowering induction and *Agrobacterium* transformation of the hardwood tree species *Eucalyptus occidentalis.* Functional Plant Biology **34:** 707–713

Southerton SG, Marshall H, Mouradov A, Teasdale RD (1998) Eucalypts MADS-box gene expressed in developing flowers. Plant Physiology **118:** 365-372

Southerton S (2002) Unusual eucalypt a genetic engineering pioneer. News in Science, Thursday, 12th December, http://abc.net.au/science/news/stories/s745443.htm

Sreekantan L (2002) Molecular studies of flowering in *Metrosideros excelsa* (Myrtaceae). PhD thesis IMBS, Massey University, Palmerston North

Sreekantan L, Clemens J, McKenzie MJ, Lenton JR, Croker SJ, Jameson PE (2004) Flowering genes in *Metrosideros* fit a broad herbaceous model encompassing *Arabidopsis* and *Antirrhinum.* Physiol Plant **121:** 163-173

Sreekantan L, McKenzie MJ, Jameson PE, Clemens J (2001) Cycles of floral and vegetative development in *Metrosideros excelsa* (Myrtaceae). International Journal of Plant Sciences **162:** 719–727

Steele MJ, Coutts MP, Yeoman MM (1989) Developmental changes in Sitka spruce as indices of physiological age. I. Changes in needle morphology. The New Phytologist **113:** 367-375

Stein OL, Fosket EB (1969) Comparative developmental anatomy of shoots of juvenile and adult *Hedera helix*. American Journal of Botany **56:** 546-55

Sung SB, Amasino RM (2004) Vernalization and epigenetics: how plants remember winter. Current Opinion in Plant Biology **7:** 4–10

Sung S, Amasino RM (2005) Remembering winter: toward a molecular understanding of vernalization. Annual review of plant biology **56:** 491-508

Sung SK, Yu GH, An G (1999) Characterization of *MdMADS2*, a member of the *SQUAMOSA* subfamily of genes, in apple. Plant Physiology **120:** 969–978

Sung ZR, Belachew A, Shunong B, Bertrand-Garcia R (1992) *EMF* an *Arabidopsis* gene required for vegetative shoot development. Science **258:** 1645-1647

Suarez-Lopez P, Wheatley K, Robson F, Onouchi H, Valverde F, Coupland G (2001) *CONSTANS* mediates between the circadian clock and the control of flowering in *Arabidopsis*. Nature **410:** 1116–1120

Sylvester AW, Parker-Clark V, Murray GA (2001) Leaf shape and anatomy as indicators of phase change in the grasses: comparison of maize, rice and bluegrass. American Journal of Botany **88:** 2157-2167

Takada S, Goto K (2003) *TERMINAL FLOWER2*, an *Arabidopsis* homolog of heterochromatin protein1, counteracts the activation of *FLOWERING LOCUS T* by *CONSTANS* in the vascular tissues of leaves to regulate flowering time. Plant Cell **15:** 2856-65

Tan FC, Swain SM (2006) Genetics of flower initiation and development in annual and perennial plants. Physiologia Plantarum **128:** 8-17

Telfer A, Bollman KM, Poethig RS (1997) Phase change and the regulation of trichome distribution in *Arabidopsis thaliana*. Development **124:** 645-654

Telfer A, Poethig RS (1998) *HASTY*: a gene that regulates the timing of shoot maturation in *Arabidopsis thaliana*. Development **125:** 1889-98

Thomas B, Vince-Prue D (1997) Photoperiodism in plants. Second edition, Acadamic Press, San Diego, CA

Thomas SC, Winner WE (2002) Photosynthetic differences between saplings and

adult trees: an integration of field results by meta-analysis. Tree Physiology **22:** 117–127

Thompson JD, Gibson TJ, Plewniak F, Jeanmougin F, Higgins DG (1997) The CLUSTAL_X windows interface: flexible strategies for multiple sequence alignment aided by quality analysis tools. Nucleic Acids Research **24:** 4876–4882

Thornley JHM, Johnson IR (1990) Plant and Crop Modelling. Oxford: Clarendon Press

Tomlinson PB (1983) Architecture of tropical plants. Annual review of ecology and systematics **18:** 1-21

Tooke F, Ordidge M, Chiurugwi T, Battey N (2005) Mechanisms and functions of flower and inflorescence reversion. Journal of Experimental Botany **56:** 2587-2599

Tsukaya H, Shoda K, Kim GT, Uchimiya H (2000). Heteroblasty in *Arabidopsis thaliana* (L.) Heynh. Planta **210:** 536 -542

van der Linden CG, Vosman B, Smulders MJ (2002) Cloning and characterization of four apple MADS box genes isolated from vegetative tissue. Journal of Experimental Botany **53:** 1025-36

Vega SH, Sauer M, Orkwiszewski JAJ, Poethig RS (2002) The *EARLY PHASE CHANGE* Gene in Maize. Plant Cell **14:** 133-147

Viser T (1964) Juvenile phase and growth of apple and pear seedlings. Euphytica **13:** 119-129

Vitousek PM (1998) Foliar and litter nutrients, nutrient resorption, and decomposition in Hawaiian *Metrosideros polymorpha.* Ecosystems **1:** 401–407

von Caemmerer S (2000) Biochemical models of leaf photosynthesis.CSIRO, Collingwood, pp 165

von Caemmerer S, Farquhar GD (1981) Some relationships between the biochemistry of photosynthesis and the gas exchange of leaves. Planta **153:** 376–387

Wada M, Cao Q, Kotoda N, Soejima J, Masuda T (2002) Apple has two orthologues of *FLORICULA/LEAFY* involved in flowering. Plant Molecular Biology **49:** 567-577

Wagner D, Sablowski, RW Meyerowitz EM (1999) Transcriptional activaton of *APETALA1* by *LEAFY.* Science **285:** 582-584

Walton EF, Podivinsky E, Wu RM (2001) Bimodal patterns of floral gene expression over the two seasons that kiwifruit flowers develop. Physiologia Plantarum **111:** 396-404

Wareing PF (1959) Problems of juvenility and flowering in trees. Journal of the Linnean Society of London Botany **56:** 282-289

Wareing PF, FrydmanVM (1976) General aspects of phase change with special reference to *Hedera helix* L. Acta horticulturae **56:** 57–68

Wareing PF, Robinson LW (1963) Juvenility problems in woody plants. Forest Commission Report for 1962 Forest Research London, pp 125-7

Warren CR (2004) The photosynthetic limitation posed by internal conductance to CO2 movement is increased by nutrient supply. Journal of Experimental Botany **55:** 2313–2321

Weigel D, Alvarez J, Smyth DR, Yanofsky MF, Meyerowitz EM (1992) *LEAFY* controls floral meristem identity in *Arabidopsis.* Cell **69:** 843-859

Welch SM, Dong Z, Roe JL (2004) Modelling gene networks controlling transition to flowering in *Arabidopsis.* Proceedings of the 4th International Crop Science Congress

Wesoly W (1985) Effect of girdling on flowering and on levels of endogenous growth regulators in embryonic shoots of Scots pine grafts (*Pinus silvestris* L.). Acta physiologica **7:** 171–179

Wilkins TA, Smart LB (1996) Isolation of RNA from Plant tissue. In: Krieg PA (ed) A laboratory guide to RNA isolation , Analysis and Synthesis, John Wiley, New York, pp 21-41

Williams DR, Potts BM, Smethurst PJ (2004) Phosphorus fertiliser can induce earlier vegetative phase change in *Eucalyptus nitens.* Australian Journal of Botany **52:** 281-284

Wiltshire RJE, Potts BM, Reid JB (1998). Genetic control of reproductive and vegetative phase change in the *Eucalyptus risdonii/E. tenuiramus* complex. Australian Journal of Botany **46:** 45-63

Witkowski ETF, Lamont BB (1991) Leaf specific mass confounds leaf density and thickness. Oecologia **88:** 486–493

Xu YL, Gage DA, Zeevaart JAD (1997) Gibberellins and stem growth in *Arabidopsis thaliana.* Effects of photoperiod on the *GA4* and *GA5* loci. Plant Physiology **114:** 1471–1476

Yan L, Loukoianov A, Tranquilli G, Helguera M, Fahima T, Dubcovsky J (2003). Positional cloning of the wheat vernalization gene *VRN1*. Proceedings of National Academy for Sciences USA **100:** 6263-8

Yanovsky MJ, Kay SA (2003) Living by the calendar: how plants know when to flower. Nature Reviews Molecular Cell Biology **4:** 265-75

Zhang H (1998). Cytokinins and phase change in *Pinus radiata*: morphological, physiological and molecular studies. PhD thesis, Plant Biology, Massey University, Palmerston North

Zimmerman RH, Hackett WP, Pharis RP (1985) Hormonal aspects of phase change and precocious flowering. Encyclopedia of Plant Physiology **11:** 79-115